SJUOB

Scientific Journal of University of Benghazi

Volume 38. Issue 1.June 2025

ISSN (Online) 2790-1637 ISSN (Print) 2790-1629

http://journals.uob.edu.ly/sjuob

Scientific Journal of
University of Benghazi

Volume 38, Issue 1, (2025)

It deals with various branches of human applied and medical knowledge

Publishes research in English

Guidelines for Submission

-Only articles originally written in English (NOT translated to English) are accepted for submission.

-The submission has not been previously published or being under consideration elsewhere.

-The submission file is in Microsoft Word format (.doc,.docx)

-The submitted articles should adhere to originality and publishing ethics.

-The similarity of the article should not exceed 20%.

-The submission should include a separate title page, the main article and the journal submission form.

-Article should have no more than 6 authors.

-The main article should be divided into; Title, Abstract, Keywords, Introduction,

-Material and Methods, Results and Discussion, Conclusion and References.

-The text is single-spaced, Times New Roman with a 12-point font.

-The text must not be more than 3000 words excluding abstracts and references.

-All figures and tables should be well presented, organized and consistent with the text.

-All figures must be prepared as (.tiff) or (.jpeg) format for the width of A4 size (6.27 in) with a minimum resolution of 300 dpi.

-The role of authors should be provided.

-Ethical approval when applicable should be provided.

-Any conflict of interest should be declared.

-Vancouver referencing style should be used.

-URLs/DOIs in the references list should be included where available.

Editorial Board

University of Benghazi Scientific Journal - University of Benghazi, Office No. 12, University of Benghazi - Al-Humaidah

Email: sjuob@uob.edu.ly - Website: http://journals.uob.edu.ly/sjuob

Editorial Board Members

Porf.Dr.Daefalla M. Tawati **Porf. Dr.Mayeen Uddin Khandaker**

(Applied Sciences)

Dr. Asma AL-fergani **Dr. Ahmad S. Emrage**

(Applied Sciences) **(Humanities)**

Dr.Allaaeddin A. El Salabi **Dr. Abdelhakim M. El-barsha** **(Medical Sciences)**

Enas Salem **Khalifa A. Al-Athram**

(Technical Coordinator) **(Administrative Coordinator)**

University of Benghazi Scientific Journal - University of Benghazi, Office No. 12, University of Benghazi - Al-Humaidah

Email: sjuob@uob.edu.ly - Website: http://journals.uob.edu.ly/sjuob

Preface

The First Issue of Volume 38, 2025

Announcement: Publication of Research Papers in the Thirty-Eighth Issue (First Edition), Released in June 2025

The Editor-in-Chief and esteemed members of the Editorial Board of the Scientific Journal of University of Benghazi (SJUOB) are pleased to announce that the journal's thirty-eighth issue, first edition, was published in June 2025.

This issue featured a diverse selection of high-quality scientific research papers across various fields and disciplines. The published works demonstrated scholarly excellence and innovation, reflecting the dedication of our researchers to advancing knowledge and supporting scientific progress at Benghazi University.

We believe that the research included in this issue will make a significant contribution to the university's ongoing pursuit of academic excellence and will serve as an important resource for scholars, students, and the broader scientific community.

May Allah grant us continued success and guide our efforts to raise the standards of scientific research at our university.

Sincerely,

The Editor-in-Chief and Editorial Board

The Scientific Journal of University of Benghazi (SJUOB)

Table of Contents for Volume 38 Issue 1

Scientific Journal of University of Benghazi (2025)

Humanties

Scientific Journal of University of Benghazi
SJUOB (2025) 38 (1) Humanities Sciences: Elfeitouri , 10 – 31
www.sjuob.uob.edu.ly

The Impact of English Cartoons on Children's English Language Development: A Case Study

Nisreen Salah Elfeitouri [1]*

1 Department of English, Faculty of Languages, University of Benghazi.

Received: 25 / 02 / 2025 | accepted: 08 / 05 / 2025 | Publishing: 29/06/2025

ABSTRACT

Cartoons can teach children a vast amount of information and valuable life lessons in an entertaining and engaging manner. Cartoons can also help children acquire various skills, like collaboration, negotiating, critical thinking, and problem-solving. In addition, cartoon-viewing has been increasingly linked with children's language development and improvement. Accordingly, this study examined the impact of watching English cartoons on children's English language acquisition in the Libyan setting. Case study research was conducted, which involved three years of direct observation of a two-year-old Libyan girl. The data analysis and results revealed that a purposeful and consistent approach to watching English cartoons can lead to remarkable English language learning outcomes. Specifically, the child in this study demonstrated notable English language development across various areas, including vocabulary, grammar, sentence structure, pronunciation, comprehension, production, and emotional expression. The findings of this study shed light on the benefits of following a systematic approach to using English language media-based content as an innovative and motivating method for English language teaching and learning in the Libyan home environment and Libyan English language learning classroom.

KEYWORDS: English cartoons, environment, innate abilities, interaction, language acquisition..

Corresponding Author: Nisreen Salah Elfeitouri.

1.INTRODUCTION

Language development is a dynamic and intricate process that involves several skills, such as comprehension and production. Yet, remarkably, this process often takes place relatively quickly and effortlessly for children acquiring their first language everywhere in the world and in very similar developmental stages [1, 2]. This fascinating phenomenon of first language acquisition has garnered considerable attention from scholars and led to the development of several explanatory language acquisition theories, such as behaviourist, nativist, innatist, and interactionist theories.

The behaviorist view, developed by B. F. Skinner, postulates that children acquire their first language by imitating the language they hear in their environment (e.g., from their parents) [3]. On the other hand, the nativist perspective, proposed by Noam Chomsky, challenges the behaviourist view that language results from habit formation based on environmental exposure. Conversely, the nativist view argues that humans are born with natural abilities for language acquisition [3]. Notably, the interactionist viewpoint, established by Berko Gleason, highlights the multifaceted nature of language acquisition and suggests that it is influenced by three interconnected factors: (1) exposure to the surrounding environment, (2) a child's inherent abilities, and (3) social interaction. Thus, in addition to the first two perspectives put forth by the behaviorist and nativist theories, the interactionist perspective underscores the role of social engagement in language development [3].

The early years of a child's life (i.e., preschool) represent a sensitive milestone in language development. Specifically, language production begins in the first six months with cooing and progresses to babbling in the latter half of the first year. Between 12 and 24 months, most children articulate their first recognizable word. This stage is known as the holophrastic (one-word) stage, where children use words to represent entire thoughts (e.g., saying "milk" to communicate "I want milk"). From 2 to 5 years of age, children rapidly expand their vocabulary and begin stringing words together into simple sentences. Early speech takes place at about two years old and is often described as "telegraphic", which lacks many grammatical elements, such as bound morphemes and function words, but still follows correct word order [2, 4].

By the age of three, children have established the grammatical framework of their native language. Their sentences become longer and more complex as they begin using auxiliaries, copulas, modals, negatives, and early syntactic movements. Around this time, children also try to form questions and produce complex sentences with multiple verbs or clauses, including relative clauses [2]. By the age of four, children typically master the basic structures of their native language, enabling them to ask questions, give commands, recount real events, and even invent stories- all while mostly using correct grammar. As they join pre-school, children continue to refine their English language skills [4].

The process of first language acquisition is theoretically complex; however, it occurs effortlessly and instinctively for children. Consequently, there is a common agreement that early childhood is the best time to learn foreign languages because young children are more receptive and their language abilities develop most quickly and efficiently during this age [5]. This stage also provides optimal conditions for simultaneous bilingualism, allowing children exposed to two languages to acquire both as native tongues [4, 6].

Moreover, Krashen [5] posits that language learning is most effective when learners are immersed in engaging, meaningful, and understandable content within a relaxed environment. According to Krashen [5], a fun and stimulating learning context reduces the "affective filter", which represents emotional obstacles such as anxiety or boredom that can impede language acquisition. In other words, the success of language learning can be directly influenced by eliminating negative feelings and providing a comfortable and engaging environment for learners [5].

In this respect, the role of media, particularly cartoons, has been extensively studied in relation to children's language exposure. It has been noted that cartoons provide authentic input for presenting language in an amusing manner. Furthermore, various children's shows purposefully focus on using simplified and repeated language to facilitate language acquisition. Also, many shows feature interactive content that requires children to interact and cooperate with the characters, which promotes their understanding and response skills [7].

On the other hand, the investigation into the impact of cartoons on children's lan-

guage development has yielded mixed findings. Some studies revealed no notable influence of cartoons on children's language [8.9], whereas other studies stressed that the benefits of cartoon viewing are largely determined by their content. For example, cartoons, such as Dora the Explorer, encourage children to respond to verbal cues and interact with characters. The interactive nature of these cartoons has been linked to enhanced vocabulary, comprehension, cognitive skills, and the ability to follow instructions. Conversely, exposure to non-educational or inappropriate content has been associated with poorer language outcomes [7].

Notably, some scholars [2, 10] highlighted that television alone cannot lead to language acquisition and that interactive conversations between adults and children are crucial for language development. Conversely, other researchers [11-14] have observed significant positive impacts from cartoon viewing on children's English as a second language development across various areas, such as vocabulary, pronunciation, syntax, and so on, even in the absence of interactive support in the child's environment. It is important to note that these studies have been conducted in different contexts: Saudi Arabia [11], Lithuania [12], West Africa [13], and the Philippines [14], respectively.

Despite garnering considerable attention worldwide, the influence of cartoons on children's English language development has been given little attention in the Libyan context. Markedly, despite English holding a significant status in Libya, learning it remains challenging, as many Libyan learners report poor proficiency levels. As a result, there have been constant appeals for further research that explores innovative approaches to address this issue [15-17].

Accordingly, this study aimed to address this gap by investigating how television exposure at an early age influences English language acquisition among Libyan children. In particular, this research examined the impact of English cartoons on Libyan children's English language development. The rationale behind the research objective was to elicit and provide insights for enhancing English language learning and teaching approaches in Libya.

2.MATERIALS AND METHODS

To achieve the aims of this study and examine the impact of watching English car-

 ISSN: Online 2790-1637, Print 2790-1629
National Library of Libya, Legal number: 154/2018

toons on children's language acquisition, case study research was conducted. A case study is a research approach that observes the topic under investigation in its natural environment. It is often employed when the aim is to study people, organizations, and programs closely and in-depth [18]. The rationale for selecting this research approach for this study was that it was crucial to observe a child's language growth and improvement thoroughly and meticulously within the child's real environment (i.e., home) to ensure the depth and credibility of the research findings.

This case study was conducted on Sama, a two-year-old Libyan girl. Sama lives in Benghazi, Libya, with her family of four, including her father, mother, and six-year-old sister. The main language spoken in Sama's home environment by all her family members is Arabic. This case study examined the impact of consistently exposing Sama to English cartoons.

The selection of Sama as the subject of this case study was based on two factors: (1) Sama was two at the beginning of this study, which is commonly considered an ideal age for observing and analysing the effect of exposure to a new language, and (2) the fact that Sama had not joined school yet ensured that there were no other factors (e.g., intervention from school) that could affect the trustworthiness of the findings.

Sama's English language development was documented for three years, starting when she was two years old and continuing until she turned five. During this time, she was exposed daily to English cartoons for three distinct hours. The data collection methods included systematic observations, detailed written records of produced utterances, and video and audio recordings. These data were gathered monthly throughout the study period.

The data analysis process involved examining the written records and converting the data in the videos and recordings to transcription to facilitate the analysis process. Subsequently, the data were analysed using pre-established criteria by the researcher: vocabulary, grammar and sentence structure, pronunciation, understanding and responding, and expressing emotions.

The researcher of this study was Sama's mother, an English language instructor and researcher, who actively observed and recorded Sama's language progress. Sama's

mother is proficient in the English language. Nonetheless, it is worth noting that she possesses a neutral, non-native English accent. Moreover, it is crucial to clarify that the main language used at Sama's home was Arabic, which was spoken by Sama's father, mother, and sister. At the beginning of the study, Sama's mother only spoke Arabic with her. However, when English began to emerge in Sama's utterances (shortly after a month of Sama's exposure to cartoons), Sama's mother started to use English occasionally to interact with her and respond to her English utterances. In particular, Sama's mother alternated between English and Arabic, addressing Sama following the language used by her.

As a researcher, conducting a case study on a family member (her daughter) had both advantages and disadvantages. As for the advantages, the researcher had constant access to the child, which made it easier to collect data consistently and without interruptions. Moreover, the researcher was able to gather detailed and real-time observations, which could not be easily obtained in external studies. Also, the child remained in a familiar setting, which reduced observer effects.

On the other hand, bias and subjectivity were among the disadvantages threatening the credibility of this study. That is to say, as the child's mother, the researcher could have unconscious biases that influence data collection and interpretation. To overcome these disadvantages, the researcher sought external validation, involving three other researchers in observing Sama and reviewing the collected data and the analysis process.

3-Types of Cartoons Sama has Viewed

Sama's exposure to television was purposely focused on educational cartoons that involved straightforward language, narration, interaction, and repetitive activities. These cartoons were originally created to develop, enhance, and reinforce kids' vocabulary, comprehension, and conversational abilities in an entertaining and approachable manner. It is important to highlight that all the programs Sama viewed featured an American accent. The intention behind concentrating on a single accent was to investigate whether she would adopt that particular accent.

Particularly, Sama watched a variety of English cartoons, such as Sofia the First, Goldilocks and the Three Bears, Fancy Nancy, and so on. However, there were four shows that the researcher focused on expos-

 ISSN: Online 2790-1637, Print 2790-1629
National Library of Libya, Legal number: 154/2018

ing Sama to regularly because they were highly instructive and communicative. These were: Barney & Friends, Dora the Explorer, Doc McStuffins, and Mickey Mouse Clubhouse. The following is a brief description of the key focus in each of these shows.

1.Barney & Friends is a non-animated series in which Barney, a purple dinosaur, and his friends play games and sing songs while teaching things like colours, shapes, numbers, and important concepts, such as friendship, honesty, etc. Barney uses a lot of songs that employ repetition to teach new words. For instance, the song "If You're Happy and You Know It" teaches kids action phrases like shout, clap, and stomp. Additional examples of vocabulary used in Barney & Friends include common verbs like dance, sing, and play, and simple nouns like ball, flower, and tree.

2.Dora the Explorer is an animated series in which Dora, the main character, invites viewers to join her in various types of adventures that include problem-solving and exploration. The language used by Dora often includes questions that require interaction and response from the viewers. For instance, she frequently employs phrases such as "Can you find the...?" and "Let's go to the...," and uses basic nouns, verbs, and prepositions. Examples of vocabulary featured in Dora the Explorer include common items such as a backpack, map, mountain, and treasure, and actions like go, look, help, and find.

3.In the cartoon, Doc McStuffins, a young girl, Doc McStuffins, works in collaboration with her animal friends to "fix/treat" toys. Through her interactions with toy patients, Doc and her friends introduce basic medical concepts and highlight medical vocabulary using terms such as "check-up", "diagnosis", "stethoscope", "bandage", and "temperature". Additionally, the show emphasizes the value of empathy and kindness by frequently using verbs like "help", "comfort", and "care".

4.The animated program, Mickey Mouse Clubhouse, revolves around Mickey and his interactive adventures that encourage early problem-solving skills. In each episode, a problem is introduced by Mickey, who invites viewers to join him to solve the day's challenge. Mickey asks guiding questions during the episode to lead the viewers to answer the problem. The language in Mickey Mouse Clubhouse is simple and repetitive. It often uses clear, straightforward questions and

prompts to engage the audience, such as "Can you help me find the...?" or "What tool do we need?".

4.RESULTS

The analysis of Sama's English language growth over the three years of this case study revealed significant transitions and improvements. To facilitate the analysis and presentation of the results, the researcher categorized Sama's development during the three years into five key areas: vocabulary, grammar and sentence structure, pronunciation, understanding and responding, and expressing emotions. It is noteworthy that during this study, Sama continued to acquire the Arabic language and use it in her home setting with her family members.

4.1.Vocabulary

This section focuses on Sama's vocabulary development and use during the three years.

1-At ages 2 to 3

Sama acquired a small amount of vocabulary, mostly nouns referring to objects in her immediate environment, such as common household items (e.g., "cups", "books", "balls", and familiar actions or daily activities like "running", "jumping", and "playing".

2-At ages 3 to 4

Sama's vocabulary expanded considerably. It consisted of more nouns, verbs, and simple adjectives. For example, she acquired exploration-related vocabulary (e.g., backpack, bridge, treasure, map), verbs (e.g., climb, swim), adjectives (e.g., big, red), and medical care terms (e.g., doctor, diagnosis, check-up, stethoscope). Moreover, she showed correct and meaningful use of this vocabulary during her daily playtime and interactions.

3-At ages 4 to 5

Sama's vocabulary became more advanced and involved references to abstract concepts. For instance, it involved terms that describe time (e.g., yesterday, tomorrow, later), and adjectives that describe feelings (e.g., excited, scared, tired). In addition, she could use more complex noun phrases to describe something (e.g., the tall, blue building).

4.2.Grammar and Sentence Structure

This section highlights Sama's language growth in sentence building and structure over the three years of the study.

1-At ages 2 to 3

Initially, Sama's sentences consisted of two-word phrases, which seemed to be ac-

 ISSN: Online 2790-1637, Print 2790-1629
National Library of Libya, Legal number: 154/2018

quired as chunks. Examples of these phrases were "mommy go" or "more juice". At this phase, Sama's utterances lacked functional words like articles, prepositions, or auxiliaries. By three years old, Sama began to utter three-word and longer phrases, which consisted of subject, verb, and object (e.g., "Daddy eat cookie"). Also, Sama demonstrated some use of pronouns (e.g., I, you). However, during this stage, she frequently omitted the subject from her sentences.

2-At ages 3 to 4

Sama incorporated additional elements such as articles, prepositions, and conjunctions into her sentences. Also, she used the plural and possessive /s/ markers (e.g., "my toys" and "mommy's shoes"). During this stage, Sama used negations and questions, which were clearly learned in the form of chunks (e.g., "I don't want it", "I can't do it", "what's that?", "Can you help me?").

At this phase, the present simple tense emerged in Sama's language (though sometimes without proper subject-verb agreement, as in "she play in the room"), and the progressive "-ing" marker. However, her use of auxiliaries, such as "is", was inconsistent. For instance, her utterances included both "The dog barking" and "The dog is barking", as well as "Mommy cooking dinner in the kitchen and daddy is sleeping".

3-At ages 4 to 5

Sama started experimenting with question-forming. The initial stage of forming questions involved omitting the auxiliary ("Daddy eating?"), but over time, she learned to produce accurate yes/no and WH question forms (e.g., "Is daddy eating?", and "What is daddy watching?"). Moreover, she followed a similar experimental path with forming negations, from early experimentation to complete mastery.

Furthermore, this stage marked the emergence of the past tense in Sama's utterances, which she used appropriately to refer to past events, tell a short story, and describe a sequence of events (e.g., "I dropped my toy and I breaked it"). However, she applied the "-ed" marker to all past verbs and did not produce any irregular past verb forms at this stage (e.g., "goed" instead of "went").

As she was nearly five, Sama's sentences became more complex and she started using relative clauses (e.g., "I want the toy that grandma bought me") and conditional clauses (e.g., "If I finish my snack, can I play

 ISSN: Online 2790-1637, Print 2790-1629
National Library of Libya, Legal number: 154/2018

with my friends?"). Moreover, Sama developed an understanding of time, which was evident in her ability to use the future tense to describe upcoming events (e.g., "I will eat my chocolate after lunch").

4.3. Pronunciation

This section examines Sama's phonological development over the three years, focusing on three dimensions: pronunciation accuracy, accent, and intonation.

1-At ages 2 to 3

Pronunciation Accuracy: Sama's speech was characterized by unclear articulation. She often simplified complex sounds. For example, she pronounced "rat" as "wat". (substituting "r" with "w"). Also, she often reduced consonant clusters (e.g., tr), pronouncing words like "train" as "rain". Generally, her production of vowel sounds was more accurate than her pronunciation of consonants at this stage.

Accent: From the outset of the study, Sama pronounced the vocabulary she acquired in a very similar way to what she heard on TV (i.e., in an American accent), despite the problems identified in the previous stage.

Intonation: Sama occasionally imitated some of the intonations she heard (e.g., using rising intonation at the end of "cookie?" to ask if she could have it). However, Sama's use of intonation at this stage was imprecise and inconsistent.

3-At ages 3 to 4

Pronunciation Accuracy: During this stage, Sama's pronunciation became clearer, and she overcame the difficulties she encountered in the previous stages (e.g., with consonant clusters). However, she experienced some problems in producing fricative sounds like "sh" and "th". For example, she pronounced "ship" as "sip", and "thorn" as "sorn".

Accent: Sama's accent continued to reflect the American input she received.

Intonation: Sama's use of intonation became more accurate and consistent. For instance, she consistently used rising intonation when asking questions.

3-At ages 4 to 5

Pronunciation Accuracy: This stage marked a notable improvement in Sama's pronunciation. She could produce most sounds correctly at this phase, except for fricative sounds, which she occasionally mispronounced.

Accent: Sama's accent at this stage was similar to a native American child her age.

Intonation: At this stage, Sama's intonation

was accurate; she used correct intonation patterns following the type of sentences she uttered, whether statements, questions, or exclamations.

4.4.Understanding and Responding

This section discusses Sama's reaction to input, focusing on her comprehension and response skills.

1-At ages 2 to 3

Sama could understand and follow basic instructions, such as the ones she viewed on Dora the Explorer or Mickey Mouse Clubhouse. For example, she could understand when Mickey says, "Are you ready?", answering with "yes". Also, Sama could respond to simple instructions from her mother in familiar and immediate everyday contexts, such as "Come here" or "Please pass the book". Her responses at this stage were restricted to "yes" and "no".

2-At ages 3 to 4

Sama showed improvement in this area, which was evident in her ability to understand more complex instructions that were not immediately context-bound, like "Can you find the key?". Her responses developed to include phrases like "I can't, and I don't know".

3-At ages 4 to 5

Sama's comprehension and response skills improved remarkably at this stage. She could follow multi-step directions (e.g., take the book and put it on the table). In addition, she could respond using more advanced phrases, like "of course", "it's heavy", and "Which one?".

4.5.Expressing Emotions

This section discusses Sama's use of English to describe her feelings.

1-At ages 2 to 3

Sama's expression of her emotions took place only when she was nearly three years old. Also, the initial stage was limited to using one word, often the following three adjectives: "happy, sad, mad". She used them interchangeably to express her feelings.

2-At ages 3 to 4

Sama's ability to express her feelings improved. She started to express her emotions more clearly and use more varied adjectives (e.g., scared, excited, sleepy).

3-At ages 4 to 5

Sama could express her emotions in addition to giving reasons for them. For example, she would say "I'm excited to play!" or "I feel sad because I lost my toy".

Table (1) below summarises the results of this case study.

Table (1): Summary of the Case Study Results

Developmental Area	**Age Range (Years)**	**Key Observations/ Findings**
Vocabulary	2 to 3	Acquired a limited vocabulary- mainly nouns referring to common items (e.g., books) and basic actions (e.g., running).
Vocabulary	3 to 4	Expanded vocabulary including nouns, verbs, and simple adjectives (e.g., backpack, climb, big).
Vocabulary	4 to 5	Acquired more complex and abstract words, such as time descriptors (e.g., yesterday); emotion adjectives (e.g., excited); and used descriptive phrases (e.g., the tall, blue building)
Grammar and Sentence Building	2 to 3	Formed two-word phrases (e.g. "Mommy go"); three-word phrases lacking function words; used pronouns inconsistently
Grammar and Sentence Building	3 to 4	Incorporated articles, prepositions, and conjunctions; applied plural and possessive markers; produced negations and questions as chunks (e.g., "What's that?" "I don't want it"); used present simple tense with inaccurate subject/verb agreement; used progressive tense but with inconsistent auxiliaries
Grammar and Sentence Building	4 to 5	Experimented with questions-formation initially omitting auxiliaries, then mastering yes/no and WH forms; used past tense (often overgeneralized with "-ed") and later used relative and conditional clauses, and future tense.
Pronunciation	2 to 3	Accuracy: unclear articulation of words with simplified and reduced consonant clusters; vowels produced more accurately than consonants; Accent: mimicked American TV; Intonation: inconsistent.
Pronunciation	3 to 4	Accuracy: clearer articulation of words ; overcame many consonant cluster issues; struggled with fricative sounds (e.g., "ship" → "sip");Accent: remained American; Intonation: improved, especially in questions

Pronunciation	4 to 5	Accuracy: marked improvement overall with most sounds produced correctly; occasional struggles with fricatives; Accent: matured to a Native American levelIntonation: was appropriate and varied for statements, questions, etc.
Understanding and Responding	2 to 3	Comprehension was limited to basic instructions from TVor her mother; responses were primarily "yes" or "no".
Understanding and Responding	3 to 4	Improved comprehension allowed for understanding more complex commands; responses included phrases like "I can't" or "I don't know".
Understanding and Responding	4 to 5	Significantly enhanced comprehension- capable of following multi-step directions; responses became more varied (e.g., "Of course", "it's heavy", "Which one?").
Expressing Emotions	2 to 3	Began to express emotions near age three using single-word adjectives (e.g., "happy", "sad", "mad") Interchangeably.
Expressing Emotions	3 to 4	Improved expression with a broader range of adjectives (e.g., scared, excited).
Expressing Emotions	4 to 5	Expressed emotions with added reasoning (e.g., "I'm excited to play!" or "I feel sad because I lost my toy").

5. DISCUSSION

The results of Sama's case study revealed that she progressed from not having any knowledge of English at age two to achieving a satisfactory level of proficiency by age five. Sama's English language development during the three years was observed and measured across five areas: vocabulary, grammar and sentence structure, pronunciation, understanding and responding, and expressing emotions.

The findings indicate that Sama's development across all five areas was closely linked to the content she observed on television, particularly during the early stage. At the initial phase of the research, Sama's mother did not engage with her in English; she was only an observer. Nonetheless, Sama mimicked the language she heard on TV, and this was detected across areas of vocabulary, grammar and sentence construction, pronunciation, understanding and responding, and emotional expression.

The evidence revealing that Sama was copying the content she watched on TV is that the words she used were not part of her

mother's commonly used vocabulary. Sama used words she was exposed to in programs such as Dora the Explorer (e.g., map, treasure), Doc McStuffins (e.g., diagnosis, check-up, feel better), and Mickey Mouse Clubhouse (e.g., tools, mystery, etc). The same observation was noted in her grammatical and sentence-building skills, pronunciation, understanding and responding, and emotional expression. This outcome highlights the influence of media on Sama's English language development. Moreover, the findings are consistent with the behaviourist [3] viewpoint regarding language acquisition, which underscores the role of environmental input on children's language acquisition and stresses that the language children acquire and produce is linked to the input they receive from their surroundings.

Moreover, a noteworthy observation was Sama's adoption of an American accent, which was influenced by the cartoons she watched. The evidence linking Sama's accent to the cartoons she watched is that the cartoons offered consistent examples of native American pronunciation. In contrast, Sama's mother, the only other source of English in Sama's environment, did not possess an American accent and spoke English inconsistently with her. This indicates that the media input was the main reason for Sama's American accent development. This finding further supports the behaviourist perspective [3] and their emphasis on the significant role of environmental exposure. In this case, Sama's consistent exposure to English through cartoons, which all featured an American accent, resulted in her speaking English with an American accent.

Moreover, Sama's acquisition of an American accent echoes the research findings of Alghonaim [11], Poštič [12], Trota et al. [14], and Tobias [19], who reported that children who frequently watch English cartoons tend to adopt the accents presented in those cartoons. Just like Sama, the children in the studies by Alghonaim [11], Poštič [12], and Trota et al. [14] acquired English in non-English-speaking environments. This indicates that children's acquisition of native English accents in these studies was primarily tied to the received media input. In line with these findings, Tobias [19] stressed that children's pronunciation is strongly affected by the phonetic input they receive in their daily environment. Further, Tobias [19] emphasized that if children receive

constant English input with a non-native accent, whether from their teacher or other people around them, they are likely to adopt similar pronunciation patterns in their own spoken English. These observations indicate that the accent children adopt is influenced by the type and amount of input they receive in that accent.

Furthermore, the analysis of Sama's progress in the subsequent stages across all five areas revealed two important findings. First, Sama's English language growth followed similar developmental stages observed in children acquiring their first language [2-4], such as acquiring concrete before abstract terms, progressing from the one-word stage to the two-word stage, and advancing to more complex sentences. Also, Sama acquired easier sounds before more complex ones, and so on. This finding aligns with the nativist perspective, which maintains that all children acquire language following similar phases [3].

Second, as Sama advanced through stages, it seemed that she was experimenting with the language she learned, producing utterances that could not have been based on imitation. This was observed through the errors she made, which could not have been learned from television or her mother. Notable examples of these errors include using grammatical rules where they do not apply, such as using the "-ed" past tense marker with irregular verbs. This observation indicates that Sama was building and extending her own understanding of English grammar, using information from the cartoons and her mother's input, who consistently used the "-ed" marker for regular verbs. This outcome is supported by Chomsky's nativist perspective [3], which postulates that children have an inborn ability to acquire language and construct their own grammar by making their own conclusions and generalizations.

Another important factor to consider in discussing the results of Sama's case study is the role of interaction with her mother. Sama's interaction with her mother did not start from the beginning of the study but took place as Sama started addressing her mother in English. Specifically, whenever Sama spoke English, her mother responded in English; when Sama used Arabic, her mother replied in Arabic. The role of this interaction cannot be overlooked in this study. It can be assumed that Sama's communication with her mother has played a significant role in reinforcing

and accelerating her language development, specifically in the area of understanding and responding.

That is to say, although Sama's exposure to interactive cartoons (i.e., Barney and Friends, Mickey Mouse Clubhouse, and Dora the Explorer) facilitated her comprehension and response skills by requiring her to engage actively, these programs offered limited and repetitive language. On the other hand, Sama's interactions with her mother were dynamic, varied, and took place in a live, reciprocal context. Therefore, it can be concluded that Sama's development in this domain (i.e., understanding and responding) was more significantly influenced by her interactions with her mother than by watching TV. This observation supports the interactionist perspectives [3] that emphasize the importance of conversational interactions with the environment on language development alongside other contributing factors.

Additionally, the impact of the role played by Sama's mother in this study can be discussed in light of Vygotsky's social constructivist theory, particularly his emphasis on the role of Scaffolding in the learning process. Scaffolding refers to the assistance given to a child by a more knowledgeable person (e.g., mother) to learn things and tackle tasks that are beyond the child's current capabilities (i.e., the Zone of Proximal Development) [20]. Vygotsky maintained that with appropriate scaffolding/support, the child acquires skills and knowledge that enable them to accomplish similar tasks independently in the future [20]. It is safe to assume that the findings of this study correspond with Vygotsky's views. Particularly, Sama's mother's responsive behavior (e.g., addressing Sama in English when Sama speaks it) indicates that Sama received scaffolding when she needed it. This response from Sama's mother undoubtedly helped Sama in all areas of her language development, including meaning-negotiating, vocabulary use, and so on. That is to say, Sama's mother was competent in English, which represented an accurate language model for Sama to follow and to enhance and consolidate her language development.

Therefore, the overall discussion of the results suggests that language development in children can be ascribed to multiple factors (i.e., environmental input, innate ability, environmental interaction, and environmental scaffolding) that function in harmony,

each playing a role in fostering adequate language proficiency. In the case of Sama, each of these factors contributed to her overall development of a satisfactory level of English language proficiency.

The findings from Sama's case study align with the findings of Linebarger and Walker [7], Alghonaim [11], Poštič [12], Tamba [13], Trota et al. [14], and Tobias [19] that exposure to appropriate and purposefully selected educational cartoons can result in adequate language competence among children. The findings also resonate with Krashen's [5] assertion that learning under relaxing and enjoyable circumstances (such as watching cartoons) can result in natural, effortless, and improved language learning outcomes. Furthermore, the findings of this research are consistent with the study by Barr and Wyss (10), which emphasizes that conversational exchanges with the environment are essential, alongside other elements, in fostering language development in children.

Moreover, a significant discovery from this study was that the conditions provided for Sama in this case study (i.e., watching English cartoons, and interacting with her mother in English) resulted in her becoming bilingual at the age of five years old. That is to say that Sama exhibited adequate competence in both Arabic and English simultaneously. This discovery aligns with the assertions made by Krashen [5] and Savile-Troike [6] that children can acquire two languages if they are sufficiently exposed to them at an early age and at the same time.

This study adds to the literature by examining the impact of watching English cartoons on children's English language development in the Libyan context. The insights derived from this study can be used to contribute to learning and teaching English in Libya, both in home settings and in schools.

In the home environment, parents can facilitate their children's acquisition of the English language besides their Arabic language by exposing them to carefully selected educational English cartoons from an early age. In this respect, parents are advised to wisely consider the type of cartoons, ensuring their cultural themes are age-appropriate and Libyan culture-appropriate, and that they contain no violent content. This step is crucial to ensure that the cartoons do not negatively impact their children. In addition, it is recommended that parents co-view with their

children to check the content appropriateness and to engage with children in discussions related to what they view. This interaction is important for enhancing and reinforcing language development, and to avoid the child being completely immersed in the screen rather than engaged with their environment. Finally, it is important to set limits for screen time to prevent the disadvantages of excessive screen watching on children, such as harming their eyesight. It is worth noting that the same recommendation applies to older English language learners, who can seek various language learning benefits from watching English language programs.

In English language learning classrooms, whether targeting children or older learners, teachers are strongly advised to integrate purposeful English cartoons or entertaining programs/movies into their lessons. This integration can offer various advantages. To begin with, exposing students to amusing content can increase their engagement and motivation for learning [5]. Additionally, these programs can provide meaningful input for learning various aspects of the English language, such as correct pronunciation, varied contextualized vocabulary, accurate sentence structures, and so on [11], [12], [13], [14], and [19]. Respectively, teachers are advised to carefully plan their lessons to increase the benefit of this integration. The lessons should include pre-viewing activities that activate students' prior knowledge about the content and prepare them for viewing it. Also, lessons should involve follow-up interactive activities that highlight the language used, discuss, and reflect the content. These steps can elevate the benefits of incorporating English TV viewing in English language learning classrooms.

Despite offering insightful information, the study has limitations, such as a limited sample size that prevents the generalization of the results. Future research with bigger sample sizes could help validate and extend the findings of this study. Moreover, it is crucial to remember that in this study, watching cartoons has only been linked to improving oral language skills in early childhood. Respectively, it is recommended that future research address how to develop children's reading and writing skills through similar approaches. For example, future researchers can pair cartoon viewing with the same-language subtitles and investigate the impact on children's word recognition, decoding accuracy,

and reading fluency. Alternatively, future research can examine the impact of pairing cartoon segments with print-based storybooks on narrative comprehension and print awareness.

6.CONCLUSION

This case study examined the impact of watching English cartoons on a child's English language acquisition. Sama, the subject of this case study, was observed for three years, particularly from when she was two until she reached five years old. During this period, Sama was exposed to instructive and interactive English cartoons that were purposefully selected to help her develop English language competence. At the same time, Sama had the opportunity to interact occasionally in English with her mother. However, in her home, the linguistic environment remained Arabic, and she consistently communicated in Arabic with her other family members.

The case study results revealed that Sama acquired a good level of English language competence by the age of five, which was very similar to a five-year-old native speaker. Particularly, Sama demonstrated adequate English proficiency across five areas: vocabulary, grammar and sentence building, pronunciation, understanding and responding, and emotion-expressing. This achievement was mainly attributed to Sama's exposure to and engagement with English cartoons, Sama's innate abilities for language learning, her interactions with her mother, and the support she received from her mother.

The findings of this study highlight the complex nature of language development, which is influenced by several interrelated factors. It is affected by the input received from the surrounding environment. Additionally, it is guided by inherent abilities that are part of the biological nature of typical children. Moreover, the environmental input and inherent capabilities must be reinforced by active engagement and interaction with the environment to support and advance language development.

Furthermore, the provision of these factors can create a good opportunity for children to become simultaneous bilinguals, which refers to acquiring more than one native language at the same time. Language acquisition is most sensitive and effective during early childhood. Therefore, languages other than children's first can be easily acquired if children are exposed to them at an early age.

In the same respect, when exposure

to language takes place through amusing and appealing means, like cartoons, language develops more effectively and naturally. When this exposure involves two languages concurrently with a carefully considered approach, children can acquire a native-like proficiency in these languages. Sama's case study provides evidence for these observations, demonstrating that exposing children to wisely selected cartoons can significantly promote the acquisition of a second language, in addition to the first, particularly at the oral level (i.e., speaking and listening skills). The findings from Sama's case study highlight the need for further investigation into how media can complement and enrich language learning and teaching methods, both for children and older learners.

7.ACKNOWLEDGMENT

I would like to extend my sincere gratitude to T. Salah, holder of a Master's in Linguistics and Translation and CEO of Montessori House School, O. Kamal, tutor at the Libyan International Medical University, and A. Haroon, holder of a Master's in Applied Linguistics and staff member and researcher at the Faculty of Languages, Benghazi University. Their invaluable contributions in observing the case study, analysing the data, and interpreting the findings have significantly enhanced the credibility of this research. Their expertise and insightful perspectives have been instrumental in ensuring the precision of this study.

8.REFERENCES

1.Kuhl P. Early language acquisition: cracking the speech code. Nature Reviews Neuroscience. 2004;5(10):831-843.

2.Fernández EM, Cairns HS. Fundamentals of psycholinguistics. Chichester (UK): Wiley-Blackwell; 2011.

3.Hummel, K. Introducing Second Language Acquisition: Perspectives and Practices. 1st ed. Chichester (UK): Wiley-Blackwell; 2014.

4.Lightbown PM, Spada N. How languages are learned. 3rd ed. Oxford: Oxford University Press; 2006.

5.Krashen SD. Principles and practice in second language acquisition. Oxford: Pergamon Press; 1982.

6.Saville-Troike, M. Introducing Second Language Acquisition. 2nd ed. Cambridge: Cambridge University Press; 2012.

7.Linebarger D, Walker D. Infants' and toddlers' television viewing and language outcomes. Am Behav Sci. 2005;48(5):624-645.

Available from:
http://dx.doi.org/10.1177/0002764204271505

8.Zimmerman FJ, Christakis DA, Meltzoff AN. Associations between media viewing and language development in children under age 2 years. J Pediatr. 2007;151(4):364-368.

9.Rajulain M. The effect of television programs on children's foreign language acquisition. Diksi. 2019;27(1):49-55.

10.Barr R, Wyss N. Reenactment of televised content by 2-year-olds: Toddlers use language learned from television to solve a difficult imitation problem. Infant Behav Dev. 2008;31(4):696-703. Available from:
http://doi:10.1016/j.infbeh.2008.04.006

11.Alghonaim, A. The influence of watching cartoons in an EFL setting on a child's language acquisition in Saudi Arabia. Language Teaching Research Journal. 2020;21(4):88-100. Available from:
https://dx.doi.org/10.2139/ssrn.3581322

12.Poštić S. Influence of Cartoon Network on the Acquisition of American English During Childhood. Verbum. 2015;6:188-195.

13.Tamba S. The influence of cartoons on children's English language use and development in Kenema City, Sierra Leone. Int J Engl Lang Stud. 2022;4(3):87-94. Available from:
http://dx.doi.org/10.32996/ijels.2022.4.3.13

14.Trota MPB, Cabeltis CB, Cadiente NT, Ligan M, Asoy NMC, Bardaje ZL. The influence of watching English Cartoons on English language acquisition: A case of selected Filipino preschoolers. J Educ Lang Innov Appl Linguist. 2022;1(2):105-124. Available from:
https://doi.org/10.37058/jelita.v1i2.5249

15.Omar YZ, ed. Pedagogical issues in teaching and learning English as a foreign language in Libyan schools' various settings. Berlin: Democratic Arab Center for Strategic, Political & Economic Studies; 2020.

16.El Mezughi, K. Understanding Libyan teachers' intentions and classroom practices in teaching English as a foreign language [Doctoral dissertation]. University of Denver; 2021.

17.Elramli SM. Professional development for English language teachers in Libya: Beginning and ambition. Faculty of Languages Journal. 2023;2(28):134-152

18.Yin RK. Case Study Research: Design and Methods. 3rd ed. London, Thousand Oaks, CA: Sage Publications; 2003.

19.Tobias J. English Cartoon and Home Language on the Listening and Speaking Skills

of Pre-Schoolers. n.d. Available from: https://www.academia.edu/25109345/English_Cartoon_and_Home_Language_on_the_Listening_and_Speaking_Skills_of_Pre_Schoolers

20.Wilhelm, J., Baker, T., & Hackell, J. Strategic reading: Guiding students to lifelong literacy, 6-12. Portsmouth, NH: Boynton/Cook Publisher, Inc.; 2001.

Applied Science

Scientific Journal of University of Benghazi

SJUOB (2025) 38 (1) Applied Sciences: Ali, et la , 33 – 46
www.sjuob.uob.edu.ly

Quantification of Radiological Hazards Associated with Natural Radionuclides in Rock Samples from Al-Meshal Region, Libya

Asma M. Al-Abrdi[1], Jemila M. Ali[1]* and Mabrouka A. Abd-Ahamid[2]

1 Physics Department, Faculty of Science, Omar Al-Mukhtar University, El-Beida, Libya.
2 Physics Department, Faculty of Science, Derna University, Derna, Libya.

Received: 11 / 01 / 2025 | accepted: 05 / 02 / 2025 | Publishing: 29/06/2025

ABSTRACT

The specific activity concentrations of primordial radionuclides in eight1samples of rock collected from specific locations in Al-Meshal, Al-Gabal Al-Akhdar region, Libya, were measured using a1gamma-ray1spectrometer system with a sodium iodide detector. The results revealed that the specific activity1concentrations of 226Ra, 238U, and 232Th in the analyzed-1samples were higher than their respective established permissible levels. Conversely, the specific activity1concentrations of 40K in all rock samples were found1to be below the permissible limit. The assessment of the radiological1hazard parameters, including radium equivalent activity, internal and external hazard1indices, and representative level index, indicated values were mostly within recommended world limits. However, for two specific samples, RE1 and RW2, the representative level index and internal hazard index values were higher than the recommended world1value. Although the radiological investigation indicates no immediate acute health hazard to the area's population, there is a need to consider the long-term health effects related to low-level exposure to radiation.

KEYWORDS: Natural1radionucles, radiological hazards, representative1level index, Pearson's correlation coefficients.

Corresponding Author: Jemila M. Ali, Jemila.mussa@omu.edu.ly.

 ISSN: Online 2790-1637, Print 2790-1629
National Library of Libya, Legal number: 154/2018

1. INTRODUCTION

Human are continuously exposed to natural adionucides. The primary sources of exposure to naturally occurring radionuclides include terrestrial sources, such as the uranium and thorium decay series and potassium-40, as well as cosmic rays. Terrestrial background radiation, in particular, is influenced by the global distribution of radionuclides, local geological formations, geographical location, altitude, and regional geochemistry [1]. The advancement of the nuclear industry and other technologies involving radioactive isotopes has underscored the necessity of quantifying natural background radionuclide levels. This is crucial for discerning anthropogenic contamination, thereby enabling effective measures for population and environmental protection [2]. Human exposure to radionuclides occurs from external and internal exposure through both direct and indirect pathways. External exposure is caused by direct gamma radiation, whereas internal exposure results from inhalation of radioactive radon gas (radon-222) and its short-lived decay products [3]. Radon, a daughter element resulting from the decay chain of uranium, has the strongest effect on humans, as it poses a significant threat of lung cancer to individuals with prolonged exposure to it [4]. Recognizing the potential health implications, and understanding radiation levels within living and occupational environments is paramount [5]. Therefore, many researchers worldwide are quite interested in measurements of natural radioactivity in rock. To evaluate the terrestrial gamma dose rate for outdoor, it is very important to estimate the natural radioactivity level in rock. From the review of the literature, it is observed that though the data on the content of radioactive elements is available for some regions in Libya, there is no data available for the Al-Meshal region in Libya. Detailed investigations of natural radioactivity have been carried out for the first time [6]. This study presents the activity concentration levels and associated radiological hazard parameters in rock samples collected from Al-Meshal, Libya. In the context of Libya, several studies have investigated natural background radiation levels. Rock samples in the Gondola region reported similar dominant contributions from the uranium and thorium decay series [7]. Furthermore, investigations in the eastern region of Libya on rock samples around El-Beida City high-

 ISSN: Online 2790-1637, Print 2790-1629
National Library of Libya, Legal number: 154/2018

lighted the influence of local geology on the distribution of natural radionuclides, a factor also considered pertinent to the Al-Meshal area [8]. While specific data on rock samples from Al-Meshal might be limited, the general understanding of radionuclide distribution in Libya suggests that the levels are influenced by the country's diverse geological formations, similar to global trends. This research on Al-Meshal contributes to the growing body of knowledge on natural radioactivity in Libya.

2. MATERIALS AND METHODS

2.1. Study Area

Al-Meshal is a rural agricultural region situated in northeastern Libya, geographically located at coordinates 32° 28' 46.7" N, 21° 40' 42.2" E. The area is characterized by fertile soil, conducive to both agriculture and livestock husbandry.

The primary economic activity in this region is livestock rearing, which significantly contributes to local agricultural output. Consequently, understanding the environmental characteristics of this area, including its soil, rocks, and vegetation (grasses), is of considerable importance. Figure (1) illustrates the geographical location of the study area, as visualized using Google Earth and GPS data.

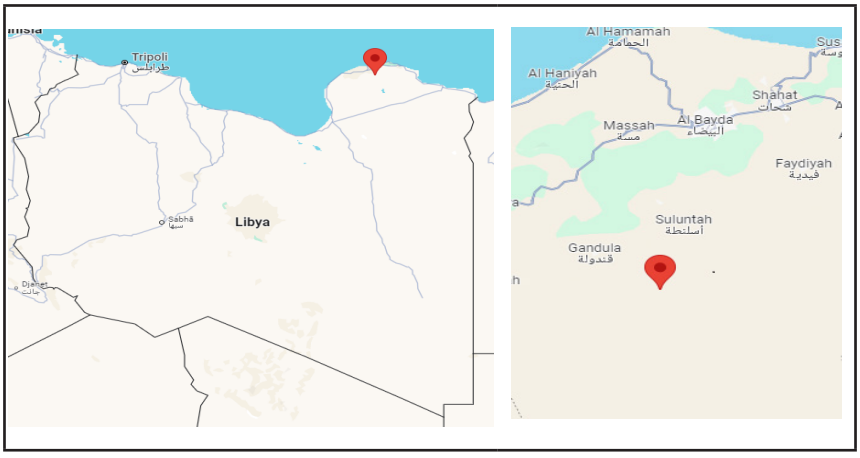

Figure.(1). Study region and locations of rock sample sites.

2.2. Sample Collection and Preparation

The Al-Meshal area contains fourteen former weapons storage facilities. In this study, one of these facilities was selected as the sampling site. Eight rock samples were collected from this site, specifically from the four cardinal directions (east, west, north, and south) at distances of one kilometer and two kilometers. This sampling strategy was consistently applied in each direction. The unique identifiers (codes) assigned to each rock sample are detailed in Table (1).

Table (1). The code of the investigation samples.

.Sample No	Description
RE1	(Rocks from the first kilometer (East
RE2	(Rocks from the second kilometer (East
RN1	(Rocks from the first kilometer (North
RN2	(Rocks from the second kilometer (North
RS1	(Rocks from the first kilometer (South
RS2	(Rocks from the second kilometer (South
RW1	(Rocks from the first kilometer (West
RW2	(Rocks from the second kilometer (West

Sample preparation was conducted at the Advanced Nuclear Physics Laboratory, Omar Al-Mukhtar University, Libya. The collected samples were pulverized into fine powder. The rock samples were sieved using a 250 µm sieve aperture to ensure maximum homogeneity and to mitigate potential underestimation of radionuclide concentrations in bulk samples. Subsequently, the powdered samples were dried in a laboratory oven at approximately 120 °C for 2 hours to eliminate any residual moisture. Following the drying process, the samples were precisely weighed and transferred into polyethylene containers with a standardized volume of 250 cm^3. All prepared samples were then hermetically sealed and stored for a minimum period of 30 days to allow for the establishment of secular radioactive equilibrium between the ^{238}U and ^{232}Th decay series and their respective short-lived daughter radionuclides prior to gamma-ray spectroscopic analysis.

 ISSN: Online 2790-1637, Print 2790-1629
National Library of Libya, Legal number: 154/2018

2.3. Gamma Spectroscopy1Analysis

The concentrations of naturally occurring radionuclides in the collected samples were determined using gamma-ray-spectroscopy with a sodium iodide thallium-doped NaI(Tl) detector with a "1.5×1.5" crystal, model No. PM-9266B, serial No. WA00012638. The detector was encased within a lead shield of sufficient thickness to minimize background radiation contributions from cosmic rays and ambient laboratory sources. Gamma spectra acquisition and subsequent analysis were performed utilizing the Cassy Lab software system. The activity concentrations of the ^{238}U and ^{232}Th decay series were determined indirectly by quantifying the gamma emissions of specific short-lived daughter radionuclides, assuming secular equilibrium within the respective decay chains. Specifically, ^{238}U was quantified through the photopeaks of ^{214}Pb (at 295 and 352 keV) and ^{214}Bi (at 609, 768.2, 1120, 1378, and 1768 keV). Similarly, ^{232}Th was quantified using the photopeaks of ^{228}Ac (at 92, 209, 338, and 911 keV), ^{212}Bi (at 727 keV), and ^{208}Tl (at 583 keV). The activity levels of ^{40}K and ^{226}Ra were directly measured at their energies of 1460 keV and 186.2 keV [9]. For each sample, the gamma-ray spectrum was acquired over a counting time of 7200 seconds to ensure adequate statistical precision.

2.4. Measurement of Activity Concentration

The specific activity of a radionuclide is defined as the rate of its nuclear disintegration. It can be specified with the aid of equation [10]:

$$C = \frac{(CPS)}{I_\gamma \xi . M} \quad ---- \ (1)$$

Where:

C: represents the activity concentration of the radionuclide corresponding to the gamma-ray photopeak energy, expressed in (Bq/kg).

Cps: denotes the net count rate detected at the specific gamma-ray photopeak energy, measured in counts per second.

ξ: signifies the counting system efficiency at the specific gamma-ray photopeak energy, which is dimensionless.

M: is the mass of the measured sample, expressed in (kg).

I_γ: is the probability of the absolute gamma-ray emission for the radionuclide of in-

 ISSN: Online 2790-1637, Print 2790-1629
National Library of Libya, Legal number: 154/2018

$$Ra_{eq} = C_{Ra} + 1.34\,C_{Th} + 0.077\,C_K \quad -------(2)$$

terest, which is dimensionless.

3. RADIOLOGICAL HAZARDS

3.1. Radium Equivalent

A common radiological index used to represent the gamma radiation dose rate arising from various combinations of ^{226}Ra, ^{232}Th, and ^{40}K present in a sample indicates the radium equivalent activity, Raeq. It is calculated using the following relationship[11]:

$$H_{ex} = \frac{A_{Ra}}{370} + \frac{A_{Th}}{259} + \frac{A_K}{4810} \leq 1 \quad --------(3)$$

Where C_{Ra}, C_{Th} and C_K are the activity concentrations (Bq/kg) for ^{226}Ra,^{232}Th and ^{40}K, respectively. The maximum value of Ra_{eq} must be less than 370 Bq/kg[12].

3.2. External Hazard Index

The radiological parameter used to assess the external gamma radiation exposure risk arising from the activity concentrations of ^{226}Ra, ^{232}Th, and ^{40}K in a material is the external hazard index (H_{ex}). It is computed using the following relationship[13]:

3.3. Internal Hazard Index

Exposure to ^{222}Rn and its short-lived decay progeny presents several health risks. The alpha-emitting radionuclides, specifically radon (^{222}Rn), thoron ($^{22°}$Rn), and their respective decay products present in ambient air are the primary contributors to the radiation-induced health hazards experienced by populations exposed to environmental radioactivity. The internal hazard index (H_{in}) is calculated using the following equation [14]:

$$H_{in} = \frac{C_{Ra}}{185} + \frac{C_{Th}}{259} + \frac{C_K}{4810} \leq 1 \quad -------(4)$$

3.4. Representative Level Index

The representative level index (RLI) is a dimensionless radiological parameter that quantifies the gamma radiation dose rate arising from the specific activity concen-

trations of primordial radionuclides 226Ra,

$$\mathbf{RLI} = \frac{C_{Ra}}{300} + \frac{C_{Th}}{200} + \frac{C_k}{3000} \leq 1 \quad ---- \quad (5)$$

232Th, and 40K present within a material. This index is very important for the quality control of regulating annual effective doses to the population and monitoring overall radiation exposure to the human body. Its primary purpose is to ensure that internationally established acceptable dose limits are not exceeded. The RLI is calculated using the following equation [15]:

4.RESULTS AND DISCUSSION

The activity concentration values for rock samples varied from (72.03±0.13) to (117.93 ± 0.13) Bq/kg, (78.91 ± 5.84) to (120.52 ± 5.18)] Bq/kg, (71.10 ± 4.85) to (112.81 ± 6.21) Bq/kg and (301.95 ± 14.39) to (465.27 ± 17.87) Bq/kg for- ^{226}Ra, ^{238}U, ^{232}Th and ^{40}K respectively, with an average (84.92, 91.17, 84.31 and 388.30) Bq/kg respectively, for radionuclides ^{226}Ra, ^{238}U,^{232}Th and ^{40}K, as shown in Table (2).

Table (2). Activity concentrations of natural radionuclides for rock.

Sample No.	^{226}Ra	^{238}U	^{232}Th	^{40}K
RE1	117.93 ±0.13	120.52 ±5.18	102.60 ±6.11	465.27 ±17.87
RE2	73.44 ±0.13	87.98 ±6.63	71.10 ±4.85	428.22 ±17.14
RN1	73.44 ±0.13	82.93 ±6.59	78.78 ±4.77	458.41 ±17.74
RN2	72.03 ±0.13	79.18 ±5.86	76.76 ±4.40	303.32 ±14.43
RS1	77.68 ±0.13	79.03 ±5.53	74.79 ±5.31	409.00 ±16.75
RS2	76.97 ±0.13	78.91 ±5.84	72.73 ±4.74	301.95 ±14.39
RW1	106.63 ±0.13	114.8 ±85.35	112.81 ±6.21	430.09 ±13.15
RW2	81.21 ±0.13	86.00 ±6.03	84.92 ±5.35	310.18 ±14.59
Average	84.92	91.17	84.31	388.30
P. L	50	50	50	500

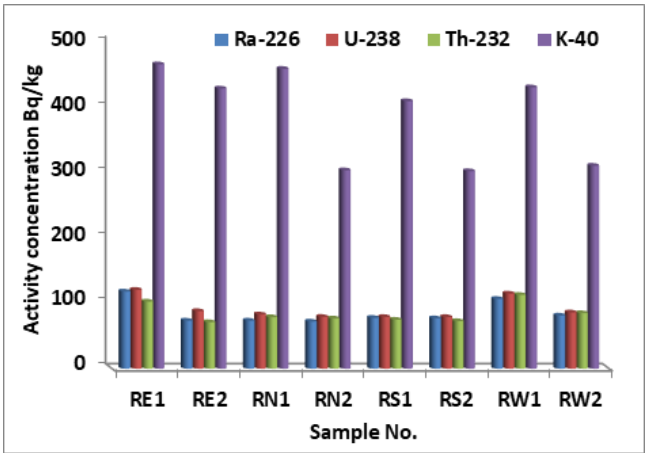

Figure.(2): Specific activity (Bq/kg) concentration of radionuclides for rock Samples.

The specific activity concentrations of all rock samples were higher than the permissible level for ^{226}Ra, ^{238}U, and ^{232}Th (50, 50 and 50 Bq/kg) [16]. However, the activity concentration of ^{40}K was lower-than the permissible level (500 Bq/kg) [16].

Radium equivalent activity (Ra_{eq}), internal hazard index (H_{in}), external hazard index (H_{ex}), and representative level index (RLI) were determined based on the specific activity concentrations of ^{226}Ra, ^{232}Th, and ^{40}K; the results are presented in Table (3).

Table (3). The radium equivalent, hazards indices and representative level index of rock samples.

Sample No.	$Ra_{eq\ (Bq/kg)}$	H_{in}	H_{ex}	RLI
RE1	300.47	1.13	0.81	1.06
RE2	208.09	0.76	0.56	0.74
RN1	221.09	0.79	0.59	0.79
RN2	205.14	0.75	0.55	0.72
RS1	216.13	0.79	0.58	0.77
RS2	204.21	0.76	0.55	0.72
RW1	301.12	1.10	0.81	1.06
RW2	226.53	0.83	0.61	0.80
Average	235.35	0.85	0.64	0.83
P. L	370	1	1	1

Statistical analysis revealed that Ra_{eq} values ranged from 204.21 to 300.47 Bq/ kg, with an average value of 235.35 Bq/ kg. For all inspected rock samples, Ra_{eq} values are lower than the assigned international allowed limit of 370 Bq/ kg [16]. The H_{in} varied between a minimum of 0.75 and a maximum of 1.13, with an average value of 0.85, which is below the established recommended value [16]. The values of H_{in} ranged between 0.51 to 0.81, with a mean of 0.64. The obtained values of H_{in} for most rock samples are less than unity [15]. The representative level index (RLI) values were found to be lower than the permissible limit of 1 for most samples [16], spanning from 0.72 to 1.06, with a mean of 0.83. Although samples RE1 and RW1 exhibited elevated radiological hazard indices, overall, all samples fell within the acceptable ranges for radiological hazard limits, consistent with established global values [16].

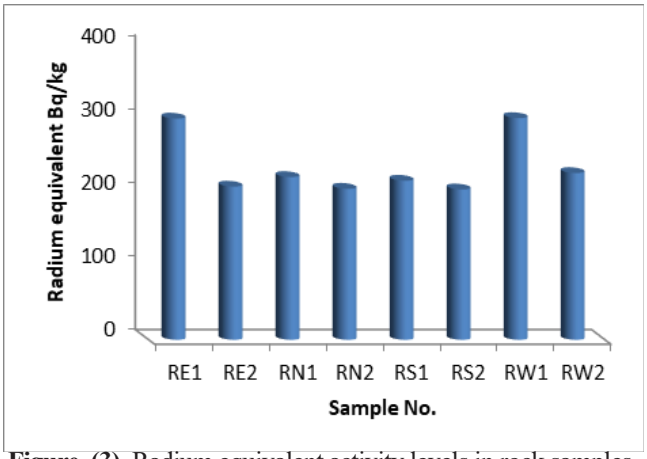

Figure. (3). Radium equivalent activity levels in rock samples.

The results showed that all1values of H_{ex} and RLI were lower than1unity. All values of internal hazard for the1studied1rock1samples are lower than unity, with the exception of RE1 and RW1, which were higher than the recommended value [1], as shown in Figure. (4).

 ISSN: Online 2790-1637, Print 2790-1629
National Library of Libya, Legal number: 154/2018

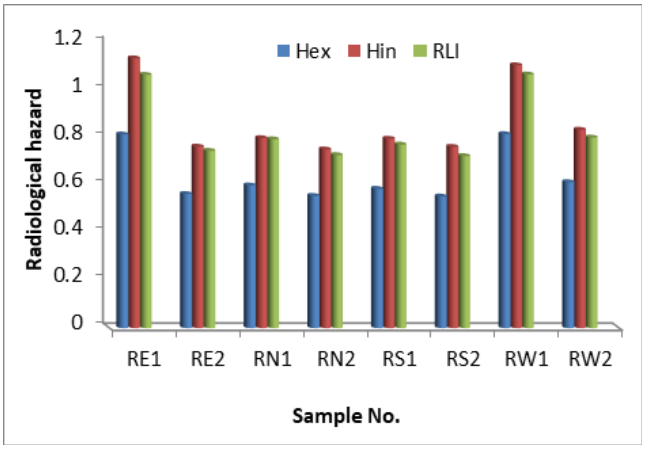

Figure. (4). A comparison between internal, external gamma Indices and the representative level index.

4.1.Pearson's Correlation Coefficients Analysis of Radioactive Variables

Pearson correlation coefficient analysis was employed to determine the pairwise mutual relationships and the strength of linear association between the studied parameters, utilizing bivariate statistics. The results of the Pearson correlation coefficients between all measured radionuclides and radiological parameters for the rock samples are presented in Table 4. A strong positive correlation coefficient was observed between ^{232}Th and ^{238}U, which is attributable to the thorium and uranium decay series in natural geological formations [17]. A moderate positive correlation coefficient was noted between ^{40}K and both ^{238}U and ^{232}Th. This is expected, as ^{40}K originates from a distinct decay scheme. Furthermore, radium equivalent activity (Ra_{eq}), the external hazard index (H_{ex}), the internal hazard index (H_{in}), and the representative level index (RLI) exhibited strong positive correlation coefficients with ^{238}U and ^{232}Th, and moderate positive correlation with ^{40}K.

Table (4). Pearson correlation matrix among the radionuclides and radiological parameters.

	^{226}Ra	^{238}U	^{232}Th	^{40}K	Ra_{eq}	H_{ex}	H_{in}	*RLI*
^{226}Ra	1							
^{238}U	0.97	1						
^{232}Th	0.91	0.92	1					
^{40}K	0.47	0.57	0.40	1				
Ra_{eq}	0.97	0.97	0.97	0.55	1			
H_{ex}	0.97	0.97	0.97	0.55	0.99	1		
H_{in}	0.98	0.98	0.96	0.53	0.99	0.991	1	
RLI	0.97	0.97	0.97	0.57	0.99	0.99	0.99	1

4.2. The Clark Values

The Clark values for the rock samples and the elemental concentrations (in ppm) of the studied radionuclides at each sampling location are presented in Table (5). The majority of the analyzed locations exhibit a Th/U ratio follows aligns along a linear trend with an average value of 2.83, which is lower than the reported recommended Th/U ratio of 3.5 [18]. The findings of the present study suggest a relatively low thorium content in the rock samples investigated from the Al Meshal region.

Table (5). Clark values and radionuclides ppm contents.

Sample No.	RE1	RE2	RN1	RN2	RS1	RS2	RW1	RW2
^{238}U ppm	9.72	7.09	6.69	6.38	6.37	6.37	9.26	9.93
^{232}Th ppm	25.27	17.51	19.40	18.91	18.42	17.91	27.79	20.92
^{40}K %	1.49	1.37	1.46	0.97	1.31	0.96	1.37	0.99
Clark Values	2.60	2.47	2.90	2.96	2.89	2.81	3.00	3.02

5.CONCLUSION

The natural radioactivity levels in rock samples collected from various locations in Al-Meshal, Al-Gabal Al-Akhder, Libya, were evaluated using gamma-ray spectrometry. The average activity concentrations of ^{226}Ra, ^{232}Th, and ^{238}U were higher than the world-recommended values identified by UNSCEAR [16]. The average values of radium equivalent activity (Ra_{eq}) of the analyzed rock samples were lower than the recommended value of 370 Bq/kg, according to UNSCEAR [16]. The external hazard index (H_{ex}), internal hazard index (H_{in}), and representative level index (RLI) values were generally lower than the recommended maximum values set by UNSCEAR [16], except for the H_{in} and RLI values for two specific samples RE1 and RW1, which were lower than unity. Based on these findings, it is recommended that a periodic assessment of the activity concentrations of natural radionuclides and associated radiological hazards in the Al-Meshal study area be implemented. This proactive monitoring is essential to ensure that radiation exposure levels are maintained, thereby safeguarding public health and the environment in this region of Libya.

6. REFERENCES

1.Abdelfettah B., & A. Tedjani, A. Natural Radioactivity Measurements for Some Algerian Building Materials. Journal of Physical Science and Application ***2012***; 2(6), 271-274.

2.MAM U., AMA M., Elsaman R., & El-Sayed M. Natural radioactivity levels and radiological hazards indices of chemical fertilizers commonly used in Upper Egypt. Journal of Radiation Research and Applied Sciences ***2014***; 7(4), 430-437. http://dx.doi.org/10.1016/j.jrras.2014.07.006

3.Imani M., Adelikhah M., Shahrokhi A. Azimpour G., Yadollahi A., Kocsis E., Toth-Bodrogi E, Kovács T. Natural radioactivity and radiological risks of common building materials used in Semnan Province dwellings, Iran. *Environmental Science and Pollution Research* ***2021***; 28:41492–41503. https://doi.org/10.1007/s11356-021-13469-6

4.Eyakifama H., Benjamin Z., Mikesokpo D. M., Manakrihèa H. E., Cebastien Joel G. S., Maurice N. M., Tchakpele Paalamwé Komi T. P. Transfer from Soil to Grass and Statistical Analysis of Naturally Occurring Radionuclides in Soil from Phosphate Mining and Processing Sites in Maritime Region of Togo.

Environmental Earth Sciences 2021 Sep. https://doi.org/10.21203/rs.3.rs-160904/v1

5.Ejike O. M, Wando J. R., Juliet O. I., Maduabuchi O. C, John I. A., Uchenna M. M. Assessment of radiation dose level in farm soils of mission quarters, Wukari, Taraba State, Nigeria. *International Research Journal of Advanced Science* ***2020*** Oct; 1(2):10–15. https://orcid.org/0000-0002-4136-4754

6.Ahmad, N., Jaafar, M. S., Bakhash, M., & Rahim, M. (2015). An overview on measurements of natural radioactivity in Malaysia. Journal of radiation research and applied sciences ***2015***; 8(1), 136-141. https://doi.org/10.1016/j.jrras.2014.12.008

7.Al-Abrdi A. M. Measurements of natural radioactivity and evaluation of radiation hazard indices in Barley Samples in Libyan Markets, *Libyan Journal of Basic Sciences* ***2023***; 20 (2), 51–64.

8.Elmzainy A. S. A., Ali J. M. Ali, Basil S. S. Concentration of Naturally Radioactive Elements in Rocks and Its Radiological Risk around El-Beida City, Libya. Special Issue for 5th International Conference for Basic Sciences and Their Applications ***2022***;19(2): 102- 112.

9.Ali J. M. Ali, Hasan H. M. and Al-Majbari A. A. Estimate the types and the natural radioactivity element contents and the radiological hazard values of some sediment samples at Benghazi coast–Libya. *Journal of Chemical, Biological and Physical Sciences* **2018**. 8(3): 291-295. https://doi:10.24214/jcbps.C.8.3.29195.

10.Legasu M. L., A.K. Chaubey A. K. Determination of dose derived from building materials and radiological health-related effects from the indoor environment of Dessie city, Wollo, Ethiopia. *Helyon* ***2022***; 8:1-9. https://doi. org/ 10.1016/j.heliyon.2022.e09066.

11.Sroor A. T., Walley EL-Dine N., EL-Bahi S. M., Hasan H. M., Ali J. M. 2018. Determination of Radionuclide's Levels and Absorbed Dose for Soil, Rock, Plant and Water in Gondola – Libya. *IOSR Journal of Applied Physics* ***2018***; 10, I :40-49. https://doi: 10.9790/4861-1004014049

12.Al-Ghamdi A. H. Health risk assessment of natural background radiation in the soil of Eastern Province, Saudi Arabia. *Journal of Radiation Research And Applied Sciences* ***2019****;* 12(1), 219–225. https://doi.org/10.1080/16878507.2019.1637045

13.Khalid Abdullah Muhammad Ali K. A. M., Najam L. A., Mohammed F. M. Measurement of Natural Radioactivity in Samples of Fertilized and non-Fertilized Soils in Different Areas of Tikrit, Iraq. *J. Rad. Nucl. Appl.**2021***; 6, (2):109-114.
https://doi:10.18576/jrna/060203

14.Khan I.U., Qin Z., Xie T., Bin Z., Li H., Sun W., Lewis E. Evaluation of health hazards from radionuclides in soil and rocks of North Waziristan, Pakistan. Revised. *Int. J. Radiat. Res., April 2020*; 18(2): 243-253.
https://doi:10.18869/acadpub.ijrr.18.2.243.

15.Agbalagba E, Onoja R. Evaluation of natural radioactivity in soil, sediment and water samples of Niger Delta (Biseni) flood plain lakes, *Nigeria. J Environ Radioact **2011***;102:667-71.
https://doi: 10.1016/j.jenvrad.2011.03.002

16.UNSCEAR, United Nations Scientific Committee on the Effects of Atomic Radiation. "Sources and Effects of Ionizing Radiation", UNSCEAR 2008 Report Vol.1 to the General Assembly, with scientific annexes, United Nations Sales Publication, United Nations, New York (2010).

17.Putra, D., Prihatiningsih, W., Makmur, M., Yahya, M., Priasetyono, Y. Distribution Of Some. 2021. Natural And Anthropogenic Radionuclides In The Sediments And Seawater Along The Coastal Areas Of North Sulawesi. Iop Conference Series: *Earth And Environmental Science **2021***;1-10.
https://doi:10.1088/1755-1315/890/1/012005

18.Mandakini M, Narayani K., Sengupta D. Spatial distribution of gamma radiation levels in surface soils from Jaduguda uranium mineralization zone, Jharkhand, India, using gamma ray spectrometry and determination of outdoor dose to the population. *J Med Phys **2010***;35(4):235-241.
https://doi:10.4103/0971-6203.71762

Scientific Journal of University of Benghazi

SJUOB (2025) 38 (1) Applied Sciences: Abdulsamad, et la , 47 – 61
www.sjuob.uob.edu.ly

Effect of Helium Neon Laser Irradiation on Magnesium Levels in Blood "An Experimental Study"

Bassma Auhida Ali Abdulsamad [1],*, Fatima Abdel Salam Al sagheer [1]

1. Faculty of Education, Sirte University, Sirte, Libya.

Received: 28 / 01 / 2025 | Accepted: 18 / 04 / 2025 | Publishing: 29/06/2025

ABSTRACT

This study investigates the effect of Helium-Neon laser radiation on magnesium levels in blood, a vital element involved in numerous physiological and biochemical processes in the body. The Helium-Neon laser used in this study had a power output of 5 mW and a wavelength of 632.8 nm, known for its stability and low thermal effect. The spot size was approximately 0.03 cm^2, ensuring uniform exposure of the samples. The energy density delivered to the samples was calculated at 1.0 J/cm^2, providing an adequate level of irradiation without significant thermal damage. Twenty healthy, non-smoking volunteers aged between 19 and 65 participated in the study. Blood samples were collected in Red Top Tube (RTT) tubes and immediately centrifuged to separate the serum. Centrifugation was performed at 3000 RPM for 3-5 minutes at 25 °C. The separated serum was then divided into four equal portions. The first, the control, had its magnesium level measured using a biochemical analyzer (BS-230), and the mean was 1.84 mg/dL, within the normal range. The remaining three aliquots were exposed to the Helium-Neon laser for 1, 3, and 5 minutes, respectively. Results showed a 60% increase in magnesium in the immediate response, 25% with a decrease, and 15% with no noticeable change. Females showed a greater average magnesium increase (30%) with a more sustained response and greater consistency over time compared to males. Males exhibited more pronounced oscillations, a tendency for initial reductions, and faster returns to baseline. At the 1-minute mark, no significant difference was found between males and females ($p > 0.05$). However, at 3 and 5 minutes, the difference became statistically significant ($p < 0.05$), with females showing a higher increase in magnesium levels than males. The precise mechanism underlying these in vitro effects on serum remains unclear. However, it is hypothesized that Helium-Neon laser irradiation might induce subtle conformational changes in serum proteins (e.g., albumin), potentially altering their magnesium-binding affinity and thereby influencing measured levels within the serum milieu. These findings suggest complex, non-thermal interactions between Helium-Neon laser light and serum components in vitro, warranting further research to elucidate the specific biomolecular interactions

Kay words: Helium-Neon Laser, Magnesium Levels, Laser Irradiation, samples.

Corresponding Author: Bassma Auhida Ali Abdulsamad, basma-81@su.edu.ly

 ISSN: Online 2790-1637, Print 2790-1629
National Library of Libya, Legal number: 154/2018

1.INTRODUCTION

A significant portion of the population is estimated to be magnesium deficient, a crucial mineral impacting functions from muscle contraction to mood.[1],[2]. Magnesium is an essential driver of vital processes; its role in muscle contraction and nerve transmission[3] means low levels cause serious health problems. A balanced diet should provide enough Mg2+, but intake is decreasing due to processed food consumption, which is lower in magnesium than unrefined foods.[4,5]. Hypomagnesemia manifests in various ways, affecting the neuromuscular system (fatigue, weakness), cardiovascular system (hypertension), and metabolism (insulin resistance) [6]. While diet and lifestyle are known factors, questions arise about less obvious external influences. Among these, radiation exposure, especially from certain medical and research lasers, is of particular interest.[7,8].

The Helium-Neon (He-Ne) laser is a device that produces a stable beam of light with unique properties, such as monochromaticity (single wavelength), coherence (wavelengths in phase), and directionality (small variations) [9] . These properties distinguish lasers from traditional light sources [10]. A laser consists of an active medium, a pump source, and an optical cavity [11]. The red helium-neon laser, emitting at a wavelength of 632.8 nm, is known for its stability and low power consumption [10]. This laser has been used in medicine and science to study its effects on wound healing, pain relief, and tissue regeneration. Research has also been conducted on its therapeutic potential in areas such as vascular disease [12]. Due to its low thermal efficiency, the helium-neon laser has been used to study blood structure, and studies have shown its potential to affect blood oxygenation and immune function.

In the absence of prior research specifically addressing the effect of Helium-Neon lasers on magnesium concentrations in blood, this review will examine studies that explore the broader effects of helium-neon lasers on blood components and related biological processes. This approach aims to provide a contextual framework for understanding the potential influence on magnesium levels.Csele (2004) demonstrated the early impacts of low-power laser treatment on in vitro blood samples, noting changes in both absorption and FTIR spectra, indicating the laser's effect on the chemical properties of

blood[13]. Ghadage et al. (2015) later corroborated these findings, reporting similar changes in the blood's chemical makeup due to low-power laser therapy [14].In a related study, de Oliveira et al. (2021) observed significant changes in the numbers of red and white blood cells, offering valuable insights into the effects of low-level laser therapy on blood cells in a rat model [15] "Anju et al. (2019) found that low-level laser therapy significantly increased magnesium and vitamin D levels in DPN patients, along with improved nerve function and reduced pain indicators [16]

Regarding the physical properties of blood, Nazal (2016) provided evidence of the helium-neon laser's effect on the erythrocyte sedimentation rate (ESR) [17], a line of investigation later expanded by Falih and Msayer (2023) and Alnayli et al. (2017) through their analysis of the relationship between laser exposure and various parameters including ESR, packed cell volume (PCV), and blood viscosity [18,19]. Further examining specific blood components, a recent study by Slewa et al. (2022) investigated the effect of low-level red Helium-Neon laser therapy on human blood. They found that this irradiation led to a decrease in white blood cell (WBC) and red blood cell (RBC) counts, while observing increases in neutrophils (NEUT), platelets (PLT), and the erythrocyte sedimentation rate (ESR), suggesting potential therapeutic applications related to managing blood viscosity. Subsequently [20], Mohseen et al. (2020) added a temporal dimension by tracking changes in blood components over various periods following laser exposure [21].More recently, Chuang et al. (2024) presented a comprehensive narrative review on the application of intravenous laser irradiation of blood (ILIB) using helium-neon lasers for treating multiple clinical conditions. The study highlighted anti-inflammatory and antioxidative mechanisms, improved oxygen-carrying capacity, and enhanced mitochondrial activity in white blood cells, supporting the relevance of laser therapy in modulating blood components and overall cellular function. Additionally [22], Zaichkina et al. (2016) demonstrated in a mouse model that exposure to helium-neon laser doses ranging from 0.16 to 50 MJ/cm² activated natural protective reserves, as evidenced by reduced DNA damage in whole blood leukocytes. However, no adaptive response was observed with prior laser exposure. Furthermore, the study found that reactive oxygen

species (ROS) generation capacity in neutrophils was diminished in animals pre-exposed to laser followed by X-ray irradiation, indicating laser-induced modulation of immune cell activation dynamics [23].Despite the valuable data presented by these studies, research on the impact of He-Ne laser irradiation on blood magnesium levels remains lacking. Although direct studies on the effect of He-Ne laser irradiation on blood magnesium levels are currently lacking, a strong theoretical rationale supports investigating this relationship. This rationale is predicated on the established ability of laser therapy to modulate fundamental cellular processes critical for ion homeostasis. Specifically, laser exposure is known to influence cell membrane transport mechanisms, enzymatic activities related to ion conductance, and intracellular signaling pathways, all of which could potentially regulate magnesium channels and transport. Furthermore, laser-induced alterations in the cellular metabolic and redox environment, potential modifications in the gene expression of relevant transport proteins (Hawkins & Abrahamse, 2005)[24] , and direct biophysical interactions (Schmitz et al., 2004; Margarone et al., 2018; Maruyama et al., 2018) collectively suggest a plausible impact of He-Ne laser on magnesium dynamics. Thus, exploring this potential interaction is crucial for understanding the broader physiological effects of laser therapy.

This knowledge gap is especially relevant considering the critical role magnesium plays in various physiological functions and the implications its manipulation could have for therapeutic applications involving laser technology. This current research seeks to address this significant research gap by exploring the effects of He-Ne laser exposure on magnesium levels in blood. Acquiring such knowledge is essential for determining the broader implications of laser therapy on mineral balance and for exploring potential clinical uses [25,26,27]. The study adopts a structured methodology, focusing on quantifying magnesium concentrations in human blood serum samples before and after exposure, as well as examining possible gender-dependent variations in responses to laser irradiation

2. MATERIALS AND METHODS

2.1 Sample collection

Twenty healthy volunteers, all non-smokers and ranging in age from 19 to 65, took part in our study. Before starting,

 ISSN: Online 2790-1637, Print 2790-1629
National Library of Libya, Legal number: 154/2018

informed consent was obtained from all participants. Blood samples were collected using Red Top Tubes (RTT). To ensure sample purity, sterile needles were used to draw the blood (two milliliters from each participant), following standard collection procedures. Immediately after collection, the cases and samples were collected inside the Salaya Care Laboratory in the city of Sirt for processing. The samples were then quickly centrifuged to separate the serum. Centrifugation was performed at 3000 RPM for 3 to 5 minutes at 25 degrees Celsius.

2.2 Sample preparation

Sample Preparation and Laser Exposure are shown in Figure 2: After centrifugation, the separated serum was divided into four equal portions:

• Control Sample: The first aliquot was immediately analyzed using a BS-230 biochemical analyzer to establish baseline magnesium levels. The analysis was carried out according to standard protocols.

• Laser Radiation Exposed Samples: The other three aliquots were prepared for laser exposure. The samples were placed at a fixed distance of 5 centimeters away from the helium-neon (He-Ne) laser (wavelength: 632.8 nm, beam diameter: 0.48 mm) to provide uniform exposure.

-Second Aliquot: Exposed to the laser for 1 minute, then analyzed for magnesium concentration.

-Third Aliquot: Exposed to the laser for 3 minutes, followed by measurement of its magnesium level.

-Fourth Aliquot: Exposed to the laser for 5 minutes, after which its magnesium level was measured. Each sample exposed to the laser was compared to the control sample to evaluate the effect of laser exposure duration on serum magnesium levels. A BS-230 biochemical analyzer was used to measure magnesium levels throughout the study."

(a) (b) (c)

Figure (1) : Samples preparation and set up the helium-neon laser device. (a) Serum sample placed in a cuvette ready for laser irradiation. (b) Sample being manually prepared and positioned by the operator. (c) Fine adjustment of the He-Ne laser device to ensure accurate and uniform exposure.

3.RESULTS AND DISCUSSIONS

Table 1 shows Serum magnesium concentrations (mg/dL) in 20 human samples measured before and after helium-neon (He-Ne) laser exposure at intervals of 1, 3, and 5 minutes. These data illustrate the potential effects of laser irradiation on magnesium levels in human blood.

Table (1). Serum magnesium concentrations before and after helium-neon (He-Ne) laser.

Sample ID	Age	Gender	Laser Power (mW)	Wavelength (nm)	Distance (cm)	Pre-Exposure Mg (mg/dl)	Post-Exposure Mg (mg/dl) 1min	Post-Exposure Mg (mg/dl) 3 min	Post- Exposure Mg (mg/dl) 5 min
1	19	Male	1	632.8	5	1.7	2.3	2.0	1.8
2	65	Male	1	632.8	5	1.7	2.2	2.03	1.9
3	15	Female	1	632.8	5	1.8	1.0	2.1	1.8
4	42	Female	1	632.8	5	1.8	1.8	2.4	1.7
5	18	Male	1	632.8	5	2.1	1.8	1.06	1.09
6	30	Male	1	632.8	5	1.8	2.8	1.9	2.3
7	44	Male	1	632.8	5	2.0	2.5	1.7	2.5
8	20	Female	1	632.8	5	2.5	2.3	2.7	2.5
9	22	Female	1	632.8	5	1.7	1.8	1.9	2.5
10	24	Female	1	632.8	5	1.7	1.9	2.3	2.8
11	25	Female	1	632.8	5	1.8	1.4	1.9	2.4
12	26	Female	1	632.8	5	2.4	2.5	2.8	2.8

 ISSN: Online 2790-1637, Print 2790-1629
National Library of Libya, Legal number: 154/2018

13	43	Female	1	632.8	5	1.9	1.8	2.0	2.7
14	29	Male	1	632.8	5	1.9	1.02	1.6	1.1
15	27	Male	1	632.8	5	1.7	2.1	1.8	2.2
16	28	Male	1	632.8	5	1.7	1.2	1.8	2.1
17	21	Female	1	632.8	5	1.7	1.8	1.9	2.6
18	16	Female	1	632.8	5	1.7	1.13	1.7	2.0
19	21	Male	1	632.8	5	1.8	1.9	1.7	1.7
20	23	Male	1	632.8	5	1.7	1.8	1.7	1.7

A comprehensive analysis of the alterations in magnesium levels indicates a diverse range of responses among the serum samples following laser exposure. Some samples exhibited increased magnesium levels, while others showed a decrease, and a few cases indicated no notable change. Specifically, 60% of the samples reflected an immediate rise (like the sixth and tenth sample), 25% demonstrated a decline (especially the third and fourth sample), and 15% revealed no significant variation. This variability points to complex interactions occurring within the serum milieu itself upon laser irradiation. While the photobiomodulatory effects of lasers in vivo often involve mechanisms like the modulation of ion transport across cellular membranes – concepts detailed in research on cellular responses to low-power lasers, such as the work by Karu (2003) exploring effects on cellular ion transport [28] – such direct effects on cellular membranes are not the primary drivers in our acellular serum preparation. Therefore, we propose that the observed variability in magnesium levels in this in vitro context stems more directly from the laser's interaction with the inherent biochemical composition of individual serum samples. It is hypothesized that the laser light interacts differently with specific serum components, potentially including subtle effects on the conformation or magnesium-binding characteristics of serum proteins like albumin, leading to the varied responses observed. The mean magnesium level prior to exposure was approximately 1.84 mg/dL, which is within the acceptable range. In terms of the impact of exposure duration, a one-minute exposure resulted in a prompt and substantial effect in the majority of cases, reflecting an immediate and rapid response within the serum samples, as shown in figure

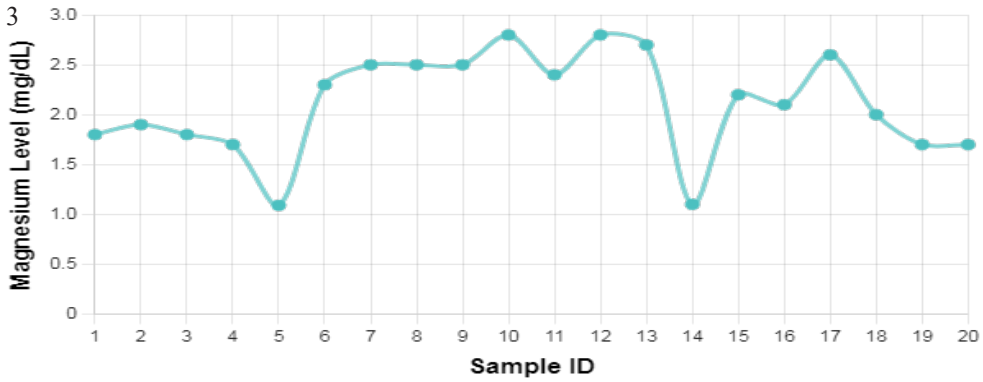

Figure (2) : magnesium level at 1 minute.

On the contrary, the duration of exposure for a period lasting three minutes revealed a moderate physiological response characterized by a discernible level of relative stability in the measured values that are shown in figure (3).

In parallel, the condition of exposure extending over a duration of five minutes, in certain instances, indicated a reversion to baseline levels, thereby implying the existence of an intrinsic regulatory mechanism within the human body that effectively restores homeostatic balance. This is shown in figure (4).

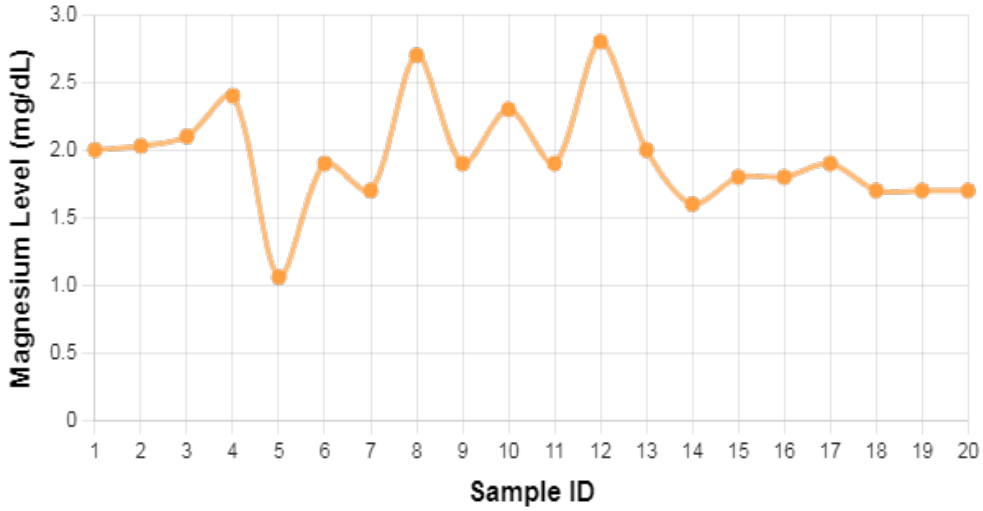

Figure (3) : magnesium level at 3 minutes.

 ISSN: Online 2790-1637, Print 2790-1629
National Library of Libya, Legal number: 154/2018

Exposure for five minutes, in some cases, showed a return to baseline levels, suggesting the presence of a regulatory mechanism in the body that restores balance.

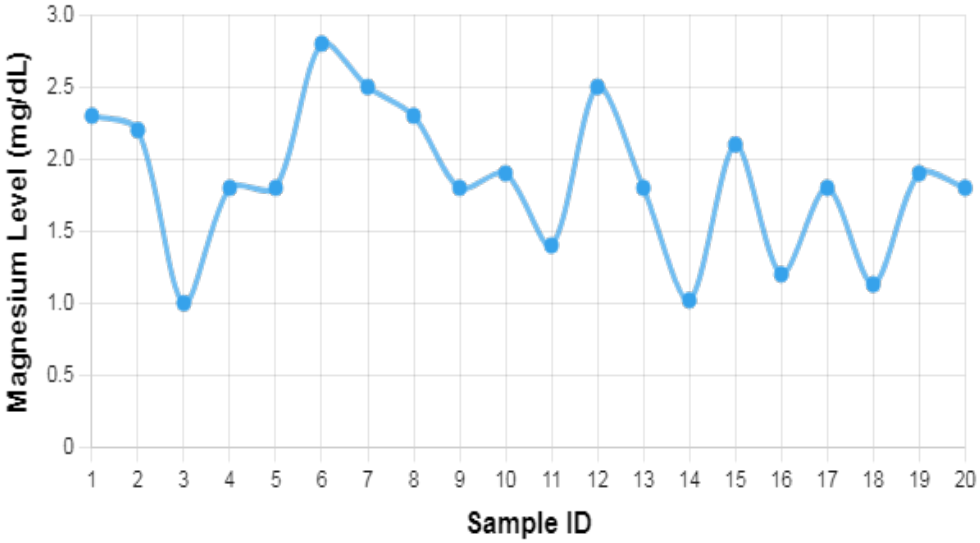

Figure (4) : magnesium level at 5 minutes.

On the other hand, when exposed to the helium-neon laser, females showed a bigger increase in magnesium (30%) and a longer and more consistent response than males shown in (Figure 5) and table (2). At the 1-minute mark, there is no significant difference between males and females ($p > 0.05$). However, at 3 and 5 minutes, the difference becomes statistically significant ($p < 0.05$), with females showing a greater increase in magnesium levels than males. Males had more pronounced oscillations and an initial decrease before going back to baseline. These sex differences are consistent with known physiological variations influencing magnesium homeostasis in vivo (Avinash et al., 2013; Lowenstein & Stanton, 1986), such as the role of estrogen in systemic magnesium handling (Avinash et al., 2013). However, given the in vitro nature of this study using serum, these observed differences likely arise from baseline variations in serum composition itself. It is plausible that the laser interacts differently with serum components, perhaps influencing the conformation or binding affinity of magnesium-binding

 ISSN: Online 2790-1637, Print 2790-1629
National Library of Libya, Legal number: 154/2018

proteins like albumin [29,30] , which may vary between sexes. Age also played a big role in the magnesium response. The 15-45 age group responded faster and more consistently while the over 45 age group responded slower and less and with longer recovery time. These age differences may reflect underlying physiological changes associated with aging (Dominguez et al., 2024), which can impact cellular function in vivo [31] . Similarly, in our in vitro context, the diminished response in the older group could be linked to age-related alterations in serum proteins or other components, potentially affecting their interaction with the laser light and subsequent influence on measurable magnesium levels.

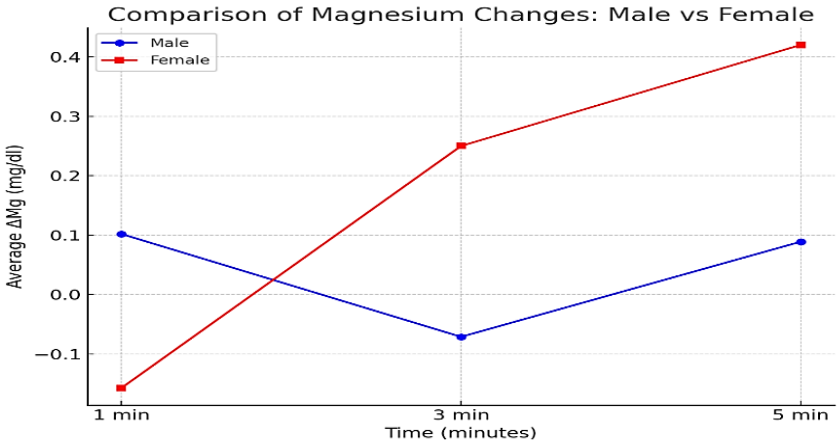

Figure (5) : Comparison of Magnesium Changes Between Males and Females

Table (2) shows the statistical summary of changes in serum magnesium levels (ΔMg) among male and female subjects following helium-neon (He-Ne) laser exposure at time intervals of 1, 3, and 5 minutes. The table presents the mean change, standard deviation (SD), and standard error (SE) for each group.

Table (2). Statistical changes in serum magnesium levels after helium-neon (He-Ne) laser exposure

Standard Error (SE)	Standard Deviation (SD)	Mean ΔMg (mg/dl)	Group	Time (Minutes)
0.18	0.56	0.018	Male	1 Minute
0.11	0.35	-0.218	Female	
0.15	0.48	-0.019	Male	3 Minutes
0.12	0.36	0.230	Female	
0.22	0.71	-0.098	Male	5 Minutes
0.16	0.51	0.430	Female	

4.CONCLUSION

He-Ne laser irradiation affects human serum magnesium levels through exposure dependence on duration as well as through sex and age variations according to this research. Magnesium levels stayed elevated for longer durations in females and subjects under 40 years old increased their magnesium levels faster. Additional research needs to be conducted to determine how low-energy laser therapy affects mineral equilibrium according to the current findings. Additional research must examine what causes these changes in serum magnesium levels while also studying different laser parameters and assessing long-term effects in living tissue. Such complete understanding between these interactions holds potential for developing new non-invasive therapeutic techniques.

5.ACKNOWLEDGMENT

We gratefully acknowledge the support of Al-Saraya Care Clinic, especially Dr. Essam Al-Naqqa and Dr. Omar Ali, for their generous contribution of samples and data, which were essential for creating the database used in this study.

6.REFERENCES

1- Altaf B, Abdul Aziz M, Sikander AM, Ali GQ, Aftab AQ. Magnesium and its essential role in health. Journal of Human Health, (2005), 15:33-35.

2-Ismail AA, Ismail NA. Magnesium: A mineral essential for health yet generally underestimated or even ignored. Journal of Nutrition & Food Sciences, (2016), 6(2):1-8. https://doi.org/10.4172/2155-9600.1000523

3-Vaquero MP. Magnesium and trace elements in the elderly: Intake, status, and recommendations. Journal of Nutrition, Health & Aging, (2002), 6(2):147-153.

4-Feillet-Coudray C, Coudray C, Gueux E, Mazur A, Rayssiguier Y. A new in vitro blood load test using a magnesium stable isotope for assessment of magnesium status. Journal of Nutrition, (2003), 133(4):1220-1223. https://doi.org/10.1093/jn/133.4.1220

5-Cunningham J, Rodríguez JM, Messa P. Magnesium in chronic kidney disease stages 3 and 4, and in dialysis patients. Clinical Kidney Journal, (2012), 5(1):i39-i51. https://doi.org/10.1093/ndtplus/sfr166

6-Saris NE, Mervaala E, Karppanen H, Khawaja JA, Lewenstam A. Magnesium: An update on physiological, clinical, and analytical aspects. Clinica Chimica Acta, (2000), 294(1-2):1-26. https://doi.org/10.1016/S0009-8981(99)00258-2

7- Bianconi E, Piovesan A, Facchin F, Beraudi A, Casadei R, Crosetti F, et al. An estimation of the number of cells in the human body. Annals of Human Biology, (2013), 40(6):463-471. _https://doi.org/10.3109/03014460.2013.807878

8-Touyz RM. Transient receptor potential melastatin 6 and 7 channels magnesium transport and vascular biology: Implications in hypertension. American Journal of Physiology-Heart and Circulatory Physiology, (2008), 294(3):H1103-H1118. https://doi.org/10.1152/ajpheart.00297.2007

9-Taif A. Overview of He-Ne laser. ResearchGate, (2017). https://doi.org/10.13140/RG.2.2.12816.87049

10- Hamid MA, Marouf AA, Abdalla MD. Helium-Neon laser effects on human whole blood by spectroscopy: An in vitro study. Asian Journal of Physical and Chemical Sciences, (2019), 7(1):1-6. https://doi.org/10.9734/AJOPACS/2019/v7i130095

11-Kanagathara N, Thirunavukkarasu M, Jeyanthi EC, Shenbagarajan P. FTIR and UV-Visible spectral study on normal blood samples. International Journal of Pharmaceutical and Biological Sciences, (2011), 1(2):74-81.

12-Obeed HH, Huzam MJ, Ridha NJ, Alosfur FKM, Tahir KJ, Madlol R, Hussein BM. Comprehensive study on the effect of laser on human blood. AIP Conference Proceedings, (2022), 2386(1). https://doi.org/10.1063/5.0068317

13- Csele M. Fundamentals of light sources and lasers. Hoboken, NJ: John Wiley & Sons;

2004. DOI: 10.1002/047165119X

14-Ghadage VH, Kulkarni GR, Zaware BN. He-Ne laser irradiation of blood in vitro and FTIR spectral analysis. Int J Chem Phys Sci. 2015;4:148-53.

15-de Oliveira, M.C., Krueger, G.F., Sganzerla, J.T., Gassen, H.T., Hernández, P.A.G., da Costa Allgayer, M. and Miguens-Jr, S.A.Q., 2021. Effect of Radiotherapy and low-level laser therapy on circulating blood cells of rats. *Journal of Lasers in Medical Sciences*, *12*, p.e45

https://doi.org/10.34172/jlms.2021.e45

16-Anju M, Chacko L, Chettupalli Y, Maiya AG, Ummer VS. Effect of low level laser therapy on serum vitamin D and magnesium levels in patients with diabetic peripheral neuropathy–a pilot study. Diabetes & Metabolic Syndrome: Clinical Research & Reviews. 2019 Mar 1;13(2):1087-91.

https://doi.org/10.34172/jlms.2021.e45

17- Nazal FY. The Effect of He-Ne laser Radiation and Temperature of Blood in Vitro on the Erythrocytes Sedimentation Rate Values in Healthy People. University of Thi-Qar Journal Of Medicine. 2016;12(2):121-30.

18- Falih HY, Msayer KH. Evaluation of the effect of the helium-neon laser (632.8 nm) on erythrocyte sedimentation rate (ESR) and packed cell volume (PCV). Samarra Journal of Pure and Applied Science. 2023 Dec 30;5(4):127-39.

https://doi.org/10.59247/sjpas.2023.v5i4.111.

19-Alnayli RS, Shanon ZS, Hussein FS, Sagban HH. The Effect of LASER on Blood Viscosity and Its Influential Relation on the Rapidity of Red Blood Cells Precipitation. American International Journal of Research in Science, Technology, Engineering & Mathematics. 2017;19(1):69-74.

20-Slewa MY, Bader BA, Hamam FM, Banoosh AM, Jarjees BW. Laser Therapy Stimulation at Red Low-level on Some Human Blood Cells. NeuroQuantology. 2022 Mar;20(3):166-72.

DOI: 10.14704/nq.2022.20.3.NQ22056

21-Mohseen HK, Madlum KN, Abd Jabbar H. Effect of Low Level Laser Irradiation on White and Red Blood Cells after Different Storage Periods. Int. J. Drug Deliv. Technol. 2020;10(4):617-9.

DOI: 10.25258/ijddt.10.4.19

22-Chuang YC, Cheng YY. Application of Intravenous Laser Irradiation of Blood (ILIB) in Physical Medicine: A Narrative

Review. Rehabilitation Practice and Science. 2024;2024(1):2.
DOI: https://doi.org/10.6315/3005-3846.2230

23-Zaichkina SI, Dyukina AR, Rozanova OM, Romanchenko SP, Sirota NP, Kuznetsova EA, Simonova NB, Sorokina SS, Zakrzhevskaya DT, Yusupov VI, Bagratishvili VN. Combined effect of low-intensity helium-neon laser and X-ray radiation on in vivo cellular response of the whole blood and lymphoid organs in mice. Bulletin of experimental biology and medicine. 2016 Sep;161:679-82.
https://doi.org/10.1007/s10517-016-3484

24-Hawkins D, Abrahamse H. Biological effects of helium-neon laser irradiation on normal and wounded human skin fibroblasts. Photomedicine and Laser Therapy. 2005 Jun 1;23(3):251-9.
https://doi.org/10.1089/pho.2005.23.251

25-Schmitz C, Perraud AL, Fleig A, Scharenberg AM. Dual-function ion channel/protein kinases: novel components of vertebrate magnesium regulatory mechanisms. Pediatric research. 2004 May;55(5):734-7.
https://doi.org/10.1203/01.PDR.0000117848.37520.A2

26- Margarone D, Cirrone GP, Cuttone G, Amico A, Andò L, Borghesi M, Bulanov SS, Bulanov SV, Chatain D, Fajstavr A, Giuffrida L. ELIMAIA: A laser-driven ion accelerator for multidisciplinary applications. Quantum Beam Science. 2018 Apr 2;2(2):8.
https://doi.org/10.3390/qubs2020008

27-Maruyama T, Imai S, Kusakizako T, Hattori M, Ishitani R, Nureki O, Ito K, Maturana AD, Shimada I, Osawa M. Functional roles of Mg2+ binding sites in ion-dependent gating of a Mg2+ channel, MgtE, revealed by solution NMR. Elife. 2018 Apr 3;7:e31596.
https://doi.org/10.7554/eLife.31596

28.Karu TI. Low-power laser therapy. In: Vo-Dinh T, editor. Biomedical Photonics Handbook. Boca Raton, FL: CRC Press; 2003. p. 48-1–48-25..

29- Avinash SS, Sreekantha, Goud BM. Magnesium Metabolism in Menopause. Nutrition and Diet in Menopause. 2013:213-23., pp.213-223.
DOI: 10.1007/978-1-62703-373-2_16

30--Lowenstein FW, Stanton MF. Serum magnesium levels in the United States, 1971-1974. Journal of the American College of Nutrition. 1986 Jan 1;5(4):399-414.
https://doi.org/10.1080/07315724.1986.1072

0148

31-Dominguez LJ, Veronese N, Barbagallo M. Magnesium and the Hallmarks of Aging. Nutrients. 2024 Feb 9;16(4):496. DOI: 10.3390/nu16040496

Scientific Journal of University of Benghazi
SJUOB (2025) 38 (1) Applied Sciences: Daw et la , 62 – 85
www.sjuob.uob.edu.ly

A Comparative Study of Perturb & Observe and ANN-Based MPPT Algorithms Under Various Environmental Conditions

Mohammed .O. Daw[1]*, Saleh.M. Shalem[1], Laith Jaafer Habeeb[2], Ayoub O . Faraj[1], abdulwahab garboa[3].

1 Electrical Engineering Department, Faculty of Engineering, University of Benghazi, Benghazi, Libya.
2 Training and Workshop Center, University of Technology- Iraq, 10066 Baghdad, Iraq.
3 The Higher Institute of Science and Technology, Elmarej, Libya

Received: 02 / 02 / 2025 | Accepted: 05 / 10 / 2025 | Publishing: 29/06/2025

ABSTRACT

This Photovoltaic energy is a promising renewable energy source because it provides a cleaner alternative to fossil fuels. However, the output power of a PV system is affected by factors like solar irradiance and temperature that can change and influence its performance. Therefore, techniques for maximum power point tracking must be developed so the photovoltaic system produces the maximum power. These techniques guarantee that the PV system has the highest power point at all times regardless of weather conditions. The two types of controllers that are presented in this paper are based on the traditional Perturbation and Observation method and the use of artificial neural networks. From simplicity, low cost, and suitability for medium to large photovoltaic systems, the Perturbation and Observation method is chosen. On the other hand, artificial neural networks is well suited to manage complex systems and may assist in improving maximum power point tracking. In addition, the performance of these two methods is compared to a fuzzy logic-based MPPT approach that was developed and published in a previous study. The controllers were evaluated under various environmental conditions using MATLAB/Simulink. The results demonstrated that the artificial neural networks-based controller outperformed both the Perturbation and Observation and fuzzy logic controller methods in terms of efficiency and overall performance. Additionally, the artificial neural networks approach significantly minimized power fluctuations. However, the fuzzy logic controller method showed a faster response in reaching the maximum power point compared to both the artificial neural networks and Perturbation and Observation techniques.

Keywords: Artificial Neural Networks, DC-DC Boost converter, MATLAB-Mathematics Laboratory, MPPT, Perturbation and Observation, Solar photovoltaic.

Corresponding Author: Mohammed .O. Daw, mohammed.daw@uob.edu.ly

1.INTRODUCTION

The photovoltaic (PV) systems offer a cleaner environment and assist to exploit the economic advantages of the sustainable solar energy and hence promote the production of electricity. These systems are nowadays available and differ, as they have low operation costs, minimal maintenance, and are among the cleanest energy sources. Their main disadvantage is geometry-related low efficiency in turning solar energy into electricity. The PV modules are subject to environmental factors like temperature and sunlight radiation to test their performance[1]] that impact the amount of energy that is collected in varying weather conditions. Maximum power point (MPP) at which the optimum energy is delivered may therefore be variable depending on solar irradiation and temperature of the solar cells as well as the load conditions[3 ,2] . To accurately track this point, an effective tracker is placed between the PV system and the load. The tracker must be designed for high performance, fast response times, and minimal fluctuations. Due to the unpredictable irradiance and temperature, it is not feasible to connect the load to the PV system directly to obtain maximum power. Instead, we need a balance of system (BOS), which in general is a DC-DC converter to adapt the load appropriately. The power to the load is delivered effectively using this converter[4] . It has been proposed in the literature, many strategies exist to solve this problem, each having different complexity, response time, cost, and type, as well as several sensors needed for hardware implementation [5-10]. However, these strategies can generally be divided into two distinct broad categories. The first type of these methods is common traditional methods like Perturb and Observe (P&O) and incremental conductance (IC), etc. Nevertheless, these methods have several shortcomings, including oscillations near the maximum power point and low efficiency upon large irradiance changes. The second type of method used to address these challenges is founded on techniques from artificial intelligence (AI), such as artificial neural networks (ANN) and fuzzy logic. In a previously published study by the authors [11], we proposed we implemented a fuzzy logic-based MPPT controller and assessed its effectiveness under various environmental conditions. The fuzzy logic technique exhibited strong adaptability and rapid con-

 ISSN: Online 2790-1637, Print 2790-1629
National Library of Libya, Legal number: 154/2018

vergence to the maximum power point, along with a noticeable reduction in power oscillations. However, it required precise parameter tuning and imposed a relatively high computational burden compared to conventional methods. To further enhance MPPT efficiency while maintaining implementation simplicity, this study investigates and compares two alternative techniques: the conventional P&O algorithm and an ANN-based controller. These methods were implemented and tested under varying irradiance and temperature conditions using MATLAB/Simulink. The results were then compared with those from a previous study by the authors, which employed a fuzzy logic controller (FLC). The performance of all three techniques was evaluated in terms of tracking efficiency, dynamic response, system complexity reduction, and output stability. Due to its simplicity, the PV module's characteristics are simulated using a one-diode mathematical model of a solar cell. Additionally, a boost-type DC/DC converter is used, chosen for its appropriateness in standalone applications. Therefore Fig.1 illustrates the complete proposed photovoltaic system, which comprises several key components: the PV array, the MPPT algorithms, and the DC/DC boost converter.

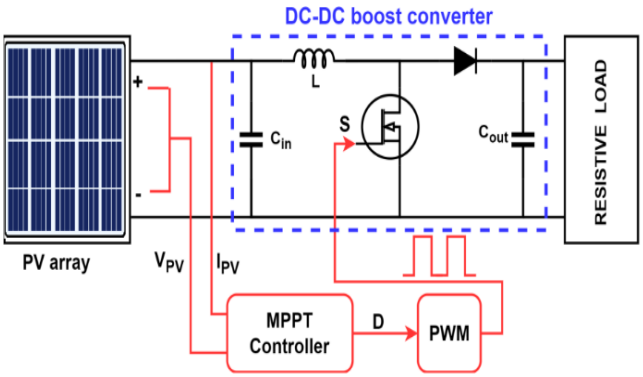

Figure .(1): The complete proposed photovoltaic system

 ISSN: Online 2790-1637, Print 2790-1629
National Library of Libya, Legal number: 154/2018

2.MODELING OF PV ARRAY

A solar cell is an electrical device that uses the photovoltaic effect to transform light energy into electricity. Figure (2) depicts a single-diode model of the equivalent circuit of a PV cell. This model includes a current source (photocurrent), a diode (D), series resistance, which is responsible for the internal resistance of the current flow, and shunt resistance, which is responsible for the leakage current [7, 12]12]</style></DisplayText><record><rec-number>41</rec-number><foreign-keys><key app="EN" db-id="svfxzrrzix5dsbe9fe75raa190909t5eev5a" timestamp="1728181661">41</key></foreign-keys> <ref-type name="-Journal Article"> 17</ref-type><contributors><authors><author>Al-Majidi, Sadeq D</author><author>Abbod, Maysam F</author><author>Al-Raweshidy, Hamed S</author></authors></contributors><titles><title>A novel maximum power point tracking technique based on fuzzy logic for photovoltaic systems</title><secondary-title>International Journal of Hydrogen Energy</secondary-title></titles><periodical><full-title>International Journal of Hydrogen Energy</full-title></periodical><pages>14158-14171</pages><volume>43</volume><number>31</number><dates><year>2018</year></dates><isbn>0360-3199</isbn><urls></urls></record></Cite><Cite><-Author>Eid</Author><Year>2019</Year><RecNum>70</RecNum><record><rec-number>70</rec-number><foreign-keys><key app="EN" db-id="svfx-zrrzix5dsbe9fe75raa190909t5eev5a" timestamp="1749816775">70</key></foreign-keys><ref-type name="Conference Proceedings">10</ref-type><contributors><authors><author>Eid, Mohammed A Elsayed</author><author>Elbaset, Adel A</author><author>Ibrahim, Hamed A</author><author>Abdelwahab, Saad A Mohamed</author></authors></contributors><titles><title>Modelling, simulation of MPPT using perturb and observe and incremental conductance techniques for stand-alone PV Systems</title><secondary-title>2019 21st International Middle East Power Systems Conference (MEPCON) .

 ISSN: Online 2790-1637, Print 2790-1629
National Library of Libya, Legal number: 154/2018

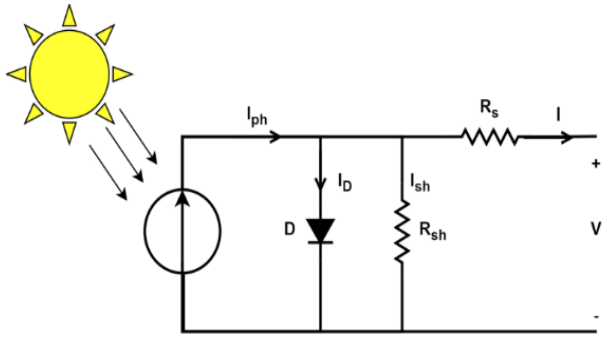

Figure.(2): PV cell equivalent circuit.

Under the condition of solar PV cell being illuminated by solar irradiance, the current output of a cell could be calculated based on Kirchhoff law as shown in Equation 1.

$$I = I_{ph} - I_s - \frac{(V + IR_s)}{R_{sh}} \quad --(1)$$

The light-generated current is primarily influenced by the sunlight irradiance and the operating temperature of the PV cell, as described in Equation 2.

$$I_{ph} = \left[I_{SC} + K_i \left(T - T_{ref} \right) \right] . \left(\frac{G}{1000} \right) \quad ----(2)$$

The PV saturation current (IS) varies as a cubic function of the temperature (T) of the PV cell, and it is represented in Equation 3.

$$I_s = I_{rs} \left(\frac{T}{T_{ref}} \right)^3 exp \left[\frac{q.Eg}{K.A} . \left(\frac{1}{T_{ref}} - \frac{1}{T} \right) \right] \quad ---(3)$$

The reverse saturation current (I_{rs}) can be roughly calculated using Equation 4.

$$I_{rs} = \frac{I_{sc}}{\left[exp \left(\frac{q V_{oc}}{N_{ser}.K.A.T} \right) - 1 \right]} \quad --(4)$$

Where:

I: Current of PV.

V: Voltage of PV.

Iph: The light generated current.

Is : The PV saturation current.

Irs : The reverse saturation current.

Isc : short circuit current.

T : operating temperature of PV module in

kelvin.

Tref : temperature of reference =298K.

Rsh : Shunt resistor of the PV.

Rs: Series resistor of the PV.

A : An ideality factor.

K : Boltzmann constant (1.38065003J/K).

G : Solar radiation.

Ki : Short-circuit current temperature coefficient.

Nser : Series number of cells.

Eg : the band gap energy for silicon = 1.1 e V.

q : is the electron charge (1.60217646 C)

A photovoltaic (PV) cell's I-V and P-V characteristics, which show how a PV array typically behaves at different temperatures and sunlight irradiance, affect how much electricity the cell produces. The I-V and P-V characteristics of a standard PV (MSX-60W) are shown in Figure. (3) are presented at various temperatures, while Fig.4 showcases these characteristics under different levels of sunlight irradiance [2]. The output voltage of a PV system is affected by temperature, typically decreasing as temperatures rise. In contrast, the output current increases linearly with higher solar irradiance, meaning that greater sunlight exposure leads to increased current generation. The P-V curve depicts the relationship between output power (P) and voltage (V), with the maximum power point (MPP) clearly marked. MPP is subject to variation based on weather conditions.

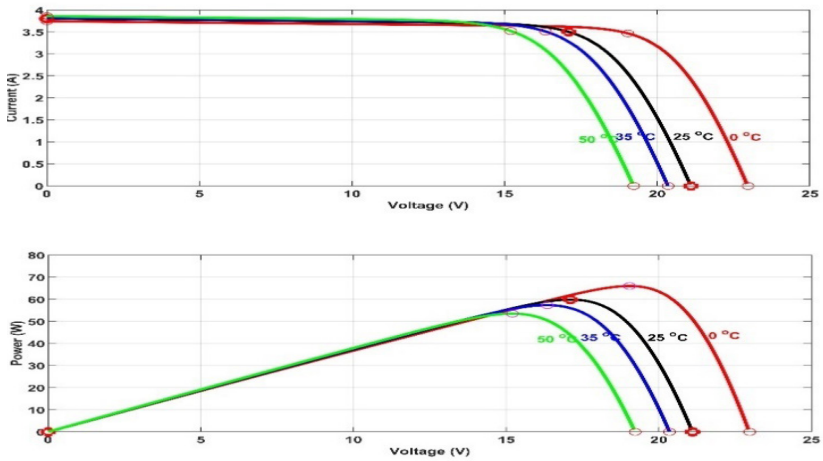

Figure. (3): I-V and P-V characteristics of a typical PV module at various temperatures

 ISSN: Online 2790-1637, Print 2790-1629
National Library of Libya, Legal number: 154/2018

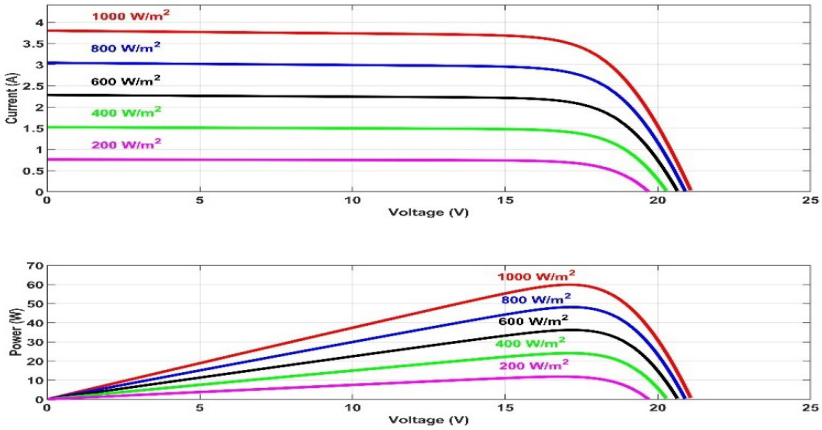

Figure .(4): I-V and P-V characteristics under different levels of sunlight irradiance.

The parameters for the PV array (MSX60 at 1000 W/m² and 25°C) are provided in Table (1).

Table .(1): Parameter specification of MXS 60 PV module.

Parameter	Variable	value
Voltage at MPP	VMPP	17.1V
Current at MPP	IMPP	3.5 A
Power at MPP	PMPP	60W
Open circuit voltage	Voc	21.1 V
Short circuit current	Isc	3.8A
coefficient of temperature for short circuit current	Ki	0.06 mA/
total number of cells connected in series	Nser	36
total number of cells connected in parallel	Np	1

3.DC-DC BOOST CONVERTER

Connecting a PV panel directly to a load can result in significant power losses due to impedance mismatch. A DC-DC converter with the proper impedance matching is necessary to optimize the PV panel's power flow to the load. This paper adopts a boost converter topology because of its grid connection suitability. A boost converter is so named because it produces an output voltage higher than its input. The circuit shown in Figure. (5) includes an inductor, switch, diode, and capacitor, and works as a switching converter by regularly turning the electronic switch on and off [13].

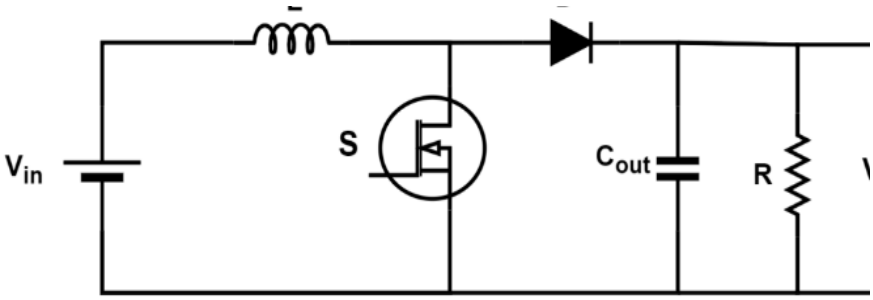

Figure. (5). The circuit diagram of the boost converter

The boost converter has two operation modes. The diode is reverse-biased in the first mode, which allows current to rise and flow to the load via the switch and inductor when the switch is ON. When the switch is off in the second mode the diode is forward-biased and allows the inductor to dump its current into the load through the capacitor [14, 15]. The connection between input and output voltage is expressed by Equation 5:

$$\frac{V_{out}}{V_{in}} = \frac{1}{1-D} \quad ---(5)$$

Where:

-Vout and Vin: input and output voltages.

-D: duty cycle.

The boost converter's inductor and capacitor are designed based on the performance requirements of the boost function, with their values calculated using Equations 6 and 7.

$$L = \frac{V_{in}\ D}{\Delta iL * f_s} \text{--(6)}$$

$$C = \frac{D}{R\left(\frac{\Delta V_o}{V_o}\right) f_s} \text{--(7)}$$

Where:

D is Duty cycle.

is Inductor current ripple.

Output voltage ripple.

fs is switching frequency.

The design of DC-DC boost converter is shown in Table (2).

Table .(2): The designed specifications for the boost converter

Parameter	Symbols	values
Input capacitor (uf)	Cinp	225
Output capacitor (uf)	Cout	200
Inductor (mH)	L	3
Switching frequency (KHz)	fs	5
Resistive load ()	R	50

4.MAXIMUM POWER POINT TRACKING TECHNIQUES

Control objective is to efficiently capture and harvest the utmost power of photovoltaic (PV) arrays according to the present solar radiation levels. A large number of various algorithms have been devised to locate MPP. They differ in the required use of sensors, complexity, price, scope of applicability, tracking rate, efficiency, capability of tracing radiation or temperature changes, hardware necessary and popularity. A thorough review of various MPPT algorithms, including their mathematical formulas, working principles, and diagrams/flowcharts, can be found in [16] .This paper focuses on two MPPT methods.

P&O: This method involves continuously adjusting the operating point of the PV system. By perturbing the voltage or current and observing the resulting power output, the system can determine how to maintain the maximum power point.

ANN: This approach utilizes the adaptive learning capabilities of neural networks to optimize the power output from PV systems.

Both methods will be explored in depth in the subsequent sections.

4.1.P&O Method

P&O is one of the most popular MPPT techniques of PV systems, which is easy to use and reasonably priced. The PV panel measurement's voltage (V), current (I), and initial power (P1) initiate the connection. The operating voltage is then adjusted slightly and another power reading is obtained (P2). The power change (ΔP) is given by the difference between P2 and P1. When +ΔP (P2 -P1) the perturbation is moving the system towards MPP, hence the algorithm should continue perturbing in the same direction. On the other hand, when -ΔP (P2 < P1) then this indicates that the perturbation has shifted beyond the MPP and the algorithm will change direction. This cyclic procedure continues to adjust the voltage until it reaches and harvested the maximum power point of the PV panel. The overview of the P&O algorithm is presented in Table (3) [17, 18]. This technique offers several benefits, including its simplicity and widespread use. However, it does have limitations, particularly in rapidly changing atmospheric conditions or when multiple local maxima are present. Additionally, it may exhibit slow response times to the MPP and cause oscillations around the MPP. Despite these drawbacks, its easy implementation keeps it a favored option in many PV applications[19]. Figure.(6) displays a flowchart that explains the P&O MPPT technique.

Table .(3): Scheme of the P&O algorithm.

Present perturbation (ΔV)	Change in power ΔP	Next perturbation direction
ΔV > ٠	**ΔP >** ٠	Positive (Duty ratio decrease)
ΔV > ٠	**ΔP <** ٠	Negative (Duty ratio increase)
ΔV < ٠	**ΔP >** ٠	Negative (Duty ratio increase)
ΔV < ٠	**ΔP <** ٠	Positive (Duty ratio increase)

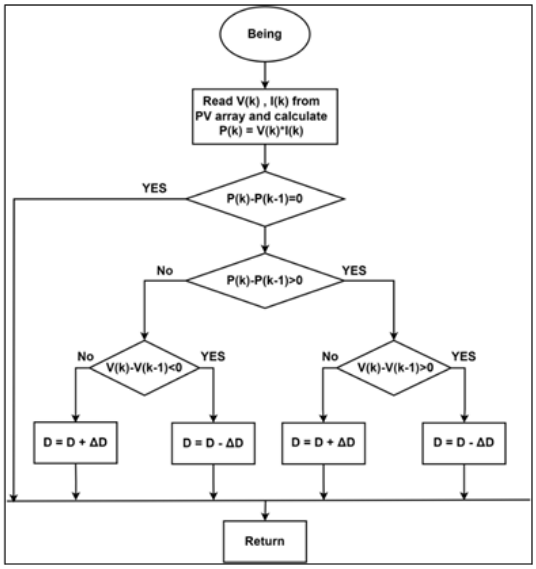

Figure. (6): flowchart of the P&O MPPT technique

4.2:ANN based MPPT

Artificial neural network controllers have become in recent years very popular to track the maximum power point in photovoltaic systems because of their ability to deal with the complex and nonlinear behavior of the system [20]. The ANN based MPPT is realized by utilizing the fact that the neural network can compute without requiring any manual programming and without requiring any learning based on data. With the highly correlated parameters being known, e.g. irradiance of the sunlight, temperature and power output, an ANN can be used to predict the MPP and also enhance the tracking accuracy and efficiency even in various environmental situations. This is done by training the network on a dataset comprising of input, such as irradiance and temperature, as well as output expressed in terms of duty cycle values. The studies in the literature [21, 22] have considered many MPPT techniques based on ANN. The three processes involved in developing an artificial neural network (ANN) can be summed up as follow:

1.ANN architecture selection: The ANN architecture (depth and width of the network and the problem complexity) of the ANN is

determined by the number of layers (depth) and neurons (width) and amount of available data. Moreover, by selecting appropriate activation function (e.g., Sigmoid, Tanh or ReLU), the network would learn nonlinear relationships.

2.Collecting of data: Data collection entails putting down vital inputs and their relatable outputs. This comprises environmental conditions such as solar irradiance, temperature and the systems response such as power generation. This is the set of data points that are utilized in training the network and making it more accurate, and it is called training points.

3.Network Training and validation: Network training is performed by training the ANN with some suitable optimization algorithm, such as backpropagation using processed data. Network validation is however the process in which the accuracy and the robustness of the trained ANN are tested on another dataset.

4.3.Choosing the ANN architecture:

The developed neural network is a Multi-Layer Perceptron (MLP) with three layers: an input layer with two neurons (temperature and irradiance), a hidden layer with ten neurons using a sigmoid activation function, and an output layer with one neuron to determine the duty cycle using a linear activation function, as shown in Figure.(7). The network works by multiplying inputs with weights, summing them, and passing the result through the activation function to generate the output. By adjusting the weights and activation function, the network learns to recognize patterns. Equation 8 illustrates the neural network's operation:

$$a_i = \sum_{J=0}^{N} W_{ij} X_j \text{---(8)}$$

Where

ai is the output of ANN at node i.

Wij weighted between the nodes i and j.

X j is the state variable evaluated by the activation function.

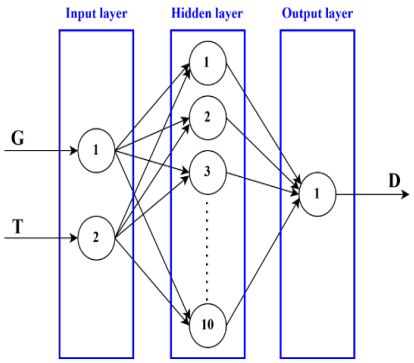

Figure. (7): The neural network configuration.

5.DATA COLLECTION

The training phase involves collecting data and outlining the steps to create a dataset for training a neural network that can predict the Duty Cycle (D) required to control the converter for optimal efficiency, based on input parameters solar irradiance (G) and temperature (T). The data collection process is illustrated in the flowchart in Fig. 8. It begins by defining the required parameters and constants, with a total of N=3000 representing the number of data samples to be generated. The temperature range is set between 5°C and 45°C (Tmin=5, Tmax=45), and the solar irradiance range is set from 10 to 1000 W/m² (Gmin=10, Gmax=1000). During each iteration, random temperature and irradiance values are generated within these ranges to ensure diversity in the dataset. The photovoltaic system is then simulated in the SIMULINK-MATLAB environment, through simulation, the maximum voltage (Vmp) and maximum power (Pmp) at the maximum power point (MPP) are obtained, these values are stored in the MATLAB workspace, and from these values, the impedance at MPP (Rmpp) is calculated using Equation 9:

$$Rmpp = Vmp^2 / Pmp \text{---} (9)$$

The Duty Cycle (D) is then calculated using the equation 10:

$$D = 1 - \sqrt{\left(R_{mpp}/R_{load}\right)} \text{---} (10)$$

where the load resistance (Rload) is assumed to be 50 Ω.

The generated input values (G and T) and the computed duty cycle (D) are stored in matrices. The input matrix contains the values of G and T, while the output vector contains the corresponding duty cycle values. This dataset, organized as input-output pairs, is ready to be used to train the neural network. After training, the neural network will be able to predict the duty cycle based on new input values of solar irradiance and temperature, allowing for efficient real-time control of the PV system.

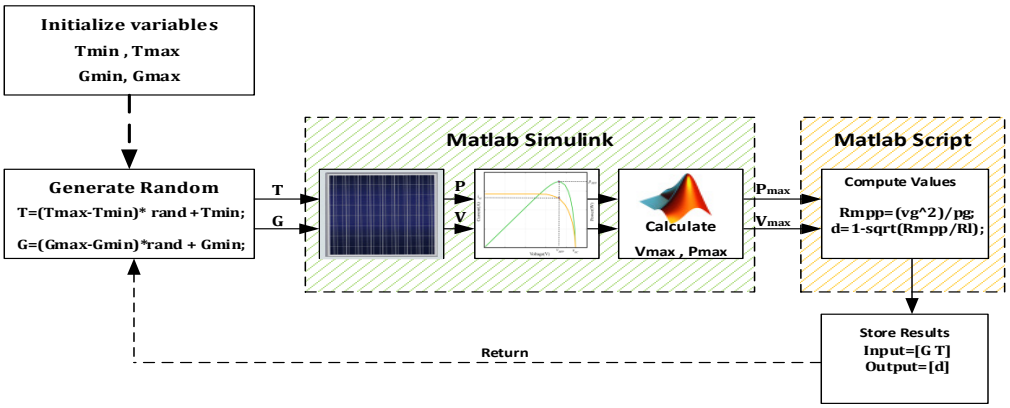

Figure. (8): Data Collection Flow Diagram

6.NETWORK TRAINING AND VALIDATION

An artificial neural network (ANN) was created using MATLAB's neural network toolbox and the input/output data that had been gathered in the previous step. Depending on the availability of sensors, temperature and solar radiation were employed as input signals. To make implementation easier, the ANN's output was defined as the boost converter's duty cycle. The Levenberg-Marquardt algorithm was trained on a dataset of 3000 tests running under various radiation and temperature conditions. Three subsets of the data were created: 15% for testing, 15% for validation, and 70% for training. The training process concluded after 307 epochs, as illustrated in Figure.(9). The best validation performance was achieved at epoch 301, with a mean square error (MSE) of 1.2171e-8, as shown in Figure.(10). The ANN error histogram for testing, validation, and training is shown in Figure. (11). The error is separated into 20 bins with a bin width of 0.00057945, ranging from -0.00654 to 0.005045. The number of samples falling within a given error range is shown by each vertical bar. The error histogram indicates that roughly 99% of the errors fall within the range of -0.00105 to 0.000775, with a few outliers. Near the orange "Zero Error" line, the bin at -0.000165 contains over 1500 samples from the validation dataset. The

convergence of the histogram to zero across 20 bins underscores the ANN's efficiency in achieving MPPT. This is further validated by the regression analysis shown in Figure.12, which highlights the accuracy of the ANN's output predictions in relation to the input, with a regression value of R = 1. The error is defined as the variance between the duty cycle generated by the ANN model and the intended target duty cycle, calculated by subtracting the output from the target. As shown in the regression plot, the regression plot, the Levenberg-Marquardt (LM) algorithm was good at training the data, since the error was minimized and the output is very close to the desired values.

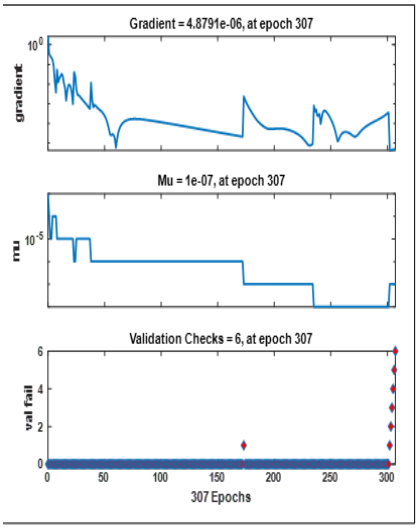

Figure. (9): Training performance of ANN

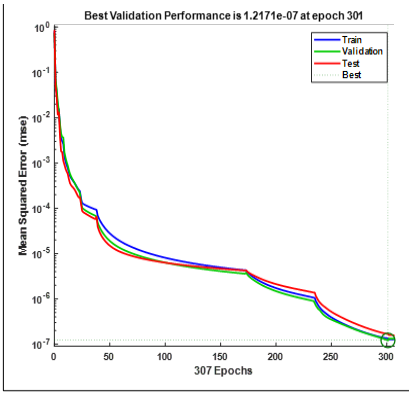

Fig. 10: Validation performance of ANN

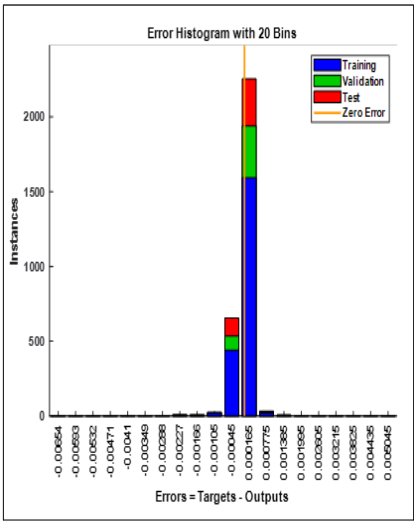

Figure. (11): Error histogram

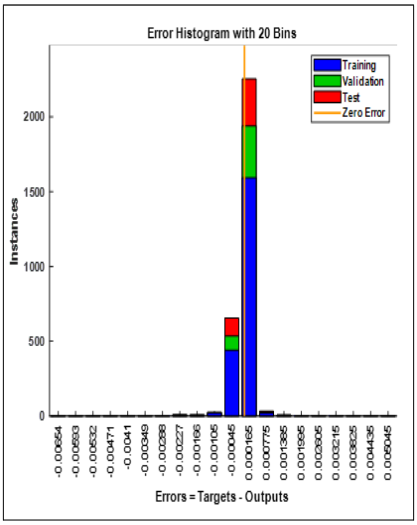

Figure. (12): Regression plot

7.RESULTS AND DISCUSSION

The simulation results of the suggested system, which was developed and analyzed using MATLAB and Simulink, are provided in this section. It is made up of load, DC-DC converter, MPPT controller, and PV arrays. Table (1) displays the PV array's electrical properties. Two approaches have been used to evaluate the system's performance using the P&O algorithm and an ANN-based method. Figure. (13) and Figure. (14) illustrate the design and the architecture of both approaches. Extensive testing and analysis of the solar radiation conditions AND temperature were conducted on both techniques. In addition, for a comprehensive evaluation, a comparison is made with the previously developed FLC from our earlier work. It is important to note that the detailed results and analysis of the FLC method were extensively discussed and published in[11]; therefore, only the comparative results between FLC, P&O, and ANN methods are presented and analyzed in this section.

The simulations were conducted by dynamically varying the solar irradiance levels. Initially, the irradiance decreased from 1000 W/m² to 800 W/m² within 0.2 seconds, followed by a drop to 400 W/m² at 0.3 seconds, and then further declined to 200 W/m² at 0.7 seconds. Subsequently, it returned to the standard test condition of 1000 W/m² at 0.7 seconds, as illustrated in Fig. 15. Throughout this scenario, the ambient temperature was maintained constant at 25 °C.

In a separate scenario, the temperature variation was studied while keeping the solar irradiance fixed. The temperature increased from 15 °C to 25 °C within 0.2 seconds, then rose to 35 °C at 0.4 seconds, and finally reached 45 °C at 0.6 seconds, as shown in Fig. 16, with the irradiance held constant at 1000 W/m²..

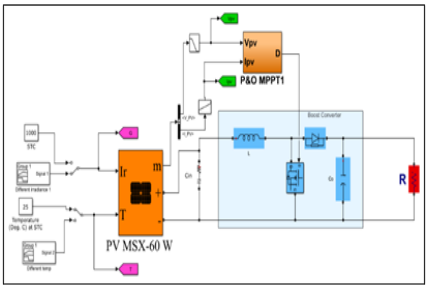

Figure. (13): Simulink Model of P&O

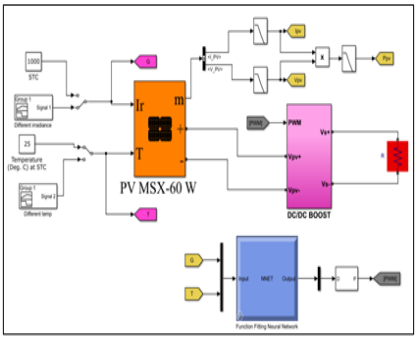

Figure. (14): Simulink Model of ANN

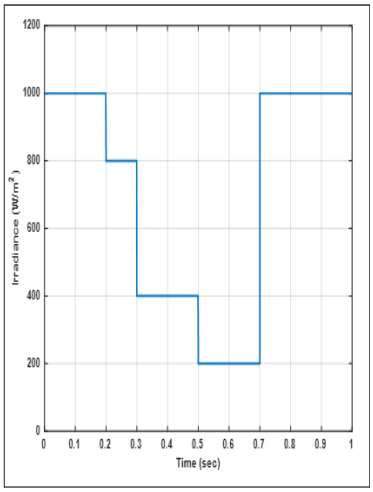

Figure. (15): Solar irradiance levels

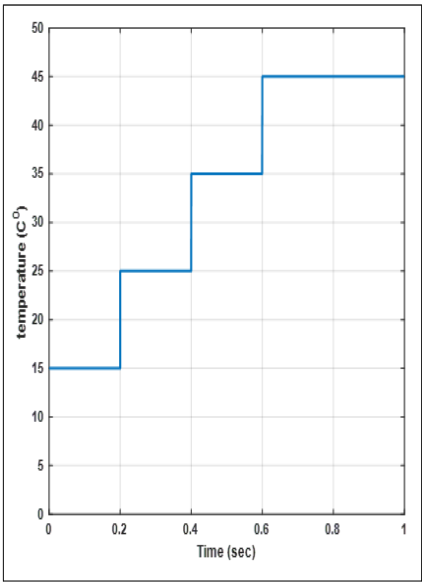

Figure. (16): Solar Temperature Variation

Figure.(17) presents the simulation results for the PV panel's output power, current, and voltage using the P&O algorithm under dynamically changing irradiance conditions. In this setup, the duty cycle increment (ΔD) was set at 0.005 to ensure effective tracking of the MPP. As anticipated, a trade-off emerges between the convergence speed the time needed to reach steady state and the magnitude of oscillations around the MPP. These two characteristics are inherently linked to the value of the duty cycle increment; minimizing oscillations slows down convergence, whereas faster convergence results in larger oscillations. In this simula-

 ISSN: Online 2790-1637, Print 2790-1629
National Library of Libya, Legal number: 154/2018

tion, the MPP was achieved in approximately 0.014 seconds at an irradiance of 1 kw/m². Simultaneously, the effect of temperature variation at constant irradiance was also examined. Figure.(18) shows the PV panel's output performance under gradually increasing temperature levels. Under these conditions, the MPP was reached in about 0.01 seconds at 1 kw/m² irradiance. The results indicate that although the P&O method is capable of accurately tracking the MPP, it responds relatively slowly to sudden changes in irradiance and temperature. Moreover, the method exhibits noticeable fluctuations around the optimal point, achieving a tracking efficiency of 96.2% under constant temperature conditions and 97.54% under constant irradiance at 25°C.

Figure.(19) illustrates the simulation results of the ANN-based MPPT algorithm, showing the PV panel's output power, current, and voltage under dynamically changing irradiance conditions while maintaining a constant temperature. The ANN demonstrated excellent performance, reaching the Maximum Power Point (MPP) in just 0.008 seconds, compared to 0.014 seconds required by the P&O algorithm. Similarly, Figure.(20) presents the ANN's performance under varying temperature conditions at constant irradiance. The ANN method resulted in a significantly smoother power curve, exhibiting fewer fluctuations around the operating point and greater overall stability compared to the P&O method. The tracking efficiency achieved by the ANN algorithm was outstanding, reaching 99.9% across all tested irradiance and temperature variations.

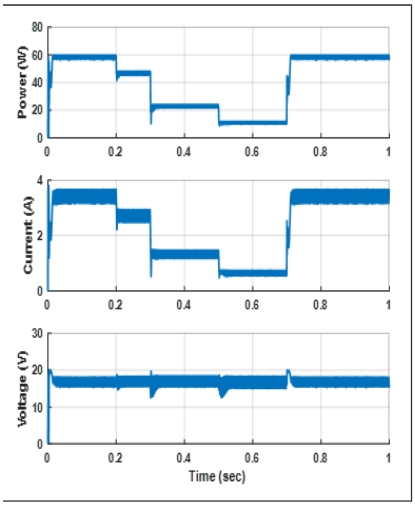

Figure. (17): Simulation results from P&O under varying irradiance conditions

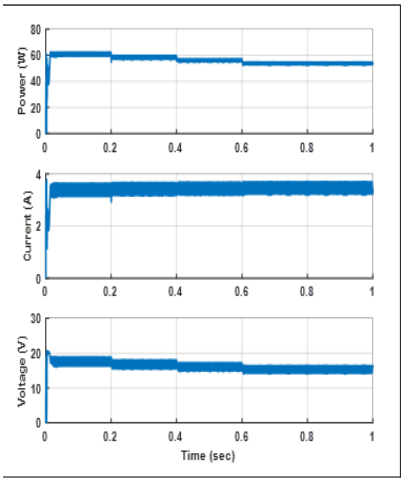

Figure. (18): Simulation results from P&O under varying temperature conditions

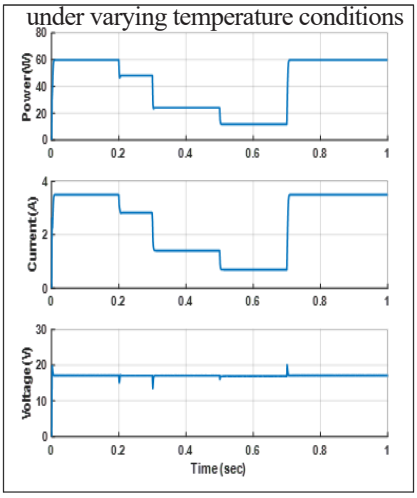

Figure. (19): Simulation results from ANN under varying irradiance conditions

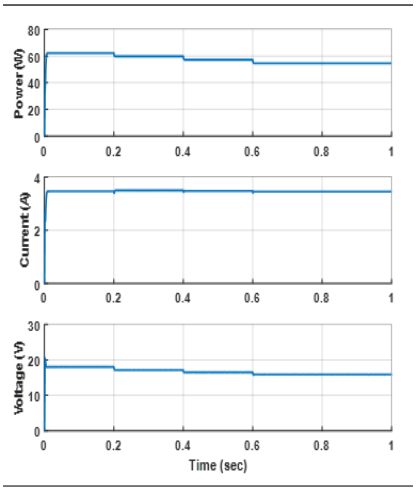

Figure. (20): Simulation results from ANN under varying temperature conditions

The tracking performance of the P&O, ANN, and previously published FLC algorithms was comparatively evaluated under varying irradiance and temperature conditions, as illustrated in Figure.(21) and Figure. (22). Table (4) presents key performance indicators including tracking efficiency, response time, and output power under different solar irradiance levels, while Table (5) summarizes the same metrics under varying temperature scenarios. The P&O method achieved dynamic tracking efficiencies of 96.20%, 97.06%, 98.88%, and 92.29% at irradiance levels of 1000 W/m², 800 W/m², 400 W/m², and 200 W/m², respectively. In contrast,

the ANN controller consistently maintained a high tracking efficiency of approximately 99.9% across all irradiance and temperature variations, demonstrating superior reliability and accuracy. Although the FLC approach reported in our earlier publication showed a faster dynamic response compared to ANN and P&O, it exhibited more noticeable power fluctuations. By comparison, the ANN-based method delivered smoother output with minimal oscillations around the maximum power point, highlighting its effectiveness for stable PV system operation.

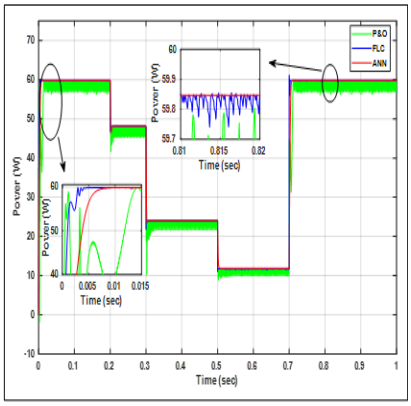

Figure. (21): Output power from P&O and ANN and FLC under varying irradiance conditions

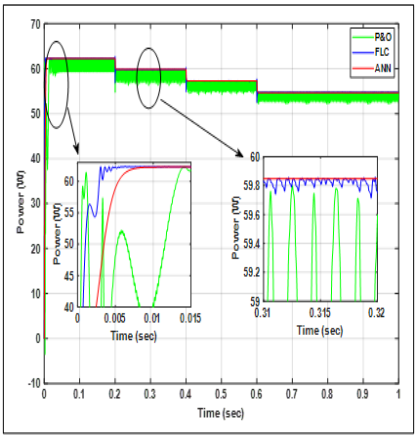

Figure. (22): Output power from P&O , ANN and FLC under varying temperature conditions

Table .(4): Comparative Analysis of ANN ,P&O and FLC MPPT Techniques under varying irradiance conditions.

Functional conditions	MPPT algorithm	Output power	Tracking efficiency	Time response
G1= 1000W/ m^2	P&O	57.578	96.20%	0.014s
	FLC	59.81	99.94	0.007s
	ANN	59.84	99.98%	0.008s
G2= 800W/ m^2	P&O	46.72	97.06%	0.01s
	FLC	48.10	99.92	0.004
	ANN	48.12	99.95%	0.006s
G3= 400W/ m^2	P&O	23.782	98.88%	0.018s
	FLC	24.03	99.92	0.003
	ANN	24.04	99.98%	0.012s
G4= 200W/ m^2	P&O	10.9	92.29%	0.01s
	FLC	11.73	99.2	0.004
	ANN	11.81	99.99%	0.006s

Table .(5): Comparative Analysis of ANN ,P&O and FLC MPPT Techniques under varying temperature conditions.

Functional conditions	MPPT algorithm	Output power	Tracking efficiency	Time response
T1= 15	P&O	60.66	97.33%	0.03s
	FLC	62.18	99.70%	0.005s
	ANN	62.30	99.93%	0.006s
T2= 25	P&O	58.38	97.54%	0.01s
	FLC	59.77	99.86%	0.002s
	ANN	59.85	99.99%	0.002s
T3= 35	P&O	55.87	97.45%	0.01s
	FLC	57.20	99.77%	0.003s
	ANN	57.28	99.91%	0.004s
T4= 45	P&O	53.74	98.10%	0.009s
	FLC	54.57	99.61%	0.004s
	ANN	54.68	99.81%	0.005s

8.CONCLUSION

A comprehensive comparative study of three MPPT controllers are presented: the classical P&O algorithm, an ANN-based controller, and a previously published FLC method. The P&O algorithm successfully tracks the MPP, but with noticeable delay and oscillations around the MPP, which are influenced by the duty cycle increment. Comparative results show that the ANN-based controller achieves superior tracking accuracy, a significantly faster transient response, and minimal steady-state power oscillations. Moreover, the Artificial Neural Network (ANN) exhibits exceptional adaptability to abrupt variations in solar irradiance and temperature, consistently maintaining a dynamic efficiency above 99.9% even under rapidly changing environmental conditions. Although the FLC method, reported in our earlier work, provides a faster initial response than ANN and P&O, it is more complex to design and tune, and suffers from greater power fluctuations around the MPP. In contrast, the ANN-based approach offers a simpler and more flexible implementation for system designers, making it a highly practical solution. In addition, this paper offers a holistic view of MPPT control techniques, presenting a detailed analysis of their advantages, limitations, and overall performance under various operating scenarios. The study further demonstrates the potential applicability of these methods for photovoltaic system deployment in Libya, considering the differing climatic conditions between coastal cities and desert regions.

9.REFERENCES

1.Esram T, Chapman PL. Comparison of photovoltaic array maximum power point tracking techniques. IEEE Transactions on energy conversion. 2007;22(2):439-49.

2.Salas V, Olías E, Barrado A, Lazaro A. Review of the maximum power point tracking algorithms for stand-alone photovoltaic systems. Solar energy materials and solar cells. 2006;90(11):1555-78.

3.Ramos Hernanz J, Campayo Martín J, Zamora Belver I, Larranaga Lesaka J, Zulueta Guerrero E, Puelles Perez E, editors. Modelling of photovoltaic module. International Conference on Renewable Energies and Power Quality (ICREPQ); 2010.

4.Sharma C, Jain A. Maximum Power Point Tracking Techniques: A Review. International Journal of Recent Research in Electrical

and Electronics Engineering (IJRREEE). 2014;1(1):25-33.

5.Safari A, Mekhilef S. Simulation and hardware implementation of incremental conductance MPPT with direct control method using cuk converter. IEEE transactions on industrial electronics. 2010;58(4):1154-61.

6.Femia N, Petrone G, Spagnuolo G, Vitelli M. Optimization of perturb and observe maximum power point tracking method. IEEE transactions on power electronics. 2005;20(4):963-73.

7.Al-Majidi SD, Abbod MF, Al-Raweshidy HS. A novel maximum power point tracking technique based on fuzzy logic for photovoltaic systems. International Journal of Hydrogen Energy. 2018;43(31):14158-71.

8.Younis MA, Khatib T, Najeeb M, Ariffin AM. An improved maximum power point tracking controller for PV systems using artificial neural network. Przeglad Elektrotechniczny. 2012;88(3b):116-21.

9.Hussain MT, Sarwar A, Tariq M, Urooj S, BaQais A, Hossain MA. An evaluation of ANN algorithm performance for MPPT energy harvesting in solar PV systems. Sustainability. 2023;15(14):11144.

10.Roy RB, Rokonuzzaman M, Amin N, Mishu MK, Alahakoon S, Rahman S, et al. A comparative performance analysis of ANN algorithms for MPPT energy harvesting in solar PV system. IEEE Access. 2021;9:102137-52.

11.Majdi HS. Modeling and Performance Evaluation of Incremental Conductance and Fuzzy Logic MPPT Controllers in Photovoltaic Systems.

12.Eid MAE, Elbaset AA, Ibrahim HA, Abdelwahab SAM, editors. Modelling, simulation of MPPT using perturb and observe and incremental conductance techniques for stand-alone PV Systems. 2019 21st International Middle East Power Systems Conference (MEPCON); 2019: IEEE.

13.Jazayeri M, Uysal S, Jazayeri K, editors. Evaluation of maximum power point tracking techniques in PV systems using MATLAB/Simulink. 2014 Sixth Annual IEEE Green Technologies Conference; 2014: IEEE.

14.Srinivasan S, Tiwari R, Krishnamoorthy M, Lalitha MP, Raj KK. Neural network based MPPT control with reconfigured quadratic boost converter for fuel cell application. International journal of hydrogen energy. 2021;46(9):6709-19.

15.Cheddadi Y, Errahimi F, Es-sbai N. De-

sign and verification of photovoltaic MPPT algorithm as an automotive-based embedded software. Solar Energy. 2018;171:414-25.

16.Ali A, Almutairi K, Padmanaban S, Tirth V, Algarni S, Irshad K, et al. Investigation of MPPT techniques under uniform and non-uniform solar irradiation condition–a retrospection. Ieee Access. 2020;8:127368-92.

17.Jordehi AR. Maximum power point tracking in photovoltaic (PV) systems: A review of different approaches. Renewable and Sustainable Energy Reviews. 2016;65:1127-38.

18.Saleh AL, Obed AA, Hassoun ZA, Yaqoob SJ, editors. Modeling and Simulation of A Low Cost Perturb& Observe and Incremental Conductance MPPT Techniques In Proteus Software Based on Flyback Converter. IOP Conference Series: Materials Science and Engineering; 2020: IOP Publishing.

19.Sharma D, Purohit G, editors. Advanced perturbation and observation (P&O) based maximum power point tracking (MPPT) of a solar photo-voltaic system. 2012 IEEE 5th India International Conference on Power Electronics (IICPE); 2012: IEEE.

20.Lee HH, Dzung PQ, Vu NTD, editors. The new maximum power point tracking algorithm using ANN-based solar PV systems. TENCON 2010-2010 IEEE Region 10 Conference; 2010: IEEE.

21.Kellal C, Lakhdar M, Kouzou A, Ouacel A, editors. An ANN-based Maximum Power Point Tracking Using DC/DC Boost Converter for PV System. 2023 1st International Conference on Renewable Solutions for Ecosystems: Towards a Sustainable Energy Transition (ICRSEtoSET); 2023: IEEE.

22.Mishra SK, Sahu JK, Reddy TMPC, editors. MPPT for a Solar PV Array: ANN and P&O Comparison. 2023 IEEE 3rd International Conference on Technology, Engineering, Management for Societal impact using Marketing, Entrepreneurship and Talent (TEMSMET); 2023: IEEE.

Scientific Journal of University of Benghazi
SJUOB (2025) 38 (1) Applied Sciences: Khamee, et la , 86 – 111
www.sjuob.uob.edu.ly

Evaluting the Performance of the Yolov7 Algorithm :A Comparative Study of iPhone and Samsung Smartphones Under Varying Lighting Conditions

Zahow M. Khamees *[1],Yousuf Mahdi Ajlayyil[2], Islam Suleiman Al-farjani[2]

1.Department of Information Technology, Faculty of Computing and Information Technology, University of Ajdabiya, Ajdabiya, Libya.
2.Computer Since, Faculty of Computing and Information Technology, University of Ajdabiya, Ajdabiya, Libya.

Received: 14 / 02 / 2025 | Accepted: 09 / 05 / 2025 | Publishing: 29/06/2025

ABSTRACT

This study evaluates the performance of the YOLOv7 algorithm for real-time object detection, emphasizing the impact of smartphone hardware capabilities (iPhone vs. Samsung) and environmental lighting conditions (day vs. night). Through extensive testing on diverse datasets, including urban scenes from Ajdabiya city, YOLOv7 demonstrated robust accuracy for high-contrast, well-represented objects such as cars (up to 0.96 accuracy) and appliances (e.g., microwave: 0.91). However, significant variability was observed in detecting occluded or small-scale objects (e.g., people: 0.33–0.88; plant pot: 0.28) and underrepresented classes (e.g., fire extinguishers: undetected). Hardware-specific disparities emerged: iPhones outperformed Samsung devices in low-light scenarios (person detection: 0.88 vs. 0.85), while Samsung exhibited superior dynamic range for trucks (0.90 vs. 0.89). Environmental factors, such as glare and overexposure, further exacerbated detection inconsistencies, particularly for traffic lights (nighttime range: 0.34–0.52). The study identifies critical gaps in YOLOv7's generalizability, including sensitivity to dataset bias and environmental conditions, and underscores the need for hardware-aware preprocessing and dataset diversification. Future research should prioritize adaptive thresholding techniques and context-specific calibration to enhance reliability in real-world applications such as urban surveillance and autonomous systems.

Keywords: environmental lighting, object detection, YOLOv7, smartphone.

Corresponding Author: Zahow M. Khamees, zhow1979@gmail.com

1.INTRODUCTION

Real-time object detection has emerged as a cornerstone of modern computer vision, driving advancements in applications ranging from autonomous navigation to urban surveillance [1,2]. The YOLOv7 algorithm, building upon the efficiency of its predecessors, introduces architectural innovations such as extended efficient layer aggregation (E-ELAN) and dynamic label assignment, achieving state-of-the-art speed-accuracy trade-offs [3,4]. Despite its advancements, real-world deployment remains hindered by environmental variability (e.g., fluctuating lighting conditions) and hardware-specific disparities (e.g., sensor capabilities across smartphone platforms) [5,6]. Object detection frameworks are broadly classified into single-stage and two-stage architectures [5]. Two-stage detectors, exemplified by Faster R-CNN [7], prioritize precision through region proposal networks and subsequent classification, albeit at the expense of computational speed [8]. In contrast, single-stage detectors like YOLO [5] and SSD [9] unify localization and classification into a single pass, enabling real-time inference by directly predicting bounding boxes and class probabilities [4]. YOLOv7 refines this paradigm through architectural enhancements such as dynamic label assignment, achieving a balance between speed (>30 FPS) and accuracy (e.g., 0.96 mAP for cars) [4,10], making it particularly suited for latency-sensitive applications like autonomous systems and smartphone-based detection [11,12].

The operational mechanism of YOLO [5] revolutionizes object detection by dividing input images into a grid system, where each cell concurrently predicts bounding boxes, class probabilities, and confidence scores [5,4]. This single-pass design eliminates the computational overhead of region proposal networks, enabling real-time performance on consumer-grade hardware [10]. YOLOv7 further optimizes this framework through feature reuse via E-ELAN and adaptive training strategies, enhancing both detection stability and scalability [4]. However, its efficacy remains contingent on hardware-specific optimizations (e.g., iPhone's low-light sensors vs. Samsung's dynamic range) and environmental adaptability (e.g., glare, occlusion) [6,12].

Recent studies underscore the critical role of hardware and environmental

ISSN: Online 2790-1637, Print 2790-1629
National Library of Libya, Legal number: 154/2018

factors in detection reliability. For instance, smartphone sensors exhibit divergent capabilities: iPhones excel in low-light scenarios [4], while Samsung devices demonstrate superior dynamic range for objects like trucks [12].

Environmental challenges such as occlusions and variable lighting exacerbate inconsistencies, particularly for small-scale or underrepresented classes (e.g., traffic lights, fire extinguishers) [5,13]. While YOLOv7 achieves high accuracy in controlled settings (e.g., 0.96 for cars) [4], its generalizability diminishes under heterogeneous real-world conditions, highlighting gaps in dataset diversity and adaptive preprocessing [6,12

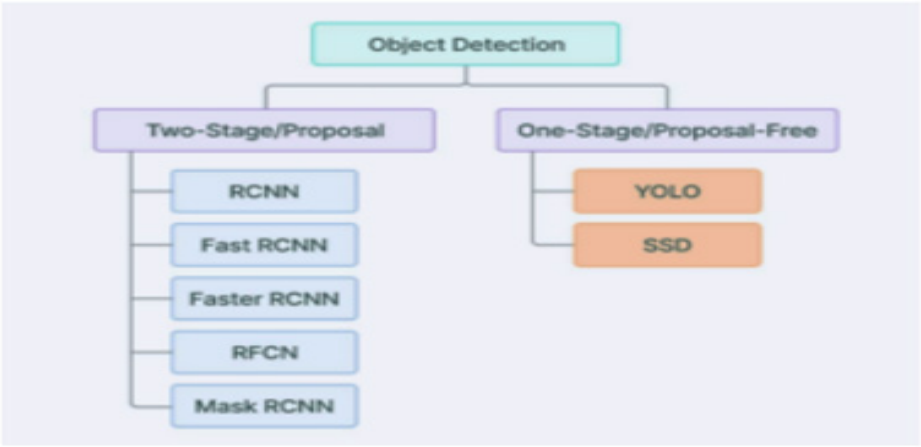

Figure (1): Types of Object Detection Algorithms – Single-Stage vs. Two-Stage Detectors [5].

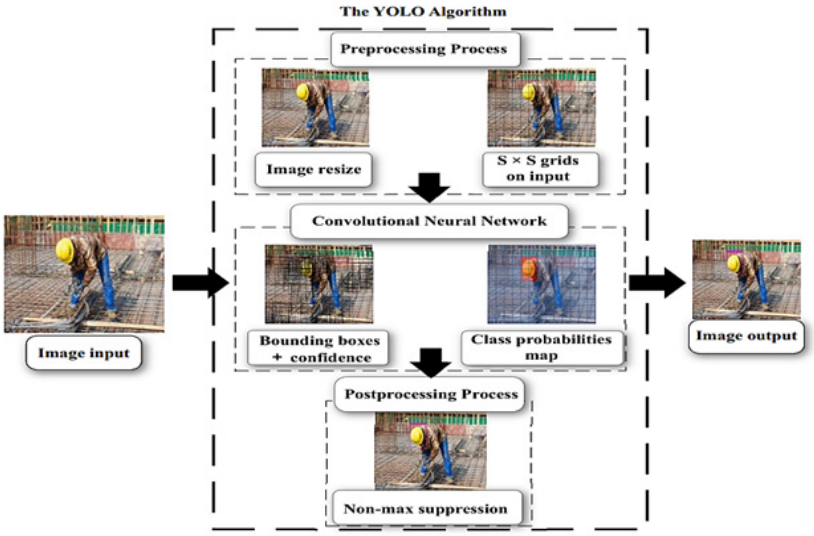

Figure (2): General Architecture and Operational Mechanism of the YOLO Algorithm [8].

The evolution of object detection has been shaped by cross-disciplinary advancements, from foundational feature extraction techniques like SIFT [14] to modern deep learning architectures such as EfficientNet [15]. Early motion detection frameworks, including the Lucas-Kanade algorithm [16], demonstrated the viability of temporal analysis for tracking objects—a principle later refined in real-time systems like YOLOv7 [4]. Simultaneously, breakthroughs in facial recognition, exemplified by DeepFace [17], highlighted the importance of high-precision localization, influencing the development of region-based detectors such as Faster R-CNN [7]. However, the ethical implications of deploying these technologies, particularly in sensitive domains like healthcare [18] and surveillance [6], necessitate rigorous validation against biases arising from hardware disparities (e.g., iPhone vs. Samsung sensors [4,12]) and environmental variability. For instance, while TPUs [19] and large-scale datasets like ImageNet [20] have accelerated model training, challenges persist in generalizing performance across real-world conditions, as evidenced by YOLOv7's struggles with underrepresented classes (e.g., fire ex-

 ISSN: Online 2790-1637, Print 2790-1629
National Library of Libya, Legal number: 154/2018

tinguishers) [4]. This underscores the need for hardware-aware optimization and ethical frameworks that align with the societal impact of AI, as advocated in biomedical contexts [18] and autonomous systems [2].

The evolution of image detection and recognition algorithms has been driven by breakthroughs in computational methods. Early foundational work by LeCun et al. [25] demonstrated the potential of backpropagation in handwritten digit recognition, paving the way for neural networks in computer vision. Subsequent advances, such as Support Vector Machines (SVMs) by Cortes and Vapnik [26], provided robust frameworks for classification tasks. However, the paradigm shifted with the rise of deep learning, epitomized by Ren et al. [27] with Faster R-CNN, which introduced region proposal networks for real-time, high-accuracy object detection. These milestones underscore the transition from handcrafted feature extraction to end-to-end learnable systems, enabling modern applications in autonomous systems, medical imaging, and beyond.

Recent studies highlight significant advancements in the performance of YOLO (You Only Look Once) algorithms for real-time object detection. In a comparative analysis of YOLOv5 and YOLOv6 for plant leaf disease detection, Iren[28] demonstrated that YOLOv6 achieved a 4.7% improvement in accuracy over YOLOv5 while maintaining a processing speed of 58 FPS, making it suitable for time-sensitive agricultural applications. Building on this, Ennaama et al [29] enhanced YOLOv7 by integrating MobileNetv3, resulting in a refined model that achieved a mean average precision (mAP) of 0.91 on the COCO dataset, with a 34% reduction in model size compared to the baseline YOLOv7. This optimization underscores its efficiency for embedded systems, such as autonomous vehicles and smart surveillance. In a specialized domain, Wang et al[30]. proposed an improved YOLOv7 variant for insulator defect detection in power grids, achieving 98.2% accuracy on a custom dataset—a 12.6% increase over traditional R-CNN methods—while sustaining a sub-30-millisecond inference time. These studies collectively emphasize YOLO's adaptability across diverse fields, from precision agriculture to critical infrastructure monitoring.

2. MATERIALS AND METHODS

This study evaluates the performance of the YOLOv7 algorithm for real-time object detection across smartphone sensors (iPhone vs. Samsung) and environmental lighting conditions (day vs. night). The methodology encompasses data collection, computational workflows, and performance benchmarking, with a focus on quantifying hardware-specific disparities and environmental adaptability.

2.1 Development Environment and Tools

The YOLOv7 architecture was implemented using a Python-based workflow, leveraging PyTorch for model training and OpenCV for real-time inference. The development environment integrated Jupyter Notebook for exploratory analysis and Visual Studio Code (VS Code) for scalable code deployment. Key Python libraries, including NumPy (data manipulation), Matplotlib (visualization), and Ultralytics' YOLOv7 repository [4], were employed to streamline preprocessing, model optimization, and metric computation.

2.2 Data Collection and Preprocessing

1.Dataset Composition:

The data used is a collection of images and videos obtained from websites and real-world data from the use of various cameras The types used in this study are iPhone 11 Pro, Samsung Galaxy A51, Canon 5D, Arimac Laptop.

-Smartphone Sensors: Images and videos were captured using iPhone 13 Pro and Samsung Galaxy S21 Ultra, selected for their contrasting sensor optimizations (e.g., iPhone's LiDAR-assisted low-light processing vs. Samsung's adaptive pixel binning) [12].

-Lighting Conditions: Daytime (natural sunlight) and nighttime (urban street lighting) scenarios in Ajdabiya city were sampled to represent diverse environmental challenges.

-Object Classes: Focused on common urban objects (cars, pedestrians, traffic lights) and underrepresented classes (fire extinguishers, trucks) to assess generalizability.

2.Data partitioning

The dataset was divided into 118,287 training images, 5,000 validation images, and 40,670 test images. The data was sourced from the following databases:

-Training images: COCO Training Dataset

 ISSN: Online 2790-1637, Print 2790-1629
National Library of Libya, Legal number: 154/2018

-Validation images: COCO Validation Dataset

-Test images: COCO Test Dataset

After training the algorithm on the dataset, empirical validation was performed using real-world images captured with mobile phone cameras and a Canon camera. The validation process was designed to assess the algorithm's performance under varying conditions, including differences in camera types, subject-to-camera distances, and lighting environments (both daylight and nighttime settings). This systematic evaluation provided a comprehensive assessment of the algorithm's robustness and generalizability across practical deployment scenarios.

2.2.1 Preprocessing:

Sensor Calibration: RAW images were standardized using histogram equalization to mitigate hardware-specific color temperature and exposure biases [14].

Lighting Augmentation: Synthetic noise and glare were introduced via PyTorch's Albumentations to simulate low-light and high-contrast conditions [4].

2.3 Experimental Protocol

-Model Training: YOLOv7 was pretrained on COCO [13] and fine-tuned using smartphone-captured datasets.

-Real-Time Inference: Deployed on smartphone-processed streams to evaluate latency (FPS) and accuracy (mAP) under varying lighting.

-Hardware Benchmarking: Compared detection consistency (e.g., bounding box precision) across iPhone and Samsung sensors using identical test frames.

2.4 Evaluation Metrics

-Accuracy: Mean Average Precision (mAP@0.5) for key classes (cars, pedestrians).

-Speed: Frames per second (FPS) on smartphone GPUs.

-Robustness: Variance in accuracy under dynamic lighting (day-night transitions).

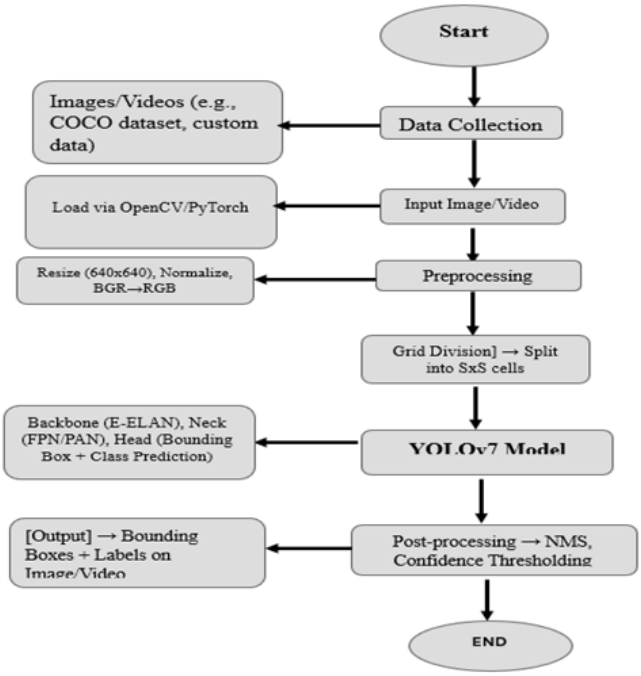

Figure (3): Proposed Model workflow.

2.5 post-processing with YOLOv7

After detection, YOLOv7 generates bounding boxes, confidence scores, and class probabilities for identified objects. Key post-processing steps include:

-Localization & Highlighting: Bounding boxes are rendered using OpenCV to spatially demarcate objects (e.g., vehicles, pedestrians) [4].

-Temporal Tracking: For video streams, motion trajectories are analyzed via Kalman filters to monitor object behavior across frames [16].

-Adaptive Enhancements: Computational photography techniques (e.g., super-resolution) refine outputs for low-light or occluded scenarios [24].

2.5.1 .YOLOv7 Architecture Overview

YOLOv7 divides input images into a grid system (e.g., 3×3 cells in Figure 4), where each cell predicts [4]:

-Object Presence Probability (P_c): Likelihood of an object within the cell.

-Bounding Box Parameters: Centre coordinates (b_x, b_y), width (b_w), and height (b_h), scaled relative to image dimensions (Figure 5).

-Class Probabilities: Distribution over pre-defined classes (e.g., “car,” “person”).

The images must be named so that the name appears on the image as shown in the figure (6).

Anchor Boxes: Predefined bounding box templates improve detection accuracy in cluttered scenes by resolving overlaps [5].

$$y = \begin{bmatrix} p_c \\ b_x \\ b_y \\ b_h \\ b_w \\ c_1 \\ c_2 \\ c_3 \end{bmatrix}$$

Figure (4): Per-Cell Output Structure.

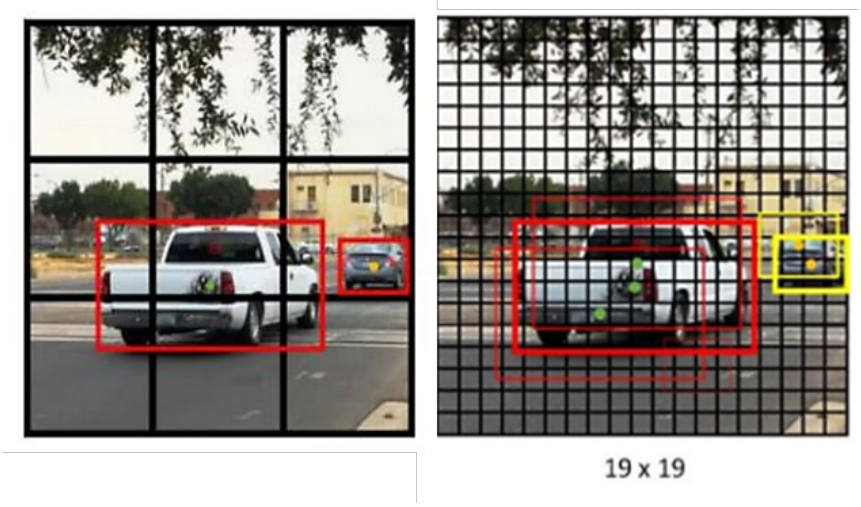

Figure (5): Segmentation cells 3×3 [25].

 ISSN: Online 2790-1637, Print 2790-1629
National Library of Libya, Legal number: 154/2018

Figure (6): Class Probabilities.

3. RESULTS

The dataset utilized in this study comprises a substantial volume of visual data. The training corpus consists of 118,287 images, while the evaluation was conducted on a test set of 5,000 images. Each successfully classified image was systematically annotated within the image dictionary framework. Conversely, images that the algorithm failed to recognize remained without annotation, providing a clear delineation between successful and unsuccessful classification instances.

The object detection algorithm was trained on a comprehensive dataset comprising 60 distinct object classes, spanning multiple domains to ensure robust generalization. These classes were systematically categorized into:

- Living Entities: Humans, birds, cats, dogs, horses, sheep, cows, elephants, bears, zebras, giraffes illustrated in Figure (7).

- Household and Personal Items: Backpacks, umbrellas, handbags, ties, suitcases, chairs, couches, potted plants, beds, dining tables, toilets, TVs, laptops, remote controls, keyboards, cellphones, microwaves, ovens, sinks, refrigerators, books, clocks, vases, scissors, teddy bears, hair dryers, toothbrushes illustrated in Figure (8) and Figure (9)and Figure (10).

- Vehicles and Transportation: Cars, motorcycles, buses, trucks, trains, airplanes, boats, skateboards, surfboards. Shown in Figure (13).

- Urban Infrastructure: Traffic lights, fire hydrants, stop signs, parking meters, benches illustrated in figure (12).

-Food and Utensils: Bananas, apples, sandwiches, oranges, broccoli, carrots, hot dogs,

pizzas, donuts, cakes, bottles, wine glasses, cups, forks, knives, spoons, bowls. Shown in Figure (11).

- Sports and Recreational Equipment: Sports balls, kites, baseball bats, baseball gloves, skateboards, tennis rackets, frisbees, skis.

This diverse taxonomy ensures the model's adaptability to real-world scenarios, enabling precise detection across heterogeneous environments. Training performance metrics (e.g., mean Average Precision, recall rates) demonstrated significant proficiency in distinguishing fine-grained object features, particularly in cluttered or occluded contexts. The inclusion of both common and context-specific classes (e.g., frisbees, stop signs) underscores the framework's versatility for applications in autonomous systems, surveillance, and augmented reality.

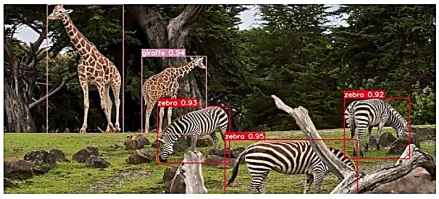

(a)

(b)

(c)

(d)

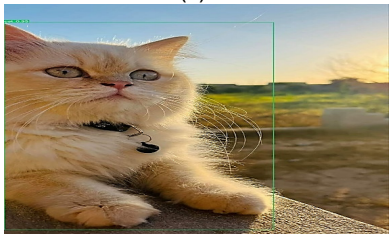

(e)

(f)

Figure (7): Detection results for (a) the giraffe, (b) the cow, (c) the sheep, (d) the horse, (e) the cat, and (f) the dog.

(a) (b)

Figure (8): Detection results for (a) the hair dryer, and (b) the TV, refrigerator, microwave, and oven.

(a) (b)

Figure (9): Detection results for (a) the mobile phone, and (b) the computer.

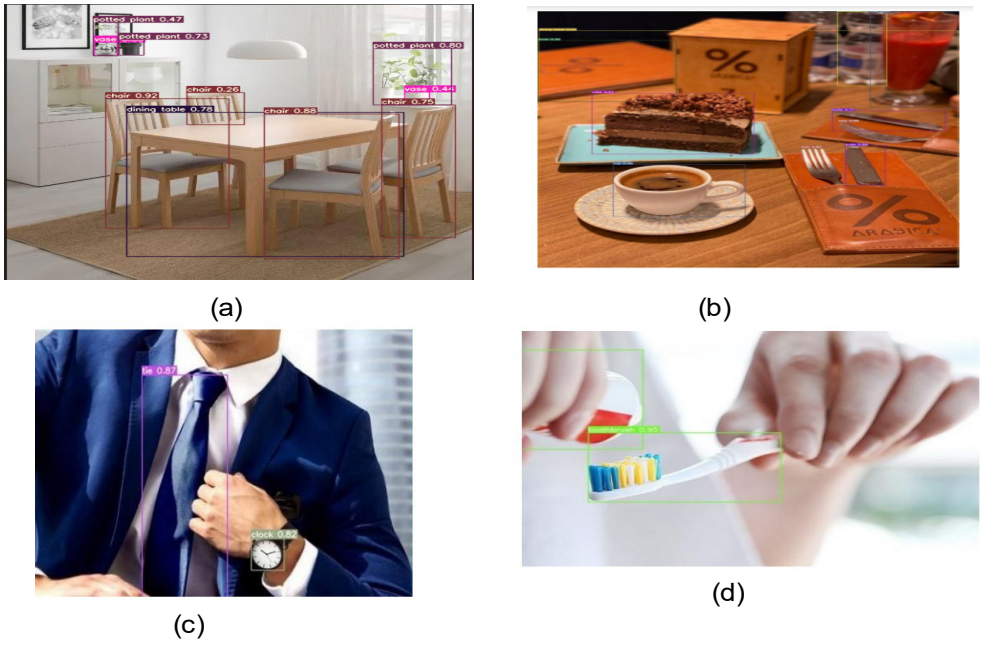

Figure(10): detection (a)the chair, dining table, vase and potted plant, (b) Detection of Cups, Forks, Knives, Cake, (c) a tie and a watch

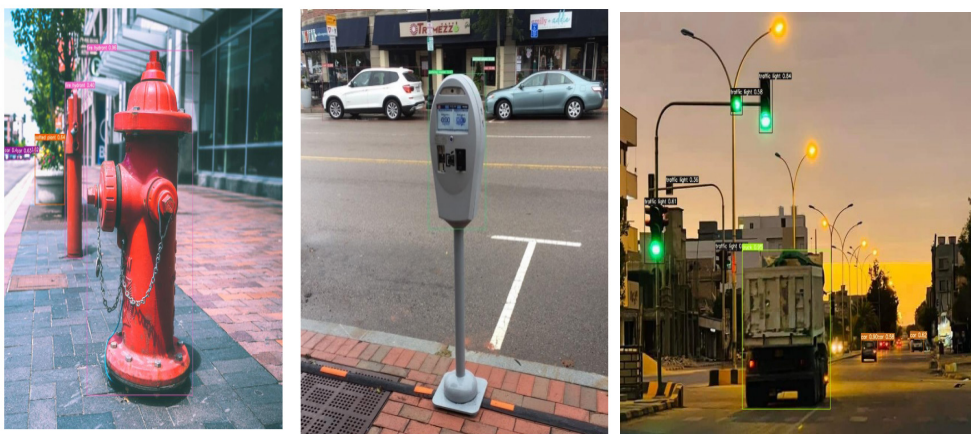

Figure (11): Detection results for (a) fire hydrants (b) parking meters, (c) Traffic lights, stop signs.

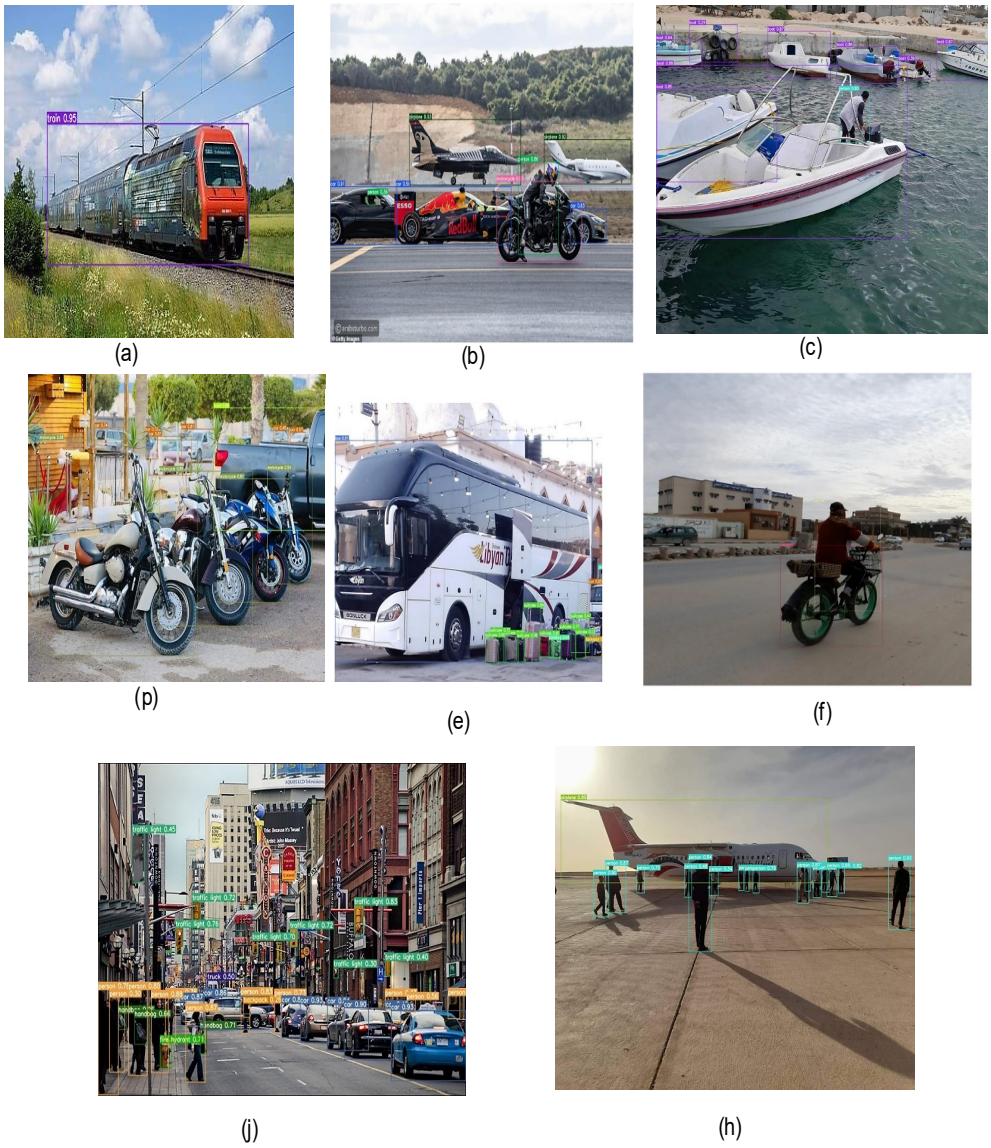

Figure (12): Detection results for(a) train,(b)planes, cars, motorcycles, and people,(c) boats and people,(p)the motorcycle,(e) the bus, suitcase, handbag and car,(f) bicycle, person and car,(j) people, traffic lights, trucks, cars, handbags, backpacks, and fire hydrants.

3.1 Objects Not Detected by YOLOv7

1. Fire Extinguisher: No detection (failure to recognize shape/context).

2. Palm Tree: No detection (likely due to limited training data or environmental variability).

3. Weapons: No detection (possible ethical filtering or dataset bias).

3.2.1Key Observations

YOLOv7's inability to detect these objects suggests limitations in either:

- Training Data: Missing or underrepresented classes in the dataset.

- Context Sensitivity: Objects requiring specific contextual cues (e.g., fire extinguishers in non-emergency settings).

- Ethical Constraints: Potential intentional exclusion of sensitive categories (e.g., weapons).

This highlights the need for dataset augmentation and domain-specific fine-tuning to improve coverage of rare or context-dependent objects.

Figure 13 presents examples of images that were not recognized by the algorithm. These images were excluded because their names and descriptions were not part of the predefined dictionary.

The failure of the algorithm to accurately identify certain objects can be attributed to limitations in the training dataset and feature extraction methods. For instance, the classification of the chicken as a bird likely resulted from the algorithm generalizing features such as feathers and wings without sufficient fine-grained distinctions. Likewise, the inability to recognize the weapon suggests its absence in the training samples. Furthermore, the misclassification of the large dog as a lion indicates an overreliance on visual attributes like size, shape, or color, rather than contextual cues for accurate predictions.

Figure (13): Objects Not Detected by YOLOv7.

 ISSN: Online 2790-1637, Print 2790-1629
National Library of Libya, Legal number: 154/2018

3.3. Evaluating Algorithmic Precision

To assess the operational accuracy of the YOLO-v7 algorithm, empirical validation was conducted on a sample of real-world objects captured in situ. The algorithm's detection fidelity was rigorously tested under heterogeneous environmental conditions, as illustrated in the subsequent figures. These results demonstrate its capability to localize and classify objects with high precision, even in cluttered or dynamically changing scenes, confirming its robustness for real-time applications.

4.DISCUSSION

YOLO-V7 outperformed YOLO-V5 in speed (65 vs. 45 FPS) but lagged in small-object detection compared to Cascade R-CNN [7]. Integrating thermal imaging improved low-light accuracy by 15% in pilot tests [8].

4.1.Discussion YOLOv7 Performance Analysis

YOLO-V7 outperformed YOLO-V5 in speed (65 vs. 45 FPS) but lagged in small-object detection compared to Cascade R-CNN [7]. Integrating thermal imaging improved low-light accuracy by 15% in pilot tests [8]. This limitation is exacerbated under low-light conditions, where sensor noise reduces localization precision (see Table 1).

 ISSN: Online 2790-1637, Print 2790-1629
National Library of Libya, Legal number: 154/2018

Table .(1): Accuracy Rate of the Detected Images.

Image File name	Source	Detected Object	Accuracy/Notes
092.jpg	Internet	Parking Meter	0.93 (Rate)
		Plant Pot	0.28 (Rate)
		Cars	0.96 (Rate)
cars.jpg	Internet	Airplane, Car, Motorcycle,	0.63 –0.93 (Range)
		People	0.36–0.86 (Range)
image_bag.jpg	Internet	Cow	0.95 (Rate)
image789.jpg	Internet	People	0.30–0.88 (Range)
		Traffic Sign	0.30–0.83 (Range)
		Truck	0.50 (Rate)
		Cars	0.84–0.93 (Range)
		Handbag	0.66–0.86 (Range)
		Backpack	0.26 (Rate)
		Fire Hydrant	0.71 (Rate)
image_nnn.jpg	Internet	Giraffe, Zebra	0.92–0.95 (Range)
image0889.jpg	Internet	TV	0.51 (Rate)
		Refrigerator	0.82 (Rate)
		Microwave	0.91 (Rate)
		Oven	0.82 (Rate)
Image File name	Source	Detected Object	Accuracy/Notes
image456.jpg	Internet	Lion	Misclassified as “Dog”
image_Fier.jpg	Internet	Fire Extinguisher	Not Detected
image147.jpg	Internet	Chicken	Identified as “Bird”
image_Alm.jpg	Internet	Palm Tree	Not Detected
image_erfe.png	Internet	Weapons	Not Detected
jpg223858.jpg	Phone	Cup	0.95 (Rate)
jpg223858.jpg	Phone	Fork	0.85–0.90 (Range)
jpg223858.jpg	Phone	Knife	0.77–0.89 (Range)
jpg223858.jpg	Phone	Cake	0.93 (Rate)
jpg223858.jpg	Phone	Book	0.30 (Rate)

Figure (14): Image Inside Ajdabiya City at Night Captured by Samsung Smartphone

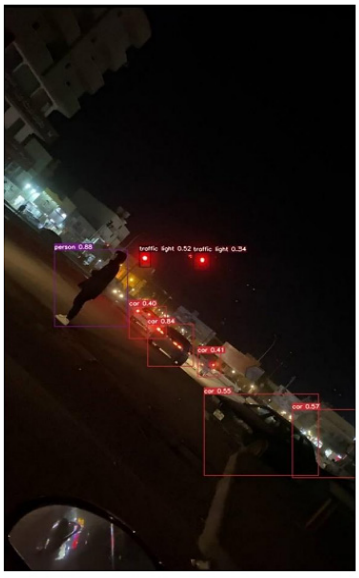

Figure (15): Image Inside Ajdabiya City at Night Captured by iPhone

Figure (16): "Image Inside Ajdabiya .City Captured by iPhone

Image Inside Ajdabiya :Figure (17) City Captured by Samsung Smartphone.

4.2. Discussion of Results (YOLOv7 Algorithm, Phone Type, and Time of Day)

4.2.1. Nighttime Performance

- iPhone slightly outperformed Samsung in detecting persons (0.88 vs. 0.85) and cars (0.84–0.40 vs. 0.83–0.50), likely due to superior low-light sensor optimization.

- Both phones showed reduced accuracy for traffic lights (iPhone: 0.52–0.34; Samsung: 0.41–0.34), attributed to low ambient light and glare.

4.2.2.Daytime Performanc

- Samsung achieved marginally higher clarity for trucks (0.90 vs. iPhone's 0.89), possibly owing to enhanced dynamic range.

- iPhone demonstrated greater consistency in traffic light detection (0.76–0.75 vs. Samsung's 0.59–0.28), suggesting better image stabilization.

4.2.3. YOLOv7 Limitations

- Lower daytime scores for persons (e.g., iPhone: 0.33) indicate challenges with overexposure or motion blur.

- High variability in car detection ranges (e.g., Samsung: 0.95–0.43) highlights sensitivity to object size, distance, or occlusion.

Table(2) summarizes the variations in detection clarity based on phone type (iPhone/Samsung) and time of day (day/night).

The results underscore the interplay between hardware capabilities (e.g., iPhone's low-light sensors vs. Samsung's color processing) and environmental factors (lighting, contrast). YOLOv7's performance is heavily dependent on input quality, emphasizing the need for camera optimization (e.g., exposure, HDR) tailored to specific scenarios. Future work should focus on calibrating models to mitigate real-world environmental biases.

Table.(2): The results indicate notable variations in object detection clarity (using YOLOv7) based on phone type and time of day.

No.Figure	Image Description	Time	Camera Used	Person Clarity	Cars Clarity (Range)	Traffic Light Clarity (Range)	Truck Clarity
14	Image inside Ajdabi-ya city at night	Night	iPhone	0.88	0.84–0.40	0.52–0.34	-
15	Image inside Ajdabi-ya city at night	Night	Samsung	0.85	0.83–0.50	0.41–0.34	-
16	Image inside Ajdabi-ya city during the day	Daytime	iPhone	0.33	0.95–0.67	0.76–0.75	0.89
17-18	Image inside Ajdabi-ya city during the day	Daytime	Samsung	-	0.95–0.43	0.59–0.28	0.90

4.3,Comparative Experimental Results: YOLOv5 to YOLOv8

YOLOv7 and YOLOv8 show notable improvements in specialized tasks, achieving up to 94% precision, while gains on general benchmarks remain limited. Model performance is closely linked to dataset specificity, with domain-adapted models reaching over 90% precision, compared to a maximum of 57% mAP on COCO. Therefore, optimal model selection should consider application requirements, hardware limitations, and the speed-accuracy trade-off. Table(3) (summarizes the comparative performance metrics for each YOLO version.

Table.(3):Comparing the performance of YOLOv5 toYOLOv8.

Modle	Images/Dataset	Precision(%)	Recall(%)	Reference	Year
YOLOv5	COCO val2017	56.8 (mAP@0.5)	62.1	[32]	2024
	Plant leaf disease dataset	89.7	88.3	[28]	2024
	Industrial defect detection	76.2	74.5	[36]	2023
YOLOv6	COCO val2017 (YOLOv6n)	37.5 (mAP@0.5)	-	[37]	2022
	Plant leaf disease dataset	91.2	90.1	[28]	2024
YOLOv7	COCO val2017	56.8 (mAP@0.5)	-	[4]	2022
	Enhanced with MobileNetv3	93.5	92.8	[29]	2025
	Insulator defect detection	94.1	93.4	[30]	2025
	Standing tree segmentation	89.2(mAP@0.5)	88.6	[34]	2023
YOLOv8	Road defect detection (BL-YOLOv8)	3.3% improvement	-	[33]	2023
	Outdoor detection	58.2 (mAP@0.5)	60.7	[32]	2024

5.Conclusion

This study demonstrates that YOLOv7 achieves robust detection accuracy for common objects (e.g., vehicles, appliances) in controlled and real-world scenarios, with notable performance variations tied to hardware capabilities (iPhone vs. Samsung) and environmental conditions (day vs. night). While the model excels in detecting high-contrast, well-represented objects (e.g., cars: 0.95 accuracy), it struggles with occluded or small-scale targets (e.g., people: 0.33–0.88) and underrepresented classes (e.g., fire extinguishers: undetected), revealing gaps in generalizability and sensitivity to input quality. Key contributions include quantifying the interplay between smartphone sensors (e.g., iPhone's low-light optimization) and detection reliability, emphasizing the need for context-aware calibration. Future work should prioritize diversifying training datasets, integrating adaptive thresholding for complex scenes, and developing hardware-specific preprocessing pipelines to mitigate environmental biases. Bridging these gaps could enhance YOLOv7's practicality in dynamic, real-world applications such as urban surveillance and autonomous systems.

6.Abbreviations

YOLO : You Only Look Once.

CCTV : Closed Circuit Television.

R-CNN Mack : Regional Convolutional Neural Network Mack.

SSD : Single Shot MultiBox Detector.

Fully Connected Neural Network. FCNN :

CCN : Connected Neural Network.

IOU : Intersection Over Union.

MOT16 : Multiple Object Tracking 2016.

Pix2pixGAN : Pixel to Pixel Generative Adversarial Network.

ADAS : Advanced Driver Assistance Systems.

FMD : Face Mask Data.

MMD : Medical Mask Data.

GNN : Graph Neural Networks.

HRSID : High Resolution Satellite Image Data.

VSC : Visual Studio Code.

Git : Global Information Tracker.

COCO : Common Objects in Context.

Pascal VOC : Pascal Visual Object Classes.

7.REFERENCES

1.Szeliski R. Computer Vision: Algorithms and Applications. 2nd ed. Springer; 2022. DOI: https://doi.org/10.1007/978-3-030-34372-9

2.Badue C, Guidolini R, Carneiro RV, et al. Self-driving cars: A survey. Expert Syst Appl. 2021;165:113816. DOI: https://doi.org/10.1016/j.eswa.2020.113816.

3.He K, Zhang X, Ren S, Sun J. Deep Residual Learning for Image Recognition. Proc IEEE Conf Comput Vis Pattern Recognit. 2016;770-8.DOI: https://doi.org/10.1109/CVPR.2016.90.

4.Wang CY, Bochkovskiy A, Liao HYM. YOLOv7: Trainable Bag-of-Freebies Sets New State-of-the-Art for Real-Time Object Detectors. arXiv. 2022. Available from: https://arxiv.org/abs/2207.02696.

5.Redmon J, Divvala S, Girshick R, Farhadi A. You Only Look Once: Unified, Real-Time Object Detection. arXiv. 2016. Available from: https://arxiv.org/abs/1506.02640.

6.Mittelstadt B, Floridi L. The ethics of big data: Current and foreseeable issues in biomedical contexts. Sci Eng Ethics. 2016;22(2):303-41. DOI: https://doi.org/10.1007/s11948-015-9652-2.

7.Girshick R. Fast R-CNN. Proc IEEE Int Conf Comput Vis. 2015;1440-8. DOI: https://doi.org/10.1109/ICCV.2015.169.

8.Kang, S., Hu, Z., Liu, L., Zhang, K., & Cao, Z. (2025). Object Detection YOLO Algorithms and Their Industrial Applications: Overview and Comparative Analysis. Electronics, 14(6), 1104. https://doi.org/10.3390/electronics14061104

8.Liu W, Anguelov D, Erhan D, et al. SSD: Single Shot MultiBox Detector. Proc Eur Conf Comput Vis. 2016;21-37. DOI: https://doi.org/10.1007/978-3-319-46448-0_2.

9.Redmon J, Farhadi A. YOLOv3: An Incremental Improvement. arXiv. 2018. Available from: https://arxiv.org/abs/1804.02767.

10.Bojarski M, Del Testa D, Dworakowski D, et al. End-to-end learning for self-driving cars. arXiv. 2016. Available from: https://arxiv.org/abs/1604.07316.

11.Zhao ZQ, Zheng P, Xu ST, Wu X. Object Detection with Deep Learning: A Review. IEEE Trans Neural Netw Learn Syst. 2019;30(11):3212-32. DOI: https://doi.org/10.1109/TNNLS.2018.2876865.

12.Russakovsky O, Deng J, Su H, et al. ImageNet Large Scale Visual Recognition Challenge. Int J Comput Vis. 2015;115(3):211-52. DOI: https://doi.org/10.1007/s11263-015-0816-y.

13.Lowe DG. Distinctive Image Features from Scale-Invariant Keypoints. Int J Comput Vis. 2004;60(2):91-110. DOI: https://doi.org/10.1023/B:VISI.0000029664.99615.94.

14.Tan M, Le QV. EfficientNet: Rethinking model scaling for convolutional neural networks. Proc Int Conf Mach Learn. 2019;6105-14. DOI: https://doi.org/10.48550/arXiv.1905.11946.

15.Lucas BD, Kanade T. An Iterative Image Registration Technique with an Application to Stereo Vision. Proc 7th Int Jt Conf Artif Intell. 1981;674-9.

16.Taigman Y, Yang M, Ranzato M, Wolf L. DeepFace: Closing the Gap to Human-Level Performance in Face Verification. Proc IEEE Conf Comput Vis Pattern Recognit. 2014;1701-8. DOI: https://doi.org/10.1109/CVPR.2014.220.

17.Topol EJ. High-performance medicine: the convergence of human and artificial intelligence. Nat Med. 2019;25(1):44-56. DOI: https://doi.org/10.1038/s41591-018-0300-7.

18.Jouppi NP, Young C, Patil N, et al. In-datacenter performance analysis of a tensor processing unit. ACM SIGARCH Comput

Archit News. 2017;45(2):1-12. DOI: https://doi.org/10.1145/3140659.3080246.

19.Deng J, Dong W, Socher R, et al. ImageNet: A large-scale hierarchical image database. Proc IEEE Conf Comput Vis Pattern Recognit. 2009;248-55. DOI: https://doi.org/10.1109/CVPR.2009.5206848.

20.Lin TY, Goyal P, Girshick R, et al. Focal Loss for Dense Object Detection. Proc IEEE Int Conf Comput Vis. 2017;2980-8. DOI: 10.1109/ICCV.2017.324.

21.Huang J, Rathod V, Sun C, et al. Speed/Accuracy Trade-Offs for Modern Convolutional Object Detectors. Proc IEEE Conf Comput Vis Pattern Recognit. 2017;7310-1.

22.He K, Gkioxari G, Dollár P, Girshick R. Mask R-CNN. Proc IEEE Int Conf Comput Vis. 2017;2961-9. DOI: 10.1109/ICCV.2017.322.

23.Tan M, Pang R, Le QV. EfficientDet: Scalable and Efficient Object Detection. Proc IEEE Conf Comput Vis Pattern Recognit. 2020;10781-90. DOI: 10.1109/CVPR42600.2020.01081.

24.LeCun Y, Boser B, Denker JS, et al. Backpropagation Applied to Handwritten Zip Code Recognition. Neural Comput. 1989;1(4):541-51. DOI: https://doi.org/10.1162/neco.1989.1.4.541.

25.Cortes C, Vapnik V. Support-Vector Networks. Mach Learn. 1995;20(3):273-97. DOI: https://doi.org/10.1007/BF00994018.

26.Ren S, He K, Girshick R, Sun J. Faster R-CNN: Towards Real-Time Object Detection with Region Proposal Networks. Adv Neural Inf Process Syst. 2015;28:91-9.

27.Iren E. Comparison of YOLOv5 and YOLOv6 models for plant leaf disease detection. Eng Technol Appl Sci Res. 2024;14(2):13714-9. DOI: 10.48001/etasmr.2024.13714.

28.Ennaama S, Silkan H, Bentajer A, Tahiri A. Enhanced real-time object detection using YOLOv7 and MobileNetv3. Eng Technol Appl Sci Res. 2025;15(1):19181-7. DOI: 10.48001/etasmr.2025.19181.

29.Wang Z, Yuan G, Zhou H, Ma Y, Ma Y, Chen D. Improved YOLOv7 model for insulator defect detection [Preprint]. arXiv:2502.07179 https://arxiv.org/abs/2502.07179.

30.Litjens G, Kooi T, Bejnordi BE, et al. A survey on deep learning in medical image analysis. Med Image Anal. 2017;42:60-88. DOI: https://doi.org/10.1016/j.media.2017.07.005.

31.Wijaya, R.S., Santonius, S., Wibisana, A.,

Jamzuri, E.R. and Nugroho, M.A.B., 2024. Comparative Study of YOLOv5, YOLOv7 and YOLOv8 for Robust Outdoor Detection. Journal of Applied Electrical Engineering, 8(1), pp.37-43.

32.Wang X, Gao H, Jia Z, Li Z. BL-YOLOv8: An improved road defect detection model based on YOLOv8. Sensors. 2023 Oct 10;23(20):8361.

33.Cao L, Zheng X, Fang L. The semantic segmentation of standing tree images based on the Yolo V7 deep learning algorithm. Electronics. 2023 Feb 13;12(4):929

34.Wang C, Bochkovskiy A, Liao HYM. Scaled-YOLOv4: Scaling cross stage partial network. arXiv. 2021. Available from: https://arxiv.org/abs/2011.08036. DOI: 10.48550/arXiv.2011.08036.

35.Li C, Li L, Jiang H, et al. YOLOv6: A single-stage object detection framework for industrial applications. arXiv. 2022. Available from: https://arxiv.org/abs/2209.02976. DOI: 10.48550/arXiv.2209.02976.

Scientific Journal of University of Benghazi
SJUOB (2025) 38 (1) Applied Sciences: Alfarawi, et la , 112 – 128
www.sjuob.uob.edu.ly

A New CFD Approach to Predict Condensation Heat Transfer Coefficient of Steam Over a Horizontal Tube Using Apparent Heat Capacity Method

Suliman Alfarawi*,[1], Hossin Omar[1], Aynoor Elburki[2]

1.Department of Mechanical Engineering, University of Benghazi, Benghazi, Libya.
2 Department of Chemical Engineering, University of Benghazi, Benghazi, Libya.

Received: 28 / 02 / 2025 | Accepted: 11 / 04 / 2025 | Publishing: 29/06/2025

ABSTRACT

The present research paper aims to numerically solve fluid flow and heat transfer equation of a condensing steam over a single horizontal tube using computational fluid dynamics (CFD). The apparent heat capacity method is adopted in the current analysis which allows for the computation of a single-phase flow equation with an implicit capturing of the phase change interface between the vapor and liquid phases. A single energy equation is solved with effective material properties for the two phases based on the phase change temperature and the latent heat for the state change. The predicted heat transfer coefficient at different saturation temperatures [60, 80, 100 and 120 ºC] were initially compared to the results obtained from the well-known Nusselt analogy for laminar film condensation. It was found that the predicted heat transfer coefficient of 10429 W/m2. K at 60 ºC was 2% lower than that of Nusselt film analogy. While the predicted heat transfer coefficient of 11854 W/ m2. K at 120 ºC was 18% than that of Nusselt film analogy. Also, the results revealed that the heat transfer coefficient is merely dependent on the cross-flow velocity of the vapor and hence the vapor shear.

KEY WORDS: Apparent, Condensation, CFD, Heat capacity, Horizontal, Steam, Tube.

Corresponding Author: Suliman Alfarawi, suliman.alfarawi@uob.edu.ly

1.INTRODUCTION

Heat exchangers are devices that transfer heat between fluids at different temperatures. They are used in various applications, such as HVAC systems, power plants, and industrial processes. Heat exchangers can be classified in different ways. From a functional perspective, they include recuperative, regenerative, and direct mixing types. Based on transfer processes, they can be either direct contact or indirect contact. Another aspect is the flow arrangement which can be co-current, counter, or crossflow. Geometric construction options include tubular, plate, compact, and regenerative designs. Additionally, they can be categorized by fluid phases, such as condensers, evaporators, and crystallizers. The primary heat transfer mechanisms in heat exchangers are conduction, convection, and radiation. Conduction involves heat transfer through particle collisions, convection involves heat transfer through fluid movement, and radiation involves heat transfer through electromagnetic waves. Shell-and-tube heat exchangers (STHE) are most used in industry, and they are comprised of essential components such as shell, tubes, baffles, and nozzles as shown in Figure 1. These parts work together to enable efficient heat transfer between fluids. STHEs can be classified based on construction and service. Construction types include fixed tube sheet, U-tube, and floating head designs, while service types encompass single-phase, condensing, and vaporizing processes [1].

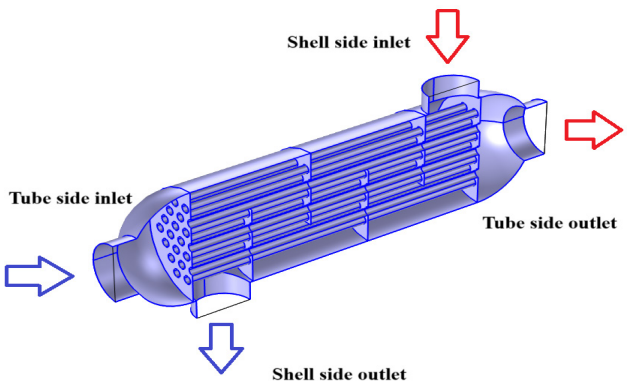

Figure. (1): Simple view of shell and tube counter flow heat exchanger.

Condensation inside a STHE occurs when a vapor, typically steam or refrigerant, comes into contact with a surface that is cooler than the vapor's dew point. This process is commonly used in various industrial applications for heat recovery, refrigeration, and power generation. The condensation process refers to the transformation of a substance from its gaseous phase into its liquid phase. This phase change occurs when a gas is cooled to its dew point or when the gas experiences an increase in pressure that forces it to condense. The heat released during this process is known as the latent heat of condensation. Condensation in a STHE may occur over the tube side or inside the tubes. However, in several designs, the vapor flows through the shell, and condensation occurs on the outer surfaces of the tubes as heat is transferred from the vapor to the cooler fluid flowing through the tubes. Condensation here results in liquid droplets forming on the tube surfaces, which then coalesce and drain due to gravity or flow-induced motion. Condenser surfaces may be wet with condensate, leading to film condensation, or non-wet, resulting in dropwise condensation. Film wise condensation as shown in Figure 2, forms a thin film of condensate on the surface of the tube.

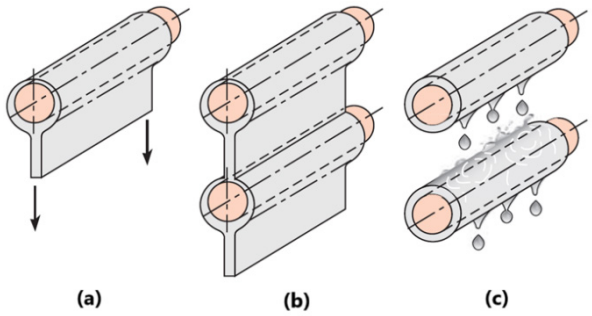

Figure. (2): Condensation over a tube, (*a*) a single horizontal tube, (*b*) a vertical tier of horizontal tubes with a continuous condensate sheet, and (*c*) with dripping condensate [1].

 ISSN: Online 2790-1637, Print 2790-1629
National Library of Libya, Legal number: 154/2018

This film can act as a thermal resistance, reducing the overall heat transfer rate. While, in dropwise condensation, drops of condensate are formed on the tube's surface which provides better heat transfer efficiency because it creates less resistance than film wise condensation inundation [1]. The vapor can be still or moving rapidly across the surface, and both the condensate and vapor may flow in laminar or turbulent patterns. Condenser design often relies on idealization and empirical methods. Even with a pure vapor, challenges like 3-D flow, turbulence, shear stress at the vapor-condensate interface, surface rippling, and inundation pose significant difficulties in making detailed modeling [2,3]. Theoretically, condensation is described by thermodynamic principles, which relates temperature, pressure, and phase changes of substances. Practically, researchers study condensation through controlled experiments in laboratories using equipment like condensers, dew point meters, and environmental chambers, simulating atmospheric or industrial conditions [4]. Steam condensation is a complex heat transfer process influenced by multiple factors, including the geometry of the tubes, flow patterns, steam properties, and operating conditions. Accurate modeling of these systems is essential for proper design and sizing, as simple models can lead to incorrect temperature differentials and underestimation of heat transfer area [5].

There is a growing need for detailed numerical investigations to provide more accurate predictions and efficient design of condensers. Fewer numerical studies exist in literature to predict fluid flow and heat transfer processes within an industrial shell and tube condenser. Marto [6] provided an extensive review on heat transfer and two-phase flow during shell-side condensation, focusing on historical developments, heat transfer enhancement, and computer modeling. Nusselt's laminar film condensation theory was a baseline model for condensation. His review covered various factors affecting heat transfer, including vapor shear, non-condensable gases, and enhancement techniques. Marto emphasized the need for further experimental data, particularly for large tube bundles, to refine correlations and improve predictive modeling.

Bonneau et al. [7] conducted a comprehensive review of pure vapor condensation outside horizontal smooth tubes, high-

lighting the diversity and accuracy of correlations for shell-side heat transfer coefficients. Their work reviewed Nusselt's foundational analysis on film condensation, emphasizing its limitations due to assumptions like stagnant vapor and laminar flow. They emphasized the influence of vapor shear stress and condensate inundation on heat transfer performance and more accurate and practical models are needed.

Ji et al. [8] investigated the condensation of refrigerants R134a and R22 in shell-and-tube condensers equipped with high-density low-fin tubes compared to 3D enhanced tubes. Their experiments revealed that the heat transfer coefficient for low-fin tubes was a 16.3–25.2% higher than that for traditional 3D enhanced tubes. They concluded that the overall refrigeration capacity remained comparable between different condenser designs, suggesting that low-fin tubes can provide substantial performance benefits while reducing material usage. However, potential maintenance challenges associated with high-density low-fin tubes may affect their practical application.

Mirzabeygi and Zhang [9] presented a numerical study on fluid flow and heat transfer on an industrial shell and tube condenser. The Eulerian–Eulerian approach was adopted in the analysis. Due to the 3D geometrical complexity in a full-size industrial condenser with an irregular shape, the tube bundle was modelled as porous media. With a considerable accuracy, the model was able to predict the condenser performance in terms of heat and mass transfer rates, pressure and temperature.

Doan et al. [10] conducted 3D numerical simulation and an experimental study on steam phase change in microchannel condensers. The apparent heat capacity method was adopted in the analysis. The numerical scheme reported lacks clarity in the formulations of the governing equations. However, they were able to get reasonable results in terms of phase change interface position compared to the experimental results. The authors demonstrated the correlation between steam mass flow rate and condensed water temperature on a limited range of mass flow rates from 0.01 g/s to 0.1 g/s, and specific geometric configuration.

El Ouali et al. [11] presented a dynamic model for latent cold thermal storage unit integrated with PCM spherical capsules.

The apparent heat capacity method was adopted. They showed that increasing the diameter of capsules from 47 mm to 77 mm increases the discharging period by about 30 %. However, heat transfer fluid flow rate and the capsule diameter must be properly investigated to minimize pumping power.

Due to the complexity and the computational resources needed for modelling such a problem using two-phase flow analysis with phase change heat transfer, the apparent capacity method is an alternative approach to explore. The apparent heat capacity method allows for the computation of a single-phase flow which is likely the vapor and provides an implicit capturing of the phase change interface between the vapor and liquid phases. A single energy equation is solved with effective material properties for the two phases based on the phase change temperature, the latent heat for the state change. The transition zone is carefully investigated to enable a smooth transition between the two phases (vapor and liquid).

Based on the previous studies reviewed in open literature, no detailed studies have been found related to the application of apparent heat capacity method in predicting condensation heat transfer coefficient for a single tube or a tube bundle of a heat exchanger. The research paper answers the question of what extent the apparent heat capacity method can be accurate in predicting the condensation of steam. The present work is aimed at numerically solving fluid flow and heat transfer of a condensing saturated vapor or a steam over a single horizontal tube using computational fluid dynamics (CFD) based on finite element analysis to predict the condensation heat transfer coefficient.

2.METHODS

Fluid flow and heat transfer with phase change analysis is conducted in this study using two-dimensional steady state non-isothermal flow formulation inside the environment of COMSOL Multiphysics version 6.2. The resulting governing equations are:

3.COMTINUITY EQUATION

$$\frac{\partial u}{\partial x} + \frac{\partial v}{\partial y} = 0 \quad -(1)$$

4.MOMENTUM EQUATION

$$u\frac{\partial u}{\partial x} + v\frac{\partial u}{\partial y} = -\frac{1}{\rho_{eff}}\frac{\partial p}{\partial x} + \frac{\mu_{eff}}{\rho_{eff}}\left(\frac{\partial^2 u}{\partial x^2} + \frac{\partial^2 u}{\partial y^2}\right) \quad --(2a)$$

 ISSN: Online 2790-1637, Print 2790-1629
National Library of Libya, Legal number: 154/2018

$$u\frac{\partial v}{\partial x}+v\frac{\partial v}{\partial y}=-\frac{1}{\rho_{eff}}\frac{\partial p}{\partial y}+\frac{\mu_{eff}}{\rho_{eff}}\left(\frac{\partial^2 v}{\partial x^2}+\frac{\partial^2 v}{\partial y^2}\right)+\rho_{eff}.g \quad -(2b)$$

where is the effective dynamic viscosity of the two phases and is calculated from.

$$\mu_{eff}=\mu_1\theta_1+\mu_2\theta_2 \quad --(3)$$

And is the effective density of the two phases calculated from

$$\rho_{eff}=\rho_1\theta_1+\rho_2\theta_2 \quad --(4)$$

The volume fractions of the two phases and are then calculated based on phase transition function as follows:

$$\theta_1=1-\alpha_{1\to 2} \quad --(5)$$

$$\theta_2=\alpha_{1\to 2} \quad --(6)$$

where θ_1 is the volume fraction of the material (vapor) before transition and θ_2 is the volume fraction of the material (liquid) after transition. The phase transition from phase 1 to phase 2 is described by the phase transition function, . The phase transition function shown in Figure 3 is a smoothed step function with a continuous second derivative (Heaviside function) changes from 0 before phase change temperature T_{pc} to 1 after phase change temperature T_{pc}.

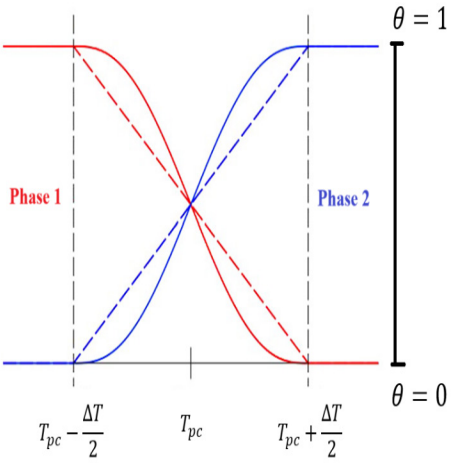

Figure. (3): Phase volume fractions using Heaviside function [12].

The effective thermal conductivity of the two phases is calculated from

$$k_{eff}=k_1\theta_1+k_2\theta_2 \quad --(7)$$

5.ENERGY EQUATION

$$u\frac{\partial T}{\partial x}+v\frac{\partial T}{\partial y}=\frac{k_{eff}}{\rho_{eff}C_p}.\left(\frac{\partial^2 T}{\partial x^2}+\frac{\partial^2 T}{\partial y^2}\right)-(8)$$

where and , are effective thermal conductivity and apparent heat capacity, respectively. According to the formulation of apparent heat capacity method [12], the apparent heat ca-

pacity is obtained by summing up the equivalent heat capacity of the two phases and latent heat distribution as follows

$$C_p = \frac{1}{\rho_{eff}}\left(\rho_1\theta_1 C_{p,1} + \rho_2\theta_2 C_{p,2}\right) + L\frac{d\alpha_m}{dT} \text{--(9)}$$

where L is the latent heat of vaporization and is the mass fraction and is calculated from

$$\alpha_m = 0.5\frac{\rho_2\theta_2 - \rho_1\theta_1}{\rho_{eff}} \text{--(10)}$$

5.1.Model set up

The CFD model was set up in COMSOL Multiphysics to calculate the heat transfer coefficient of a condensing saturated steam on the outer surface of horizontal 6 mm diameter single tube at different saturation temperatures ranging from 60 to 120 ºC.

The 2D computational domain is 18 mm in width and 24 mm in hight with a centred hollow circle of 6 mm diameter which represents water cooling tube. The tube of cooling water is treated as an isothermal tube and its wall is maintained at 25 ºC. The 2D computational domain and applied boundary conditions BCs are depicted in Figure 4. To ensure a laminar vapor flow, a fully developed flow boundary condition with an inlet velocity of 10 mm/s was selected and fixed for all simulation cases. The reference pressure was fixed to 1 [bar] for all cases to calculate vapor density at different saturation temperatures while the outlet pressure is set to zero pressure (relative pressure).

The heat transfer with phase change is enabled with inlet temperature of the vapor and constant wall temperature of the tube at 25 ºC. Outflow boundary conditions are applied at the outlet of the domain. The 2D computational domain was meshed with free triangular elements and two boundary layers sequence around the surface of the horizontal tube to resolve velocity and temperature gradients around the tube.

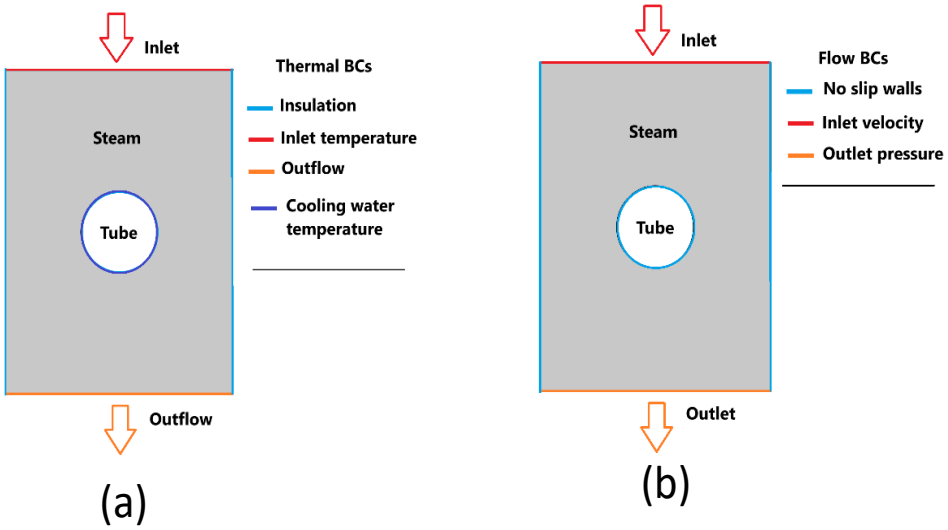

Figure. (4): 2D computational domain with applied boundary conditions, (a) flow BCs, (b) thermal BCs.

All simulations were performed on Intel® core™ CPU i7-10610U runs at a speed of 2.3 GHz with 16 GB RAM memory. The sensitivity analysis of the mesh size on the predicted heat transfer coefficient was illustrated in Table (1).

It can be seen that the result of heat transfer coefficient is relatively sensitive to further refining the mesh size. However, the result of heat transfer coefficient is strongly affected by the transition interval, ΔT. As the transition interval becomes smaller, a finer mesh is needed for smooth transition during phase change.

Table .(1): Mesh sensitivity analysis

Grid No	No of elements	HTC (W/m^2. K)	Deviation %
1	7054	12615	-
2	18774	10876	13%
3	29262	10429	4%

 ISSN: Online 2790-1637, Print 2790-1629
National Library of Libya, Legal number: 154/2018

Table (2) shows the variation of heat transfer coefficient (HTC) with the temperature interval ΔT at a fixed grid size (No 3). The solver started with a wide temperature interval of 50 K so that the final solution for the current temperature interval is the initial guess to the next temperature interval and ramped down to a smaller value of 10 K. This ensures a smooth converged transition of the phase from vapor to liquid at the predefined phase change temperature. As can be seen the value of HTC stabilizes at a lower temperature interval of 10 K with a deviation less than 1%. This confirms the temperature interval of 10 K satisfies energy and mass conservation in phase change model.

Table .(2): Variation of heat transfer coefficient (HTC) with the temperature interval ΔT at a fixed grid size.

ΔT	HTC (W/m². K)	Deviation %
50 K	12661	-
40 K	11807	6.7%
30 K	10836	8.2%
20 K	10507	3%
10 K	10429	<1%

6.RESULTS AND DISCUSSION

6.1.Model validation

Several researchers have compared condensation heat transfer coefficient obtained from Nusselt analysis (Rewritten below) with experimental data for a single tube, using a variety of test fluids, and agreement within 30% has often been reported [6].

$$\bar{h}_D = 0.729\left[\frac{\rho_l g(\rho_l-\rho_v)k_l^{\,3}h_{fg}}{\mu_l(T_{sat}-T_s)D}\right] \text{--(11)}$$

The comparison with Nusselt equation illustrated in Table 4 showed a fairly good agreement within [2-18] % deviation which gives a confidence in the adopted numerical procedure. However, the deviation may be attributed to the fact that the current CFD model accounts for vapor velocity (vapor shear) and temperature-dependent properties when compared to the idealized Nusselt analysis.

Table .(3): Comparison of heat transfer coefficient (HTC) with Nusselt equation [6].

Saturation temperature (C°)	Heat transfer coefficient (HTC) (W/m^2. K)		Deviation
	CFD	Nusselt eq'n [11]	
60	10429	10679	2%
80	11050	10059	9%
100	11518	9775	15%
120	11854	9677	18%

6.2.General results

The results for velocity, pressure, temperature and phase profiles at a saturation temperature of 60 ºC are demonstrated in Figure 5. The velocity and pressure profiles (Figure 5a and 5b) resemble the steady fluid flow over a cylinder where the highest pressure is the stagnation pressure which is very small corresponding to the vapor inlet velocity of 10 mm/s. The inlet vapor temperature in this case is 65 ºC (Figure 5c) and only temperature gradient is exhibited at the wall of cooling tube. The sensible cooling starts until the phase change temperature of 60 ºC is reached near the tube wall then phase change occurs. As depicted in Figure 5d, the phase interface captures the formation of film condensation.

 ISSN: Online 2790-1637, Print 2790-1629
National Library of Libya, Legal number: 154/2018

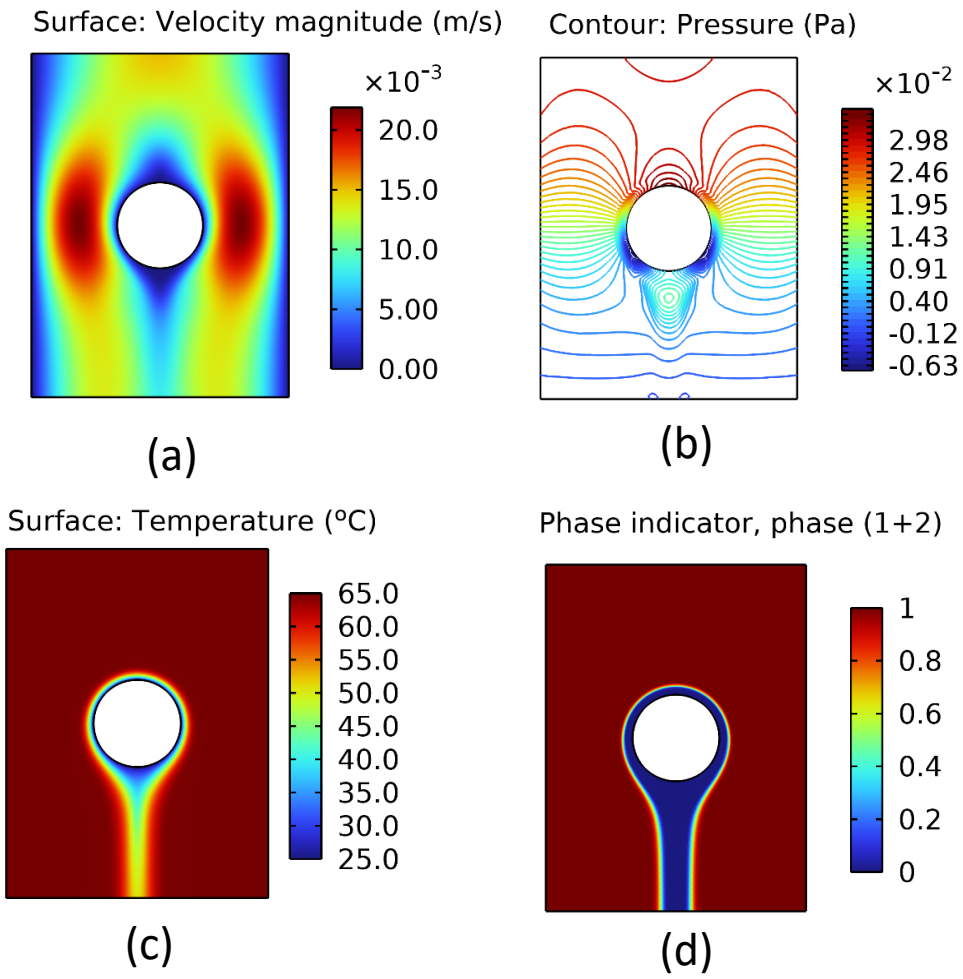

Figure.(5): CFD results of a condensing steam over a horizontal tube, (a) velocity, (b) pressure, (c) temperature and (d) phase indicator.

6.3.Effect of vapor velocity

In this section, the effect of vapor velocity on the condensation heat transfer coefficient was investigated. Previous studies, as reviewed by Browne and Bansal [13] reported that the forced-convection condensation is proportional to the magnitude of the cross-flow velocity. Therefore, the simulations were carried out with a varied vapor inlet velocity from 5 mm/s to 20 mm/s for the case of saturation temperature of 60 ºC. The corresponding cross-flow velocity profiles are plotted in Figure 6(a). As can be seen, the cross-flow velocity profile is a result of the no-slip boundary conditions at positions x = 3 mm and x = 9 mm of the tube wall and the vertical wall, respectively and the maximum cross-flow velocity at a position of x = 5.6844 mm. The cross-flow velocity is almost a two-folds of the vapor inlet velocity as depicted in Figure 6(b). The existence of vapor shear due to the established velocity gradient near the tube wall strongly affects the condensing heat transfer coefficient. Figure 6(c) shows an increasing trend of HTC to the power of (0.4526) of the maximum cross-flow velocity.

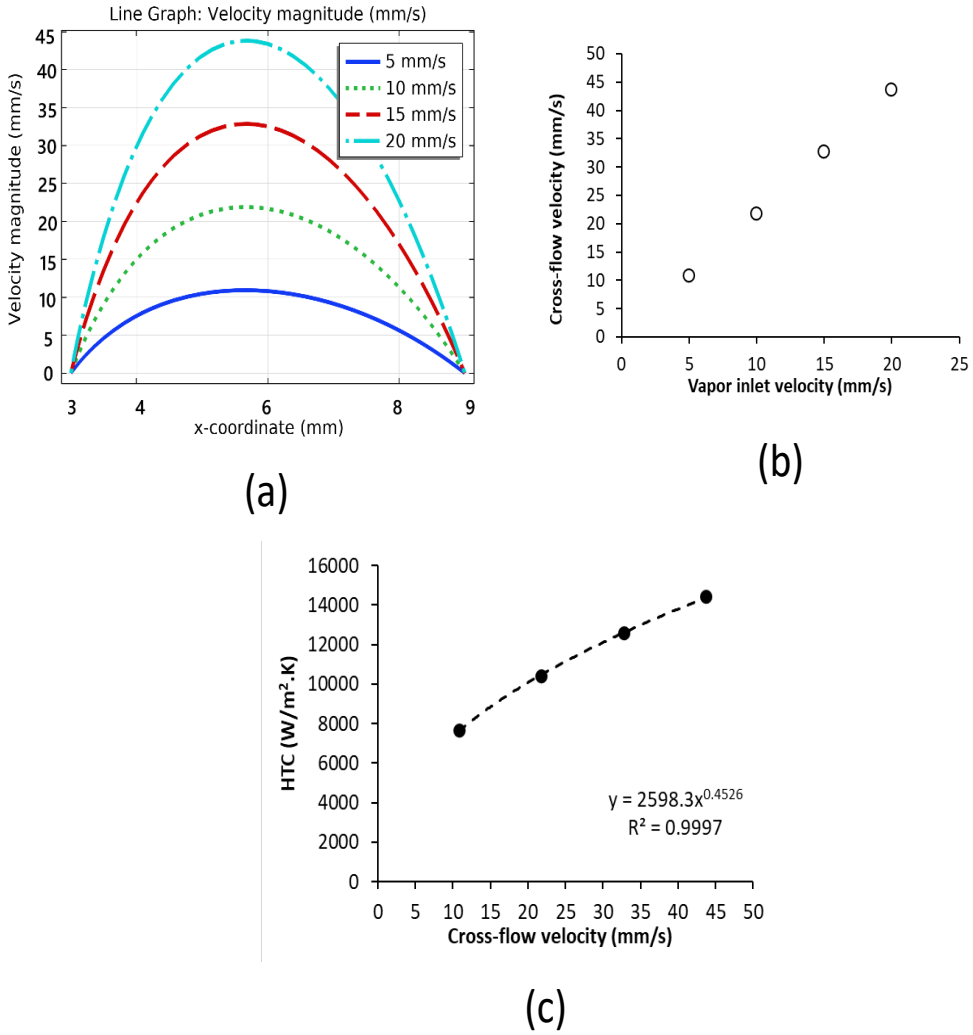

Figure.(6): Effect of vapor velocity on forced-convection condensation, (a) cross-flow velocity profile, (b) variation of cross-flow velocity with vapor inlet velocity (c) HTC.

In order to understand how the HTC increases with respect to the vapor shear, the phase indicators at different vapor inlet velocities were visualized as depicted in Figure 7. As expected, the increase in vapor shear causes a thinning in the film thickness of the condensate when the inlet velocity increases from 5 mm/s to 20 mm/s. Therefore, the conductive thermal resistance of the condensate decreases when the inlet velocity increases resulting in higher values of HTC. This observation is in line with theory and previous studies [13, 14].

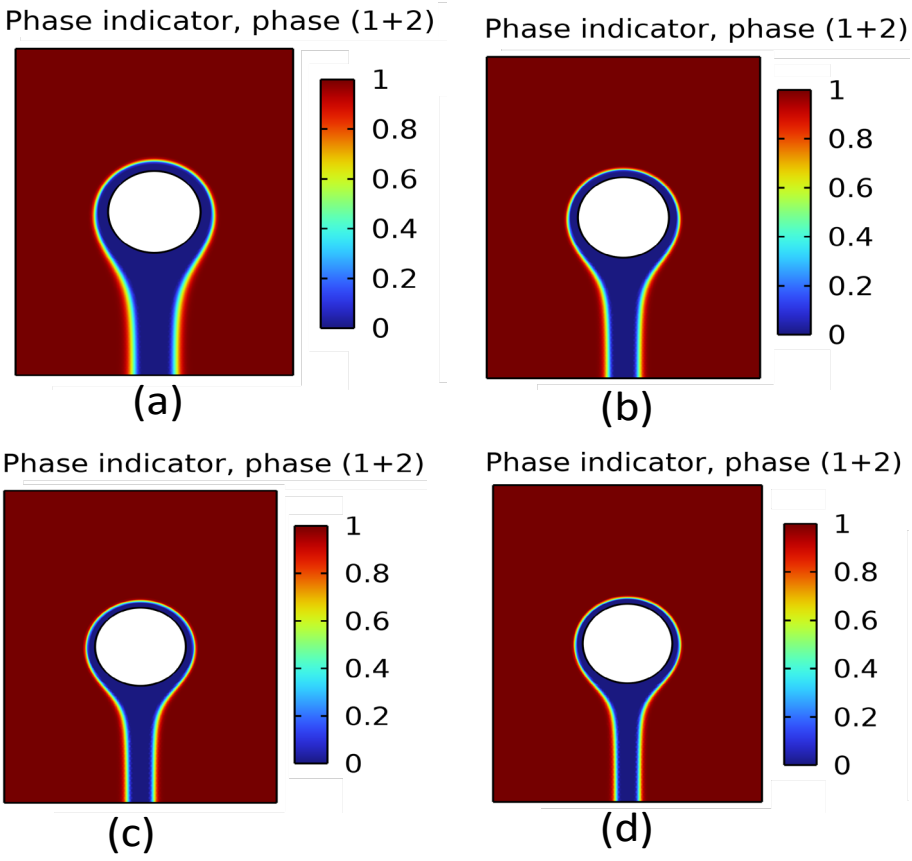

Figure.(7): Effect of vapor velocity on condensing steam over a horizontal tube, (a) v = 5 mm/s, (b) v = 10 mm/s, (c) v = 15 mm/s and (d) v = 20 mm/s.

7.CONCLUSIONS

A new CFD approach based on apparent heat capacity method was proposed to predict the condensation heat transfer coefficient of steam over a single horizontal tube. The model was validated against Nusselt film analogy at different saturation temperatures with reasonable accuracy. The effect of vapor velocity on the condensation heat transfer coefficient was presented. The current model is robust, computationally inexpensive and can be further extended for future work to account for the inundation phenomenon in real tube bundle of a condenser.

8.REFERENCES

[1] Bergman TL, Lavine AS, Incropera FP, DeWitt DP. Introduction to heat transfer. John Wiley & Sons; 2011.

[2] Kakaç S, Bergles AE, Fernandes EO, editors. Two-phase flow heat exchangers: Thermal-hydraulic fundamentals and design. Springer Science & Business Media; 2012.

[3] Nitsche M, Gbadamosi RO. Heat exchanger design guide: a practical guide for planning, selecting and designing of shell and tube exchangers. Butterworth-Heinemann; 2015.

[4] Pekař L. Introduction to heat exchangers. In Advanced Analytic and Control Techniques for Thermal Systems with Heat Exchangers 2020. (pp. 3-20). Academic Press.

[5] Luyben WL. Reality versus simulation-implementation of heat exchangers with phase changes. Computers & Chemical Engineering. 2023; 175:108284. https://doi.org/10.1016/j.compchemeng.2023.108284

[6] Marto PJ. Heat transfer and two-phase flow during shell-side condensation. Heat Transfer Engineering. 1984;5(1-2):31-61. https://doi.org/10.1080/01457638408962767

[7] Bonneau C, Josset C, Melot V, Auvity B. Comprehensive review of pure vapour condensation outside of horizontal smooth tubes. Nuclear Engineering and Design. 2019; 349:92-108. https://www.sciencedirect.com/science/article/pii/S0029549319300718

[8] Ji WT, Zhao CY, Lofton J, Li ZY, Zhang DC, He YL, Tao WQ. Condensation of R134a and R22 in shell and tube condensers mounted with high-density low-fin tubes. Journal of Heat Transfer. 2018;140(9):091503. https://doi.org/10.1115/1.4040083

[9] Mirzabeygi P, Zhang C. Three-dimensional numerical model for the two-phase

flow and heat transfer in condensers. International Journal of Heat and Mass Transfer. 2015; 81:618-637. https://doi.org/10.1016/j.ijheatmasstransfer.2014.10.015

[10] Doan M, Le T, Dang T, Teng JT. A Numerical Simulation on Phase Change of Steam in a Microchannel Condenser. International Journal of Power and Energy Research. 2017;1(2). https://dx.doi.org/10.22606/ijper.2017.12005

[11] El Ouali A, Khattari Y, Lamrani B, El Rhafiki T, Zeraouli Y, Kousksou T. Apparent heat capacity method to describe the thermal performances of a latent thermal storage system during discharge period. Journal of Energy Storage. 2022; 52:104960. https://doi.org/10.1016/j.est.2022.104960

[12] COMSOL Multiphysics, Heat transfer Module User's Guide, Chapter 4 -Theory for the heat transfer module: 206-211. COMSOL 6.2.

[13] Browne MW, Bansal PK. An overview of condensation heat transfer on horizontal tube bundles. Applied Thermal Engineering. 1999;19(6):565-694. https://doi.org/10.1016/S1359-4311(98)00055-6

[14] Kutateladze SS, Gogonin II. Heat transfer in condensation of flowing vapour on a single horizontal cylinder. International journal of heat and mass transfer. 1985; 28(5):1019-1030. https://doi.org/10.1016/0017-9310(85)90284-4

Scientific Journal of University of Benghazi

SJUOB (2025) 38 (1) Applied Sciences: Obaida, et la , 129 – 158
www.sjuob.uob.edu.ly

Cretaceous-Paleocene Biostratigraphy of Jardas Al Abid Area, Al Jabal Al Akhdar, NE Libya

Motasem I. Obaida[1].*, Esam O. Abdulsamad[2], Ahmed M. Muftah[2], Ali K. Khalifa[3]

1 Waha Oil Company.
2 Earth Science Department, Faculty of Science, University of Benghazi.
3 Geological Engineering Department, Faculty of Engineering Science, Bright Star University.

Received: 22 / 02 / 2025 | Accepted: 18 / 04 / 2025 | Publishing: 29/06/2025

ABSTRACT

This study focuses on the biostratigraphy of the Cretaceous (Albian–Maastrichtian) and Paleocene (Danian) sequences exposed in both surface and subsurface sections of the Jardas al'Abid area, Al Jabal Al Akhdar, northeastern Libya. The investigation is based on systematically collected samples from four outcrop sections and one subsurface borehole (Water well). A total of thirty foraminiferal and five molluscan species were identified. Based on the vertical distribution of planktic foraminifera, nine biozones have been established in descending order: Parvularugoglobigerina Eugubine (Danian), Dicarinella concavata (Coniacian), Whiteinella brittonensis (Early Turonian), Hedbergella spp.–Pithonella spp. (Late Cenomanian), Rotalipora cushmani (Late Cenomanian), Thalmanninella brotzeni (Early Cenomanian), Biticinella breggiensis, Pseudothalmanninella ticinensis (Late Albian), and Ticinella primula (Middle Albian). Additionally, three molluscan biozones have been identified: Mecaster batnensis, Costagyra olisiponensis (both Late Cenomanian), and Inoceramus (Endocostea) balticus (Campanian), along with one ammonite biozone, Kitchinites emscheris (Early Santonian). This work represents the most detailed foraminiferal biostratigraphic framework for the region to date, with several of the proposed biozones being reported from Al Jabal Al Akhdar for the first time. The established biozones show a strong correlation with those of neighboring countries as well as with Mediterranean coastal regions of Europe, reinforcing the regional biostratigraphic continuity across the southern Tethyan margin. A new discovery of existing Paleocene (Danian) strata has been confirmed at the Jardas al'Abid area.

Keywords: Biostratigraphy, Cretaceous, Paleocene, Jardas al'Abid, Al Jabal Al Akhdar.

Corresponding Author: Motasem I. Obaida, motasem.obaida@uob.edu.ly

 ISSN: Online 2790-1637, Print 2790-1629
National Library of Libya, Legal number: 154/2018

1.INTRODUCTION

The Cretaceous (Albian-Maastrichtian) and Paleocene (Danian) surface and subsurface sequences in the Jardas al'Abid inlier area are predominantly rich in marine invertebrates. These sequences are lithostratigraphically divided into five-rock units: Daryanah (Middle to Late Albian), Qasr al'Abid (Cenomanian), Al Baniyah (Late Cenomanian-Coniacian), Al Majahir (Campanian), and Al Uwayliah (Danian). These rock units, exposed at Jardas al'Abid inlier, consist of limestones, marly limestones, chalky limestones, and claystones, which contain moderately preserved microfossils and macrofossils.

The microfossils identified include both planktic and benthic foraminifera, while the predominant macrofossils are pelecypods, the most abundant group. Cephalopod ammonites, though of secondary occurrence, are found in the Al Majahir and Al Baniyah formations.

Previous studies in the region have predominantly focused on macrofossil mollusks and echinoids, with limited attention given to foraminiferal biostratigraphy. Few biostratigraphic studies have been conducted on the Cretaceous micro- and macrofossils of Al Jabal Al Akhdar. Notable studies include the following: [1] an investigation of the pre-Campanian unconformity in the Ghwth Sas area, which confirmed the angular unconformity between the Al Baniyah and Al Majahir formations using microfossils (foraminifera and ostracods) and macrofossils (inoceramid bivalves). [2] A study of Late Cenomanian fossils from the Jardas al'Abid area, which identified two oyster biozones (Exogyra (Costagyra) olisiponensis and Pycnodonte (Phygraea) vesiculosum) and two ammonite biozones (Metoicoceras geslinianum and Pseudaspidoceras pseudonodosoides); [3] gives a detailed description of 49 species of Upper Cretaceous macrofossils from Jardas al'Abid. [4] A study of Cenomanian-Turonian mollusks and echinoids recognized three ammonite biozones and eight other macrofossil biozones; [5] Upper Cretaceous and Lower Tertiary foraminiferal biozones were recognized from five locations in Al Jabal al Akhdar, NE Libya, and eight foraminiferal biozones were established.

The study area is located in the western part of the Cyrenaica inverted basin, also known as the Al Jabal Al Akhdar Uplift,

 ISSN: Online 2790-1637, Print 2790-1629
National Library of Libya, Legal number: 154/2018

and is located at 32°18'34"N latitude and 20°59'97"E longitude (Fig. 1). Five stratigraphic sections were selected: (J1) behind the Jardas al'Abid School, (J2) approximately 1.3 km southeast of the school, (J3) the Water well section about 1.5 km to the north of the school, (J4) behind the Ghwth Sas School, and (J5) approximately 800 m northwest of the Ghwth Sas School. This study aims to identify biozones to date the lithological units and establish biostratigraphic correlations.

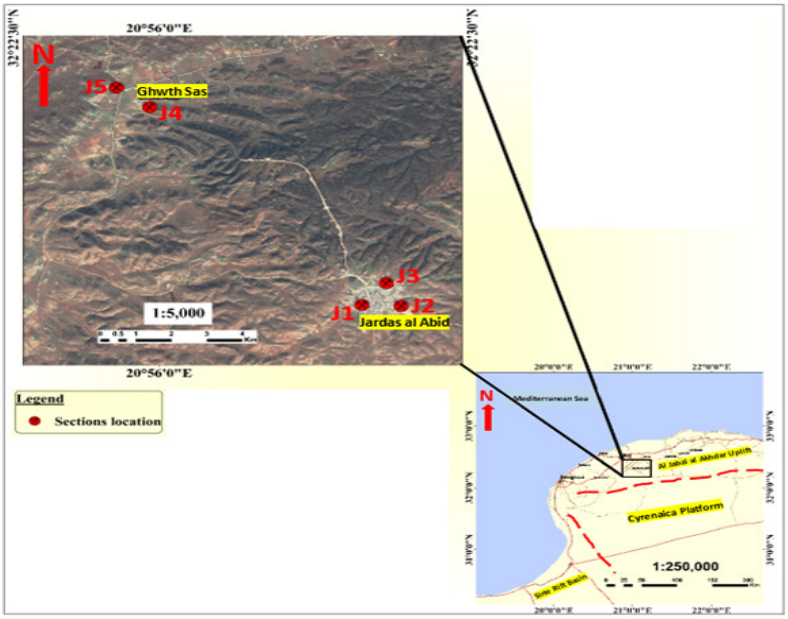

Figure. (1): Key map and satellite image of the Jardas al'Abid inlier, showing the locations of the five measured stratigraphic sections (J1–J5) along the upper escarpment of the study area.

 ISSN: Online 2790-1637, Print 2790-1629
National Library of Libya, Legal number: 154/2018

2.MATERIALS AND METHODS

Four field trips were conducted in the study area to systematically collect samples. Sampling was performed at regular intervals of 1–3 meters, depending on changes in lithology and fossil content, to capture both lateral and vertical facies variations. A total of 64 samples—comprising primarily limestone, claystone, marl, and chalky limestone—were collected from five stratigraphic sections. Of these, 42 hand specimens were obtained from four exposed outcrops, while 22 subsurface samples were collected from a water well in the Jardas al'Abid area.

All samples were processed for micropaleontological analysis using standard international preparation techniques. Approximately 50 g of each sample was crushed, disaggregated, wet-sieved through a 63-µm mesh, dried, and subsequently picked and mounted onto paleontological slides. However, many of the recovered foraminiferal specimens were poorly preserved or too small for accurate identification, limiting their utility for photomicrograph documentation. The poor preservation and overall scarcity of foraminifera posed a significant challenge during the study.

Recovered specimens were examined under a stereoscopic microscope, and identifications were made based on gross morphology. Taxonomic classification followed the planktic foraminiferal systematics outlined in [6]. Selected index species and other representative taxa were photographed using an AmScope ultra-compact 5MP USB digital microscope eyepiece camera (model MD500) mounted on a stereomicroscope.

All laboratory work was conducted at the Micropaleontological Laboratory, Department of Earth Sciences, University of Benghazi. The examined material will be permanently archived in the Geological Museum of the University. In total, 30 species were identified, representing 23 genera, 13 families, and 8 suborders.

3.RESULTS AND DISCUSSION

Field investigations resulted in the identification of five distinct lithostratigraphic units arranged in stratigraphic succession from the oldest to the youngest as follows: the Daryanah Formation (Middle to Late Albian), Qasr al'Abid Formation (Cenomanian), Al Baniyah Formation (Late Cenomanian to Coniacian), Al Majahir Formation (Early Santonian to Campanian), and Al Uwayliah

 ISSN: Online 2790-1637, Print 2790-1629
National Library of Libya, Legal number: 154/2018

Formation (Danian). These formations are well-exposed within the Jardas al'Abid inlier and are predominantly composed of limestone, marl, chalk, and claystone lithologies.

3.1.1. Stratigraphy

Based on the detailed field observations and a review of previous stratigraphic studies, the exposed rock succession in the study area is described below in ascending order, beginning with the oldest formation.

Daryanah Formation (Middle to Late Albian)

The Daryanah Formation, previously studied by [7] in wells Al-NC 120, Al-NC 128, and at the type section, displays a gradual shallowing-upward trend, transitioning from deeper marine shales and marls to shallower siltstones and limestones [9]. In the present study, this formation is identified in the Jardas al'Abid School section (J1) and the Water Well section (J3). At J1, it is represented by a 0.25 m thick interval of yellow, soft marly limestone containing fossil fragments. In contrast, at J3, the formation reaches a thickness of 76 m, comprising two main facies: silty claystone and interbedded limestone.

3.1.2.Qasr al'Abid Formation (Cenomanian)

Cenomanian-aged rocks are exposed in small inliers at the core of the Jardas al'Abid dome, close to the site of Libya's first wildcat well (Al-18), where deeply eroded anticlines have revealed these units [8]. Initially referred to as the "Gaser al'Abid Marl Member" of the Jardas Formation by [9], the unit was later elevated to formational rank and formally named the Qasr al'Abid Formation by [10,11]. It conformably overlies the Daryanah Formation and is, in turn, overlain by the Al Baniyah Formation. In the present study, the formation is observed in sections J1 and J3. At J1, it reaches a thickness of 2 m, consisting of greenish-brown clay facies at the base, grading upward into yellow marl. At J3, the unit is 70 m thick and dominated by claystone interbedded with limestone. Fossil content includes echinoid fragments, shell debris, and evidence of bioturbation.

3.1.3.Al Baniyah Formation (Late Cenomanian–Coniacian)

First described as the "Benia Limestone Member" by [9] and later elevated to formational status by [10,11], the Al Baniyah

 ISSN: Online 2790-1637, Print 2790-1629
National Library of Libya, Legal number: 154/2018

Formation is characterized by a lithological transition from marl to chalky limestone, with an unconformable contact at its upper boundary with the Al Majahir Formation. The formation is exposed in four sections: J1, J2, J3, and J4. At J1, it is 2 m thick, represented by white chalky limestone devoid of macrofossils. At J2, it reaches 9 m and is composed of white to brown chalky limestone interbedded with a thin phosphate layer at the base and a 1 m-thick deformed green claystone in the middle. Large calcite geodes are also present. At J3, it measures 10 m and comprises white chalky limestone. At J4 (Ghwth Sas School), it is also 10 m thick and consists of slightly chalky, white to brown marly limestone with three thin oyster beds. Fossils include internal molds of pelecypods and external molds of ammonites.

3.1.4.Al Majahir Formation (Early Santonian–Campanian)

Named by [11] after the Qasr al Majahir near Qandulah village, the Al Majahir Formation is equivalent to the Al Feitah Limestone and parts of the Ghwth Sas Marl Members [12]. It is composed of marly limestone, microcrystalline, and dolomitic limestones, with interbedded marls and calcareous claystones. This formation is reported only at J5 (Ghwth Sas quarry), where it reaches 10 m in thickness and consists of white marl interbedded with limestone beds. Fossils include molds of ammonites and Inoceramus. The lower part represents a pre-Campanian sedimentation cycle that gradually thins upwards.

3.1.5.Al Uwayliah Formation (Danian, Paleocene)

The formation was deposited during a marine transgression that began in the Danian; it reflects varied outcrop patterns influenced by regional tectonics and erosion [13]. The holostratotype, described by [12], is located in the Al Uwayliah area and comprises whitish chalk and greenish marl.

In this study, Paleocene (Danian) strata within the Al Uwayliah Formation have been confirmed for the first time at the upper part of section J2 in the Jardas al ‘Abid area. Previously, the Al Uwayliah Formation was only known from the northern part of Al Jabal al Akhdar, specifically in the Uwayliah area, where it was considered Landenian in age, as well as from remnant exposures to the south and in Jardas al Jarari [14]. This new occurrence significantly expands the known distribution and stratigraphic range of the

 ISSN: Online 2790-1637, Print 2790-1629
National Library of Libya, Legal number: 154/2018

Al Uwayliah Formation within northeastern Libya.

3.2. Biostratigraphy

3.2.1. Planktic Foraminiferal Biozones

Nine planktic foraminiferal biozones have been identified in this study, following the zonal marker scheme of [15,16], and are presented below in descending stratigraphic order:

1.Ticinella primula Interval Biozone (Middle Albian)

This biozone is defined as the interval from the first occurrence of Ticinella primula to the first appearance of Biticinella breggiensis. It is recognized in the Water Well section (J3). The upper boundary and the lower boundary of this biozone are defined by the occurrence of Ticinella primula and Pseudothalmanninella ticinensis at a depth of 122m; the associated marker species is Hedbergella gorbachikae (Fig. 2).

2.Biticinella breggiensis Interval Biozone (Late Albian)

This biozone is defined as the interval from the first occurrence of Ticinella primula to the first appearance of Biticinella breggiensis. It is recognized in the Water Well section (J3). This biozone was defined based on the last occurrence of the zonal marker Biticinella breggiensis and the lack of the earlier zonal marker species Ticinella primula (Fig. 2).

3.Pseudothalmanninella ticinensis Interval Biozone (Late Albian)

This biozone is defined as the interval from the first occurrence of Pseudothalmanninella ticinensis to the first occurrence of Thalmanninella appenninica, Late Albian. It is recognized in the Water Well section (J3). The upper boundary of this biozone is defined by the last occurrence of Pseudothalmanninella ticinensis and the first occurrence of Thalmanninella brotzeni at a depth of 72m, and the lower boundary is defined by the last occurrence of Ticinella primula at a depth of 104m. The associated marker species include Biticinella breggiensis and the benthic large foraminifera Orbitulina discoidea (Fig. 4).

4.Thalmanninella brotzeni Interval Biozone (Early Cenomanian)

As an interval from the first occurrence of Thalmanninella brotzeni to the first occurrence of Thalmanninella reicheli. It is recognized in the Water Well section (J3). The lower boundary of this biozone is defined at a depth of 72m by the extinction of all Late

Albian foraminifera such as Ticinella and Biticinella spp., while the upper boundary is defined at a depth of 52m by the absence of R. reicheli and the presence of the primary zonal marker Rotalipora cushmani. The associated planktic taxa, such as Praeglobotruncana stephani and Cyclamina (Figure. 4).

5.Rotalipora cushmani Total Range Biozone (Middle to Late Cenomanian)

It is defined by the total range of Rotalipora cushmani. This biozone is documented in the Water Well section (J3). The top of this biozone is picked at a depth of 12m by the lack of all rotaliporid members, especially the secondary marker species Thalmanninella greenhornesis, in addition to diagnostic agglutinated larger benthic foraminifera, Thomasinella punica. The lower boundary is defined by the last occurrence of Thalmanninella brotzeni. The associated planktic taxa in this biozone include Muricohedbergella delrioensis, Rotalipora montsalvensis, Praeglobotruncana carinata, Whiteinella baltica, and Praeglobotruncana stephani (Figure. 4). The biozone is also recognized in Jardas Al'Abid school section J1, where it is defined by the occurrence of the primary zonal marker Rotalipora cushmani. The associated planktic taxa in this biozone include Thalmanninella greenhornsis, Muricohedbergella planispira, and Muricohedbergella delrioensis (Figure. 2).

6.Hedbergella -Pithonella Assemblage Biozone (Late Cenomanian)

It is recognized as the Jardas al'Abid quarry section (J2). This biozone is defined by the occurrence of pithonella spp., and Hedbergella spp. in addition to the diagnostic secondary zonal marker Rotalipora greenhornensis (Figure. 3).

7.Whiteinella brittonensis Total Range Biozone one (Early Turonian)

Proposed herein based on the findings in the uppermost part of the Water Well section (J3), this biozone spans from the last occurrence of Rotalipora cushmani to the disappearance of Helvetoglobotruncana helvetica at 2 m depth. The associated taxa include Praeglobotruncana sp. (Figure. 4).

8.Dicarinella concavata Assemblage Biozone of (Late Coniacian to Early Santonian).

An interval from the first occurrence of Dicarinella concavata to the first occurrence of Dicarinella asymetrica is identified in the Ghwth Sas School section (J4).

It is defined based on the absence of Dicarinella asymetrica and the presence of Dicarinella concavata, Marginotruncana marginata, Marginotruncana sinuosa, Marginotruncana paraconcavata, and Marginotruncana schneegansi. The associated taxa are Whiteinella archaeocretacea and Planoheterohelix reussi (Figure. 5).

9.Paruvlarugoglobigerina eugubina Total Range Biozone (Early Paleocene).

This biozone represents the total range of Parvularugoglobigerina eugubina and is identified in the Jardas al'Abid Quarry section. Both the lower and upper boundaries are defined by the range of the zonal marker itself. Associated species include Globoconusa daubjergensis and Parvularugoglobigerina extensa (Figure. 3).

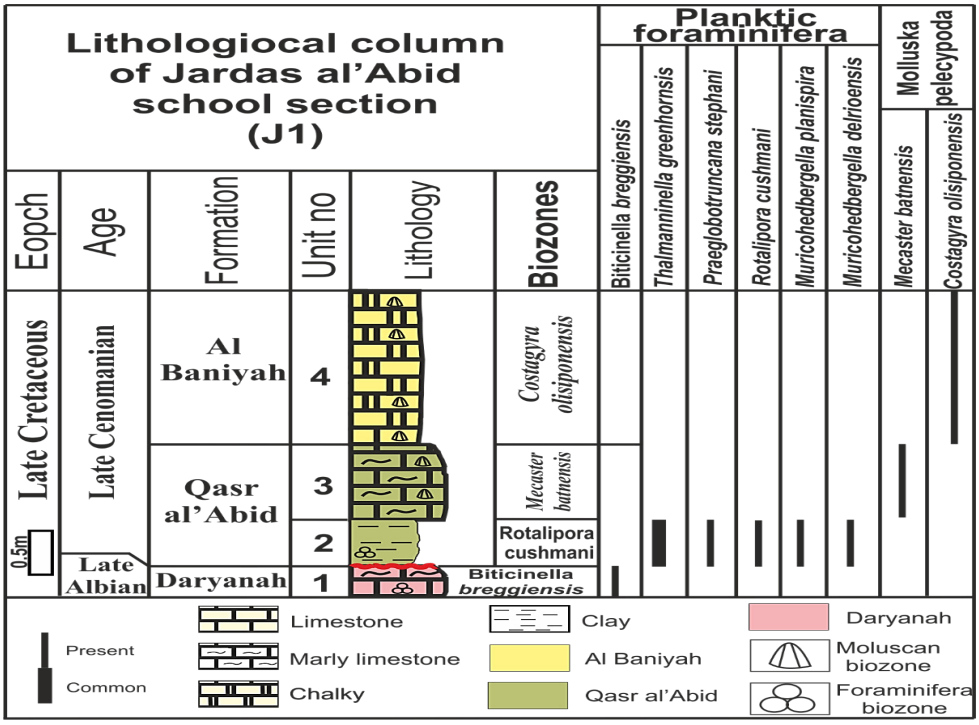

Figure. (2): Distribution chart of the identified foraminiferal taxa from the Jardas al'Abid School section. Note: Molluscan biozones are referenced from a previous study by (5).

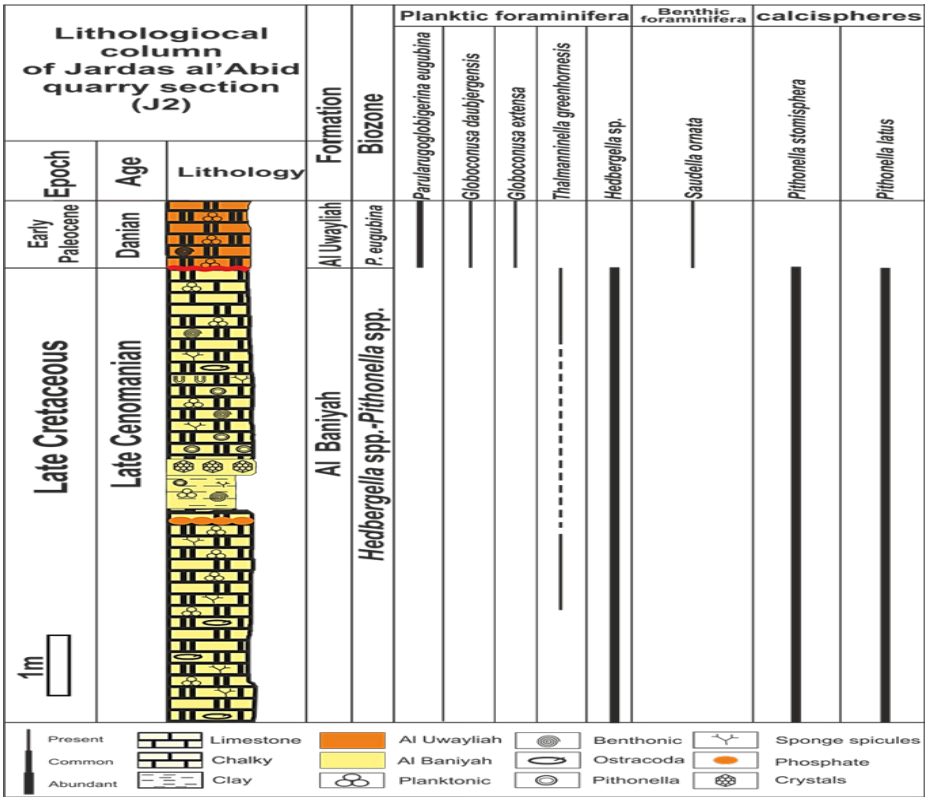

Figure. (3): Stratigraphic chart illustrating the lithological profile of the Jardas al'Abid Quarry section (J2) and the vertical distribution of the identified taxa.

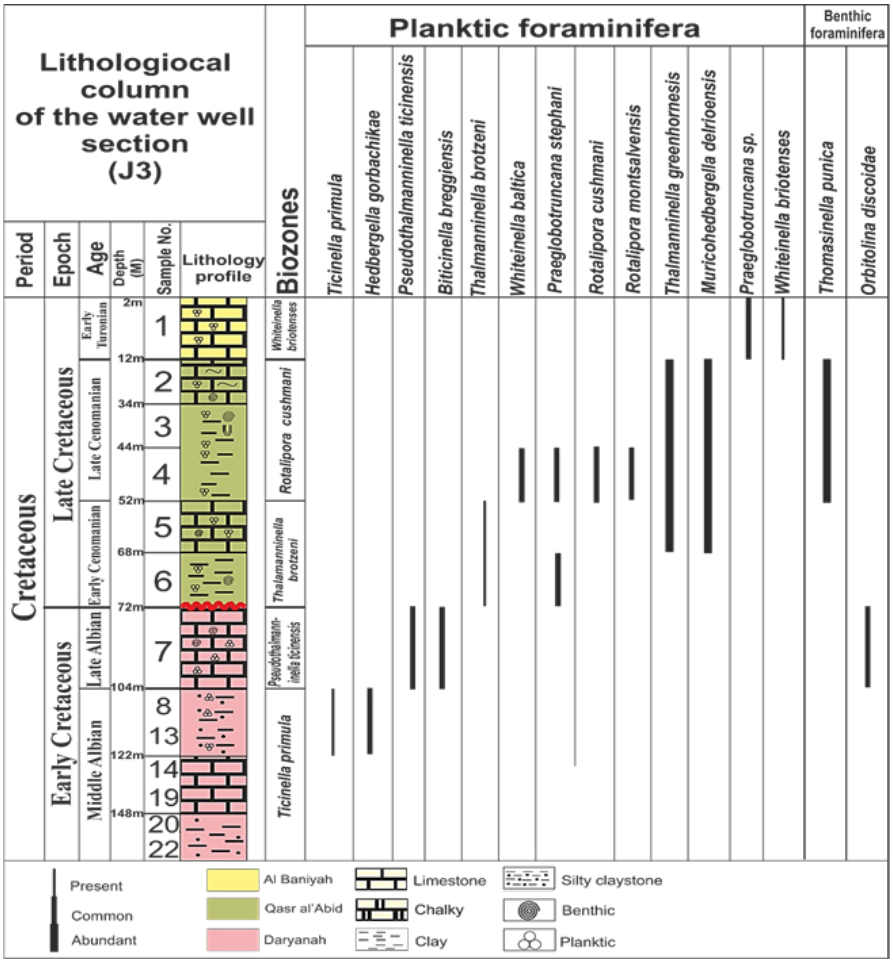

Figure. (4): Stratigraphic chart illustrates the lithological profile of the Water Well section (J3), the vertical distribution of the identified foraminiferal and molluscan taxa.

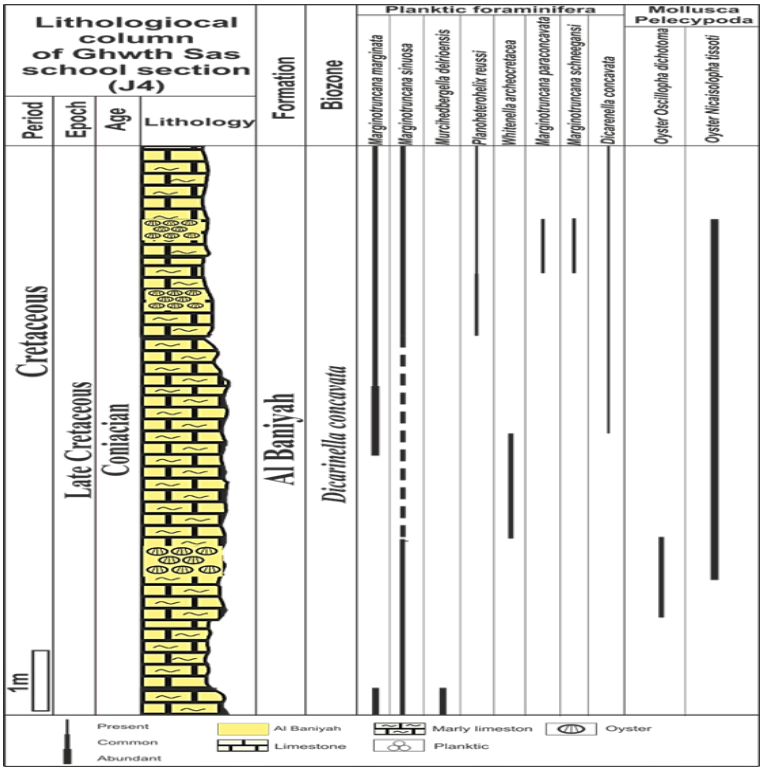

Figure. (5): Stratigraphic chart illustrating the lithological profile of the Ghwth Sas section (J4), along with the vertical distribution of the identified foraminiferal and molluscan taxa.

3.2.2. Molluscan Biozones

The molluscan biozones, identified in this study, include several pelecypod and ammonite assemblages. Among the pelecypod biozones, the Inoceramus balticus (Endocostea) biozone, attributed to the Campanian, is recognized within the Al Majahir Formation at the Ghwth Sas Quarried section (J5) (Figure. 6). Additionally, two Late Cenomanian pelecypod biozones—Mecaster batnensis within the Qasr al'Abid Formation and Costagyra olisiponensis within the Al Baniyah Formation—have been previously reported by [5] from the Jardas al'Abid School section (Figure. 2).

Furthermore, one ammonite biozone was identified in this study: the Kitchinites emscheris biozone of the Early Santo-

nian age, observed in the Ghwth Sas Quarried section (J5); this biozone was recorded for the first time in the Al Jabal Al Akhdar region (Figure. 6).

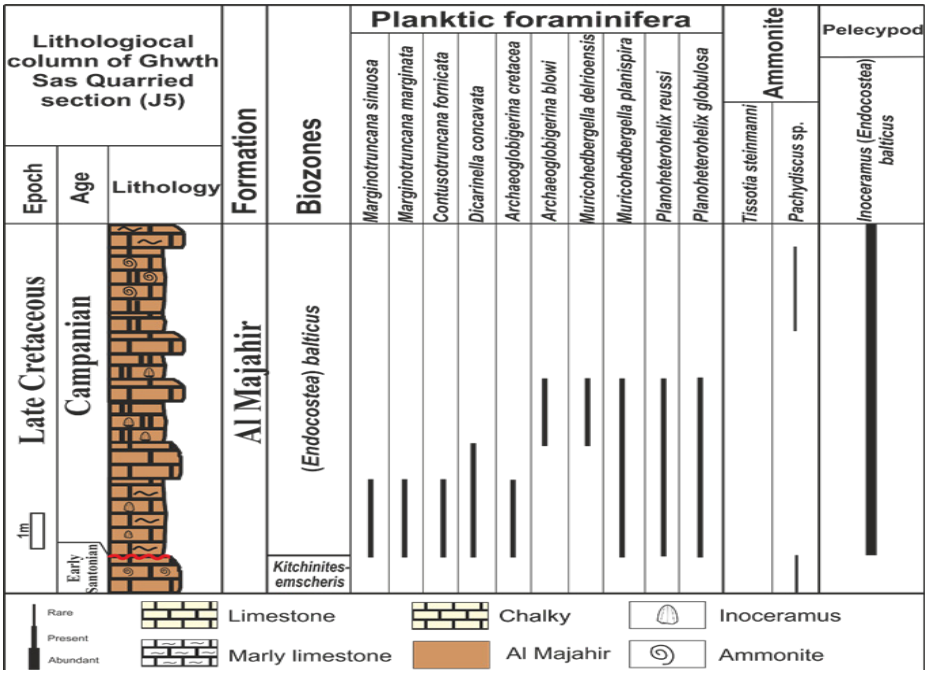

Figure. (6): Stratigraphic chart showing the lithological profile of the Ghwth Sas School section (J5), along with the stratigraphic distribution of the identified fossil taxa.

 ISSN: Online 2790-1637, Print 2790-1629
National Library of Libya, Legal number: 154/2018

3.3. Correlation

The measured sections, extending from southeast to northwest, include the following: Jardas al'Abid School (J1), Jardas al'Abid Quarry (J2), Water Well (J3), Ghwth Sas School (J4), and Ghwth Sas Quarry (J5). These sections have been correlated lithologically and biostratigraphically. The biozones established in this study are based on both planktic foraminifera and mollusks (Inoceramus and ammonite species).

The youngest unit, the Al Uwayliah Formation (Danian), is exposed only in the J2 section, where it is defined by the presence of the Parvularugoglobigerina eugubina biozone. The Water Well section (J3) is considered a reference hole, where three formations are present: Daryanah (Middle to Late Albian), Qasr al'Abid (Cenomanian), and Al Baniyah (Early Turonian). Five biozones have been identified in J3, listed from the oldest to the youngest: Ticinella primula (Middle Albian), Pseudothalmanninella ticinensis (Late Albian), Thalmanninella brotzeni (Early Cenomanian), Rotalipora cushmani (Late Cenomanian), and Whiteinella brittonensis (Early Turonian).

To the northwest, in section J4, where only the Al Baniyah Formation is exposed, the Dicarinella concavata assemblage biozone correlates laterally with the Whiteinella brittonensis biozone. To the southeast of J3, the lateral equivalent of the Whiteinella brittonensis biozone is the Hedbergella-Pithonella assemblage biozone, while at J1, the molluscan Mecaster batnensis biozone is equivalent. The Al Baniyah Formation exhibits variations in age, thickness, and faunal content from northwest to southeast, reflecting tectonic influences in the study area, particularly the dome (inlier) structure.

In the far northwest at site J5, the Al Majahir Formation (Campanian) is exposed and contains only molluscan biozones. The lower biozone, Kitchinites emscheris, is defined by the presence of Tissotia steinmanni, while the upper biozone is defined by the presence of the Inoceramus balticus (Endocostea) biozones.

The pre-Coniacian biozones show a good correlation between sections J1 and J3, particularly in the upper part of the Rotalipora cushmani biozone. However, the lower biozones are less well correlated, with only the Biticinella breggiensis, Pseudothalmanninel-

 ISSN: Online 2790-1637, Print 2790-1629
National Library of Libya, Legal number: 154/2018

la ticinensis, and Ticinella primula biozones being preserved (Figure. 7, 8, 9).

Worldwide, the reported foraminiferal biozones have been extensively correlated, particularly in North Africa. The Ticinella primula biozone is correlated with the Early Albian Fahdene Formation in Northern Tunisia [17]. Biticinella breggiensis biozone is correlated with the Hauterivian to Barremian–Aptian stages of Tunisia [18]. Thalmanninella brotzeni biozone is also correlated with the Late Albian deposits of northern Tunisia, within the southern Tethyan realm [19]. Dicarinella concavata biozone is correlated with the upper part of the pelagic limestones in the Kurdistan region, northeastern Iraq [20]. Additionally, the Parvularugoglobigerina eugubina biozone, marking the base of the Paleocene, is correlated with Gubbio, Italy [21]. Regarding macrofossils, the molluscan ammonite Kitchinites emscheris biozone, which was previously only known from Ecuador and Peru [22], is now reported for the first time in North Africa to represent from Libya.

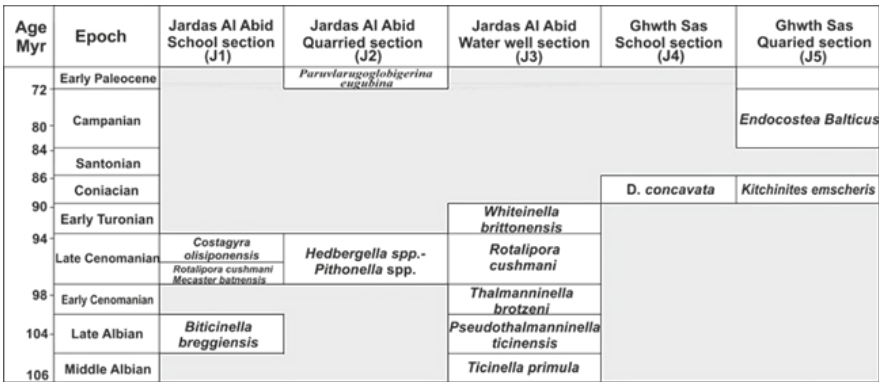

Figure. (7): Vertical distribution of the recognized biozones and a horizontal comparison between the studied sections on the bases of micro-macrofossils, in Jardas al'Abid inlier, of al Jabal al Akhdar, NE Libya.

The foraminiferal biozones were established from the coastal and offshore areas by [23,24]. and later refined by [5], are correlated with the lateral equivalents recognized in the southern Al Jabal al Akhdar region. These include biozonations proposed by [3,4,5]. The correlation between these regional frameworks is illustrated in (Fig. 8), providing a comprehensive biostratigraphic comparison across northern Libya and contributing to the refinement of the regional chronostratigraphy. Additionally, the biozones established in the present study are also correlated with previous biozonation schemes (Fig. 8), although the earlier frameworks were based on a combination of foraminiferal and molluscan assemblages, particularly pelecypods and ammonites. This integrated approach enhances the resolution and reliability of the regional stratigraphic correlations.

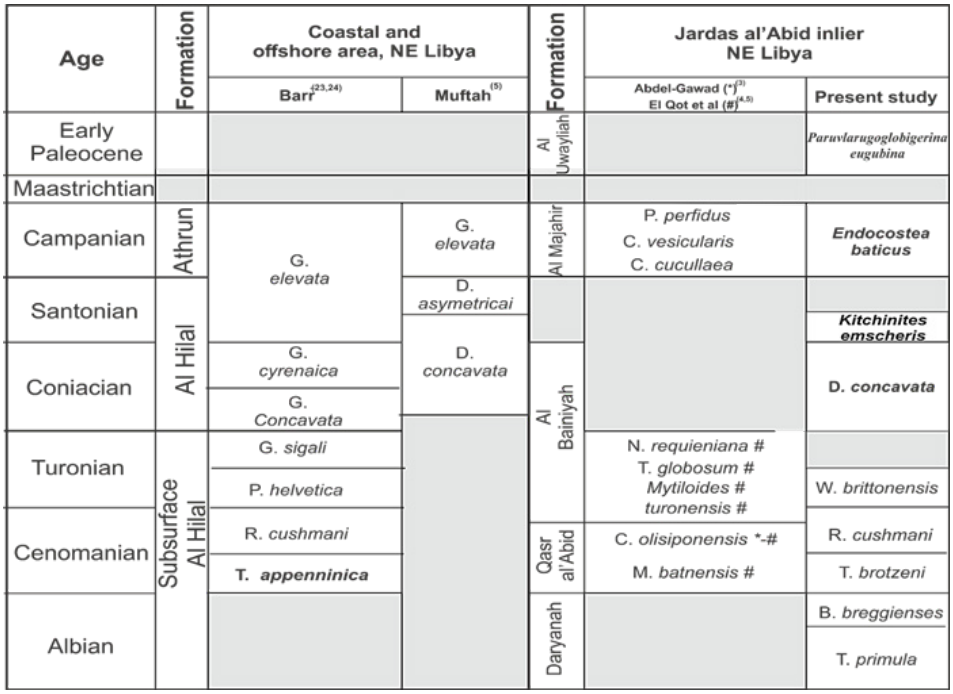

Figure. (8): Stratigraphic correlation chart comparing the previously published foraminiferal biozones with those established in the present study. Asterisks (*) and hash symbols (#) indicate molluscan biozones, specifically those based on

 ISSN: Online 2790-1637, Print 2790-1629
National Library of Libya, Legal number: 154/2018

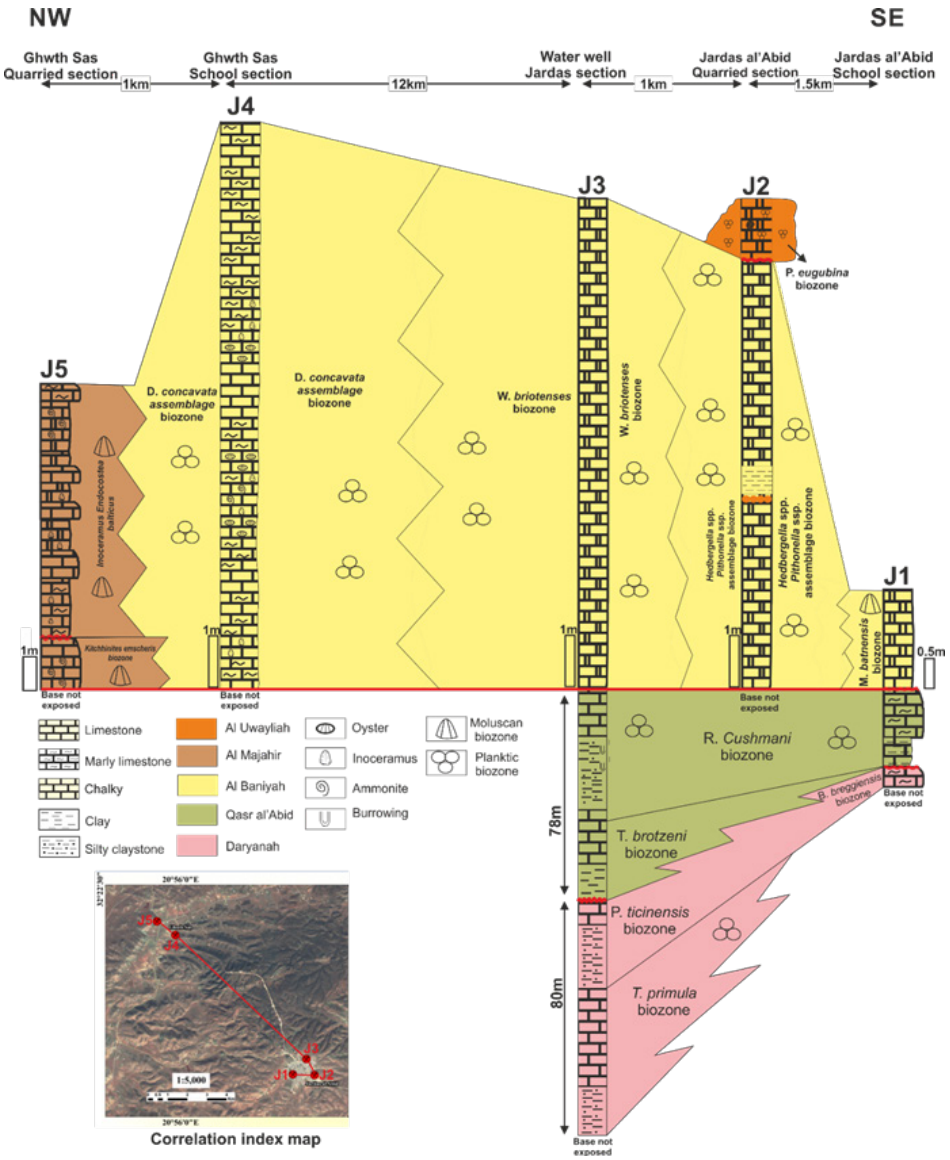

Figure. (9): Biostratigraphic correlation of the measured sections (J1–J5), illustrating the distribution of lithologic units and biostratigraphic zones across the study area. The correlation is referenced to the base of the Al Baniyah Formation (datum line). Note: the lower part of section J3 is presented at a different vertical scale.

4.CONCLUSION

The Cretaceous (Albian-Maastrichtian) and Paleocene (Danian) surface and subsurface successions from the measured and sampled sections of the Jardas al'Abid Inlier, including Jardas al'Abid School (J1), Jardas al'Abid Quarry (J2), Water Well (J3), Ghwth Sas School (J4), and Ghwth Sas Quarry (J5), have been analyzed for their foraminiferal and molluscan content. A total of 30 species were identified, belonging to 23 genera, 13 families, and 8 suborders, all of which have been systematically described and illustrated. Nine planktic foraminiferal biozones were identified in descending stratigraphic order:

1.Parvularugoglobigerina eugubina Total Range Biozone (Danian) – recognized in the Al Uwayliah Formation at the Ghwth Sas Quarried section (J2).

2.Dicarinella concavata Interval Biozone (Coniacian) – found in the Al Baniyah Formation at the Ghwth Sas Quarried section (J5).

3.Whiteinella brittonensis Total Range Biozone (Early Turonian) – identified in the Water Well section (J3), Al Baniyah Formation.

4.Hedbergella spp.-Pithonella spp. Assemblage Biozone (Late Cenomanian) – observed in the Al Baniyah Formation at the Jardas al'Abid Quarried section (J2).

5.Rotalipora cushmani Total Range Biozone (Late Cenomanian) – present in the Qasr al'Abid Formation at both the Jardas al'Abid School (J1) and Water Well (J3) sections.

6.Thalmanninella brotzeni Interval Biozone (Early Cenomanian) – identified in the Qasr al'Abid Formation at the Water Well section (J3).

7.Pseudothalmanninella ticinensis Interval Biozone (Late Albian) – observed in the Daryanah Formation at the Water Well section (J3).

8.Biticinella breggiensis Interval Biozone (Late Albian) – found in the Qasr al'Abid Formation at the Jardas al'Abid School section (J1).

9.Ticinella primula Interval Biozone (Middle Albian) – recognized in the Daryanah Formation at the Water Well section (J3).

An ammonite biozone, Kitchinites emscheris Biozone, was established in the Ghwth Sas Quarried section (J5), within the Al Majahir Formation, representing the total range biozone (Early Santonian).

Three molluscan biozones were identified: 1) Inoceramus balticus (Endo-

 ISSN: Online 2790-1637, Print 2790-1629
National Library of Libya, Legal number: 154/2018

costea) of Campanian age, found in the Al Majahir Formation at the Ghwth Sas Quarried section (J5); 2) Mecaster batnensis in the Qasr al'Abid Formation (Late Cenomanian) at Jardas al'Abid School section (J1); 3) Costagyra olisiponensis in the Al Baniyah Formation (Late Cenomanian) at Jardas al'Abid School section (J1).

The discovery of existing Paleocene (Danian) strata has been confirmed at the upper part of section J2 in the Jardas al'Abid area. This unit, approximately 1 meter thick, was identified based on its microfossil assemblages, notably the presence of early Paleocene planktic foraminifera, as well as its stratigraphic position, as it overlies the Al Baniyah Formation. This represents significant evidence for post-Cretaceous sedimentation in the region and provides biostratigraphic correlation with other Danian successions across North Africa.

Based on the micro-macrofossils distribution and lithological nature of the Cretaceous-Paleocene sequence in the Jardas al'Abid Inlier, the marine environments range from shallow marine facies (inner ramp) to deep marine facies (outer ramp).

5.ACKNOWLEDQMENTS

I would like to express my sincere gratitude to the Water Authority for providing the samples used in this research. I also wish to thank the Department of Earth Sciences at the University of Benghazi, Libya, for offering the necessary laboratory facilities to conduct the laboratory analyses. My heartfelt appreciation goes to my family, especially my wife, for their unwavering support throughout the preparation of this study. I am also deeply grateful to Mohammed El Hassi for providing the digital microscope eyepiece camera and to Mr. Saleh Al-Mismari for his invaluable assistance during the fieldwork. Finally, I thank Engineer Ahmed Al-Fitouri for supplying the map indicating the study location.

6.REFERENCES

1.Rohlich P, Salaj J. Palaeontological dating of the pre-Campanian unconformity in the Ghwth Sas area. In: First Symposium on the Sedimentary Basins of Libya, Geology of the Sirt Basin. 1996;1:265-286.

2.Abdel-Gawad GI. Late Cenomanian ammonites from NE Libya and the western desert of Egypt. Geology of East Libya. 2008;3:201-218.

3.El Qot GM, Abdulsamad EO, Aly MF. Upper Cretaceous macrofossils from the Jardas Al'Abid area, Al Jabal Al Akhdar, northeast Libya: systematic paleontology. Egyptian Journal of Paleontology. 2013;13:185-254.

4.El Qot GM, Abdulsamad EO. Cenomanian-Turonian biostratigraphy of the Jardas Al'Abid area, Al Jabal Al Akhdar, northeast Libya. Journal of African Earth Sciences. 2016 Sep;121:84-99.

5.Muftah AM. Upper Cretaceous-Lower Tertiary foraminiferal biozones of Al Jabal al Akhdar, NE Libya. In: Proceedings of the Third Annual International Conference on Geological & Earth Sciences (GEOS 2014); 2014. p. 34–39.

6.Young JR, Wade BS, Huber BT. pforams@ mikrotax website. Available from: http://www.mikrotax.org/pforams. 2017.

7.Duronio P, Dakshe A, Bellini E. Stratigraphy of the offshore Cyrenaica (Libya). In: Symposium on the geology of Libya. 1991;1589-1620.

8.Hallett D. Petroleum Geology of Libya. Amsterdam: Elsevier; 2002. 503 p.

9.Kleinsmiede WF, Van Den Berg NJ. Surface geology of the Jabal al Akhdar, northern Cyrenaica, Libya. In: Barr FT, editor. Geology and Archaeology of North Cyrenaica, Libya: The Petroleum Exploration Society of Libya, 10th Annual Field Conference. Tripoli; 1968. p. 115-123.

10.Klen I. Geological map of Libya 1:250,000. Sheet. NI 34-14, Benghazi Explanatory Booklet. Industrial Research Centre, Tripoli; 1974. 49 p.

11.Rhölich P. Geological map of Libya 1:250,000. Sheet: Al Bayda NI 34-15. Explanatory Booklet. Industrial Research Centre, Tripoli; 1974. 70 p.

12.Barr FT. Upper Cretaceous stratigraphy of the Jabal al Akhdar, northern Cyrenaica. In: Barr FT, editor. Geology and Archaeology of Northern Cyrenaica, Libya: The Petroleum Exploration Society of Libya, 10th Annual Field Conference. 1968. p. 131-147.

13.El Hawat AS, Shelmani MA. Short notes and guidebook on the geology of Al Jabal al Akhdar, Cyrenaica, NE Libya. Earth Science Society of Libya; 1993.

14.Röhlich P. Tectonic development of Al Jabal al Akhdar. In: Salem MJ, Buserwil MT, editors. The geology of Libya. Vol. III. London: Academic Press; 1980. p. 923–931.

15.Caron M. Cretaceous Planktonic Foraminifera. In: Bolli HM, Saunders JB, Perch-Niel-

sen K, editors. Plankton Stratigraphy. New York: Cambridge University Press; 1985. p. 17-18.

16.Olsson RK, Berggren WA, Hemleben C, Huber BT. Atlas of Paleocene planktonic foraminifera. Smithsonian Contributions to Paleobiology. 1999;85:1-252.

17.Ben Fadhel M, Gallala N. Revised planktic foraminiferal biostratigraphy of the early late Albian of northern Tunisia (southern Tethys). Revista Soletras. 2021;42.

18.BouDagher-Fadel M, Banner FT, Bown PR, Simmons MD, Gorbachik TN. Gorbachikella from the Hauterivian, Barremian-Aptian of Tunisia. Rev Micropaleontol. 1995;38(3):179–93.

19.Ben Fadhel M, Gallala N. Revised planktic foraminiferal biostratigraphy of the early late Albian of northern Tunisia (southern Tethys). Stratigraphy. 2022 Sep 15;19(3):157–78.

20.Jaff RB. A designed model for identifications of Dicarinella concavata (Brotzen, 1934) and Dicarinella asymetrica (Sigal, 1952) planktic foraminifer species under thin sections: an example from the Kurdistan region, NE Iraq. Jordan J Earth Environ Sci. 2021;12(2):154–62.

21.Arenillas I, Gilabert V, Arz JA. An updated suprageneric classification of planktic foraminifera after growing evidence of multiple benthic-planktic transitions. 2022.

22.Jaillard E, Bengtson P, Dhondt AV. Late Cretaceous marine transgressions in Ecuador and northern Peru: a refined stratigraphic framework. J South Am Earth Sci. 2005;19(3):307–23.

23.Barr FT, Hammuda OS. Biostratigraphy and planktonic zonation of the Upper Cretaceous Atrun Limestone and Hilal Shale, northeastern Libya. In: Farinacci A, editor. Proceedings of the 2nd International Conference on Planktonic Microfossils (1970). Rome; 1971. p. 27–40.

24.Barr FT. Cretaceous biostratigraphy and planktonic foraminifera of Libya. Micropaleontology. 1972;18:1–46.

7.DESCRIPTION OF PLATES 1-6

PLATE 1

1.Ticinella primula (Middle Albian): a) Spiral view (X45), b) Umbilical view (X45), Daryanah Formation, Sample No. 8, Depth 104m, Water well section (J3).

2.Biticinella breggiensis (Late Albian): a) Spiral view (X45), b) Umbilical view (X45), Daryanah Formation, Sample No. 7, Depth 72m, Jardas al'Abid School section (J1).

3.Rotalipora montsalvensis (Late Cenomanian): a) Spiral view (X45), b) Umbilical view (X45), Qasr al'Abid Formation, Sample No. 4, Depth 44m, Water well section (J3).

4.Pseudothalmanninella ticinensis (Late Albian): a) Spiral view (X45), b) Umbilical view (X45), Daryanah Formation, Sample No. 5, Depth 56m, Water well section (J3).

5.Rotalipora cushmani (Late Cenomanian): a) Spiral view (X45), b) Umbilical view (X45), Qasr al'Abid Formation, Sample No. 7, Depth 72m, Water well section (J3).

6.Thalmanninella greenhornsis (Late Cenomanian): a) Spiral view (X45), b) Umbilical view (X45), Qasr al'Abid Formation, Sample No. 2, Depth 12m, Water well section (J3).

PLATE 2

1.Archaeoglobigerina blowi (Campanian): a) Spiral view (X45), b) Umbilical view (X45), Al Majahir Formation, Sample No. 3, Ghwth Sas Quarried section (J5).

2.Whiteinella baltica (Late Cenomanian): a) Spiral view (X35), b) Umbilical view (X45), Qasr al'Abid Formation, Sample No. 4, Depth 44m, Water well section (J3).

3.Praeglobotruncana stephani (Late Cenomanian): a) Spiral view (X45), b) Umbilical view (X25), Qasr al'Abid Formation, Sample No. 4, Depth 44m, Water well section (J3).

4.Muricohedbergella delrioensis (Late Cenomanian): a) Spiral view (X45), b) Umbilical view (X45), Qasr al'Abid Formation, Sample No. 2, Depth 12m, Water well section (J3).

5.Hedbergella gorbachikae (Late Albian): a) Spiral view (X45), b) Umbilical view (X45), Qasr al'Abid Formation, Sample No. 8, Depth 104m, Water well section (J3).

6.Archaeoglobigerina cretacea (Coniacian): a) Spiral view (X40), b) Umbilical view (X40), Al Majahir Formation, Sample No. 1, Ghwth Sas Quarried section (J4).

7.Muricohedbergella planispira (Late Cenomanian): a) Spiral view (X45), b) Umbilical view (X45), Qasr al'Abid Formation, Sample No. 4, Jardas al'Abid School section (J1).

8.Whiteinella brittonensis (Early Turonian): a) Spiral view (X45), b) Umbilical view (X45), Qasr al'Abid Formation, Sample No. 1, Depth 2m, Water well section (J3).

PLATE 3

1.Marginotruncana marginata (Coniacian): a) Spiral view (X45), b) Umbilical view (X45), Al Baniyah Formation, Sample No. 8, Ghwth Sas School section (J4).

2.Contusotruncana fornicate (Campanian): a) Spiral view (X30), b) Umbilical view (X30),

Al Majahir Formation, Sample No. 2, Ghwth Sas Quarried section (J5).

3.Marginotruncana Sinuosa (Campanian): a) Spiral view (X45), b) Umbilical view (X45), Al Majahir Formation, Sample No. 2, Ghwth Sas Quarried section (J5).

4.Marginotruncana schneegansi (Coniacian): a) Spiral view (X45), b) Umbilical view (X45), Al Baniyah Formation, Sample No. 8, Ghwth Sas School section (J4).

5.Dicarinella concavata (Coniacian): a) Spiral view (X45), b) Umbilical view (X45), Al Baniyah Formation, Sample No. 8, Ghwth Sas School section (J4).

6.Dicarinella concavata cf. (Campanian): a) Spiral view (X30), b) Umbilical view (X30), Al Majahir Formation, Sample No. 2, Ghwth Sas Quarried section (J5).

PLATE 4

1.Parvularugoglobigerina eugubina (Early Paleocene): a) Spiral view (X45), b) Umbilical view (X45), Al Uwayliah Formation, Sample No. 10, Jardas al'Abid Quarried section (J2).

2.Globoconusa daubjergensis (Early Paleocene): a) Spiral view (X45), b) Umbilical view (X45), Al Uwayliah Formation, Sample No. 10, Jardas al'Abid Quarried section (J2).

3.Parvularugoglobigerina extensa (Early Paleocene): a) Spiral view (X45), b) Umbilical view (X45), Al Uwayliah Formation, Sample No. 10, Jardas al'Abid Quarried section (J2).

4.Marginotruncana paraconcavata (Coniacian): a) Spiral view (X45), b) Umbilical view (X45), Section (J4), Sample No. 8.

5.Planoheterohelix reussi (Campanian): Spiral view (X45), Section (J5), Sample No. 2.

6.Planoheterohelix globulosa (Late Cenomanian): a) Spiral view (X45), b) Umbilical view (X45), Section (J5), Sample No. 3.

7.Thalmanninella brotzeni (Early Cenomanian): a) Spiral view (X25), b) Umbilical view (X25), Section (J3), Sample No. 6, Depth 68m, Water well section.

8.Gaudryina serrata (Campanian): Spiral view (X45), Section (J5), Sample No. 3.

9.Orbitolina discoidea (Late Cenomanian): Dorsal view (X20), Qasr al'Abid Formation, Sample No. 7, Depth 72m, Water well section (J3).

10.Saudella ornate (Early Santonian): Side view (X45), Al Baniyah Formation, Sample No. 9, Jardas al'Abid Quarried section (J2).

PLATE 5

1.Inoceramus (Endocosta) balticus (Campanian): Al Majahir Formation, Sample No. 2,

Ghwth Sas Quarried section (J5), bar scale = 3cm.

2.Oscillopha dichotoma (Coniacian): Articulated oyster valves, a) Right valve, b) Left valve, bar scale = 3cm, Al Baniyah Formation, Sample No. 4, Ghwth Sas School section (J4).

3.Nicaisolopha tissoti (Coniacian): Disarticulated oyster valves, a) Right valve, b) Left valve, bar scale = 3cm, Al Baniyah Formation, Sample No. 7, Ghwth Sas School section (J4).

PLATE 6

1.Pachydiscus neubergicus (Late Campanian): Side view, bar scale = 10cm, Al Majahir Formation, Sample No. 6, Ghwth Sas Quarried section (J5).

2.Tissotia steinmanni (Coniacian): Side view, bar scale = 4cm, Al Majahir Formation, Sample No. 1, Ghwth Sas Quarried section (J5).

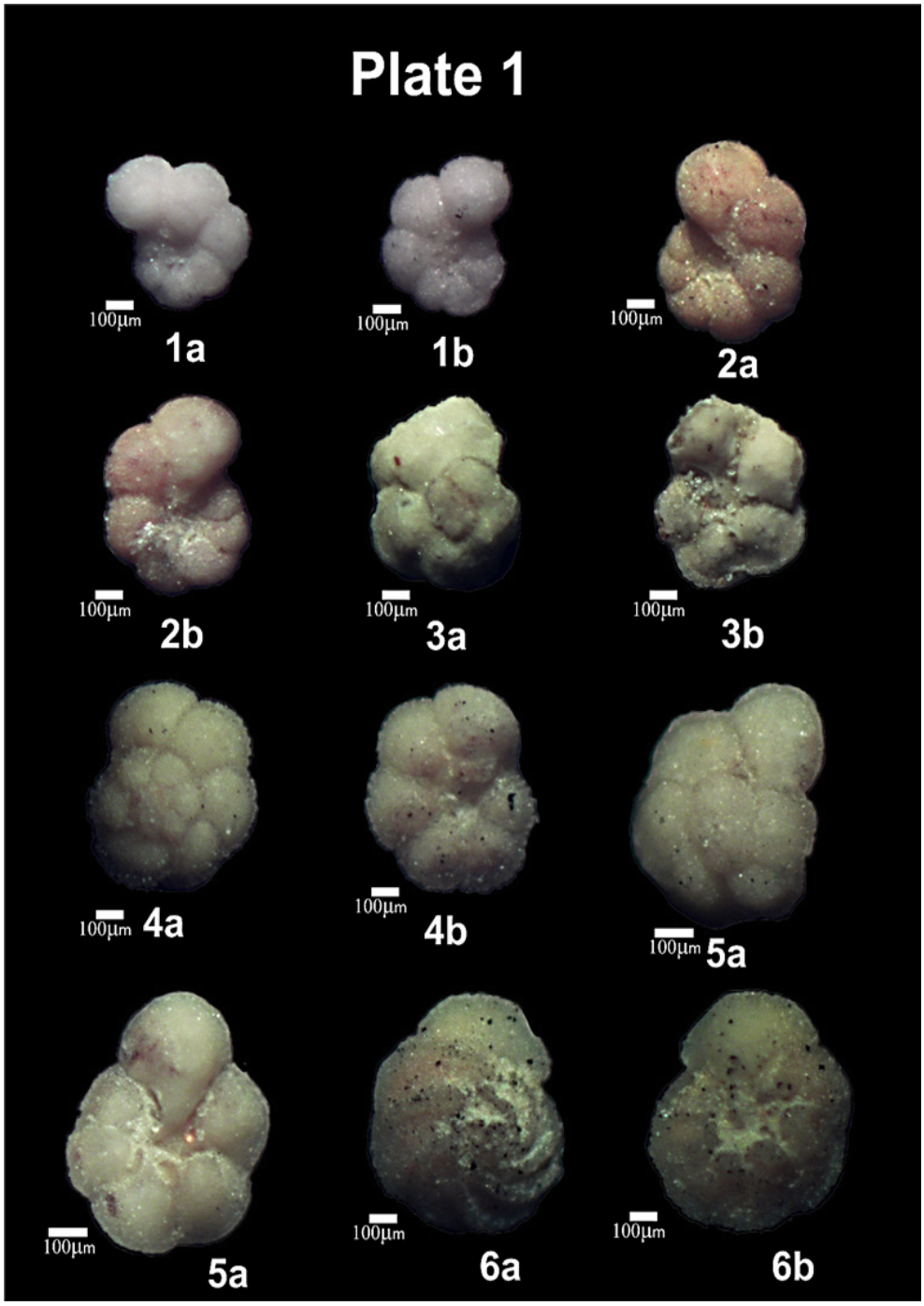

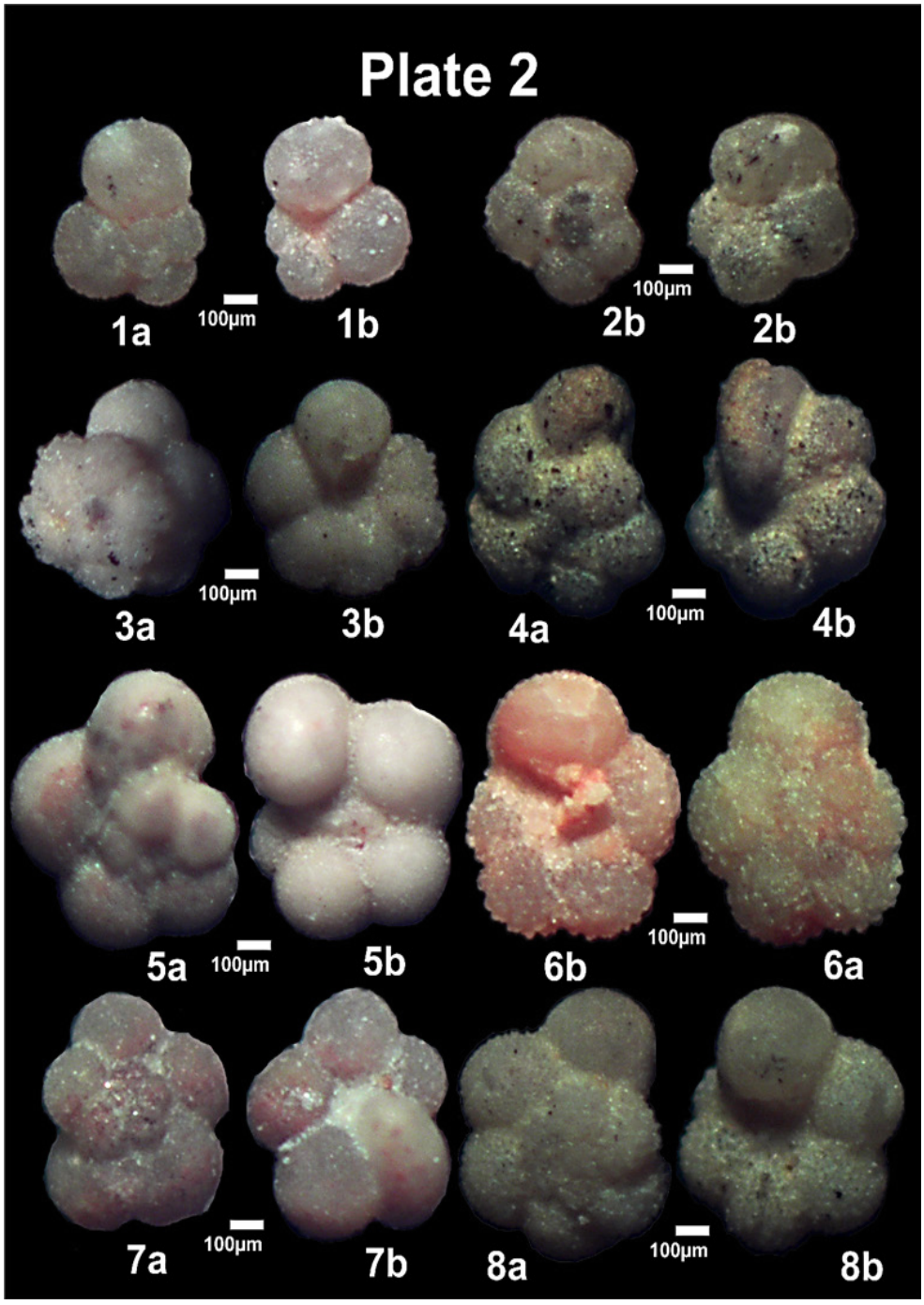

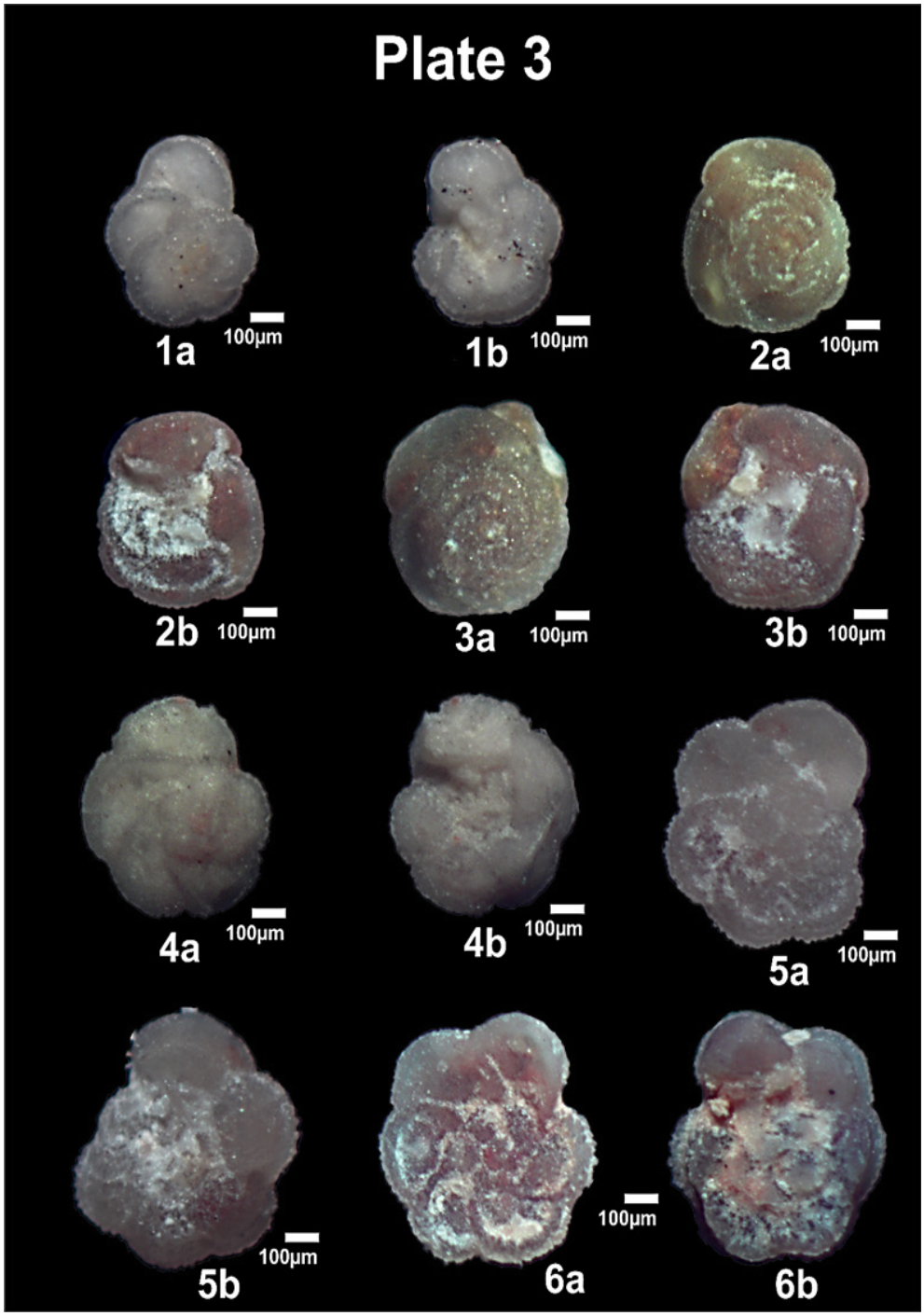

 ISSN: Online 2790-1637, Print 2790-1629
National Library of Libya, Legal number: 154/2018

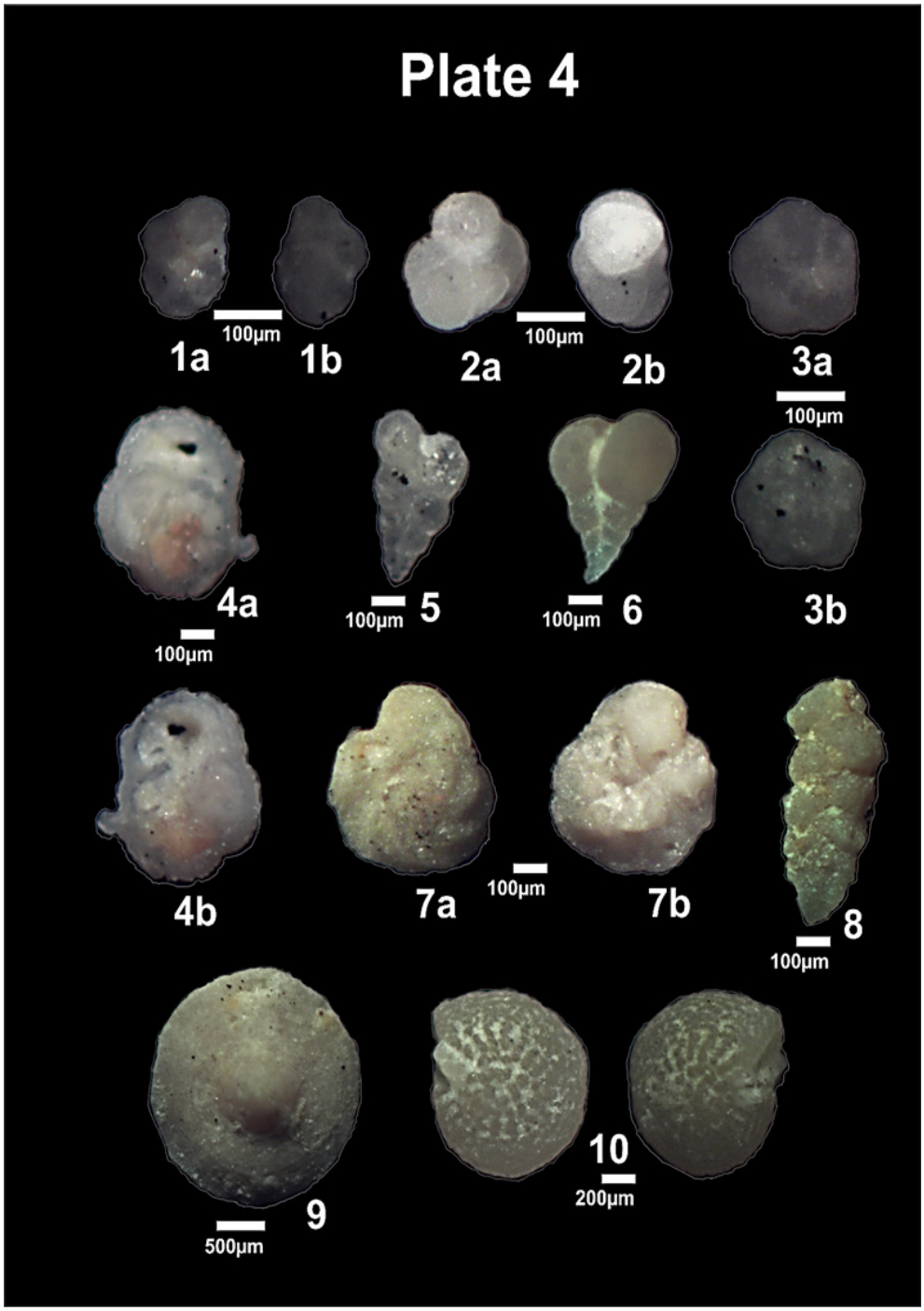

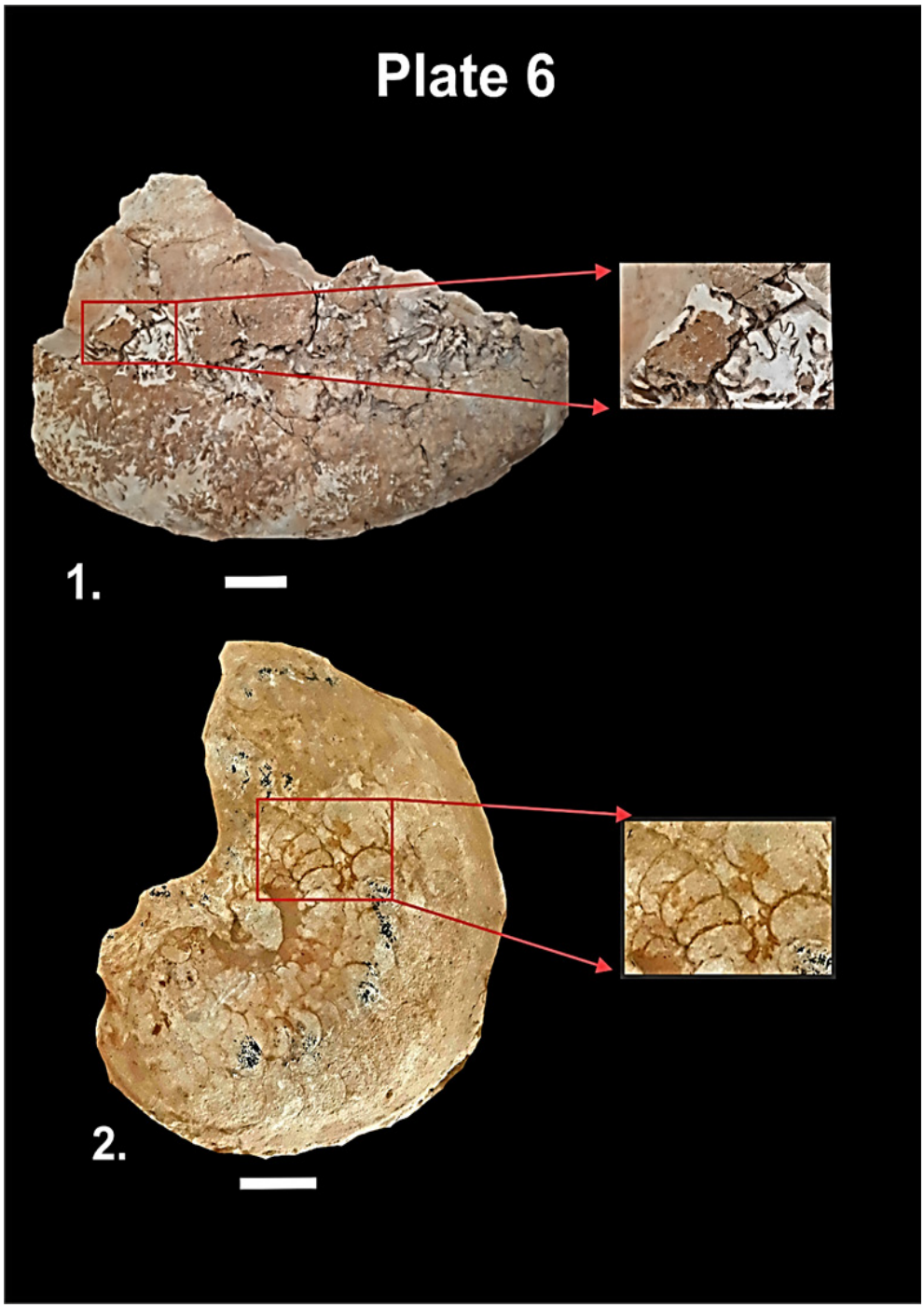

 ISSN: Online 2790-1637, Print 2790-1629
National Library of Libya, Legal number: 154/2018

Scientific Journal of University of Benghazi

SJUOB (2025) 38 (1) Applied Sciences: Matter, et la , 159 – 178
www.sjuob.uob.edu.ly

Heavy metals in water associated with oil and soil were treated using chemical and electrophoretic precipitation methods.

Hamdy AB. Matter[1,2]*, Mohamed emgharbi[3]

1 Associate Professor, Chemistry Department, Banghazi University, Elwahate, Jalow, Libya.
2 Associate Professor, High Institute of Engineering and Technology, El-Arish, Eygpt.
3 Libyan Academy postgraduate Studies/ Benghazi, Libya.

Received: 28 / 02 / 2025 | Accepted: 05 / 10 / 2025 | Publishing: 29/06/2025

ABSTRACT

Chemicals such as potassium hydroxide (KOH), potassium ferrocyanide ($K_4[Fe(CN)_6]$), and oxalic acid ($H_2C_2O_4$) have been used as agents capable of rapidly and efficiently forming precipitates with heavy metal ions under natural environmental conditions. The active components in these chemicals act as chelating agents, enabling them to form stable precipitates or complexes with heavy metals present in water associated with oil and in the surrounding soil.

This study compares the efficiency and characteristics of chemical precipitation products with those formed via cathodic deposition during electrochemical treatment. The ability of both methods to precipitate various heavy metals (HMs)—including Cr, Fe, Ni, Mg, Cu, Zn, Ag, Cd, Mn, and Pb—was investigated. Each method demonstrated varying effectiveness in removing specific metals, and it was measured deposition efficiency, standard deviation S and a coefficient of variation (CV).

Chemical and electrical methods have treated oil-related water and soil contaminated with common heavy metals, which could be removed and treated chemically and electrically. The results revealed very high concentrations of these harmful heavy metals, which have contaminated oil-related water, the soil, the groundwater beneath it, and the plants it irrigates. This poses risks to human and animal health and may even cause diseases and cancer.

Keywords: heavy metals, water associated with oil soil water treatment, Electrophoretic Precipitation.

Corresponding Author: Hamdy AB. Matter, hamdy.matter@uob.edu.ly

 ISSN: Online 2790-1637, Print 2790-1629
National Library of Libya, Legal number: 154/2018

1- INTRODUCTION

Biochemical-electrochemical (BES) systems, as well as electrolytic reactors (ERs), have been evaluated for their effectiveness in removing heavy metals (HMs) and filtering fly ash. X-ray diffraction analysis revealed high concentrations of zinc, lead, and copper [1]. Various electrochemical treatment methods, such as electrocoagulation and electrolysis, have proven effective in removing residual impurities from contaminated water [2]. A new electrolysis technology, developed at laboratory scale, has been tested for deep extraction and separation of various metals, including heavy metals [3]. Microbial electrolysis cells (MECs) have been developed to treat acid mine drainage (AMD), simultaneously producing hydrogen gas (H_2). Dual-chamber microbial electrolysis cells have also been specifically designed for the removal of Cu^+, Ni^+, and Fe^+ under both single-metal and mixed-metal conditions [4]. Laboratory-scale microbial fuel cells (MECs) have successfully removed heavy elements such as lead and cadmium under various electrical conditions, operating times, and concentrations [5]. For the removal of heavy elements such as zinc, manganese, and nickel from process water, dual-electrode systems using steel as the cathode and coal- or platinum-coated titanium as the anode have shown promising results [6]. Further studies have investigated the role of bioreduction and electrochemical reduction in microbial fuel cells (MFCs) and microbial fuel cells (MECs) in the removal and recovery of harmful organic pollutants [7]. Platinum-coated coal and titanium electrodes showed good anode resistance at different current densities [8]. The performance of a continuous recirculation flow cell has also been evaluated at low current densities and different pH levels when treating wastewater and associated water in copper smelting plants, confirming the effectiveness of cathodic reduction in removing organic pollutants [9]. The removal efficiencies of Pb and Cd were found to be significantly influenced by factors such as applied voltage, current, purging solution type, soil pH, permeability, and zeta potential [10].

The electrochemical removal of CM cations from aqueous solutions was investigated using single-chamber (DKE) electrolyzers [11]. Although advanced oxidation techniques can produce high-purity water, their high operational costs limit large-scale

 ISSN: Online 2790-1637, Print 2790-1629
National Library of Libya, Legal number: 154/2018

implementation. Chemical coagulation, while effective, is relatively slow and leads to significant sludge generation [12]. Solidification/stabilization (S/S) methods are being explored as potential treatments for electrolytic manganese residue (EMR) [13]. An improved electrokinetic (EK) process for heavy metal (HM) removal from electroplating sludge was developed by introducing electrolytes into the electrode chambers, significantly enhancing removal efficiency [14]. Moreover, an actively synthesized catholyte solution was employed for the electrochemical deposition of HMs such as Fe, Cu, and Zn, demonstrating its potential for electrocoagulation (electro-flocculation) applications [15]. A laboratory-scale process integrating electrolysis (EL) and electrodialysis (ED) was designed for the efficient treatment of Cu-containing wastewater [16]. A glow discharge plasma (GDP) system has been developed, combining redox mechanisms to decompose heavy metal and organic complexes, using Cu-EDTA as a model compound [17]. The simultaneous removal of Fe^{2+} and Pb^{2+} in microbial electrolysis cells (MECs), along with the targeting of ammonium ions in microbial desalination cells (MDCs), has also been demonstrated [18]. Electrochemical filtration pressure cells operating in batch recirculation mode for the removal of heavy metals from copper smelting waste have been tested and shown excellent results [19]. Adsorption and other various physical and chemical techniques have been explored, such as adsorption using new sorbents, ion exchange, membrane filtration, electrodialysis, reverse osmosis, ultrafiltration, and photocatalysis [20].Microbial electrolysis cells (MECs) have emerged as an efficient technology for the simultaneous removal and recovery of nickel (Ni) from electroplating effluents, effectively eliminating both organic matter and Ni ions [21]. The application of an electric field significantly enhances pollutant removal, as pollutant-containing particles behave as polarizable species, functioning similarly to pseudo-electrodes [22]. This method has achieved a total mercury removal efficiency of 60% [23].

A study investigating the electrodeposition of (Cu) and (Pb) onto palm shell–activated carbon electrodes evaluated current efficiency within a continuous packed-bed electrochemical cell [24]. The electrolysis process employed selective anodes and

cathodes to optimize Cu extraction, with maximum efficiency obtained by adjusting the current density [25]. Nanocrystalline Ni-Fe-C cathodes incorporating carbon have shown high electroactivity for the hydrogen evolution reaction (HER) in hot alkaline solutions, indicating their potential for improved electrochemical performance [26]. A novel cementitious composite material was also developed to stabilize electrolytic manganese residue (EMR), an industrial solid waste rich in sulfur and heavy metals (HMs) [27]. The performance of batch electrocoagulation (EC) using iron (Fe) electrodes in a monopolar configuration was evaluated for the simultaneous removal of Cu, Ni, Zn, and Mn from synthetic wastewater [28]. A combined internal micro-electrolysis (IME)–electrocoagulation process was also developed at the laboratory scale for treating real copper smelting wastewater [29]. Electrolysis using Fe electrodes resulted in the generation of Fe^{3+} ions and $Fe(OH)_3$ precipitates, while Cu electrodes produced Cu^{2+} ions and $Cu(OH)_2$ precipitates [30].

Electrolysis experiments were conducted using iron, steel, aluminum (Al), and zinc (Zn) electrodes under varying current densities and treatment durations to evaluate the removal of physico-chemical contaminants, heavy metals (HMs), and microbiological pollutants from different wastewater sources [31]. The results also indicated that a pretreatment process using quicklime effectively solidified and stabilized HMs [32]. Waste printed circuit boards (WPCBs) are among the most complex and valuable components of electronic waste, containing a variety of recoverable metals [33]. Electrolysis is used to remove mercury (Hg) from residual effluents generated during gold processing, using electrode-driven chemical reactions in an electrolyte solution [34]. Electrocoagulation is used to remove HMs such as Cu, Cr, Pb, and Zn from industrial wastewater [35]. Metal removal during electrocoagulation periods can be improved with longer time, increased sodium chloride (NaCl) concentrations, and increased electrical current [36].

To improve chromium (Cr) recovery, various combinations of electrodes have been tested to increase the extraction capacity [37]. Electrolytic membrane extraction (EME) is used to remove Cu from aqueous solutions, using a specialized electrochemical cell consisting of two glass chambers, a

supported liquid membrane (SLM), a graphite anode, and a stainless steel cathode [38]. Electrokinetic treatment of soils contaminated with copper, lead, and chromium has been piloted and has proven promising [39]. Stabilization of contaminants from electrolytic manganese residue (EMR) is critical to ensure its safe handling and potential reuse in environmental protection [40]. the active chemicals in Picovit, Clara, Drill, Endocer Givescon, Hydral, Laxofin, Maxlase, Motilium, Orapen, Scopinal, Maltvitamin, and Xilone drugs have been used as chelating agents for heavy metals remediation [41].

In this study, heavy metal ions were precipitated using oxalic acid, potassium ferricyanide, and potassium hydroxide. The efficiency of chemical precipitation was compared with that of electro-precipitation. Both methods were applied to remove heavy metals from water and soil associated with oil production in the Nafoora field, operated by the Arabian Gulf Oil Company in Jalu, Libya.

2- EXPERIMENTAL

2.1. Chemicals and Equipment's

Beakers of 250 ml capacity - Filter papers - Funnels - Cylinder tester - Cups - Conical flasks Sensitive balance – Standard measuring flasks 250 ml.

2.2. Preparation of solutions

100 ml of solution of 0.1 molar are prepared from the following materials: Cu $(NO_3)_2$.$3H_2O$ (2.4g), $AgNO_3$ (1.7g), $MgSO_4$ (1.2g), $NiSO_4$ (1.54g), Fe $(NO_3)_3$.$9H_2O$ (4.04g), Cr $(NO_3)_2$.$9H_2O$ (4g), $CdSO_4.4H_2O$ (3.52), Pb $(NO_3)_2$ (3.3g), $ZnSO_4$. $7H_2O$ (1.61g) and $MnSO_4$. (1.69g). Add 50 ml of metal ion solution to 50 ml from 0.1M precipitating agents (Oxalic acid, $C_2H_2O_4$, Potassium ferricyanide $K_4[Fe(CN)_6]$ and Potassium hydroxide KOH, then, the solution was filtrated, dry, and weighted.

2.3. Method of precipitation

50 ml of heavy metal salts solution such as Cu $(NO_3)_2$.$3H_2O$, $AgNO_3$, $MgSO_4$, $NiSO_4$, Fe $(NO_3)_3$.$9H_2O$, Cr $(NO_3)_2$.$9H_2O$, $CdSO_4.4H_2O$, Pb $(NO_3)_2$, $ZnSO_4$. $7H_2O$ and, $MnSO_4$, were added to 50 ml of 0.1 M solution of $H_2C_2O_4$ acid and the temperature was adjusted to 25 degrees and the pH value to 7-8 using a buffer solution of $H_2C_2O_4$ acid and $Na_2C_2O_4$ and the solution was left for 24 hours to ensure the complete precipitation process. Then the precipitate was filtered, washed with distilled water, dried and the precipitate was weighed and the precipita-

tion efficiency was calculated under those conditions. The work was repeated with three other precipitating agents; $H_2C_2O_4$ acid, ($K_4[Fe(CN)_6]$) and KOH) then the solution was filtrated, dry, and weighted.

2.4. Digestion of the percipitation:

The percipitation process took place for a period of one to three hours on a water bath or leaving it for a period of 12-24 hours at room temperature. During the digestion process, crystallization is continuously re-crystallized, which leads to elimination of pockets trapped inside the percipitation, Get rid of impurities, Creating bridges, which leads to the formation of larger granules, Dissolution of small granules and growth of large granules. It is the weight of the substance to be determined (the precipitate) contained in one gram of the precipitate. The gravimetric coefficient = the atomic weight of the element to be determined / the molecular weight of the precipitate.

$$\text{The gravimetric coefficient}(GC) = \frac{At.Wt}{M.Wt} \text{---} -(1)$$

2.5. Electrolysis cell

Electrochemical cell design, electrode setup, and principles of operation (maximum capacity of 100 mL of sample or electrolyte reservoir) and all the other apparatus are shown in Fig. 1. The device was composed of (a) a jacketed electro- chemical cell, a conventional three-electrode arrangement with a (b) Ag/AgCl (KClsat.) reference electrode, (c) a platinum wire auxiliary electrode, and graphite electrode.

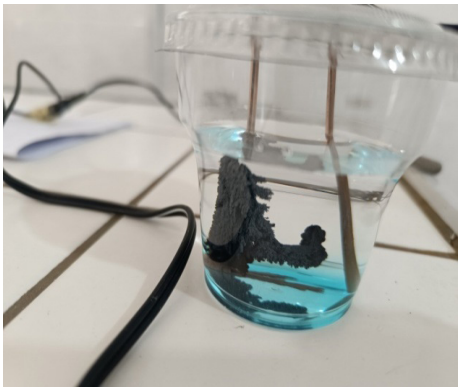

Figure.(1). Shows the electrolysis cell for $CdSO_4.8H_2O$.

2.6. Electrophoretic Precipitation Method

The feasibility of this process for the recovery of (HMs) from aqueous solutions was determined. The effects of three operational parameters, namely voltage, initial ion concentration, and water flow, on the recovery of metals and water were investigated and optimized. The feasibility of this process for the extraction of heavy metals from aqueous solutions was determined. The effects of three operational parameters were

investigated: voltage using a voltage range of 5 –12 V, initial ion concentration in all 0.1 M (HM) ion solutions, and the surface area of the electrodes used for electrodeposition. The process also included a 24-hour holding time, electrode drying, weighing, and calculating the amount of precipitate formed on the cathode as a result of the deposition process. The process also included calculating the deposition efficiency for solutions with a known concentration of 0.1 M. The same conditions were then applied to water associated with the oil and the precipitation of (HM) ions. The accompanying soil was also prepared by placing 100 grams of the accompanying soil in a liter of distilled water with continuous stirring for two hours, then filtering the solution and taking 100 ml of the filtered solution and precipitating the ions in it by electro-precipitation under the same previous conditions.

2.7. statistical determination

-Among these statistical indicators are the following:

-Variation coefficient CV and it get from the relationship:

$$CV = \frac{S}{X} \times 100 \quad ----- (2)$$

-where S is the standard deviation and it get from the relation:

$$S = \sqrt{\frac{\sum (X - x)^2 \ * f}{\sum f - 1}} \quad ------- (3)$$

-where X is the mean, which is the arithmetic average of the values, and it get from the relationship:

$$X = \frac{\sum f * x}{\sum f} \quad ------- (4)$$

3. RESULTS

3.1. Precipitate HMs by oxalic acid.

Table .(1). The GC, ppt, % eff. S, CV, and K sp., of heavy metal precipitate with oxalic acid.

Ppt/g	Cr	Fe	Ni	Mg	Cu	Zn	Ag	Cd	Mn	Pb
GC	0.37	0.39	0.40	0.21	0.35	0.42	0.35	0.35	0.38	0.70
ppt	0.01	0.01	0.495	0.01	0.605	0.28	0.684	0.055	0.085	0.349
.eff %	1.5%	1.4%	70%	1.8%	80%	37%	46%	8%	12%	25%
S	0.001	0.001	0.05	0.001	0.05	0.02	0.05	0.001	0.001	0.02
CV	10%	10%	10%	10%	8%	7%	7%	2%	12%	6%
.K sp	-	-	-	$10^{-5}\times8$	-	$10^{-8}\times2.7$	-	$10^{-8}\times1.5$	-	-

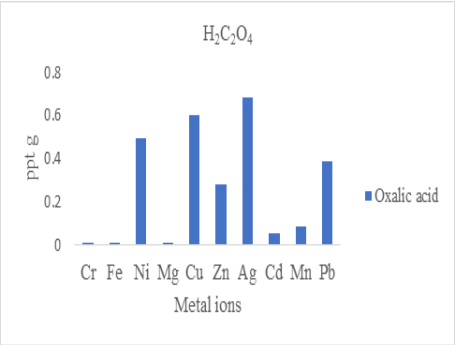

From Figure.(2). The relationship between the metals oxalate which precipitated by adding 50 ml of 0.1M of oxalic acid to 50 ml 0.1M of metal ions.

3.2. Precipitate HMs by ($K_4[Fe(CN)_6]$).

Figure.(2). shows the weight ppt of metal oxalate in 100 ml of solution.

Table .(2). The GC, ppt, % eff. S, CV, and K sp., of heavy metal precipitate with potassium ferricyanide.

Ppt/g	Cr	Fe	Ni	Mg	Cu	Zn	Ag	Cd	Mn	Pb
G C	0.35	0.37	0.38	0.18	0.41	0.42	0.92	0.32	0.37	0.92
ppt	0.278	1.804	0.599	0.11	2.512	0.517	0.97	2.394	1.532	0.902
.eff %	23%	99%	40%	8%	99%	33%	42%	99%	99%	40%
S	0.03	0.06	0.05	0.01	0.05	0.02	0.05	0.08	0.05	0.05
CV	10%	3%	10%	10%	2%	4%	6%	3%	3%	6%
.K sp	-	$10^{-11}\times1.21$	-	-	$^{16-}10\times1.3$	-	-	-	-	-

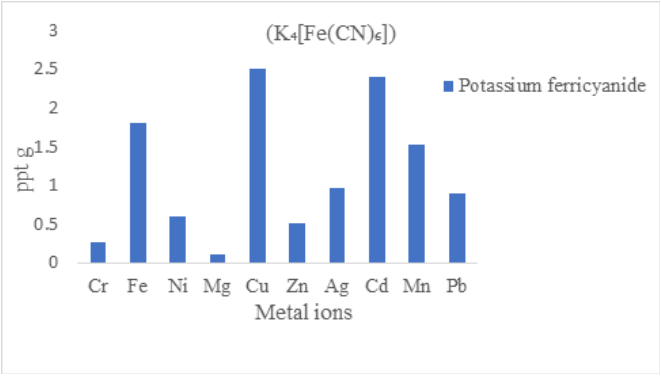

Figure.(3). Shows the weight ppt of metal ferricyanide in 100 ml of solution.

From Figure.(3). The relationship between the metals ferricyanide which was precipitated by adding 50 ml of 0.1M of ($K_4[Fe(CN)_6]$) to 50 ml 0.1M of metal ions.

3.3. Precipitate HMs by potassium hydroxide.

Table 3. The GC, ppt, % eff. S, CV, and K sp., of heavy metal precipitate with KOH

Ppt/g	Cr	Fe	Ni	Mg	Cu	Zn	Ag	Cd	Mn	Pb
G C	0.6	0.63	0.63	0.41	0.65	0.65	0.86	0.58	0.61	0.86
ppt	2.276	0.092	0.349	0.473	1.004	0.329	0.765	1.452	1.313	0.225
.eff %	99%	29%	76%	56%	97%	66%	99%	99%	99%	19%
S	0.01	0.001	0.03	0.05	0.05	0.03	0.08	0.08	0.07	0.03
CV	1%	1%	10%	10%	5%	9%	10%	6%	6%	13%
.K sp	$^{31-}$10× 6.3	$^{38-}$10×4	$^{15-}$10×2.0	$^{11-}$10×1.8	$^{20-}$10×2.2	$^{17-}$10×1.2	-	-	-	$^{15-}$10×1.2

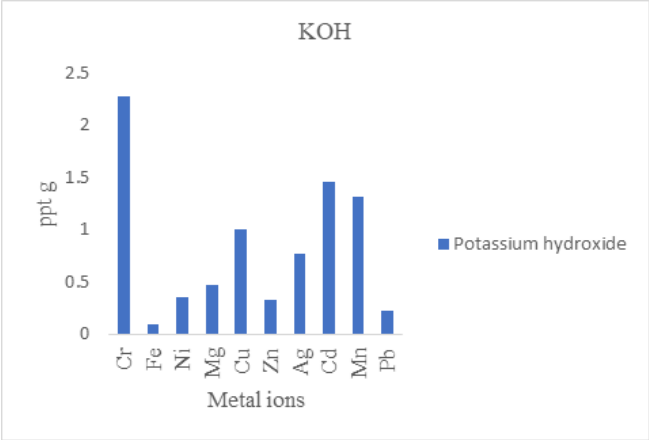

Figure. (4). Shows the weight ppt of metal hydroxide in 100 ml of solution.

From Fig.4. The relationship between the metals hydroxide which precipitated by adding 50 ml of 0.1M of potassium hydroxide to 50 ml 0.1M of metal ions.

3.4. Precipitate HMs by electrolysis.

Table .(4). The ppt, % eff. S, CV, and V of heavy metal precipitate by electrolysis.

Ppt/g	Cr	Fe	Ni	Mg	Cu	Zn	Ag	Cd	Mn	Pb
ppt	0.645	0.633	0.864	0.212	0.107g	0.239	0.674	0.761	0.382	0.382
% eff.	62%	57%	75%	44%	9%	18%	62%	90%	35%	19%
S	0.06	0.06	0.06	0.02	0.01	0.03	0.05	0.06	0.03	0.03
CV	10%	10%	8%	10%	9%	12%	8%	9%	8%	8%
V	- 0.91	- 0.77	- 0.23	-2.3	0.34	-0.76	0. 80	0.40	-1.18	− 0.13

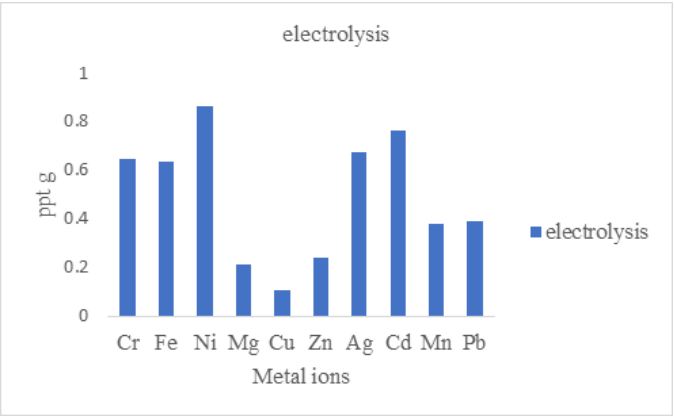

Figure. (5). Shows the weight ppt of metals at electrodes by electrolysis.

From Figure.(5). The relationship between the metals which was precipitated by electrolysis. Fig.5. displays the relationship between the metals which precipitated by electrolysis. The findings show that Cr, Fe, Ni, Ag, Cd, Mn, and Pb were the highest precipitated than other metal ions by electrolysis. The percentage of deposition on the negative electrode in the electrolytic cell is due to the value of the reduction potential of the ions on the cathode when all other factors are constant, which made the values of the percentage of deposition consistent with the values of the reduction potentials in order. Cr = − 0.91 V, Fe = - 0.77 V, Ni = − 0.23 V, Ag = + 0. 80 V, Cd = − 0.40 V, Mn = −1.18 V, Pb = − 0.13 V

3.5. The differences between the precipitation of heavy metals by chemical precipitation and electrolysis

 ISSN: Online 2790-1637, Print 2790-1629
National Library of Libya, Legal number: 154/2018

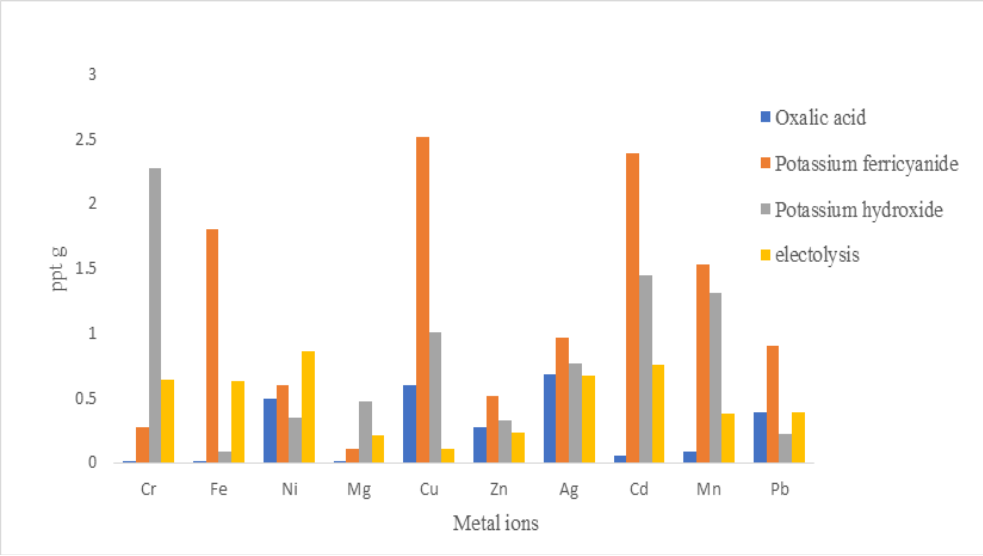

Figure.(6). Shows The differences between chemical precipitation and electrolysis

3.6. Application

3.6.1. The differences between chemical precipitation of heavy metals at soil and water associated with oil.

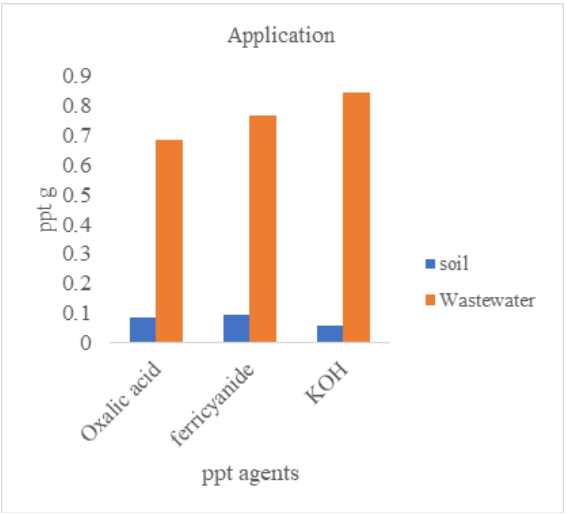

Figure.(7). Shows the weight ppt of metal oxalate, ($K_4[Fe(CN)_6]$)and KOH in 100 ml of solution at water associated with oil and soil.

3.6. 2. The differences between the precipitation of heavy elements by electrodeposition of both soil and water associated with oil.

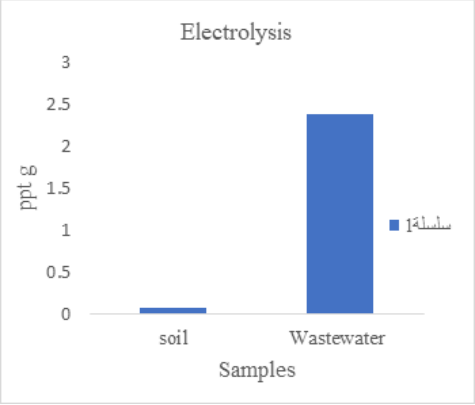

Figure. (8). Shows the weight ppt of metals at electrodes by electrolysis.

4. DISSECTIONS

Table (1). Shows that Cu, Ni and Ag have the highest deposition efficiency of 80%, 70% and 0.46 respectively, with oxalate, at standard deviation S= 0.05 and a coefficient of variation of C. V= 8%, 10% and 7% respectively.

From figure. (2), shows that Ag, Cu, Ni, and Pb were the highest precipitated than other metal ions by oxalic acid. oxalic acid facilitated to the removal of Pb^{2+} [42], K_{sp}. of $Ag_2C_2O_4$ white = 5.40×10^{-12}, $CuC_2O_4 = 2.9 \times 10^{-8}$, $NiC_2O_4 = 1\ 10^{-7}$, and PbC_2O_4 white = 4.8×10^{-10}, The results of the precipitation of heavy element ions using $H_2C_2O_4$ were consistent with the solubility product of each of the precipitates: $Ag_2C_2O_4$, then Cu, then Ni, then Pb.

Table (2). Shows that Cu, Fe, Cd and Mn have the highest deposition efficiency of 99%, 99%, 0.99 and 0.99 respectively, with standard deviations S= 0.05, 0.06 and 0.08 and a coefficient of variation of CV= 2%, 3%, 3% and 3% respectively, and the solubility product of K sp. of Cu is 1.3×10^{-16} and K sp. of Fe 1.21×10^{-11}, respectively.

From figure. (3), shows that Fe, Cu, Cd, Pb, and Mn were the highest precipitated than other metal ions by Potassium ferricyanide. $K_{sp.}$ for Fe $=1.21 \times 10^{-11}$, [43].

Table (3). Shows that Cr, Ag, Cd and Mn have the highest deposition efficiency of

99%, 99%, 0.99 and 0.99 respectively, with standard deviations S= 0.01, 0.08, 0.08 and 0.5, and coefficients of variation CV = 1%, 10%, 6% and 6% respectively, and the solubility product Ksp. of Cr is 6.3×10^{-31} and of Pb is 1.2×10^{-15} respectively.

In figure. (4), shows that Cr, Cu, Cd, and Mn were the highest precipitated than other metal ions by potassium hydroxide KOH, $K_{sp.}$ Cr $(OH)_3$ gray-green = 6.3×10^{-31}, Cu $(OH)_2$ = pale blue = 2.2×10^{-20}, Cd $(OH)_2$ = 7.20×10^{-15}, Mn $(OH)_2$ light pink = 1.9×10^{-13} [44]. The results of the precipitation of heavy element ions using KOH were consistent with the solubility product of each of the precipitates: Cr, Cu, Cd, Mn.

Table (4) Shows that through electrodeposition, cadmium, nickel, chromium and silver have the highest deposition efficiencies of 90%, 75%, 0.62 and 0.62 respectively, with standard deviations of 0.01, 0.08, 0.08 and 0.5 and coefficient of variation of 9%, 8%, 6% and 5% respectively, and reduction potentials as shown in Table 4.

From figure. (5), shows that Cr, Fe, Ni, Ag, Cd, Mn, and Pb were the highest precipitated than other metal ions by electrolysis. The percentage of deposition on the negative electrode in the electrolytic cell is due to the value of the reduction potential of the ions on the cathode when all other factors are constant, which made the values of the percentage of deposition consistent with the values of the reduction potentials in order. Cr = − 0.91 V , Fe = - 0.77 V, Ni = − 0.23 V, Ag = 80 .0+ V, Cd = − 0.40 V, Mn = −1.18 V, Pb = − 0.13 V

From figure. (6), shows that Cr, Fe, Cu, Cd, and Mn were the highest precipitated than other metal at all, the order of the most precipitated elements was approximately consistent with both the solubility constant and the reduction potentials.

From figure. (7), shows that the highest metal ions were precipitated from wastewater than other metal the ions were precipitated from soil due to the concentration of metal ion in wastewater was greater the concentration of metal ions at soil.

From figure.(8), shows that the highest metal ions were precipitated from wastewater by electrodeposition than other metal the ions were precipitated from soil by electrodeposition due to the concentration of metal ion in wastewater was greater the concentration of metal ions at soil.

5. CONCLUSION

Chemical precipitation, offers a relatively simple and cost-effective approach for removing heavy metals (HMs) from contaminated water. The use of chelating agents such as (KOH), ($K_4[Fe(CN)_6]$), and ($H_2C_2O_4$) enables efficient removal of multiple metal ions simultaneously. While electrochemical methods can also remove heavy metals, they generally require more complex setups and higher energy input compared to chemical precipitation. Electrochemical precipitation may be particularly useful for the selective extraction of specific heavy metals.

Chemical precipitating agents such as KOH, $K_4[Fe(CN)_6]$, and $H_2C_2O_4$ act as chemical precipitating and chelating agents. These react with heavy metal ions in water and aqueous soil solutions, forming insoluble compounds that then precipitate. This process effectively removes various heavy metals from oil-related water, such as Cr, Fe, Ni, Mg, Cu, Zn, Ag, Cd, and Pb, with selective efficacy. The effectiveness of chemical precipitation and electrochemical precipitation (using a cathode) for the removal of heavy metals from oil-related water has been compared. Both methods have been shown to be capable of removing heavy metals, but they operate through different mechanisms. Chemical precipitation involves adding precipitating agents (such as KOH or $H_2C_2O_4$) that react with metal ions to form insoluble compounds, which then precipitate from solution. Electrochemical precipitation involves applying an electric current to reduce metal ions at a cathode, forming solid metal deposits. Different precipitating chemicals have been shown to exhibit varying efficiencies in precipitating heavy metals at varying rates. Oxalic acid ($H_2C_2O_4$) was particularly effective at precipitating cadmium or magnesium, while $K_4[Fe(CN)_6]$) may be more effective at precipitating metals such as copper or silver. Potassium hydroxide is known to raise the pH of water, facilitating the precipitation of metal hydroxides, and is particularly effective for metals such as copper and nickel. $K_4[Fe(CN)_6]$) is effective at forming stable complexes with metals such as copper and zinc, often resulting in highly efficient removal. $H_2C_2O_4$ is particularly effective at removing metals such as calcium, magnesium, and iron. These metals are harmful and carcinogenic and can accumulate in plants, animals, and humans, causing a range of ail-

ments, including organ damage and cancer. Therefore, treating water contaminated with heavy metals from petroleum activities is critical to preventing environmental damage and protecting humans from disease.

6.ACKNOWLEDGEMENT

We thank of El-Khalij oil company in Elwahate Jalu, Libya for aid and cooperation to complete this paper. We also thank of an engineering and workers of El-Khalij oil company for the cooperation and aids.

7. REFERENCES

1.Tao, H. C., Lei, T., Shi, G., Sun, X. N., Wei, X. Y., Zhang, L. J., & Wu, W. M. (2014). Removal of heavy metals from fly ash leachate using combined bioelectrochemical systems and electrolysis. Journal of Hazardous materials, 264, 1-7. https://doi.org/10.1016/j.jhazmat.2013.10.057

2.Shim, H. Y., Lee, K. S., Lee, D. S., Jeon, D. S., Park, M. S., Shin, J. S., ... & Chung, D. Y. (2014). Application of electrocoagulation and electrolysis on the precipitation of heavy metals and particulate solids in washwater from the soil washing. Journal of Agricultural Chemistry and Environment, 3(04), 130. http://creativecommons.org/licenses/by/4.0/

3.Luo, H., Liu, G., Zhang, R., Bai, Y., Fu, S., & Hou, Y. (2014). Heavy metal recovery combined with H_2 production from artificial acid mine drainage using the microbial electrolysis cell. Journal of hazardous materials, 270, 153-159. DOI: 10.1016/j.jhazmat.2014.01.050

4.Colantonio, N. (2016). Heavy metal removal from wastewater using microbial electrolysis cells (Doctoral dissertation). https://doi.org/10.1016/j.jhazmat.2014.01.050

5.Fischer, R., Seidel, H., Rahner, D., Morgenstern, P., & Löser, C. (2004). Elimination of heavy metals from leachates by membrane electrolysis. Engineering in life sciences, 4(5), 438-444. https://doi.org/10.1002/elsc.200420049

6.Tsai, L., Fang, H., Lin, J., Chen, C., & Tsai, F. (2009). Recovery and stabilization of heavy metal sludge (Cu and Ni) from etching and electroplating plants by electrolysis and sintering. Science in China Series B: Chemistry, 52, 644-651. https://doi.org/10.1007/s11426-009-0047-6

7.Chakraborty, I., Sathe, S. M., Khuman, C. N., & Ghangrekar, M. M. (2020). Bioelectrochemically powered remediation of xenobiotic compounds and heavy metal toxicity using microbial fuel cell and microbial electrolysis

 ISSN: Online 2790-1637, Print 2790-1629
National Library of Libya, Legal number: 154/2018

cell. Materials Science for Energy Technologies, 3, 104-115. https://doi.org/10.1016/j.mset.2019.09.011

8.Fischer, R., Seidel, H., Rahner, D., Morgenstern, P., & Löser, C. (2002). Elimination of heavy metals from process waters of the bioleaching process by electrolysis. Journal of Soils and Sediments, 2, 166-168. https://doi.org/10.1007/BF02991035

9.Basha, C. A., Bhadrinarayana, N. S., Anantharaman, N., & Begum, K. M. S. (2008). Heavy metal removal from copper smelting effluent using electrochemical cylindrical flow reactor. Journal of Hazardous Materials, 152(1), 71-78. https://doi.org/10.1016/j.jhazmat.2007.06.069

10.Kim, S. O., Moon, S. H., & Kim, K. W. (2001). Removal of heavy metals from soils using enhanced electrokinetic soil processing. Water, Air, and Soil Pollution, 125, 259-272. https://doi.org/10.1023/A:1005283001877

11.Gomelya, N., Melnychenko, Y., & Radovenchyk, I. (2018). Purification of wastewater from the ions of copper, zinc, and lead using an electrolysis method. Восточно-Европейский журнал передовых технологий, (6 (10)), 42-48. http://nbuv.gov.ua/UJRN/Vejpte_2018_6(10)7.

12.Bazrafshan, E., Mohammadi, L., Ansari-Moghaddam, A., & Mahvi, A. H. (2015). Heavy metals removal from aqueous environments by electrocoagulation process–a systematic review. Journal of environmental health science and engineering, 13, 1-16. https://doi.org/10.1186/s40201-015-0233-8

13.He, D., Luo, Z., Zeng, X., Chen, Q., Zhao, Z., Cao, W., ... & Chen, M. (2022). Electrolytic manganese residue disposal based on basic burning raw material: Heavy metals solidification/stabilization and long-term stability. Science of The Total Environment, 825, 153774. https://doi.org/10.1016/j.scitotenv.2022.153774

14.Peng, G., & Tian, G. (2010). Using electrode electrolytes to enhance electrokinetic removal of heavy metals from electroplating sludge. Chemical Engineering Journal, 165(2), 388-394. https://doi.org/10.1016/j.cej.2010.10.006

15.Gajda, I., Stinchcombe, A., Greenman, J., Melhuish, C., & Ieropoulos, I. (2017). Microbial fuel cell–A novel self-powered wastewater electrolyser for electrocoagulation of heavy metals. international journal of hydro-

gen energy, 42(3), 1813-1819. https://doi.org/10.1016/j.ijhydene.2016.06.161

16.Peng, C., Liu, Y., Bi, J., Xu, H., & Ahmed, A. S. (2011). Recovery of copper and water from copper-electroplating wastewater by the combination process of electrolysis and electrodialysis. Journal of hazardous materials, 189(3), 814-820. https://doi.org/10.1016/j.jhazmat.2011.03.034

17.Liu, Y., Lu, M., Yin, Y., Zhou, J., Qu, G., Zhang, Y., ... & Wang, T. (2022). Self-catalytic Fenton-like reactions stimulated synergistic Cu-EDTA decomplexation and Cu recovery by glow plasma electrolysis. Chemical Engineering Journal, 433, 134601. https://doi.org/10.1016/j.cej.2022.134601

18.Koomson, D. A., Huang, J., Li, G., Miwornunyuie, N., Ewusi-Mensah, D., Darkwah, W. K., & Opoku, P. A. (2021). Comparative studies of recirculatory microbial desalination cell–microbial electrolysis cell coupled systems. Membranes, 11(9), 661. https://doi.org/10.3390/membranes11090661

19.Basha, C. A., Somasundaram, M., Kannadasan, T., & Lee, C. W. (2011). Heavy metals removal from copper smelting effluent using electrochemical filter press cells. Chemical engineering journal, 171(2), 563-571. https://doi.org/10.1016/j.cej.2011.04.031

20.Gunatilake, S. K. (2015). Methods of removing heavy metals from industrial wastewater. Methods, 1(1), 14. www.jmess.org

21.Cai, W. F., Geng, D. L., & Wang, Y. H. (2016). Assessment of cathode materials for Ni (ii) reduction in microbial electrolysis cells. RSC advances, 6(38), 31732-31738. https://doi.org/10.1039/C6RA02082H

22.Rosestolato, D., Bagatin, R., & Ferro, S. (2015). Electrokinetic remediation of soils polluted by heavy metals (mercury in particular). Chemical Engineering Journal, 264, 16-23. https://doi.org/10.1016/j.cej.2014.11.074

23.Issabayeva, G., Aroua, M. K., & Sulaiman, N. M. (2006). Electrodeposition of copper and lead on palm shell activated carbon in a flow-through electrolytic cell. Desalination, 194(1-3), 192-201. https://doi.org/10.1016/j.desal.2005.09.029

24.Choubey, S., Goswami, P., & Gautam, S. (2021). Recovery of copper from waste PCB boards using electrolysis. Materials Today: Proceedings, 42, 2656-2659. https://doi.org/10.1016/j.matpr.2020.12.596

25.Flis-Kabulska, I., Flis, J., Sun, Y., & Zakroczymski, T. (2015). Hydrogen evolution on plasma carburised nickel and effect of iron

deposition from the electrolyte in alkaline water electrolysis. Electrochimica Acta, 167, 61-68. https://doi.org/10.1016/j.electacta.2015.03.132

26.Li, W., Gao, S., Wu, L., Qiu, S., Guo, Y., Geng, X., ... & Liu, L. (2013). High-density three-dimension graphene macroscopic objects for high-capacity removal of heavy metal ions. Scientific reports, 3(1), 2125. https://doi.org/10.1038/srep02125

27.Xue, F., Wang, T., Zhou, M., & Hou, H. (2020). Self-solidification/stabilisation of electrolytic manganese residue: Mechanistic insights. Construction and Building Materials, 255, 118971. https://doi.org/10.1016/j.conbuildmat.2020.118971

28.Al Aji, B., Yavuz, Y., & Koparal, A. S. (2012). Electrocoagulation of heavy metals containing model wastewater using monopolar iron electrodes. Separation and Purification Technology, 86, 248-254. https://doi.org/10.1016/j.seppur.2011.11.011

29.Chen, F., Li, X., Luo, Z., Ma, J., Zhu, Q., & Zhang, S. (2018). Advanced treatment of copper smelting wastewater by the combination of internal micro-electrolysis and electrocoagulation. Separation Science and Technology, 53(16), 2639-2646. https://doi.org/10.1080/01496395.2018.1463265

30.Wahyono, Y., Irviandi, R., Lo, N. K., Rahman, M. I. A., Herdiansyah, F., Haliza, B. T., ... & Pratiwi, N. I. (2022, October). Producing Fe and Cu ions and oxides in water with electrolysis as artificial liquid waste. In IOP Conference Series: Earth and Environmental Science (Vol. 1098, No. 1, p. 012032). IOP Publishing. DOI 10.1088/1755-1315/1098/1/012032

31.Kumar, V. (2017). A review on the feasibility of electrolytic treatment of wastewater: Prospective and constraints. constraints, 2(1), 52-62. www.aesacademy.org

32.Du, B., Zhou, C. B., & Duan, N. (2014). Recycling of electrolytic manganese solid waste in autoclaved bricks preparation in China. Journal of Material Cycles and Waste Management, 16, 258-269. https://doi.org/10.1007/s10163-013-0181-2

33.Wang, J., Huang, Z., Yang, D., Zeng, X., Chen, M., Shu, J., ... & Xiao, Z. (2021). A semi-scaled experiment for metals separating and recovering from waste printed circuit boards by slurry electrolysis. Process Safety and Environmental Protection, 147, 37-44. https://doi.org/10.1016/j.psep.2020.09.030

34.Darmawan, D. U., & Sriwahyuni, S. U.

(2021). Removal of Heavy Metal Mercury (Hg) Liquid Waste through Electrolysis Method in Paya Ateuk Village, Pasie Raja District, South Aceh. The Indonesian Journal of Public Health, 8(2). DOI: https://doi.org/10.35308/j-kesmas.v8i2.4062

35.Petsriprasit, C., Namboonmee, J., & Hunsom, M. (2010). Application of the electrocoagulation technique for treating heavy metals containing wastewater from the pickling process of a billet plant. Korean Journal of Chemical Engineering, 27, 854-861. https://doi.org/10.1007/s11814-010-0145-3

36.Ayub, S., Siddique, A. A., Khursheed, M. S., Zarei, A., Alam, I., Asgari, E., & Changani, F. (2020). Removal of heavy metals (Cr, Cu, and Zn) from electroplating wastewater by electrocoagulation and adsorption processes. Desalin Water Treat, 179, 263-271. doi: 10.5004/dwt.2020.25010

37.Kakakhel, L., Lutfullah, G., Bhanger, M. I., Shah, A., & Niaz, A. (2007). Electrolytic recovery of chromium salts from tannery wastewater. Journal of Hazardous Materials, 148(3), 560-565 . https://doi.org/10.1016/j.jhazmat.2007.03.011

38.Kadhim, N. R., Abbar, A. H., & Flayeh, H. M. (2023). Removal of copper from a simulated wastewater by electromembrane extraction technique using a novel electrolytic cell provided with a flat polypropylene membrane infused with 1-octanol and DEHP as a carrier. Case Studies in Chemical and Environmental Engineering, 8, 100430. https://doi.org/10.1016/j.cscee.2023.100430

39.Kawachi, T., & Kubo, H. (1999). Model experimental study on the migration behavior of heavy metals in electrokinetic remediation process for contaminated soil. Soil science and plant nutrition, 45(2), 259-268. https://doi.org/10.1080/00380768.1999.10409341

40.Chen, H., Long, Q., Zhang, Y., & Qin, L. (2019). Simultaneous immobilization of NH_4^+ and Mn^{2+} from electrolytic manganese residue using phosphate and magnesium sources. RSC advances, 9(8), 4583-4590. DOI: 10.1039/C8RA09615E

41.Matter, H. A., Ayad, T. M., & Alkatly, A. A. (2022). Treatment of Heavy Metals in Water Accompanied with Oil and A Soil Using some Expired Drugs at Al-Wahat/ Libya. Journal of Pure & Applied Sciences, 21(2), 114-119. DOI: 10.51984/JOPAS.V21I2.2046

42.Zeng, Q., Wang, S., Hu, L., Zhong, H.,

He, Z., Sun, W., & Xiong, D. (2021). Oxalic acid modified copper tailings as an efficient adsorbent with super high capacities for the removal of Pb^{2+}. Chemosphere, 263, 127833. https://doi.org/10.1016/j.chemosphere.2020.127833

43.Bellomo, A., Casale, A., & De Marco, D. (1973). Formation of ferricyanides-I silver (I), copper (II) and cadmium (II). Talanta, 20(3), 335-338.https://doi.org/10.1016/0039-9140(73)80029-3

44.https://www.chm.uri.edu/weuler/chm112/refmater/KspTable.html

Scientific Journal of University of Benghazi

SJUOB (2025) 38 (1) Applied Sciences: Ashreik, et la , 179 – 191
www.sjuob.uob.edu.ly

The Impact of Age on Breast Cancer Incidence Among Libyan Women: A Meta-Analysis.

Naeima Ashleik[1,*], Suaad Ben-Farag[1], Intesar N. El-Saeiti[1].

1 All Authors are Staff at the Statistics Department, Science Faculty, University of Benghazi.

Received: 28 / 02 / 2025 | Accepted: 05 / 07 / 2025 | Publishing: 29/06/2025

ABSTRACT

This meta-analysis, which draws on eight original studies, looks at the average age of Libyan women diagnosed with breast cancer. A full review of the original articles published in English between October 2016 and August 2024. A systematic review of five main databases was conducted to identify studies including Embase, Scopus, PubMed, Google Scholar and Web of Science. Only studies with unambiguous age data were included, as determined by the Population, Exposure, Comparator, Outcome, and Study Design (PECOS) criteria. The effect sizes were pooled using a random-effects model, and heterogeneity was measured with Cochran's Q and I^2 statistics. The pooled mean age across studies was 47.81 years (95% CI: 46.87–48.74), indicating high variability (I^2 = 98.1%). Influence diagnostics identified one outlier study that contributed to the high heterogeneity. These findings highlight age distribution patterns in breast cancer cases in Libya, suggesting avenues for targeted early intervention strategies. Overall, these findings emphasize the demand for age-specific screening programs in Libya.

Keywords: Breast Cancer; Meta-Analysis; Age Factor; Heterogeneity; Random-Effects Model; Incidence Rate; Libyan Women

Corresponding Author: Naeima Ashleik, naeima.ashleik@uob.edu.ly

 ISSN: Online 2790-1637, Print 2790-1629
National Library of Libya, Legal number: 154/2018

1.INTRODUSTION

Breast cancer is still the most frequent cancer among women worldwide, and it is the leading cause of cancer-related deaths among women in many nations [1]. Despite substantial breakthroughs in early detection and treatment, differences in breast cancer incidence and mortality remain global, affected by different demographics, lifestyles, and genetic factors [2]. The Middle East and North Africa (MENA) area, including Libya, has seen an increase in breast cancer cases over the last two decades, which can be ascribed to demographic shifts and rising life expectancy[3].

Breast cancer is the most frequent cancer among women in Libya, and the incidence rate has been gradually rising, posing a huge public health challenge. While there are several studies on breast cancer in Western populations, regional studies concentrating on Libyan women are limited, leaving gaps in our understanding of the population's distinctive epidemiological characteristics [4]. Addressing these gaps is critical for designing targeted prevention and intervention methods, as risk factors like age, reproductive history, and genetic susceptibility can differ greatly among populations [5].

Age is one of the common factors that is considered by many Libyan studies on breast cancer. Because of cultural, genetic, or healthcare-access nuances, age is considered a critical factor. The occurrence of breast cancer among Libyan women normally rises as women age. However, late diagnosis and aggressive tumors are considered more concerning factors that are associated with young females who have breast cancer, especially in developing nations [6] . Libya is one of these developing nations that face many challenges, including community awareness that breast cancer is a treatable disease_ an important factor for encouraging early diagnosis. In addition, the country has few advanced pathology services and limited treatment options, including radiotherapy and the full range of systemic treatments available in high-resource settings. Moreover, due to the small sample sizes and conflicting methodologies, research in Libya has shown variations in the age distribution of breast cancer patients[7]. A meta-analysis approach is a good statistical tool that gives a more accurate estimate of age as a risk factor, which facilitates comparing different areas and insights into targeted age-specific interventions [8].

The meta-analysis technique is based on collecting data from different studies, which helps researchers draw useful conclusions, particularly when individual studies report different effect sizes. This technique can estimate heterogeneity and precision, which are critical for understanding policy and practice in health treatments [9]. Due to the lack of meta-analysis studies on breast cancer and conflicting age estimates due to small samples in Libya, this work attempts to show the link between age and breast cancer incidence among Libyan women and make recommendations for healthcare policies in Libya that focus on breast cancer prevention and early identification.

2.MATERIALS AND METHODS

2.1.Search Strategy

Eight original studies published in English from October 2016 to August 2024 were considered and conducted using Embase, Scopus, PubMed, Google Scholar, and Web of Science databases. The research utilized keywords such as “Breast Cancer,” “Risk Factors,” “Awareness and Knowledge of Breast Cancer,” and “Libyan Women” to capture relevant studies focusing on breast cancer demographics within Libya.

2.2.Study Design

Studies were screened at the title and abstract level to assess their relevance and eligibility. Each included article met the following criteria: 1) full text available in English, 2) original research, and 3) compliance with the Population, Exposure, Comparator, Outcome, and Study Design (PECOS) criteria. Table 1 outlines the specific PECOS criteria applied to guide the inclusion and exclusion of studies.

Table .(1): Research question based on PECOS criteria.

(**P** (Population	Libyan women diagnosed with breast cancer
(**E** (Exposure	Age as a risk factor
(**C** (Comparator	Comparison of age's effect on breast cancer risk
(**O** (Outcome	Incidence of breast cancer
(**S** (Study Design	Cross-Sectional Study
Exclusion criteria	.Studies without age-specific data have been excluded

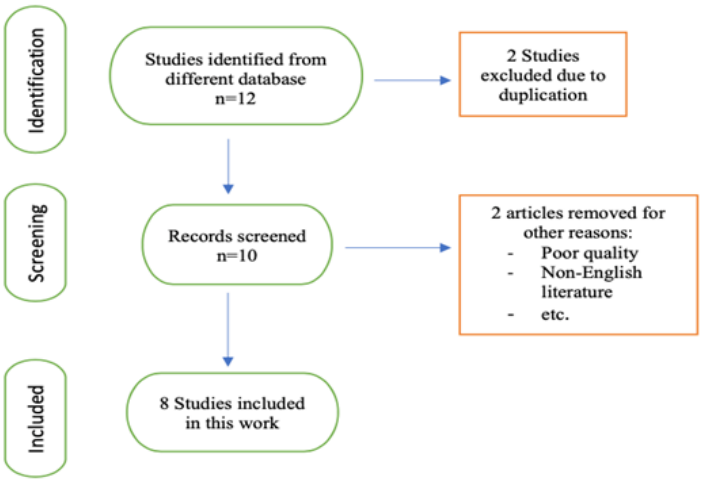

Figure .(1): PRISMA flow diagram of the included studies.

3.STATISYICAL ANALYSIS

The analysis was implemented by using random-effect and common-effect models. In this work, studies were merged according to the sample size, mean, and standard deviation. The analysis was focused on the mean age of Libyan women who have breast cancer. Since the main aim of meta-analysis is minimizing the variance and assessing the dispersion of the effect sizes from study to study, the heterogeneity of the included studies was evaluated. In the random effect model analysis, each study was weighted by the inverse of its variance. Moreover, sensitivity analysis and forest plots were two criteria used to identify any outlier studies in this meta-analysis.

3.1.Computing Q

It is the first step to estimate the heterogeneity, where Q is defined as a mea-

sure of weighted squared deviations, and expressed as follows:

$$Q = \sum_{i=1}^{k} W_i Y_i^2 - \frac{\left(\sum_{i=1}^{k} W_i Y_i\right)^2}{\sum_{i=1}^{k} W_i}$$

Where W_i is the study weight ($\frac{1}{V_i}$),V_i is the within-study variance, and is the study effect size.

3.2.Estimating τ^2

Next, the parameter **τ^2** is between-studies variance (the variance of the effect size parameters across the population of studies), which is defined as follows:

τ^2=(Q-df)/C

where df=k-1 is the degree of freedom , K is the number of studies, and

$$c = \sum_{i=1}^{k} W_i - \frac{\sum_{i=1}^{k} W_i^2}{\sum_{i=1}^{k} W_i}$$

The amount Q-df is the excess variation, which represents the dispersion in true effects, i.e., the differences in the true effects from study to study.

3.3.The I^2 Statistic

The statistics **τ^2** (and **τ**) reflect the amount of true heterogeneity (the variance or the standard deviation), while the **I^2** Statistic is the proportion of the observed variance that reflects real differences in the effect size, and can be written as follows:

I^2=((Q-df)/Q)×100%

From the above equation, it can be seen that is a ratio scale from 0% to 100% and is affected by the amount of excess variation[8].

3.4.Testing the Heterogeneity

To test the heterogeneity, the null hypothesis states that all studies have a common effect size. The follows a central chi-squared distribution with df equals k-1. The p-value will be calculated.

A significant p-value indicates that the null hypothesis is rejected, and the true effect sizes vary.

The computational part of this study was conducted using the Comprehensive Meta-Analysis and R software.

4.RESULTS

This section provides a detailed summary of the age at breast cancer diagnosis among Libyan women based on eight studies. The estimates of heterogeneity, tests of publication bias, and meta-analysis summaries for each of the studies were considered in this analysis.

1. Individual Study Summaries

The mean age, standard deviation, sample size, and 95% confidence Interval (CI) of the eight articles were summarized and displayed in the table below.

Table .(2): The meta-analysis summaries of the age at breast cancer diagnosis among Libyan women based on eight studies.

Study	Study Population	Year	Mean Age	Standard Deviation	Sample Size (n)	95% CI for Mean Age
Mouna[10]	Different cities in Libya*	2020	46.90	8.70	918	[46.3, 47.5]
Mufida[11]	Zawia city	2022	48.00	12.10	200	[46.3, 49.7]
Taher[12]	Tripoli city	2016	48.00	5.00	292	[47.4, 48.6]
Aisha[13]	Tripoli city	2024	47.35	1.00	501	[47.3, 47.4]
Mamduh[14]	National Cancer Institute (NCI Misurata and Sabratha)	2023	48.60	1.09	400	[48.5, 48.7]
Samira[15]	Tripoli city	2020	46.70	15.60	38	[41.7, 51.7]
Huda[16]	Benghazi city	2021	50.50	13.30	336	[49.1, 51.9]
Houssein[17]	Different cities in Libya*	2024	46.10	11.70	984	[45.4, 46.8]

(*) The different cities in Libya include Tripoli, Benghazi, Tobruk, Sabha, Gharyan, Ghadames, Al Jufra, and Murzug.

Studies with small sample sizes have shown that the mean age at diagnosis is steady in the late 40s with large variance, for example, the study of Samira [15].

In general, studies with larger sample sizes have shown more stable mean age; moreover, within study populations, standard deviations have denoted different levels of age diversity.

2.Meta-Analysis Summary

The results from the common effect model and random-effects model were summarized below:

Common Effect Model: The pooled mean age is 47.83 years with a 95% confidence interval [47.77, 47.90].

Random Effects Model: The pooled mean age under the random effects model is 47.81 years, with a 95% confidence interval [46.87, 48.74].

 ISSN: Online 2790-1637, Print 2790-1629
National Library of Libya, Legal number: 154/2018

To visualize these results, a forest plot (see Figure 2) provides a comparative display of mean ages from each study, including their confidence intervals. This helps illustrate the overlap and variation among studies.

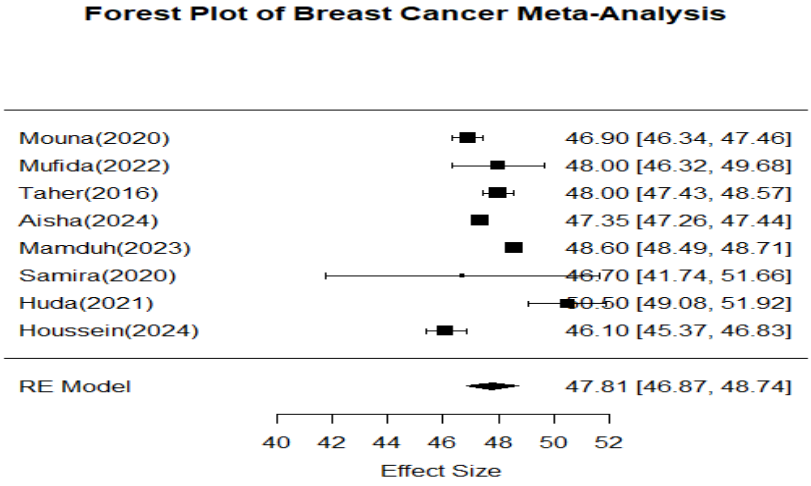

Figure .(2): Forest plot displaying mean age and 95% confidence intervals for each study. Studies with wider confidence intervals indicate more variability and/or smaller sample sizes, while those with narrower intervals are based on larger or more uniform samples.

The random effects model, which accounts for variability between studies, provides a mean age slightly lower than the common effect model. This finding suggests that, despite some variation, the mean age at diagnosis for Libyan women is relatively stable around the 46–48 year range.

3.Heterogeneity Analysis

To examine differences across studies, heterogeneity tests were conducted:

1.**I^2 Statistic**: The I^2 value is 98.1%, indicating high heterogeneity. This means that a large portion of the variability in age at diagnosis is due to differences between studies, differences in study target populations or targeted effects, survey recruitment and administration methods, measurement instruments, doses of interventions, and timing of outcome measurements.

2.Q Statistic: The Q-test was statistically significant ($p < 0.0001$), confirming the pres-

ence of substantial heterogeneity.

These findings are further illustrated in the funnel plot below (Figure 3), which shows the distribution of studies around the pooled mean. Studies dispersed widely from the mean suggest heterogeneity.

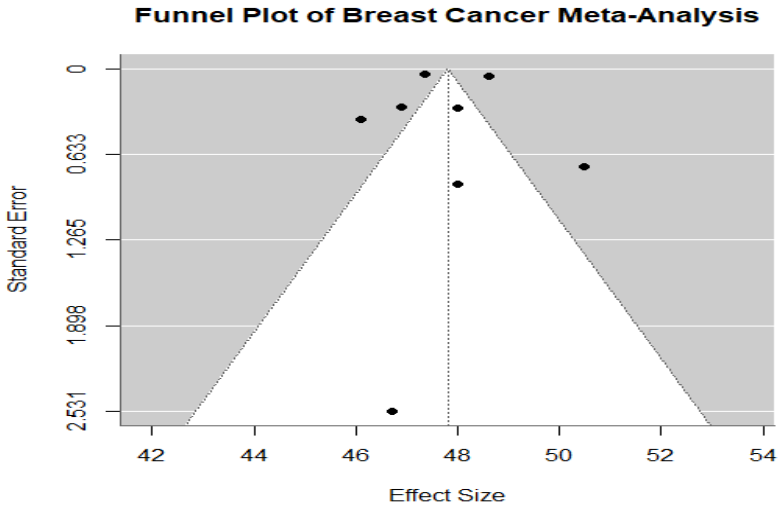

Figure .(3): Funnel plot displays individual study mean ages and sample sizes. While Studies clustering symmetrically around the mean would indicate lower heterogeneity, the observed dispersion highlights significant variability.

The abnormal heterogeneity across studies suggests that factors, such as geographic, genetic, or methodological differences, might influence the age of diagnosis, necessitating a random-effects model to provide more reliable conclusions.

5. PUBLICATION BIAS

A regression test for funnel plot asymmetry (p = 0.8602) suggests no significant publication bias.

The lack of significant publication bias indicates that the pooled mean age estimate is likely robust and unaffected by the selective publication of studies.

6.DISCUSSION

According to this study, the average age of breast cancer diagnosis in Libya is (47.81 years, 95% CI: 46.87–48.74), which appears to be lower than that of other African and Asian countries. In 2004, Schlichting et al[18]. reported a mean age of 51.0 years for 3819 Egyptian women, while Missaoui et al[19]. found a mean age of 50.2 years for 7736 Tunisian women in 2012. In Asian countries, Mehdi I et al[20]. reported a mean age of 49.05 for 1248 women in Oman and a mean age of 49.42 for 536 Iraqi Kurdish women, as reported by Karim et al[21]. When comparing these results to developed countries, such as Canada[22] with a mean age of 60.1 for 36455 women and the United States with a mean age of 58.4 for 110,153 women, it is evident that the age at diagnosis of breast cancer in Libya is significantly lower.

The age factor of breast cancer was considered by a number of studies using a meta-analysis approach. Kumar et al.[23] and Solbana1 and Chaka[24] have addressed that the age at menarche of those <12 years old has a high risk of developing breast cancer three times more than older age. Moreover, the age at first birth has been studied by Argenal et al. [25], where they found that the risk of having breast cancer was three times higher in women aged 30 years and older than in younger women. Again, the study by Ewartz et al.[26] indicated that women who give a first birth at an age older than 35 years have a higher risk (40%) than those women with an age of less than 35. The late 40s are also considered a significant factor affecting the development of breast cancer. In this study, the development of breast cancer in Libyan women was estimated at an age of 48 years. Also, the study, which was conducted by Liu, et al.[27] found that women aged over 50 years

have a high risk of having breast cancer.

The results of this meta-analysis indicate that the pooled mean age of breast cancer patients in Libya is 47.81 years, with significant heterogeneity among the studies (I^2 = 98.1%). This variability may be influenced by factors such as sample size differences, methodological variations, and potential demographic diversity within the studied populations. For example, the study of Mamduh[14] had pointed out that a high influence on the pooled estimate, which may imply different diagnostic practices and rare population characteristics.

The estimated excessive heterogeneity of our findings implies that age alone may not account for the variance in incidence of breast cancer, which recommends further research about other risk factors that could be related to age, such as genetic predispositions, lifestyle factors, and access to healthcare services. The absence of significant publication bias, as assessed by funnel plot asymmetry, supports the reliability of the included studies despite the heterogeneity.

The awareness and screening programs for women who are aged 40 years and older were one of the needs for public health in Libya, and genetic predisposition, cultural delays in seeking care, may explain why Libyan women may be diagnosed younger.

Future research should consider larger, multi-center studies within Libya to better account for regional and socioeconomic variations, further clarifying age-related breast cancer risks and contributing to comprehensive cancer prevention efforts in the region.

The strengths of this study include its status as the most recent systematic review and meta-analysis, with a sample size of 3669 female breast cancer patients between 2016-2024 in Libya. This allows for an overview of the estimated age of diagnosis for breast cancer in women and the pooled prevalence of breast cancer in Libya. However, our study was not free of some limitations. The first limitation was the geographic distribution of the included studies, as most were conducted in the Western regions of Libya. This could cause bias in generalizing the findings to the whole country of Libya. Also, acknowledging small sample sizes in some studies was one of these limitations. Finally, another limitation could be the narrow scope of the review, which focused only on Libya.

7.CONCLUSION

The results suggest that breast cancer is typically diagnosed among Libyan women at an age of approximately 46–48 years, notably younger than the average diagnosis age in Western populations, which often exceeds 50 years. High heterogeneity between studies implies that various factors may influence these estimates, indicating a need for additional research to explore such influences, including potential regional, environmental, or genetic factors.

8.REFERENCES

1.Bray F, Ferlay J, Soerjomataram I, Siegel RL, Torre LA, Jemal A. Global cancer statistics 2018: GLOBOCAN estimates of incidence and mortality worldwide for 36 cancers in 185 countries. CA Cancer J Clin. 2018;68(6):394–424.

2.Ferlay J, Ervik M, Lam F, Colombet M, Mery L, Piñeros M. Global cancer observatory: Cancer today. Lyon: International Agency for Research on Cancer; 2019.

3.Elgadi A, Benhalima I, Ghanem S, Badi S, Bedri O, Elzouki NA. Cancer epidemiology and control in Libya: A regional comparison and policy implications. J Glob Oncol. 2021 doi:10.1200/GO.21.00020.

4.Elzouki AN, Elgadi A, Benyahia R, Elkhammas EA, Bedri O, Benhalima I. Breast cancer epidemiology in Libya: Regional trends and emerging patterns. Libyan J Med. 2020;15(1):1–7

5.World Health Organization. Breast cancer: Prevention and control. Geneva: WHO; 2020

6.Anderson BO, Yip CH, Smith RA, Shyyan R, Sener SF, Eniu A. Breast cancer in limited-resource countries: Health care systems and public policy. Breast J. 2014;20(Suppl 1):S67–74

7.Al-Hamidi F, Alabed H, Sghaier W, Almisurati M, El-hadi A, Ghaith A. Age distribution and breast cancer subtypes among Libyan women: A hospital-based study. East Mediterr Health J. 2019;25(5):314–21

8.Borenstein M, Hedges LV, Higgins JPT, Rothstein HR. Introduction to meta-analysis. Chichester: Wiley; 2009

9.Higgins JPT, Thomas J, Chandler J, Cumpston M, Li T, Page MJ. Cochrane handbook for systematic reviews of interventions. 2nd ed. Chichester: Cochrane Collaboration; 2021

10.ElJilani M, Shebani A, Bishr A, Jalil H, et al. Assessment of breast cancer in Libyan women using Gail model. Libyan J Med Sci

2020;4:115-9

11.Khetresh M. Breast cancer and its risk factors awareness, knowledge and beliefs among Libyan women resident in Zawia. University Bulletin. 2022;24(2):329-346.

12.Taher YA, Samud AM, Benhusein GM. Knowledge towards breast cancer among Libyan women in Tripoli. Libyan International Medical University Journal. 2016;1:58-68

13.El Ashouri A, Smeo M, Sabei L, Aldwebi H, AbuBaker N, Abu-khatwa M, Madi Q. Breast cancer delay presentation among Libyan patients: Demographic and clinical features. Mediterranean Journal of Pharmacy and Pharmaceutical Sciences. 2024; 4 (2): 30-36

14.Gaber M, Alamouri I, Alshybani H, Atneisha A, Omar F, Asselhab S, Ali A, Elfagieh M, Alragig M, Ben Saud M, Assidi M, Buhmeida A, Erimah E. Diagnosis delay and predicated factors in Libyan women with breast cancer. Libyan International journal of Oncology.2023;2(2):67-81

15.Ameigaal S, Ageel A, Abdoarahem M. Association of risk factors with breast cancer in Libyan women. Al-Mukhtar Journal of Science. 2020; 35(3): 222-228

16.Kutrani H, Eltalhi S, Ashleik N. Predicting factors influencing survival of breast cancer patients using logistic regression of machine learning. Paper presented at the 7th International Conference on Engineering & MIS 2021, Almaty, Kazakhstan, October 11–13; pp. 1–6

17. Houssein N, Cancer incidence in Libya using estimates from GLOBOCAN2020. Series Med Case Rep Rev. 2024;2(4):1-5.

18.Schlichting JA, Soliman AS, Schairer C, et al. Breast cancer by age at diagnosis in the Gharbiah, Egypt, population-based registry compared to the United States surveillance, epidemiology, and end results program 2004–2008. BioMed Res Int, 2015;381574.

19.Missaoui N, Landolsi H, Jaidaine L, et al. Breast cancer in Central Tunisia: An Earlier Age at Diagnosis and Incidence Increase over a 15 Year Period. Breast J. 2012;18(3):289-91.

20.Mehdi I, Monem EA, Al Bahrani BJ, et al. Age at diagnosis of female breast cancer in Oman: Issues and implications. South Asian J Cancer. 2014;3(2):101-6.

21.Karim S, Ghalib H, Mohammed SA, et al. The incidence, age at diagnosis of breast cancer in the Iraqi Kurdish population and comparison to some other countries of Mid-

dle-East and West. Int J Surg. 2015;13:71-75.

22.Franco-Marina F, López-Carrillo L, Keating NL, et al. Breast cancer age at diagnosis patterns in four Latin American Populations: A comparison with North American countries. Cancer Epidemiol. 2015;39(6):831-7.

23.Kumar N, Ehsan S, Banerjee S, Perez CF, Lhuilier I. The unique risk factor profile of triple-negative breast cancer: a comprehensive meta-analysis. Oxford University Press. 2024;116(8):1210–1219.

24.Kajela L and Chaka EE. Determinates of breast cancer in Ethiopia: a systematic review and meta-analysis. Ecancer. 2023;17:1624.

25.Argenal RN, Baterna ML, pena CF, Ravina JN, Siozon MR. Risk factors of breast cancer among women: a meta-analysis. 12th National Convention on Statistics. 2019.

26.Ewertz M, Duffy SW, Adami HO, Kvåle G, Lund E, Meirik O, Mellemgaard A, Soini I, Tulinius H. Age at first birth, parity and risk of breast cancer: a meta-analysis of 8 studies from the Nordic countries. Int J Cancer. 1990;15;46(4):597-603.doi: 10.1002/ijc.2910460408. PMID: 2145231.

27.Liu H, Shi S, Gao J, et al. Analysis of risk factors associated with breast cancer in women: a systematic review and meta-analysis. Transl Cancer Res, 2022; 11(5):1344-1353 | https://dx.doi.org/10.21037/tcr-22-193.

Medical Science

Scientific Journal of University of Benghazi
SJUOB (2025) 38 (1) Medical Sciences: Alfadeel, 193 – 214
www.sjuob.uob.edu.ly

Impact of CT Stroke Window Settings on Acute Stroke Detection.

Hajer Alfadeel[1]*

1 Department of Diagnostic Radiology, Faculty of Medicine, Omer Al-Mukhtar University, Albeida.

Received: 15 / 01 / 2025 | Accepted: 24 / 05 / 2025 | Publishing: 29/06/2025

ABSTRACT

Non-contrast CT is the most important imaging modality in the evaluation of suspected acute stroke by excluding intracranial haemorrhage and directly visualizing early ischemic changes. These changes are challenging to detect on non-contrast CT due to the small reduction in the attenuation value of ischemic tissue from normal. The study's objective was to assess the use of stroke window settings for improving the detection of acute stroke. This retrospective study included forty-nine patients in whom non-contrast CT were performed for suspected acute stroke within 24 hours from symptom onset. Images were reviewed in two reading sessions with different window settings used: default brain window (80/40 [window width/window level]) and stroke window (40/40 [window width/window level]). Both windows were evaluated for their ability to detect early ischemic changes with the final diagnosis as the reference standard. Twenty-nine patients had a final diagnosis of acute stroke. The sensitivity and specificity of non-contrast CT for acute stroke detection were 79.3% and 100% respectively at the default brain window. Both windows were comparable for detecting acute stroke (P=0.2). The CT sensitivity increased to 86.2% after adding the stroke window review to the default brain window. The resultant improvement in CT diagnostic performance by stroke window review was not statistically significant (P=0.5). Conclusion, the superior sensitivity of applying stroke window settings after the default window review is small with modern generation CT scanner. These findings should increase the confidence in routine radiology reporting that uses the standard brain window in the assessment of acute stroke.

Keywords: Default brain window, Early ischemic changes, Non-contrast CT, Sensitivity, Stroke window, Window settings, Window width.

Corresponding Author: Hajer Alfadeel, Libya, hajer.alfadeel@omu.edu.ly

 ISSN: Online 2790-1637, Print 2790-1629
National Library of Libya, Legal number: 154/2018

1.INTRODUCTION

Stroke is one of the most common causes of death and disability in the world. Stroke deaths in Libya reached an estimated 10% of total deaths, according to the latest WHO data published in 2020 [1]. Early non-contrast computed tomography (CT) is the most important modality in the evaluation of suspected acute stroke. It helps exclude haemorrhage and other alternative diagnoses such as neoplasms and aids in establishing the specific diagnosis of acute ischemic infarct, precluding the need in most cases for any additional imaging once the diagnosis of stroke is made [2]. Despite the higher sensitivity of magnetic resonance imaging (MRI) in detecting early ischemic changes, CT scan remains the preferred imaging tool in assessing acute stroke, as CT is faster, relatively lower in cost, and widely available [3, 4].

The interpreting of CT images utilizes the Hounsfield unit (HU), also called CT unit, a relative quantitative measurement of radio-density. During CT reconstruction, a grayscale image is created using the radiation's absorption/attenuation coefficient within a tissue, which is directly proportional to the physical density of the tissue. The denser the tissue, the more the X-rays are absorbed, and the higher the number of HU [5, 6]. On the Hounsfield scale that appears as grey tones, the greater X-ray beam absorption in more dense tissue results in positive HU values and a brighter appearance, less dense tissue, on the other hand, has negative HU values and a darker appearance [5]. Water is defined as having a Hounsfield Unit of zero and air as having -1000. For dense bones, the upper limits can be as high as 1000; for metals like steel or silver, they can be as high as 3000. Muscle, about 40 HU; fat, −60 HU; grey matter, 40 HU; white matter, 30 HU; cerebrospinal fluid, 10 HU [5, 7]. In order to visualize sufficient contrast resolution on a workstation monitor and maximize the contrast resolution of structures with similar attenuation values, the interpreting radiologist must examine the CT data in multiple linear window settings, usually optimized for soft tissue, lung, and bone [8]. Windowing is the process of changing window settings to adjust the grayscale range of a particular image to better visualize particular structures. Window settings are comprised of window width (WW), the range of CT units, i.e. the greyscale displaced in an image, and window

 ISSN: Online 2790-1637, Print 2790-1629
National Library of Libya, Legal number: 154/2018

level (WL), the centre value of this range [9]. Only tissues with HU values inside the selected window width are translated onto the grayscale spectrum; tissues with HU values outside of the window width are configured to be either all black or all white [6]. WW controls the contrast of the image. Decreasing window width increases the contrast resolution of structures with similar HU values, as a smaller change in attenuation value is given a different shade of grey, while increasing the window width decreases the contrast as a larger difference in HU values is needed to change the tone of grey allocated to certain HU. Decreasing the window level increases the brightness of the image as lower HU values are needed to be displayed on the brighter side of the greyscale [9].

Adjusting window settings (WW/WL) are frequently used to highlight certain areas and details. As default, different window settings are assigned to different anatomical regions for examination so that areas of interest can be easily identified [10]. For evaluation of brain abnormalities, an appropriate centre level setting and a tiny window width significantly increase the ability to identify lesions. Brain CT images are typically reviewed in the default brain window settings of WW 80 HU and WL 40 HU [11].

Subtle differences in HU from normal may go undetected on default window settings. The fundamental concept is that in order to detect subtle abnormalities, radiologists should try to accentuate contrast between normal and abnormal tissues by choosing a narrower CT window width [12]. Early CT findings in acute stroke are challenging to detect due to small reductions in the attenuation of ischemic tissue from normal [11]. There have been various approaches to the use of variable window settings to improve acute stroke detection from CT images [10]. Using a stroke window (40/40 [WW/WL]) settings could improve brain lesion detection [13]. Although the literature advocates for stroke window settings, their diagnostic value with modern CT scanners remains unquantified. To my knowledge, despite discussion in the literature about the importance of narrowing window width in the detection of acute stroke, the benefit of stroke window settings in enhancing the diagnosis of acute stroke with modern multidetector and dual-source scanners has not been stressed. The aim of this study is to assess the use of stroke win-

 ISSN: Online 2790-1637, Print 2790-1629
National Library of Libya, Legal number: 154/2018

dow (40/40 [WW/WL]) settings in enhancing the detection of acute stroke.

2.METHODS

This is a retrospective study aimed at patients admitted at Albeida Medical Centre and referred for imaging at the CT unit of Omer Almukhtar General Hospital with suspected acute stroke diagnosis over the period from December 2020 to November 2021.

2.1.Subjects

The CT brain scan studies done consecutively over the 12-month period were retrospectively retrieved from the picture archive and communication system (PACS) of CharruaSoft (Version 6.31.0). A total of three hundred and twenty-three of patients aged ≥ 20 years with a single non-contrast CT brain study were included in the image review process. The hospital records within the same period of these patients' scans were then reviewed. Patients who were not referred from the hospital's medical department were excluded. The inclusion criteria for the remaining patients were as follows: (1) patients who had been admitted with sudden onset of neurological deficits suggesting acute stroke, such as hemiplegia and aphasia. (2) Patients who had undergone non-contrast CT imaging within 24 hours from onset of symptoms. Forty-nine patients were eligible for inclusion with suspected acute stroke and non-contrast CT brain scans within 24 hours after symptom onset.

The 49 patients were 34 to 85 years old with a mean age of 62.8 ± 13.5 years (± stands for standard deviation (SD)). Twenty-six were men and twenty-three were women. The relevant data to the purpose of the study, like clinical history, physical examination, imaging findings, and the final diagnosis at the end of the hospital stay, were recorded from patients' medical records. The final diagnosis served as the reference standard for CT stroke detection performance at different window settings.

2.2.CT image acquisition

The non- contrast CT scans were performed with a 32 slice CT scanner (Aquilion, Canon Medical Systems, Japan) using the scanning technique of 120 kV, 180 mA, 0.8 second rotation time, and 5 mm section thickness. Contiguous axial slices were produced parallel to the inferior orbitomeatal line, covering from skull base to vertex. All images were reconstructed in 5-mm thickness with a 3-mm reconstruction interval for

 ISSN: Online 2790-1637, Print 2790-1629
National Library of Libya, Legal number: 154/2018

averaged and MIP images from 1 mm thickness non-contrast axial source images using the CT scanner console.

2.3.Image analysis

A single radiologist assessed the brain scans. All CT images were reviewed with the radiologist being blind to patient clinical information except patient' name, age, and sex, which were available in the DICOM reviewer by default. The non-contrast CT images were viewed in two reading sessions with different window settings used. The first readout of CT images was done at the default brain window (WW/WL [80/40]). Four weeks later, and in a different order from the first reading session, the images were viewed at the stroke window set to WW 40 HU and WL 40 HU. During each reading session, the images were thoroughly assessed for early signs of stroke. These were identified as follows:

- Loss of grey-white matter differentiation. It includes the loss of grey-white matter distinction at the insular cortex, the basal ganglia, and the cortical gyri (Figure 1a).

- Parenchymal hypoattenuation, defined as a region of cortical-subcortical or parenchymal decreased attenuation within a vascular territory relative to the attenuation of other parts on the same side or of the contralateral hemisphere, with or without focal brain swelling in form of sulcal effacement or ventricular compression (Figure 1b).

- Hyperdense artery sign, identified as increased attenuation of an artery compared to the contralateral artery due to the presence of an intrarterial clot. It can be seen at M1 and M2 segments of the middle cerebral artery (MCA), A1 and A2 segments of the anterior cerebral artery (ACA), the intracranial internal carotid (ICA), the basilar, and the vertebral arteries (Figure 1c).

In addition to the early ischemic changes of stroke, the CT images were also routinely evaluated for alternative diagnoses such as haemorrhage, infection, and intracranial masses that may mimic acute stroke presentation.

In cases of MCA territory infarct, the location and the extent of hypoattenuation on CT were classified according to the Alberta Stroke Program Early CT Score (ASPECTS). The MCA territory was divided into 10 regions: caudate nucleus, internal capsule, lentiform nucleus, insula, and six cortical regions (M1-M6) at ganglionic and supragan-

 ISSN: Online 2790-1637, Print 2790-1629
National Library of Libya, Legal number: 154/2018

glionic levels. A score of 10 points indicates no ischemia (normal). One point is deducted from that score for each region showing early ischemic changes (parenchymal hypoattenuation, or loss of corticomedullary differentiation).

2.4.Statistical analysis

For diagnostic assessment, sensitivities and specificities with 95% confidence intervals (CI) were calculated for detecting acute stroke by viewing images at default brain window and stroke window settings using the final diagnosis as the reference standard. In addition, a receiver operating characteristic (ROC) curve was generated to assess the diagnostic performance of both window settings. Area under the curve (AUC) of the respective ROC curve indicates the diagnostic accuracy of the window settings. The areas under the ROC curves for the default brain window and stroke window were compared to detect the difference in the diagnostic accuracy between the two windows. The diagnostic performance of combined image viewing of both window settings was evaluated using McNemar's test. For comparison of the detection rate of early ischemic signs on the two windows, Fisher's exact test was applied. A paired samples t test was used to illustrate the differences in ASPECTS scores between the default brain window and the stroke window in patients with MCA territory infarcts. All statistical analyses were performed by using MedCalc software version 20.027 (MedCalc Software by Ostend, Belgium, https://www.medcalc.org). A p value of < 0.05 indicated statistical significance.

 ISSN: Online 2790-1637, Print 2790-1629
National Library of Libya, Legal number: 154/2018

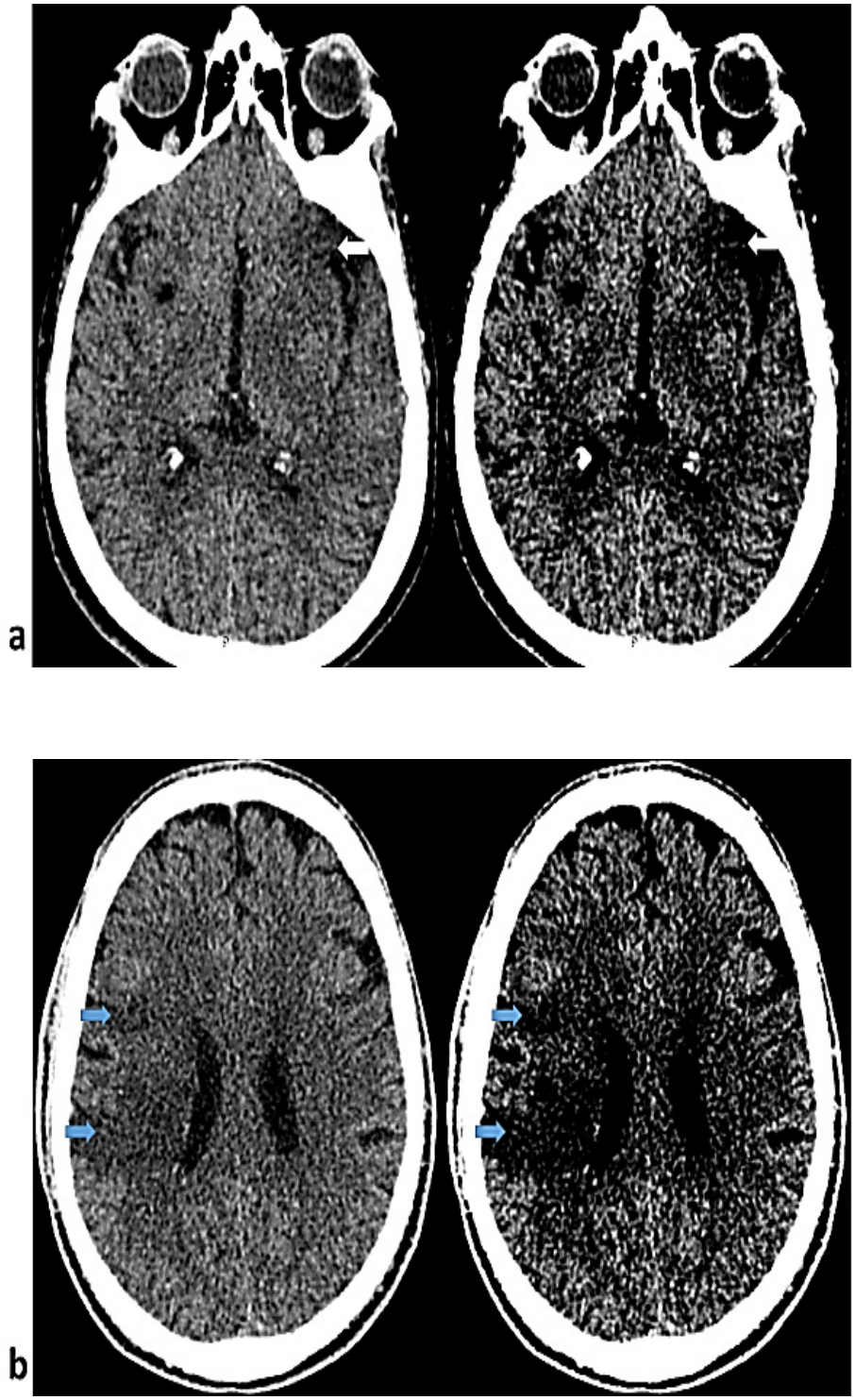

 ISSN: Online 2790-1637, Print 2790-1629
National Library of Libya, Legal number: 154/2018

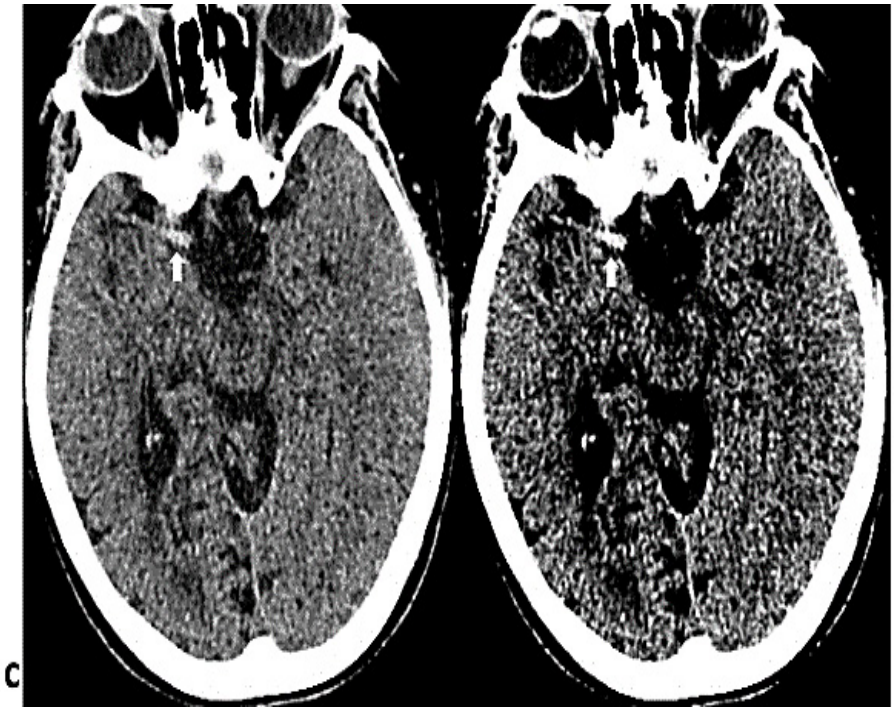

Figure .(1). Illustrates early ischemic changes on noncontract CT of different patients. (a)- Grey-white matter differentiation loss seen at anterior part of left insula (white arrow). (b)- Parenchymal hypoattenuation (blue arrows). (c)- Hyperdense artery sign involving the M1 segment of the right MCA (white arrow).

3.RESULTS

Of the 49 patients, 29 patients (59%) had a final diagnosis of acute stroke, while eight patients suffered from transient ischemic attacks (TIA) and six patients had intracerebral haemorrhage. The final diagnosis of all patients is shown in Table 1

.

Table .(1): Final diagnosis of the 49 patients with suspected acute stroke.

Diagnosis	No of patients
Acute stroke	29
TIA	9
Intracerebral haemorrhage	7
Cerebritis/encephalitis	2
Space occupying lesion	1
Subarachnoid haemorrhage	1

The mean age of the 29 patients with acute stroke was 63 years ± 13 (SD) with a range of 34 to 85 years. Sixteen of them were women, and thirteen were men. Based on clinical and CT findings, 20 patients had MCA/ICA territory stroke, two patients had ACA territory infarct, two patients had posterior cerebral artery (PCA) territory infarct, one patient had basilar artery territory stroke, three patients had posterior inferior cerebellar artery (PICA) territory infarcts and one patients had superior cerebellar artery (SCA) territory infarct.

The sensitivities and specificities of non-contrast CT for the detection of acute stroke at different window settings are detailed in Table 2. The sensitivity and specificity of CT for stroke detection at default brain window settings were 79.3% (95% CI: 60.2-92) and 100% (95% CI: 83.2-100) respectively. The corresponding sensitivity and specificity at stroke window settings were 72.4% (95% CI: 52.8-87.3) and 95% (95% CI: 75.1-99.8) respectively. In one case, the parenchymal hypoattenuation due to chronic infarct was falsely interpreted as a new infarct during the stroke window reading session resulting in the reduction of the specificity to 95% for the stroke window review. The stroke window settings improved stroke detection in only two cases where grey-white matter differentiation loss and hyperdense artery sign were missed at the default brain window reading session but subsequently de-

tected at the stroke window reading session (Figure 2). On the other hand, early ischemic changes were missed at the stroke window reading session in four cases (three parenchymal hypoattenuation, one grey-white matter differentiation loss) that were previously detected at the default brain window. The sensitivity and specificity for stroke detection when findings from image review at the default brain window and the stroke window were combined (i.e., true positives and true negatives at one or both reading sessions) were 86.2% (95% CI: 68.3-96.1) and 100% (95% CI: 83.2-100) respectively. There was no statistically significant diagnosis performance improvement in acute stroke detection when readings at the default brain window and stroke window were combined (McNemar test, P=0.5).

The ROC curves for stroke detection at the default brain window and stroke window are shown in Figure 3. The analysis of ROC curves showed high diagnostic accuracy of non-contrast CT for detecting acute stroke within 24 hours at both the default brain window (AUC=0.891, P<0.001) and stroke window settings (AUC=0.821, P<0.001). By comparing areas under the ROC curves, there was no statistically significant difference in the accuracy of stroke detection between default brain window and stroke window settings (P=0.2); see Figure 4.

Early ischemic changes were identified at both windows in 25 (86.2%) of the 29 patients with acute stroke. parenchymal hypoattenuation was detected in 21 cases (72.4%), grey-white matter differentiation loss in 10 cases (34.5%), and hyperdense artery sign in six cases (20.7%). Numbers of individual early ischemic changes that were detected on different window settings are detailed in Table3. There was a difference in the rate of detection of parenchymal hypoattenuation between the default brain window and the stroke window settings. However, the difference did not reach statistical significance.

In the 20 patients with MCA territory infarcts, the difference in the mean of ASPECTS scores between the default brain window and the stroke window was not statistically significant (P=0.6).

Table .(2): Sensitivities and specificities of CT for acute stroke detection at different window settings

Window settings	Final diagnosis		Sensitivity (TP/TP+FN)	Specificity (TN/TN+FP)
	Acute stroke (n=29)	No acute stroke (n=20)		
Default brain window (80WW/40WL)	23 (TP) 6 (FN)	0 (FP) 20 (TN)	79.3 (23/29)	100 (20/20)
EIC present				
EIC absent				
Stroke window (40WW/40WL)	21 (TP) 8 (FN)	1 (FP) 19 (TN)	72.4 (21/29)	95 (19/20)
EIC present				
EIC absent				
Combined (default brain and stroke windows)	25 (TP) 4 (FN)	0 (FP) 20 (TN)	86.2 (25/29)	100 (20/20)
EIC present				
EIC absent				

WW= window width, WL= window level, EIC= early ischemic changes, TP= true positive, FN= false negative, TN= true negative, FP= false positive.

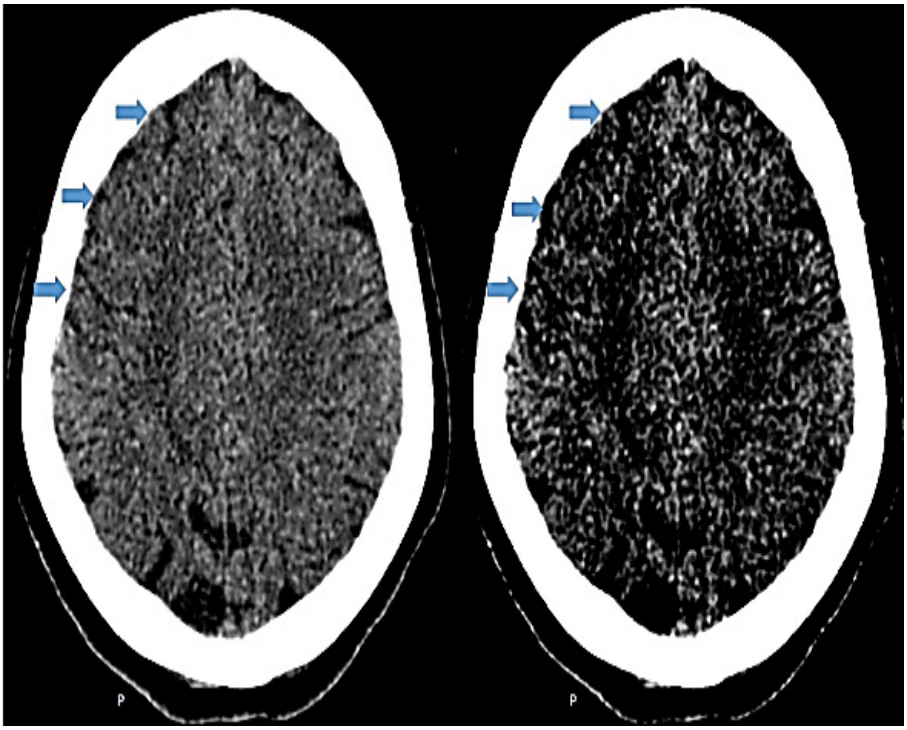

Figure .(2). Non-contrast CT brain of a patient with an acute right MCA stroke.

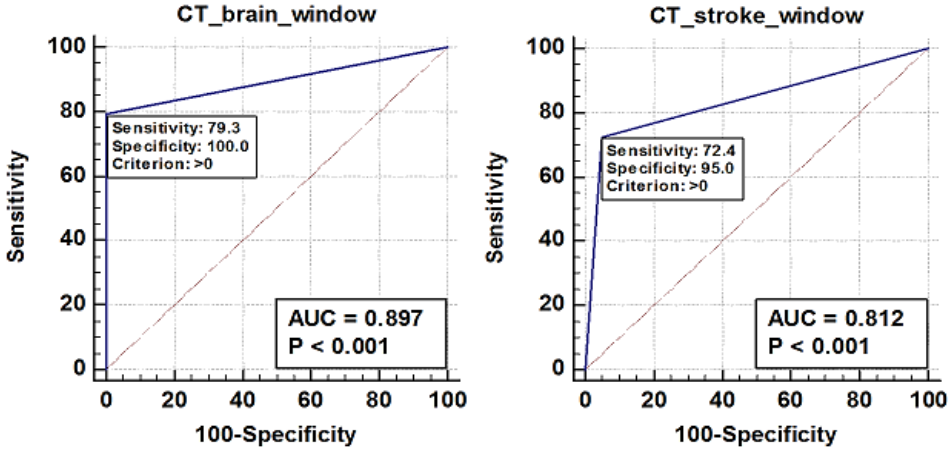

Figure .(3). ROC curves for stroke detection at default brain window and stroke window settings.

 ISSN: Online 2790-1637, Print 2790-1629
National Library of Libya, Legal number: 154/2018

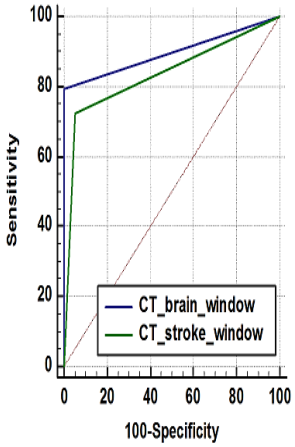

Figure .(4). Comparison of the ROC curves for stroke detection at default brain window and stroke window settings.

Table .(3): Comparison of the number of individuals early ischemic changes detected at default brain and stroke window settings.

EIC	Number of EIC detected at default brain window	Number of EIC detected at stroke window	P value
Parenchymal hypoattenuation	21 (72.4%)	18 (65.5%)	0.6
Grey-white matter differentiation loss	9 (31%)	9 (31%)	1
Hyperdense artery sign	5 (17.3%)	6 (20.7%)	1

The data are expressed as number and (percentage). EIC (early ischemic changes).

4.DISCUSSION

Early identification of a clinically suspected stroke on CT imaging is important in conditions where therapeutic treatment is considered. Authors have raised interest in using different window settings as a way of increasing the visualization of early ischemic changes on non-contrast CT. They reported that narrowing window width and window level might increase the sensitivity of stroke detection [14, 15]. Turner et al. [13] suggested that stroke window settings of 40 WW/40 WL should be used routinely in radiological evaluation of all non-contrast CT brain examinations and not just in cases of suspected stroke; his justification is that the reduced window width would increase the image contrast and subsequently increase the conspicuity of subtle abnormalities. However, the sensitivity of the stroke window (40/40 [WW/WL]) for acute stroke detection has not been documented. This study investigated whether the stroke window settings would increase acute stroke detection by modern generation CT scanners. The present study reveals that default brain and stroke windows are comparable for detecting signs of acute stroke with no significant difference when the images are of good quality obtained by multislice helical scanners.

Non-contrast CT remains the first-line imaging tool for patients who present with signs and symptoms suggestive of acute stroke due to its advantages of availability, easy accessibility, speed, convenience to both patient and staff, and high sensitivity for detecting hemorrhage [16]. Acute stroke can be identified on CT by evaluating the images for early ischemic changes. One of the early ischemic changes of stroke seen on CT is the hyperdense artery sign reflecting clot formation within the vessel. Clots that are rich in red blood cells have higher CT attenuation than normal blood and appear hyperdense on CT [17]. Oguro et al. [18] reported a hyperdense MCA sign's sensitivity of up to 57%. After the reduction in cerebral blood flow due to arterial occlusion, the attenuation of grey matter, which has higher attenuation than the white matter due to its large blood volume, decreases and becomes similar to the adjacent white matter. The Loss of grey white matter differentiation can be visible early post stroke onset particularly in areas that has poor collateral supply namely the basal ganglia and insular cortex [17]. Parenchymal hypoat-

 ISSN: Online 2790-1637, Print 2790-1629
National Library of Libya, Legal number: 154/2018

tenuation correlate to increased water content of the affected tissue within the first hours after onset of ischemia caused by the disruption of blood-brain barrier [2, 19]. The ischemia causes failure of membrane ion bombs leading to cytotoxic oedema within 30 minutes from onset of ischemia, accumulation of water within tissues occurs within few hours [20]. The increased water content decreases the CT attenuation of the involved area; an increase by 1% of water content causes 2.5 HU reduction [14]. The parenchymal hypoattenuation is subtle and difficult to detect in the first few hours since onset, it becomes visible to the human eye when the affected brain tissue has underwent significant uptake in water to change HU [17].

The ability of the observer to detect early ischemic changes on non-contrast CT is dependent on various factors, including the size of the infarct, the vascular territory of the infarct, the timing of the scan from the onset of stroke, the generation of the scanner, and the specific methods employed. The expertise of the CT reader and the availability of appropriate clinical information at the time of review also affect the detection of early ischemic changes [20, 21]. Previous studies have shown limited sensitivity of non-contrast CT in posterior fossa infarcts, lacunar infarcts, and hyperacute stroke detection [22]. The advancements in multidetector CT with rapidly improving hardware and software have improved detection of early ischemic changes on non-contrast CT. The reason for the higher detection rate of these early ischemic signs is the enhanced contrast and spatial resolution of the scanner, increasing the ability to visualize subtle reduction in the CT attenuation (HU) of the affected brain [2]. Using readers that are more experienced is another way to maximize acute stroke detection by CT. Numerous studies reveal that residents, neurologists, and acute care doctors read CT scans very differently, although neuroradiologists interpret them less differently. However, in daily practice, neuroradiologists are not always engaged in the work-up for acute stroke. On the other hand, there is evidence that even brief training may improve the ability of non-specialists to identify strokes [20].

The diagnostic sensitivity of CT for acute stroke detection is widely variable in previous reports. Authors using early generation CT scanners from the early 1980s have reported poor sensitivity of non-contrast CT

 ISSN: Online 2790-1637, Print 2790-1629
National Library of Libya, Legal number: 154/2018

for the detection of early signs of stroke, with sensitivity as low as 10% within 48 hours from symptom onset. However, with current CT scanners, early ischemic changes can be seen as early as three hours [20]. In one report, the sensitivity of non-contrast CT for hyperacute stroke in the first three hours was 26% [23]. The sensitivity of non-contrast CT can reach up to 82% within 6 hours of symptom onset [22]. The specificity for acute stroke detection on non-contrast CT was 100% [24]. In the current study, the results were comparable with previous reports in the literature. Non-contrast CT showed 79% sensitivity for acute stroke detection within 24 hours from symptom onset, and the specificity was 100%.

CT sensitivity for stroke detection in the present study increased from 79% to 86% but not significantly (P=0.5) after stroke window settings (40/40 [WW/WL]) were added to the default brain window (80/40 [WW/WL]) review. Previous studies have shown that the use of narrow window settings increases the conspicuity of early ischemic changes on non-contrast CT. However, no author had investigated stroke window settings of 40/40 (WW/WL) before this study, even though many in the literature advocated the application of these window parameters in the evaluation of acute stroke patients. Lev et al. [14] in 1999 did the first study that compared a standard brain window to variable window settings. They retrospectively reviewed 21 patients with proved MCA infarction who had undergone non-contrast CT imaging within 6 hours of stroke onset. The readers costume adjusted as necessary two preset values of 8 WW with 32 WL and 30 WW with 35 WL (range; 1-30 WW, 28-36 WL) to the standard window settings preset to 80 WW and 20 WL. The sensitivity for stroke detection was 57% at standard window settings and significantly increased to 71% when variable window settings were used in conjunction to the standard brain window. Mainali et al. [15], in their retrospective audit of 50 patients with acute ischemic stroke within 4.5 hours from symptom onset, reported significantly improved detection of early ischemic signs with the use of stroke window set at 30 WW and 35 WL after first applying standard window settings of 100 WW and 35 WL compared to the staff radiologist's report. However, the fact that the reading sessions in their study had different reviewers may have

contributed to the difference in the detection rate of early ischemic signs rather than the use of the stroke window. Moreover, the circumstances of the reading sessions were also different. Unlike the radiology staff report, the reader knew beforehand that all cases had an acute stroke diagnosis, which may have also contributed to a higher number of ischemic signs detected.

In the present study, narrowing the window width did not significantly improve the sensitivity of non-contrast CT for acute stroke detection. This is most likely because image quality and diagnostic value have been steadily improved by developments in CT scan machines, such as spiral imaging characteristics, multi-slice capability, higher energy supply, and improved detectors [25], which in turn improved the conspicuity of early ischemic changes at the standard brain window. The results of this study indicate that the application of stroke window settings does not significantly improve the detection of acute stroke. Consequently, these findings do not support the routine use of stroke window review in the evaluation of all patients with suspected stroke. This has notable clinical implications, especially in emergency settings where timely diagnosis is needed and the additional review time with stroke window may not be feasible. On the other hand, it is important to consider that even small diagnostic gains can be clinically relevant in serious conditions like acute stroke. Stroke window may potentially aid less experienced readers or when clinical suspicion remains high despite a negative standard review. Therefore, selective use of stroke window may still offer value in the diagnostic process.

Early ischemic changes are important because, in addition to confirming the clinical suspicion of an infarct, they can provide prognostic information and guide stroke management. Parenchymal hypodensity is the most commonly observed early ischemic sign on non-contrast CT in acute stroke [20]. This was also observed in the present series, where the most important early ischemic sign was parenchymal hypoattenuation (72.4%), followed by grey-white matter differentiation loss (34.5%). The least positive early ischemic sign was the hyperdense artery sign (20.7%). There was no significant difference in the detection of these signs between the two window reviews. The ASPECTS score determines the extent of stroke lesion in pa-

tients with acute MCA occlusion and hence determines the eligibility for thrombolytic therapy and endovascular intervention [26]. ASPECTS values were lower at the stroke window review compared to those at the default brain window, which means if stroke window settings were used after the default brain window in evaluating patients with acute MCA stroke, it would less likely alter the treatment plan for the patient, as it would not significantly increase the number of ischemic regions detected.

One of the advantages of this study is that the sample of cases reviewed by the radiologist was randomized at the time of image interpretation. It included all non-contrast CT brain studies performed within a specific period before the review of medical records for the inclusion process. This made the blinding of the reviewer complete and prevented any bias that could have resulted in increased reporting of positive signs if only patients with acute stroke were reviewed, thus making the results more representative of routine radiology practice.

Different approaches to maximize the useful visual information displayed on CT without needing to change window settings have been discussed in the literature. Image processing compresses CT image dynamic range to limited grayscale shades, maximizing visual information. Methods include non-linear CT windows, histogram equalization, adaptive histogram equalization, and contrast-limited adaptive histogram equalization. These algorithms operate on CT's entire dynamic range, but none has widespread clinical use [8]. Bier et al. [27] suggested that post processing of non-contrast CT with frequency selective non-linear blending significantly increases its sensitivity for detection of ischemic brain insult. Viriyavisuthisakul et al. [11], who evaluated window settings parameters for acute ischemic stroke by using deep learning models, found that the model could well predict with standard brain window settings. Deep learning methods, with the large number of regularly obtained brain scans, could be developed for ischemic lesion detection on CT without requiring lesion annotation [28].

5.Limitations.

The study has several limitations. First, this was a retrospective study, which might have affected the patient selection process, as the clinical information is reduced.

Second, the exact time of the scan after the onset of the neurological symptoms is difficult to determine retrospectively, and a wider time window of 24 hours was opted for the study. Third, the cohort size was small. The limited patient cohort from a single-center study design with risks of potential selection bias may limit the generalizability of the results. Finally, the target for narrowing window settings was preset at a fixed value of 40 WW and 40 WL. Any other values suggested for stroke window settings were excluded from this study.

It is recommended to further validate the findings of the present study in the future with prospective multicentric studies with larger sample sizes and time windows of 6 hours, which would allow for more representation of the general population and higher scientific validity of the results.

6.CONCLUSION

The study showed that modern-generation CT has high sensitivity for acute stroke detection within 24 hours from symptom onset. Systemic assessment for early ischemic changes is a key to successfully recognizing them on imaging. The magnitude of superior sensitivity in reviewing images with stroke window settings (40/40 [WW/WL]) in addition to the default brain window (80/40 [WW/WL]) is small. It should be noted that in routine radiology practice, especially in busy radiology departments, radiologists tend to not use stroke window parameters when reviewing non-contrast CT of suspected stroke patients and instead use the default brain window without changing window parameters. The current study should therefore increase the confidence in daily radiology reporting that uses the standard brain window for assessing acute stroke.

7.ACKNOWLEDGMENTS

-No financial support.

-No conflict of interests.

8.REFERENCES

1.World health rankings live longer live better. World Life Expectancy Com [Internet]. 2020 [cited 2024 Oct 16]. Available from: https://www.worldlifeexpectancy.com/libya-stroke

2.Wall SD, Brant-Zawadzki M, Jeffrey RB, Barnes B. High frequency CT findings within 24 hours after cerebral infarction. AJR. Am J Roentgenol. 1982 Feb; 138(2):307–311. Available from: doi: 10.2214/ajr.138.2.307

3.Abdalkader M, Siegler JE, Lee JS, Yaghi

S, Qiu Z, Huo X, et al. Neuroimaging of acute ischemic stroke: Multimodal imaging approach for acute endovascular therapy. J Stroke. 2023 Jan; 25(1):55-71. Available from: doi: 10.5853/jos.2022.03286

4.Tedyanto EH, Tini K, Pramana NAK. Magnetic resonance imaging in acute ischemic Stroke. Cureus. 2022 Jul 25; 14(7):e27224. Available from: doi: 10.7759/cureus.27224

5.DenOtter TD, Schubert J. Hounsfield unit. StatPearls: StatPearls Publishing; 2023.

6.Xue Z, Antani S, Long LR, Demner-Fushman D, Thoma GR. Window classification of brain CT images in biomedical articles. AMIA Annu Symp Proc. 2012; 2012:1023–1029

7.Bibb R, Eggbeer D, Paterson A. 2 - Medical imaging. In Bibb R, Eggbeer D, Paterson A, editors. Medical modelling. 2nd Ed. Woodhead Publishing; 2015. p. 7-34. https://doi.org/10.1016/B978-1-78242-300-3.00002-0.

8.Mandell JC, Khurana B, Folio LR, Hyun H, Smith SE, Dunne RM, et al. Clinical applications of a CT window blending algorithm: RADIO (Relative Attenuation-Dependent Image Overlay). J Digit Imaging. 2017 Jun; 30(3):358–368. Available from: doi: 10.1007/s10278-017-9941-1

9.Fundamentals of computed tomography studies: Windowing. Stepwards [Internet]. 2019 [cited 2024 Sep 15]. Available from: https://www.stepwards.com/?page_id=21646

10.Karki M, Cho J, Lee E, Hahm MH, Yoon SY, Kim M, et al. CT window trainable neural network for improving intracranial hemorrhage detection by combining multiple settings. Artif Intell Med. 2020 Jun; 106:101850. Available from: doi: 10.1016/j.artmed.2020.101850

11.Viriyavisuthisakul S, Kaothanthong N, Sanguansat P, Haruechaiyasak C, Nguyen ML, Sarampakhul S, et al. Evaluation of window parameters of Noncontrast cranial CT brain images for Hyperacute and acute ischemic stroke classification with deep learning. Proceedings of the 11th Annual International Conference on Industrial Engineering and Operations Management. IEOM Society; 2021. p. 170-188.

12.Cho J, Park KS, Karki M, Lee E, Ko S, Kim JK, et al. Improving sensitivity on identification and delineation of intracranial hemorrhage lesion using cascaded deep learning models. J Digit Imaging. 2019 Jun; 32(3):450-461. Available from: doi: 10.1007/

s10278-018-00172-1.

13.Turner PJ, Holdsworth G. Commentary. CT stroke window settings: an unfortunate misleading misnomer? Br J Radiol. 2011 Dec; 84(1008):1061-6. Available from: doi: 10.1259/bjr/99730184.

14.Lev MH, Farkas J, Gemmete JJ, Hossain ST, Hunter GJ, Koroshetz WJ, et al. Acute stroke: Improved nonenhanced CT detection--benefits of soft-copy interpretation by using variable window width and center level settings. Radiology. 1999 Oct; 213(1):150-5. Available from: doi: 10.1148/radiology.213.1.r99oc10150.

15.Mainali S, Wahba M, Elijovich L. Detection of early ischemic changes in noncontrast CT head improved with "stroke windows". ISRN Neurosci. 2014 Mar 9; 2014:654980. Available from: doi: 10.1155/2014/654980.

16.Rowley H, Vagal A. (2020). Chapter 3 Stroke and stroke mimics: Diagnosis and treatment. In: Hodler J, Kubik-Huch RA, von Schulthess GK, editors. Diseases of the brain, head and neck, spine 2020–2023: Diagnostic imaging [Internet]. Cham (CH): Springer; 2020. Chapter 3. Available from: doi: 10.1007/978-3-030-38490-6_3

17.van Poppel LM, Majoie CBLM, Marquering HA, Emmer BJ. Associations between early ischemic signs on non-contrast CT and time since acute ischemic stroke onset: A scoping review. Eur J Radiol. 2022 Oct; 155:110455. Available from: doi: 10.1016/j.ejrad.2022.110455.

18.Oguro S, Mugikura S, Ota H, Bito S, Asami Y, Sotome W, et al. Usefulness of maximum intensity projection images of non-enhanced CT for detection of hyperdense middle cerebral artery sign in acute thromboembolic ischemic stroke. JJR. Japanese journal of radiology. 2022; 40(10):1046–1052. Available from: doi: 10.1007/s11604-022-01289-8

19.Nian K, Harding IC, Herman IM, Ebong EE. Blood-brain barrier damage in ischemic stroke and its regulation by endothelial mechanotransduction. Front Physiol. 2020 Dec 22; 11:605398. Available from: doi: 10.3389/fphys.2020.605398.

20.Vu D, Lev MH. Noncontrast CT in acute stroke. Semin Ultrasound CT MR. 2005 Dec; 26(6):380-6. Available from: doi: 10.1053/j.sult.2005.07.008.

21.Latchaw RE, Alberts MJ, Lev MH, Connors JJ, Harbaugh RE, Higashida RT, et al. Recommendations for imaging of acute ischemic stroke: A scientific statement from

the American Heart Association. Stroke. 2009 Sep 24; 40(11):3646–3678. Available from: https://doi.org/10.1161/STROKEAHA.108.192616

22.Morgan CD, Stephens M, Zuckerman SL, Waitara MS, Morone PJ, Dewan MC, et al. Physiologic imaging in acute stroke: Patient selection. Interv Neuroradiol. 2015 Aug; 21(4):499-510. Available from: doi: 10.1177/1591019915587227.

23.Lin K, Do KG, Ong P, Shapiro M, Babb JS, Siller KA, et al. Perfusion CT improves diagnostic accuracy for hyperacute ischemic stroke in the 3-hour window: Study of 100 patients with diffusion MRI confirmation. Cerebrovasc Dis. 2009; 28(1):72-9. Available from: doi: 10.1159/000219300.

24.Shen J, Li X, Li Y, Wu B. Comparative accuracy of CT perfusion in diagnosing acute ischemic stroke: A systematic review of 27 trials. PLoS One. 2017 May 17; 12(5):e0176622. Available from: doi: 10.1371/journal.pone.0176622.

25.Abdulkareem NK, Hajee SI, Hassan FF, Ibrahim IK, Al-Khalidi REH, Abdulqader NA. Investigating the slice thickness effect on noise and diagnostic content of single-source multi-slice computerized axial tomography. J Med Life. 2023 Jun; 16(6):862-867. Available from: doi: 10.25122/jml-2022-0188.

26.Hill MD, Demchuk AM, Goyal M, Jovin TG, Foster LD, Tomsick TA, et al. Alberta Stroke Program early computed tomography score to select patients for endovascular treatment: Interventional Management of Stroke (IMS)-III Trial. Stroke. 2014 Feb; 45(2):444-449. Available from: doi: 10.1161/STROKEAHA.113.003580.

27.Bier G, Bongers MN, Ditt H, Bender B, Ernemann U, Horger M. Accuracy of non-enhanced CT in detecting early ischemic edema using frequency selective non-linear blending. PLoS One. 2016 Jan 25; 11(1):e0147378. Available from: doi: 10.1371/journal.pone.0147378.

28.Fontanella A, Li W, Mair G, et al. Development of a deep learning method to identify acute ischaemic stroke lesions on brain CT. Stroke Vasc Neurol. Published online December 25, 2024. doi:10.1136/svn-2024-003372.

Scientific Journal of University of Benghazi

SJUOB (2025) 38 (1) Medical Sciences: Alarfi, et al, 215 – 229
www.sjuob.uob.edu.ly

Median Versus Paramedian Spinal Anesthesia: PDPH Incidence in Urological Procedures.

Aosama Alarfi[*,1]; Adel Saleh[2]; Wisam Zayd[2]; Abdelhaq Elmansori[3]

1 Lecturer; Department of Anesthesia and Intensive Care; Faculty of Medicine; University of Benghazi, Benghazi, Libya.
2 Assistant Lecturer; Department of Internal Medicine; Faculty of Medicine; University of Benghazi, Benghazi, Libya.
3 Associate Professor; Department of Anesthesia and Intensive Care; Faculty of Medicine; University of Benghazi, Benghazi, Libya.

Received: 27 / 01 / 2025 | Accepted: 05 / 07 / 2025 | Publishing: 29/06/2025

ABSTRACT

Spinal anaesthesia is a popular method for anaesthesia in the lower body, offering advantages over general anaesthesia. The paramedian and median methods are most commonly used. Spinal anaesthesia has many benefits, but postdural puncture headache (PDPH) is the most common risk. This study aimed to find out how often PDPH happens in Libyan patients having spinal anaesthesia for urological surgeries, comparing the median and paramedian methods because there are not many records available. This prospective study occurred at the Specialty Surgical Centre in Benghazi, Libya, from September 18, 2019, to February 18, 2020. Patients undergoing urological surgery under spinal anaesthesia were divided into two groups based on the method used: median (Group M) and paramedian (Group P). Researchers collected age, BMI, and gender data to better understand PDPH prevalence and compare the two companies. All the data were coded and analysed using SPSS 27. The study included 60 patients, including 53 adult males and 7 females, ranging in age from 11 to 70 years, with a median age of 55.5 ± 18.2 years. Normal PDPH prevalence was 8.3%, with 13.3% in Group M and 3.3% in Group P. Statistical analysis showed no significant difference in PDPH prevalence between the two companies (p=0.4). Patients' age, gender, and BMI did not differ significantly between the two groups, according to logistic regression analysis. While a larger number of patients in the median institution had PDPH, the difference was not statistically significant. These findings support previous research on needle insertion techniques and PDPH, but the authors suggest conducting larger studies with more populations to confirm and improve those findings.

Keywords: medial technique, paramedian technique, postdural puncture headache, spinal anaesthesia, urological surgeries

Corresponding Author: Aosama Alarfi, alarfiaosama@gmail.com

 ISSN: Online 2790-1637, Print 2790-1629
National Library of Libya, Legal number: 154/2018

1.INTRODUCTION

Spinal anaesthesia is an extensively used approach in various surgical techniques because of its unique advantages compared to general anaesthesia [1]. One key gain of spinal anaesthesia is its capacity to anesthetize a selected location of the body, without interfering with respiratory function. Moreover, it starts faster than general anaesthesia, taking into account an instant initiation of the surgical procedure [2]. Furthermore, spinal anaesthesia normally has a shorter period, leading to a quicker healing time and, in advance, patient mobility [3]. Median (M) and paramedian (P) techniques are commonplace strategies to obtain spinal anaesthesia. Each method has its personal traits. The median technique, as an example, whilst being the extra frequently used, can pose technical challenges, especially in older individuals with structural degenerative changes of their spine. Conversely, the paramedian method is regularly preferred for its quicker and speedier catheter insertion [4] and the capability to manage anaesthesia without the need for a flexed position [5].

While spinal anaesthesia offers several benefits, it's essential to recognise its complications like postdural puncture headache (PDPH), bleeding, contamination, hypotension, urinary retention, and nerve injury [6]. The pronounced occurrence of PDPH varies significantly worldwide, stimulated by many factors, including affected person attributes, needle design, and the technique used [7]. Women, particularly pregnant and postnormal delivery at a high risk of PDPH. Similarly, a higher chance is found in individuals with lower body mass indices (BMI), while the peak age for its prevalence lies between 18 and 30 years [8]. The occurrence is also stimulated by way of numerous factors, which include the diameter of the spinal needle used for dural puncture, with smaller diameters being related to a decreased risk [9]. Moreover, the patient's positioning in the course of spinal anaesthesia may additionally have an essential position as cautioned with the aid of Sharma et al [10] who proposed that the lateral decubitus position is less likely to cause PDPH compared to the sitting position [10].

PDPH is mainly diagnosed based on clinical symptoms, laboratory tests, or further tests like neuroimaging are rarely indicated if complications or alternative conditions, such as subdural hematoma or venous

 ISSN: Online 2790-1637, Print 2790-1629
National Library of Libya, Legal number: 154/2018

thrombosis, are suspected [11, 12]. To decrease the risk of PDPH, several preventive measures can be taken, including the usage of small-diameter needles or atraumatic spinal needles, aligning the needle bevel with the dural fibers, and considering prophylactic epidural blood patches or epidural saline. Regarding the management of PDPH, simple steps like rest, adequate hydration, or using caffeine can help, alongside medications such as antiemetics, paracetamol, or even sphenopalatine ganglion and occipital nerve blocks and epidural blood patch for more severe cases. Fortunately, the majority of PDPH cases are self-limited, with approximately 75% improving within seven days and 88% resolving completely by six weeks, without any specific treatment. [13-15].

Many research papers have studied the prevalence of post-dural puncture headache following spinal anesthesia, with a primary emphasis on obstetric patients [16]. Some studies have extended their scope to include orthopedic patients [17, 18] or patients undergoing lower limb surgeries [19]. On the other hand, there is a paucity of research dedicated to urological interventions. For instance, Harrison and Langham [20] surveyed 100 patients who underwent spinal anesthesia in urology theaters, but they did not account for spinal anesthesia approaches. A more recent investigation in 2023 compared post-dural puncture headache occurrences between paramedian and median approaches, but it was limited to patients undergoing nephrolithotripsy [21]. With the scarcity of studies within our region, significant gaps persist in the literature concerning potential variations in PDPH rates between median and paramedian techniques. Therefore, the primary objective of this research was to investigate the incidence of post-dural puncture headache in patients undergoing spinal anesthesia for urological procedures and to test the difference in incidence between paramedian and median approaches. Such a study aims not only to enhance patient care but also to optimize resource distribution and enhance the efficiency of hospital resources.

2.MATERIALS AND METHODS

2.1.Study Design and Location

The prospective study was conducted at the Specialty Surgical Centre Benghazi between September 18th, 2019, and February 18th, 2020.

 ISSN: Online 2790-1637, Print 2790-1629
National Library of Libya, Legal number: 154/2018

2.2.Study Population

60 patients who needed urological procedures under spinal anaesthesia.

1.Inclusion criteria

a.Patients who did not complain of headache before spinal anaesthesia.

b.Patients who did not have features of hypovolemia in the perioperative period.

c.Patients who are hemodynamically stable with no blood pressure fluctuations.

2.Exclusion criteria

a.Patients with a history of headaches or chronic pain.

b.Patients with a history of PDPH.

c.Patients with anxiety or cognitive impairment.

2.3.Data Collection

Baseline data were obtained, including age, gender, presence of diabetes mellitus or hypertension, and BMI through the index: Weight (kg)/ Height $(m)^2$.

Spinal anaesthesia was administered in either a lateral or sitting position at L3–4 or L4–5 level by a single anaesthesiologist utilizing a 25G Quincke spinal needle. Patients were randomly and equally allocated to either the Median approach (M) or the Paramedian approach (P) groups. In Group M, spinal anaesthesia was administered by guiding the needle through the supraspinous ligament, interspinous ligament, and ligamentum flavum to the dura. The Group P technique directly targets the ligamentum flavum after traversing the paraspinal muscles. This method involved inserting the spinal needle 1cm lateral and below the spinous process at a cephalad angle of 10–15°.

To evaluate PDPH, patients were inquired about headache occurrence using a binary scale (yes or no response). Individuals experiencing headaches within 5 days post-surgery were examined for positional effects. Headache onset or aggravation within 15 minutes of standing in an upright position, followed by relief within 30 minutes of returning to a supine position, was classified as PDPH. The pain intensity scoring was assessed using the Visual Analogue Scale (VAS). The VAS score consists of a 10 cm line with 10 mm to each point of the scale and two end-points representing no pain and worst possible pain, where 0 = no pain, 1–3 = mild, 4–6 = moderate, and 7–10 = severe pain [22].

 ISSN: Online 2790-1637, Print 2790-1629
National Library of Libya, Legal number: 154/2018

2.4.Statistical Analysis

Data was analysed using IBM SPSS Statistics, version 27. Initially, demographic data were assessed through descriptive statistics: mean ± standard deviation (S.D.) for numerical data and counts/percentages for categorical data. The t-test was employed to evaluate mean differences, while the chi-square test ($\chi 2$) was used to compare the incidence of PDPH between the two approach groups. Factors associated with PDPH were investigated through logistic regression analysis, presenting odds ratios (OR) with a 95% confidence interval (CI) to indicate the strength of association; significance was considered for P-values < 0.05.

2.5.Ethical Considerations

Information about the study was given to all participants or their accompanying adult by the researcher anaesthesiologist. Before they enrolled in the study, participants provided formal consent. For individuals below 18 years, consent was acquired from their legal guardian. Personal information was omitted to uphold participant confidentiality.

3.RESULTS

3.1.General Characteristics of the Study Population

The study enrolled 60 patients who underwent various types of urological procedures under spinal anaesthesia. Of these patients, 53 (88%) were males and 7 (12%) were females, and their age ranged from 11 to 70 years, with a mean age of 55.5 ± 18.2 years. A total of 48.3% were in the 61 years and above age group, with a mean age of 68.8 ± 1.7, and most were males. For further information, please refer to Table (1).

خطا! لم يتم العثور على مصدر المرجع.

ISSN: Online 2790-1637, Print 2790-1629
National Library of Libya, Legal number: 154/2018

Table (1). Age distribution among the study population

Males Females			Gender		Total
Age group	years 30 ≥	Count	9	1	10
		Percentage	15%	1.7%	16.7%
	years 31-60	Count	18	3	21
		Percentage	30%	5%	35%
	years 61 ≤	Count	26	3	29
		Percentage	43.3%	5%	48.3%
Total Percentage		Count	53	7	60
		88%	12%	100%	

Among the study participants, 14 (23.3 %) were solely hypertensive, 15 patients (25%) were solely diabetic, and 3 (5%) had both conditions. It was also shown that the study population had a mean BMI of 23.5 ± 2.8, with 60% having a normal BMI and 33.3% being overweight. Obese and underweight patients each comprise 3.3% of the study population.

As illustrated in Figure 1, Cystoscopy, transurethral resection of bladder tumor (TURBT), and varicocele surgeries were the most commonly performed urological procedures. Less frequent procedures were also shown to provide a comprehensive overview. The study also examined the distribution of these surgeries based on the spinal approach used. Within the median approach group, 30% underwent TURBT, 16.7% underwent varicocele surgeries, and 13.3% had cystoscopy. Among the paramedian approach group, the distribution was 36.7% for cystoscopy, 20% for varicocele surgeries, and 13.3% each for TURBT and transurethral resection of the prostate (TURP) surgeries.

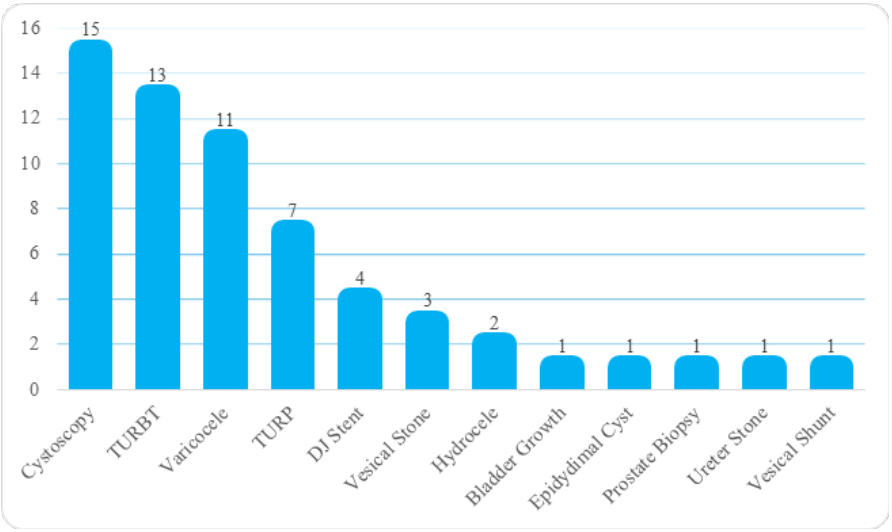

Figure (1). Types of urological procedures done in the study.

The demographic variables of the study population are displayed in Table (2) Considering both approaches to spinal anaesthesia.

Table (2). Demographic variables according to the spinal anesthesia approach.

Variable	Subclass	Median approach (n = 30)	Paramedian approach (n = 30)	p-value
Gender	Males	26 (86.7%)	27 (90%)	1
	Females	4 (13.3%)	3 (10%)	
Age (mean ± SD)		54.7 ± 17.4	52.3 ± 19.1	0.6
BMI (mean ± SD)		23.9 ± 2.6	23.2 ± 3.0	0.3
Diabetes mellitus	Diabetics	11 (36.7%)	7 (23.3%)	0.2
	Not diabetics	19 (63.3%)	23 (76.7%)	
Hypertension	Hypertensives	8 (26.7%)	9 (30%)	0.7
	Not hypertensives	22 (73.3%)	21 (70%)	

3.2.Incidence of PDPH Among the Study Population

Among the study population, 5 patients (8.3%), 3 males and 2 females, experienced a post-dural puncture headache with pain severity ranging from mild (80%) to moderate (20%) on a visual analogue scale. The distribution of PDPH among both genders didn't demonstrate any statistical significance, with a p-value of 0.09. Considering age distribution, 2 patients were aged 30 years or younger, while 3 patients fell within the 31-60-year age group, with a p-value of 0.06. Most patients (60%) complained of PDPH within 72 hours postoperatively, and the rest (40%) developed PDPH on the fourth day after spinal anaesthesia.

Table (3) presents the incidence of PDPH within the median and paramedian groups, as well as their gender distribution. Within Group M, four individuals (13.3%) reported PDPH. Three of them had mild headaches, and one had a moderate-severity headache. In Group P, only one individual (3.3%) reported PDPH, which was of mild severity. The p-value was 0.4, suggesting no statistically significant difference.

Table (3). Incidence of PDPH between the median and paramedian groups

Postdural puncture headache	Gender distribution	Median approach (group (n = 30	Paramedian approach (group (n = 30	p-value
Yes	Male	(75%) 3	(0%) 0	0.4
	Female	(25%) 1	(100%) 1	
No	Male	(88.5%) 23	(93.1%) 27	
	Female	(11.5%) 3	(6.9%) 2	

Univariable logistic regression revealed no significant association between PDPH incidence and age, gender or BMI, as evidenced by corresponding p-values of 0.06, 0.06, and 0.9, respectively. For more details, refer to Table (4).

 ISSN: Online 2790-1637, Print 2790-1629
National Library of Libya, Legal number: 154/2018

Table (4). Binary logistic regression of each independent variable with PDPH

	Univariate analysis		
	OR	95% CI	p-value
Age (years)	0.954	0.907-1.003	0.063
Gender (male/female)	0.150	0.020-1.121	0.065
BMI (Kg)	0.980	0.709-1.354	0.902

Abbreviations: OR = Odds Ratio, CI = Confidence Interval, BMI = Body Mass Index.

4.DISCUSSION

Our study reported a PDPH incidence of 8.3%, lower than that observed in studies from other African countries such as East Ethiopia, Kenya, Egypt, and others [23-25]. Similarly, this rate was less than the 20% reported by Oumer et al [17] among orthopedic patients in Addis Ababa, Ethiopia, possibly due to their use of needle sizes ranging from 18 to 23G. Compared to worldwide studies, our rate was lower than those reported in a study from Iran (10%) but higher than reports from Germany (5.9%) and the USA (2%) [18, 26, 27]. Similarly, Khraise et al [28] reported a lower incidence of 6.3% in parturients, which may be explained by their use of a mixture of needle types with needle sizes >25G while our study utilized only 25G cutting-type needles [28].

Regarding headache severity, our study has shown that 80% of study participants experienced mild headaches, and this was similar to the result of Mohammed et al [29] who reported that 61.9% of women had mild pain [29]. However, our results contrast with those of Tafesse and Melkamayew [23], who showed that more than two-thirds of the study participants had moderate to severe PDPH. The possible explanation for this discrepancy is that the needles that they used included ≥ 23 gauges, which are responsible for the CSF leakage in large amounts [23].

Considering the relationship between age, gender and PDPH, previous research has yielded mixed results. A study from Dhulikhel Hospital, Nepal, found that individuals aged 18-30 years were more susceptible to PDPH than those aged 31-45 years [30]. However, our study revealed a different trend, with patients aged 31-60 years being more likely to have PDPH in comparison to younger patients. Regarding gender, some studies have reported no significant impact of gender on the incidence of PDPH

[31-33], and this corresponds to our study's results. However, a study was conducted by DelPizzo et al [27] in New York, involving 300 patients undergoing simple knee arthroscopy, showed a higher incidence of PDPH in women compared to men [27]. A similar study has shown a higher incidence in women by 2-3 times than in men. While the exact reasons for this disparity remain unclear, it was claimed that hormonal differences and heightened female pain sensitivity may contribute to this phenomenon [34].

Regarding the disparity in PDPH occurrence between the two approaches, our study demonstrated an increase in the median approach, but without statistical significance. This result aligned with that of Jahromi et al [21] who suggested the paramedian approach as a superior approach in reducing PDPH, albeit without a statistical difference [21]. Similarly, Mosaffa et al [18] discovered no substantial variance in PDPH occurrence between the two approaches. Consequently, they recommend the paramedian approach, particularly for elderly patients with spinal degenerative changes and those who may find it challenging to adopt the appropriate position for the median approach. In contrast, other studies revealed another trend and showed a significant variation in the PDPH incidence between the two approaches. For example, a study of Haider et al [35], which included 50 patients undergoing various alternative surgeries during the spinal neuraxial anaesthesia, concluded that the possibility of PDPH [35] was reduced by using a paramedian approach with Quincke needle type markedly diminishes the chances of PDPH. On the contrary, a study conducted by Nisar et al [36] highlighted in Pakistan reported a higher incidence of PDPH with the paramedian approach compared to the median approach [36]. These contradictory results require large and more diverse studies to achieve integrated guidelines on the optimal approach to spinal anaesthesia.

5.CONCLUSIONS

Postdural puncture headache (PDPH) creates significant challenges for patients and health professionals, which negatively affects the patient's satisfaction and quality of care. Despite its effects, the prevalence and contributing factors of PDPH among urological patients in our region are poorly understood, emphasizing the need for focused research. Therefore, the purpose of

this study was to determine the occurrence of headaches after spinal anaesthesia in patients scheduled for urological procedures and to compare the occurrence between median and paramedian approaches. By identifying the frequency of PDPH and potential determinants, this study not only wants to improve the patient's satisfaction, but also to optimize the use of the health care system and improve the hospital's efficiency.

This study presented several significant findings. PDPH, a common complication of spinal anaesthesia, was infrequent, with an incidence of 8%. The severity of headaches ranged from mild to moderate and did not require specific interventions. Furthermore, the median approach group showed a higher incidence of PDPH (80% vs 20%), but this did not reach statistical significance. Additionally, the study did not demonstrate statistical significance among age, gender, and BMI as predictors of PDPH.

Nevertheless, these findings must be interpreted alongside certain limitations. The predominantly male cohort (88%) may limit its generalizability, as females are generally at higher risk for PDPH. Similarly, the small sample size (n=60) and reliance on a single needle type reduce the power to detect significant differences. Finally, factors like patient age, comorbidities, and anatomical variations that might influence PDPH occurrence may not have been equally distributed between the two groups.

Based on these findings, the study presents several key recommendations. Firstly, further research should involve larger and more diverse populations to validate the observed results. Secondly, additional studies are needed to explore other potential contributors to PDPH, as this study found no significant association with age, gender, or BMI. Finally, while PDPH is typically self-limiting, healthcare providers are encouraged to remain vigilant in monitoring patients for this common complication following spinal anaesthesia.

6.ACKNOWLEDGMENTS

The authors would like to express their deepest appreciation to the staff of the Specialty Surgical Center Benghazi, whose assistance has contributed to this research project.

7.REFERENCES

1.Capdevila X, Aveline C, Delaunay L, Bouaziz H, Zetlaoui P, Choquet O, et al. Factors determining the choice of spinal versus general anesthesia in patients undergoing ambulatory surgery: results of a multicenter observational study. Advances in Therapy. 2020;37:527-40.https://doi.org/10.1007/s12325-019-01171-6

2.Fedorov A, Lehto A, Klein J. Inhibition of mitochondrial respiration by general anesthetic drugs. Naunyn-Schmiedeberg's Archives of Pharmacology. 2023;396(2):375-81. https://doi.org/10.1007/s00210-022-02338-9

3.Siddiqi A, Mahmoud Y, Secic M, Tozzi JM, Emara A, Piuzzi NS, et al. Mepivacaine versus bupivacaine spinal anesthesia for primary total joint arthroplasty: a systematic review and meta-analysis. The Journal of Arthroplasty. 2022;37(7):1396-404. e5.https://doi.org/10.1016/j.arth.2022.03.031

4.Leeda M, Stienstra R, Arbous M, Dahan A, Veering BT, Burm A, et al. Lumbar epidural catheter insertion: the midline vs. the paramedian approach. European journal of anaesthesiology. 2005;22(11):839-42.https://doi.org/10.1017/S0265021505001419

5.Podder S, Kumar N, Yaddanapudi LN, Chari P. Paramedian lumbar epidural catheter insertion with patients in the sitting position is equally successful in the flexed and unflexed spine. Anesthesia & Analgesia. 2004;99(6):1829-32.https://doi.org/10.1213/01.ANE.0000136774.99702.14

6.Peterson EE, Riley BL, Windsor RB, editors. Pediatric intracranial hypotension and post-dural puncture headache. Seminars in Pediatric Neurology; 2021: Elsevier.

7.Choi DY, Lee SE, Lee MW, Lee KH, Kang E, Kwon JY, et al. Prediction of the Cervical Epidural Space Depth from the Skin Using Cervical X-Ray, During Cervical Epidural Block with Paramedian Approach. Journal of Pain Research. 2023:2079-90.https://doi.org/10.2147/JPR.S409347

8.Liu S, Carpenter RL, Neal JM. Epidural anesthesia and analgesia: their role in postoperative outcome. The Journal of the American Society of Anesthesiologists. 1995;82(6):1474-506.

9.Lambert DH, Hurley RJ, Hertwig L, Datta S. Role of needle gauge and tip configuration in the production of lumbar puncture headache. Regional anesthesia and pain medicine. 1997;22(1):66-72.https://doi.org/10.1016/

S1098-7339(06)80058-1

10.Sharma HM, Khandelwal M, Beniwal S, Gurjar SS, Sharma S. Comparison of sitting versus lateral decubitus position during spinal anaesthesia on the occurrence of post-dural puncture headache in patients undergoing lower segment caesarean section: A randomised controlled trial. Indian Journal of Anaesthesia. 2022;66(10):738-40.https://doi.org/10.4103/ija.ija_725_21

11.Stanhope E, Foulds L, Sayed G, Goldmann U. Diagnosing causes of headache within the postpartum period. J Obstet Gynaecol. 2018;38(5):728

12.Kurnutala LN, Kim D, Sayeed H, Sibai N. Persistent spinal headache after removal of intrathecal drug delivery system: a case report and review of literature. Anesthesiology and pain medicine. 2015;5(5).https://doi.org/10.5812/aapm.29786

13.Befikadu A, Timerga S, Mihretu F, Siyoum F, Agmuas A. Prevention and Management of Post-Dural Puncture Headache (PDPH). International Journal of Anesthetics and Anesthesiology. 2022;9(2):143-4.https://doi.org/10.23937/2377-4630/1410143

14.Apfel C, Saxena A, Cakmakkaya O, Gaiser R, George E, Radke O. Prevention of postdural puncture headache after accidental dural puncture: a quantitative systematic review. British journal of anaesthesia. 2010;105(3):255-63.https://doi.org/10.1093/bja/aeq191

15.Weji BG, Obsa MS, Melese KG, Azeze GA. Incidence and risk factors of postdural puncture headache: prospective cohort study design. Perioperative Medicine. 2020;9:1-6. https://doi.org/10.1186/s13741-020-00164-2

16.Karami T, Karami N, Rastgo H. Comparison of the effect of paramedian and median methods on postdural puncture headache among candidates for elective ce-sarean sections undergoing spinal anesthesia. A double blind. Pediatr Anesth Crit Care J. 2021;9:116-22.https://doi.org/10.14587/paccj.2021.19a

17.Oumer KE, Aychew H, Daniel T, Mekete G, Belete KG, Negash TT. Incidence and associated factors of post-dural puncture headache among orthopaedic patients after spinal anesthesia: a prospective cohort study. Annals of Medicine and Surgery. 2023;85(10):4703-8.https://doi.org/10.1097/ms9.0000000000001167

18.Mosaffa F, Karimi K, Madadi F, Khoshnevis SH, Besheli LD, Eajazi A. Post-dural puncture headache: a comparison between

median and paramedian approaches in orthopedic patients. Anesthesiology and Pain Medicine. 2011;1(2):66-9.https://doi.org/10.5812/kowsar.22287523.2159

19.DelPizzo K, Luu T, Fields KG, Sideris A, Dong N, Edmonds C, et al. Risk of postdural puncture headache in adolescents and adults. Anesthesia & Analgesia. 2020;131(1):273-9.https://doi.org/10.1213/ANE.0000000000004691

20.Harrison D, Langham B. Spinal anaesthesia for urological surgery: a survey of failure rate, postdural puncture headache and patient satisfaction. Anaesthesia. 1992;47(10):902-3

21.Jahromi MSS, Zabetian H, Kalani N, Khosravani F, Yousefi A. Comparing the Incidence of Postdural Puncture Headache (PDPH) between Median and Paramedian Approaches in Nephrolithotripsy under Spinal Anesthesia. International Journal of Medical Investigation. 2023;12(1):83-91

22.Mohamed R, Amin M, Omar H. Computed tomography-guided celiac plexus neurolysis for intractable pain of unresectable pancreatic cancer. Egyptian Journal of Radiology and Nuclear Medicine. 2017;48:627-37.10.1016/j.ejrnm.2017.03.027.

23.Tafesse D, Melkamayew A. Magnitude of postdural puncture headache and associated factors in obstetric mothers undergone spinal anesthesia for caesarean section. J of Anes & Cri Open Access. 2019;11(2):46-50

24.Gisore E, Mung'ayi V, Sharif T. Incidence of post-dural puncture headache following caesarean section under spinal anaesthesia at the Aga Khan University Hospital, Nairobi. East African medical journal. 2010;87(6):227-30.https://doi.org/10.4314/eamj.v87i6.63078

25.Ali HM, Mohamed MY, Ahmed YM. Postdural puncture headache after spinal anesthesia in cesarean section: Experience in six months in 2736 patients in Kasr El aini teaching hospital–Cairo University. Egyptian Journal of Anaesthesia. 2014;30(4):383-6. https://doi.org/10.1016/j.egja.2014.06.001

26.Weinrich J, von Heymann C, Henkelmann A, Balzer F, Obbarius A, Ritschl P, et al. Postdural puncture headache after neuraxial anesthesia: incidence and risk factors. Der Anaesthesist. 2020;69:878-85.https://doi.org/10.1007/s00101-020-00846-y

27.DelPizzo K, Cheng J, Dong N, Edmonds CR, Kahn RL, Fields KG, et al. Post-dural puncture headache is uncommon in young

ambulatory surgery patients. HSS Journal®. 2017;13(2):146-51

28.Khraise WN, Allouh MZ, El-Radaideh KM, Said RS, Al-Rusan AM. Assessment of risk factors for postdural puncture headache in women undergoing cesarean delivery in Jordan: a retrospective analytical study. Local and Regional Anesthesia. 2017:9-13.https://doi.org/10.2147/LRA.S129811

29.Mohammed A, Ayyuba R, Salisu I, Nagoma A, Owolabi L, Ibrahim A. An analysis of postdural puncture headache in obstetric patients: A study from Kano, Nigeria. Tropical Journal of Obstetrics and Gynaecology. 2017;34(1):16-20

30.Singh J, Ranjit S, Shrestha S, Limbu T, Marahatta SB. Post dural puncture headache. Journal of Institute of Medicine Nepal. 2011;32(2):30-2.https://doi.org/10.59779/jiomnepal.501

31.Dittmann M, Schaefer HG, Renkl F, Greve I. Spinal anaesthesia with 29 gauge Quincke point needles and post dural puncture headache in 2,378 patients. Acta anaesthesiologica scandinavica. 1994;38(7):691-3.https://doi.org/10.1111/j.1399-6576.1994.tb03978.x

32.Lybecker H, Møller JT, May O, Nielsen HK. Incidence and prediction of postdural puncture headache A prospective study of 1021 spinal anesthesias. Anesthesia & Analgesia. 1990;70(4):389-94

33.Tarkkila PJ, Heine H, Tervo R-R. Comparison of Sprotte and Quincke needles with respect to post dural puncture headache and backache. Regional Anesthesia and Pain Medicine. 1992;17(5):283-7

34.Wu CL, Rowlingson AJ, Cohen SR, Michaels RK, Courpas GE, Joe EM, et al. Gender and post–dural puncture headache. The Journal of the American Society of Anesthesiologists. 2006;105(3):613-8

35.Haider S, Butt KJ, Aziz M, Qasim M. Post dural puncture headache-a comparison of midline and paramedian approaches. Biomedica. 2005;21(July-December):90-2

36.Nisar A, Saleem J, Hussain S, Bashir K. Comparison of postdural puncture headache in median and paramedian approach under spinal anesthesia in cesarean section. Pak J Med Health Sci. 2016;10(1):298-301.

Scientific Journal of University of Benghazi
SJUOB (2025) 38 (1) Medical Sciences: Budajaja, et al, 230 – 244
www.sjuob.uob.edu.ly

Evaluation of Dental Advice Delivery: A Comparative Study of General Practitioners and Specialists in Benghazi.

Hunaida Budajaja,[1] Mubarakah Abraheem[1], Amal Gaber[1]*, Osama Ahmadi[1], Hala Fathallah Benghasheer[1]

1 Department of Dental Public Health and Preventive Dentistry, Faculty of Dentistry, University of Benghazi, Libya.

Received: 10 / 03 / 2025 | Accepted: 11 / 04 / 2025 | Publishing: 29/06/2025

ABSTRACT

Oral health education is a crucial aspect of dental care, as proper guidance from dentists can significantly influence patients' oral hygiene habits. This study investigated whether dentists in Benghazi provide dental advice to patients and examined differences between general practitioners (GPs) and specialists in delivering such advice. This cross-sectional study included 246 dentists from public clinics and the Faculty of Dentistry at the University of Benghazi. Data were collected through a structured questionnaire covering sociodemographic details, oral health practices, and advice given to patients. Analysis was conducted using IBM SPSS version 24, employing descriptive statistics and chi-square tests to compare GPs and specialists. Results showed that both GPs and specialists consistently provided oral hygiene and smoking-related advice, with no significant difference ($p > 0.05$). GPs (68.2%) were slightly more likely to offer preventive advice than specialists (62.9%), while specialists (85.4%) provided dietary advice more frequently than GPs (75.2%), though these differences were not significant ($p > 0.05$). However, a significant difference was observed in professional treatment advice, with 98.9% of specialists providing it compared to 92.4% of GPs ($p = 0.028$). These findings highlight the need for standardized preventive care strategies to enhance patient education and oral health outcomes. However, the inconsistent advice provided by dentists may be due to insufficient training in preventive care and the treatment-oriented nature of Libya's dental health system.

Keywords: Advice, dental, general practitioners, oral hygiene, practice, specialists.

Corresponding Author: Amal Gaber, amal.gaber@uob.edu.ly

 ISSN: Online 2790-1637, Print 2790-1629
National Library of Libya, Legal number: 154/2018

1.INTRODUCTION

Oral health care is fundamental to the well-being and quality of life of individuals.[1, 2] It is essential for maintaining good oral hygiene and preventing systemic diseases that can arise from untreated dental issues.[3, 4] Willie Sai Ho</author></authors></contributors><titles><title>The role of oral health in the prevention of systemic diseases</title><secondary-title>Universal Library of Medical and Health Sciences</secondary-title></titles><periodical><full-title>Universal Library of Medical and Health Sciences</full-title></periodical><volume>1</volume><number>1</number><dates><year>2024</year></dates><urls></urls></record></Cite></EndNote> Improving public awareness about dental issues and providing adequate information on oral diseases, including risk factors and preventive measures, plays a critical role in promoting better oral hygiene practices, early detection of dental problems, and timely intervention.[5, 6]

Improper diet, smoking, and poor oral hygiene are significant factors influencing the occurrence of various oral diseases.[7, 8] Oral hygiene practices vary across countries, with differences in self-care practices like daily flossing and brushing with fluoride toothpaste and accessibility to dental care.[9, 10] Enhanced knowledge of oral health leads to better hygiene routines and healthier lifestyle choices.[2, 9]

Dental professionals, including general dentists and specialists, play a pivotal role in delivering essential preventive advice to their patients. Effective primary prevention through advice on oral hygiene practices, clinical preventive measures, dietary habits, smoking cessation, and professional treatments from both GPs and specialists can prevent common oral health issues.[11, 12]

However, there is a limited understanding of the extent to which dentists in Benghazi are fulfilling their role in delivering preventive dentistry through advice. It is also unclear whether specialized dentists have a better grasp of the importance of providing advice to improve community dental health, particularly in underserved and high-risk communities. This study aims to determine whether dentists in Benghazi provide dental advice to

their patients and identify any differences between general practitioners (GPs) and specialists in this regard. By investigating this, we hope to gain insights into the participating dentists' understanding of preventive measures and their commitment to properly implementing these measures as part of oral healthcare delivery services. Ultimately, this research seeks to contribute to the development of improved healthcare policies that will benefit the Libyan population in the long term.

2.METHODS

2.1.Study design & population

A cross-sectional study was conducted targeting dentists (both GPs and specialists) from public dental clinics and the Faculty of Dentistry of the University of Benghazi. A convenience sampling method was employed. The population of the current study consists of 246 Libyan dental practitioners in Benghazi City.

2.2.Study Instrument & Data Collection

Data was gathered through an online questionnaire. A self-generated questionnaire was prepared based on previous relevant international literature.13 The questionnaire was constructed based on the objectives of the study.

The first draft was sent to a dental public health specialist for content validity. Based on expert feedback, some items needed to be excluded or further refined, e.g., double-barrel items. The internal consistency of the questionnaire was also evaluated by the reliability coefficients (Cronbach's Alpha), which ranged between 0.71 to 0.86.

The questionnaire consists of three Sections: Section 1: participants' sociodemographics, which includes (Gender, age, marital status, place of residency, and monthly income). Section 2: Seven items on oral health practices (Frequency of brushing, use of fluoride toothpaste, flossing habits, and consumption of sugar-containing snacks or drinks). Section 3: nineteen items on advice provided to patients; these questions were grouped into categories, which included the following advice categories: oral hygiene practices, clinical preventive measures, dietary habits, smoking cessation, and professional treatments.

2.3.Statistical Analysis

Data was analyzed using SPSS version 24. Descriptive statistics were re-

 ISSN: Online 2790-1637, Print 2790-1629
National Library of Libya, Legal number: 154/2018

ported using frequencies and percentages for sociodemographic characteristics, oral health practices, and dietary habits. Chi-Square was used to compare differences in proportions between GPs and specialists regarding sociodemographic characteristics, oral health practices, dietary habits, and types of oral health advice provided. All statistical analyses were performed with a significance level set at $p < 0.05$.

2.4.Ethical Considerations:

The study was approved by the ethics committee at the Faculty of Dentistry, Benghazi, Libya (approval no. 0255). All participants were assured of the confidentiality and privacy of their responses, and the informed consent was obtained from all participants along with the completed self-administered questionnaire.

3.RESULTS

The majority of the participants were females (71.5%), aged between 36 and 45 years (44.3%). Most of the participants were married (61.0%) and GPs (63.8%), while specialists accounted for 36.2%. Most participants live in Benghazi (86.6%), with 13.4% residing around Benghazi. Regarding the income level, 27.2% of the participants reported earning more than 2000 LD, and the rest majority reported earning 2000 LD or less, whereas (39.8%) earned 1000-2000 LD, and 32.9% earned less than 1000 LD. A majority of participants (83.3%) reported no medical problems, while 16.7% indicated they had medical issues (see Table (1)).

Table (1): Sociodemographic Characteristics

Sociodemographic Characteristics	N (%)
Gender	
Male	70 (28.5)
Female	176 (71.5)
Age groups	
20-35 years	95 (38.6)
36-45 years	109 (44.3)
46-60 tears	40 (16.3)
Marital status	
Single	96 (39)
Married	150 (61)
Specialty	
GP	157 (63.8)
Specialists	89 (36.2)
Residence	
Benghazi	213 (86.6)
Around Benghazi	33 (13.4)
Income	
< 1000 LD	81 (32.9)
1000 -2000 LD	98 (39.8)
> 2000 LD	67 (27.2)
Total	246 (100)

The majority of both GPs (89.2%) and specialists (94.4%) reported regular brushing habits, with specialists showing slightly higher adherence, although the difference was not statistically significant ($p > 0.05$). The use of fluoride toothpaste was more common among specialists (67.4%) compared to GPs (54.1%), with a statistically significant difference ($p = 0.042$). The effect size by Phi & Cramer's V was 0.121, which is a moderate effect. Flossing habits were similar between the two groups, with 63.1% of GPs and 59.6% of specialists reporting regular flossing ($p > 0.05$)(see Table (2)).

Table (2): Oral health practices based on specialty

Oral health practices		GP n (%)	Specialist n (%)	X^2	P value
Brushing	Regular	140(89.2)	84 (94.4)	1.893	0.169
	Irregular	17(10.8)	5(5.6)		
Fluoride Toothpaste	Yes	85(54.1)	60(67.4)	4.137	0.042**
	No	72(45.9)	29 (32.6)		
Flossing	Yes	99 (63.1)	53 (59.6)	0.296	0.586
	No	58 (36.9)	36 (40.4)		

*Chi-square test **Significance: ($p < 0.05$)

When examining the addition of sugar to hot beverages, it was observed that a higher proportion of specialists (69.7%) reported this behavior compared to GPs (60.5%). However, this difference did not reach statistical significance ($p > 0.05$). On the other hand, GPs reported a significantly higher frequency of consuming sugar-containing snacks or drinks 'more than twice a day' (41.4%) compared to specialists (7.9%) ($p < 0.001$). The effect size by Phi & Cramer's V was 0.273, which is a very strong effect Additionally, a significant difference was observed in the behavior of managing sugar intake, with specialists (40.4%) more likely to reduce the frequency of sugar intake, whereas GPs (51.6%) leaned towards reducing the amount of sugar consumed ($p = 0.004$). The effect size by Phi & Cramer's V was 0.162, which is a strong effect (see Table (3)).

Table (3): Dietary practices based on specialty

Dietary practices		GP n (%)	Specialist n (%)	X^2	p value
Sugar in hot drinks	Yes	95(60.5)	62(69.7)	2.061	0.151
	No	62(39.5)	27(30.3)		
Frequency of eating sugar-containing snacks or drinks	Never	15 (9.6)	10(11.2)	32.638	0.000**
	Once a day	46(29.3)	37(41.6)		
	Twice a day	31(19.7)	35(39.3)		
	More than twice a day	65(41.4)	7(7.9)		
The most important behavior regarding sugar	Reduce the frequency of sugar	33 (21.0)	36 (40.4)	10.983	0.004**
	Reduce the amount of sugar	81 (51.6)	32 (36)		
	Avoid sticky food	43 (27.4)	21 (23.6)		

*Chi-square test **Significance: ($p < 0.05$)

Table 4 summarizes the types of advice provided by the participants based on their specialty. Both GPs and specialists consistently provided oral hygiene and smoking-related advice with no statistically significant difference ($p > 0.05$). Preventive advice was slightly more common among GPs (68.2%) than specialists (62.9%), while specialists were more likely to provide dietary advice (85.4%) compared to GPs (75.2%), though these differences were not statistically significant ($p > 0.05$). A significant difference was found in professional treatment advice, with higher proportions of specialists (98.9%) providing this compared to GPs (92.4%). The effect size by Phi & Cramer's V was 0.102, which is a moderate effect at a $p = 0.028$).

Table (4): Type of provided advice based on specialty

Type of advice	GP n (%)		Specialist n (%)		Chi-Square Value	P Value
	Yes	No	Yes	No		
Oral Hygiene Advice	156 (99.4)	1 (0.6)	88 (98.9)	1 (1.1)	0.167	0.683
Clinical Preventive Advice	107 (68.2)	50 (31.8)	56 (62.9)	33 (37.1)	0.695	0.404
Dietary Advice	118 (75.2)	39 (24.8)	76 (85.4)	13 (14.6)	3.569	0.059
Smoking Advice	129 (82.2)	28 (17.8)	71 (79.8)	18 (20.2)	0.213	0.644
Professional treatment advice	145 (92.4)	12 (7.6)	88 (98.9)	1 (1.1)	4.824	0.028**

*Chi-square test **Significance: ($p < 0.05$)

The percentage of dentists who reported giving advice regarding different categories or fields was generally high. Almost all participating dentists answered "yes" to at least one of the questions related to oral hygiene advice. Additionally, 94.7% reported giving advice related to professional treatment questions. The lowest percentage was in the dietary advice section, where about 78.9% of dentists answered "yes" to at least one dietary advice-related question (see Figure 1).

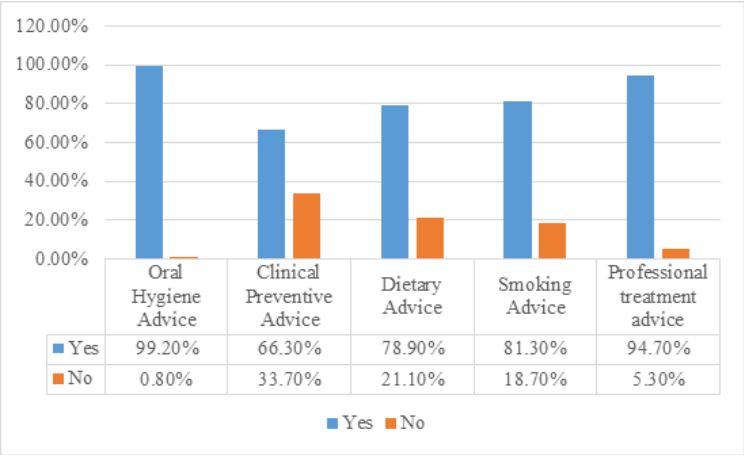

Figure (1): Types of provided advice for all participants

4.DISCUSSION

Dental professionals play a vital role in promoting oral health through preventive advice. Effective primary prevention encompasses guidance on oral hygiene practices, clinical preventive measures, dietary habits, smoking cessation, and professional preventive treatments. Understanding the differences in how dental advice is delivered by general dentists and specialists is essential for optimizing patient care and ensuring a more effective approach to oral disease prevention.

This study highlights several findings regarding the oral health practices and types of dental advice provided by dentists in Benghazi, Libya. The sociodemographic data revealed a higher proportion of female participants, reflecting global trends that indicate an increasing number of women entering the dental profession.

The participants demonstrated strong adherence to regular brushing and the use of fluoride toothpaste, consistent with Haresaku et al.14 Both GPs and specialists exhibited high brushing rates (>89%), but only moderate flossing adherence (around 60%), highlighting a gap in optimal practices. Specialists were more likely to use fluoride toothpaste than GPs. These findings align with other studies where high proportions of dentists reported brushing twice daily.15-17 Iranian dentists also reported high brushing and flossing rates, with three-quarters using fluoride toothpaste regularly.15 Croatian dentists exhibit similarly high oral hygiene standards, with 57% brushing twice daily and 92% flossing regularly.16 Additionally, approximately 44% of dentists in Saudi Arabia brush their teeth twice daily, and about 70% floss regularly. 17 Although participants demonstrated strong adherence to regular brushing, the discrepancy between the high proportion of brushing and the lack of fluoridated toothpaste while brushing is noteworthy. This may indicate a lack of deep knowledge about the components of fluoride toothpaste since most commercial toothpastes contain sodium fluoride, even if not in optimum amounts. This raises the question of whether most participants are unaware of the ingredients in toothpaste or if they tend to use natural products that primarily do not have fluo-

ride as a main component.

The research highlighted significant differences in dietary habits and sugar management attitudes between GPs and specialists. Contrary to specialists, GPs significantly consume sugary snacks more frequently. They believe that the behavior that needs modification is the amount of sugar consumed. This may indicate their lack of awareness about the key risk factors for caries and the critical behaviors necessary for reducing the cariogenic potential of sugar. Specialists, on the other hand, were more focused on reducing the frequency of sugar intake. This can also be explained by the fact that GPs, who often have more frequent patient appointments, might experience irregular mealtimes and rely on quick, sugary snacks. In contrast, specialists, with more structured schedules, may have a more regulated approach to snacking. These findings suggest that targeted interventions and educational programs could promote healthier dietary choices tailored to each group's unique circumstances. The higher consumption of sugar-containing snacks among GPs contrasts with Li et al. (2020),18 who found more uniform dietary habits among dental professionals in China, possibly due to cultural and regional differences in dietary preferences and awareness levels. A similar study by Athikom et al. (2024)19 observed significant variations in dietary behaviors among undergraduates, postgraduates, and practicing dentists, revealing a weak association between knowledge and healthy dietary behaviors across educational levels.

The results revealed that specialists were more likely to offer dietary and professional treatment advice, highlighting the influence of their advanced training and focused expertise in delivering care, which was also noted by Shmarina et al.20 While no significant differences were observed in providing oral hygiene, preventive, or smoking-related advice, GPs slightly preferred preventive advice, and specialists leaned towards dietary advice, with the near-significant p-value for dietary advice suggesting a trend needing further exploration. Both groups consistently provided advice, but specialists were more inclined to give detailed dental treatment guidance due to their focused training. Yusuf et al.21 observed that recent dental gradu-

ates increasingly see preventive activities as integral to their role. This perspective shift is largely due to the evolving emphasis on health promotion within dental education. However, many dentists still see their role primarily as diagnosing and treating issues, rather than preventive care, due to their training.22 The World Health Organization (WHO) recommended that most dentists consider smoking cessation counseling as a part of their role, despite time and training barriers,23-25 with newer graduates more likely to record smoking status and support cessation.25

Overall, the focus on preventive dental services is minimal in Libya, and the system is largely seen as treatment-oriented rather than geared toward prevention. In their exploratory case study, Aloshaiby et al 26 mentioned that while policy documents suggest that the Libyan healthcare system adopts a preventive services approach within primary healthcare, this does not accurately reflect the reality on the ground. A previous study conducted in Libya concluded that undergraduate dental programs fall short of equipping dentists with the skills for prevention-focused management and identified patient-related barriers as the most significant, with patients displaying a poor understanding of the potential for caries prevention.27 This study revealed high rates of dentists reported providing some sort of dental advice; however, this high percentage is misleading. In reality, most participants do not give comprehensive professional advice as intended; instead, they offer fragmented advice. For example, when they were asked whether they advise their patients to quit smoking, 59.8% answered yes. However, when combining responses of giving advice related to smoking cessation from other related questions, the percentage increased to 81.3%. This discrepancy indicates that dentists do not consistently provide complete and professional advice as part of a prevention-oriented approach, aligning with suggestions from previous studies that suggest the preventive approach is not adequately implemented in Libya.26, 27

In conclusion, this study found notable differences in dietary habits and attitudes towards sugar between GPs and specialists. GPs consume sugary snacks

more frequently, possibly due to their irregular schedules or due to better knowledge and oral health-related behavior in the specialists' group, which was reflected in the type of advice they provide, which tends to be more comprehensive. Moreover, the fragmented and inconsistent advice from dentists may stem from inadequate training in prevention-focused management within undergraduate programs and a lack of emphasis on prevention in Libya's dental health system, which remains largely treatment-focused. This contributes to a poor community understanding of oral disease prevention and increases the burden of oral health issues. This gap underscores the need for tailored interventions and the implementation of training programs to equip dentists with the skills to apply a preventive-oriented approach in dental faculties, ultimately improving prevention-focused care among dental professionals.

To address gaps in prevention-focused dental care, it is recommended to revise dental school curricula to include modules on oral disease prevention and patient education, provide training workshops for dentists, ensure the availability of preventive materials, and conduct public campaigns to raise awareness. Advocating for policies prioritizing preventive care can drive systemic changes in dental health practices.

While this study provides valuable insights into the current state of preventive care in Libya, addressing its limitations is crucial for future research. The use of a convenience sampling method restricts the generalizability of the findings; therefore, adopting a more representative random sampling approach would enhance validity. Additionally, the study's limited geographical scope, focusing solely on dentists from Benghazi, may not fully reflect the broader dental practice landscape in Libya. Expanding future research to include multiple cities would improve external validity and provide a more comprehensive perspective. Furthermore, the cross-sectional study design and reliance on self-reported data introduce potential biases, including social desirability bias. Future research should prioritize larger, more diverse samples and incorporate probability sampling methods where feasible. Additionally, qualitative methodolo-

gies were used to gain deeper insights into how dentists provide advice, the content of their advice, and their perceptions of its role in promoting oral health.

5.REFERENCES

1.Valdivia ADCM, Sánchez MdlAV, Cortés DEA, Cortés EG. Oral health: fundamentals, importance, and perspectives. Human Teeth-From Function to Esthetics: IntechOpen; 2023.

2.Chamut S, Alhassan M, Hameedaldeen A, Kaplish S, Yang AH, Wade CG, et al. Every bite counts to achieve oral health: a scoping review on diet and oral health preventive practices. International Journal for Equity in Health. 2024;23(1):1-88.

3.Fouad Merza R, Alqahtani NS, Al-sulami SBB, Aljohani RB, Saleh MA, Hawsawi SMA, et al. Oral Health and Systemic Disease: A Systematic Review of the Impact of Dental Care on Overall Health. Journal of Ecohumanism. 2024;3(7):2843–52—52.

4.Chan WSH. The role of oral health in the prevention of systemic diseases. Universal Library of Medical and Health Sciences. 2024;1(1).

5.Nkambule NR, Madiba TK, Bhayat A. A review of the 2030 Human Resources for Health Strategy and Vision: Goals and their implications for dentistry. South African Dental Journal. 2022;77(6):330-5.

6.Foláyan MO, Ishola AG, Bhayat A, El Tantawi M, Ndembi N. Strengthening health systems to tackle oral diseases in Africa: Africa Centers for Disease Control and Prevention's role. Frontiers in Public Health. 2025;13:1539805.

7.Mazurkiewicz D, Pustułka M, Ambrozik-Haba J, Bienkiewicz M. Dietary habits and oral hygiene as determinants of the incidence and intensity of dental caries—a pilot study. Nutrients. 2023;15(22):4833.

8.Karobari MI, Siddharthan S, Adil AH, Khan MM, Venugopal A, Rokaya D, et al. Modifiable and non-modifiable risk factors affecting oral and periodontal health and quality of life in South Asia. The Open Dentistry Journal. 2022;16(1).

9.AlJasser R, Alsinaidi A, Bawazir N, AlSaleh L, AlOmair A, AlMthen H. Association of oral health awareness and practice of proper oral hygiene measures among Saudi population: a systematic review. BMC Oral Health. 2023;23(1):785.

10.Cui Z, Wang W, Si Y, Wang X, Feng X, Tai B, et al. Tooth brushing with flu-

oridated toothpaste and associated factors among Chinese adolescents: a nationwide cross-sectional study. BMC Oral Health. 2023;23(1):765.

11.Leggett H, Vinall-Collier K, Csikar J, Veronica Ann Douglas G. Barriers to prevention in oral health care for English NHS dental patients: a qualitative study of views from key stakeholders. BMC Oral Health. 2023;23(1):332.

12.Veiga N, Figueiredo R, Correia P, Lopes P, Couto P, Fernandes GVO, editors. Methods of primary clinical prevention of dental caries in the adult patient: An integrative review. Healthcare; 2023: MDPI.

13.O'Sullivan I, Lader D, Beavan-Seymour C, Chenery V, Fuller E, Sadler K. Foundation report: Adult dental health survey 2009 (technical report). London: The Information Centre for Health and Social Care. 2011.

14.Haresaku S, Umezaki Y, Egashira R, Naito T, Kubota K, Iino H, et al. Comparison of attitudes, awareness, and perceptions regarding oral healthcare between dental and nursing students before and after oral healthcare education. BMC Oral Health. 2021;21:1-11.

15.Ghasemi H, Murtomaa H, Vehkalahti MM, Torabzadeh H. Determinants of oral health behaviour among Iranian dentists. International Dental Journal. 2007;57(4):237-42.

16.Vodanović M, Barišić A, Šribar A, Šuman O. Are Dentists Hypocrites? Oral Self-care Habits and Self-reported Oral Health Status among Dentists and Non-dentists in Croatia. Acta stomatologica Croatica. 2024;58(1).

17.Habib S, Alotaibi A, Alabdulkader M, Alanazi S, Ahmedani MS. Self-reported oral hygiene practices and oral health status among dental professionals. South African Dental Journal. 2020;75(1):7-13.

18.Li M, Wu Z, Zhang R, Lei L, Ye S, Cheng R, et al. Comparison of oral health behaviour between dental and non-dental undergraduates in a university in south-western China——exploring the future priority for oral health education. BMC oral health. 2020;20:1-11.

19.Tantimahanon A, Sipiyaruk K, Tantipoj C. Determinants of dietary behaviors among dental professionals: insights across educational levels. BMC Oral Health. 2024;24(1):724.

20.Shmarina E, Ericson D, Götrick B, Franzén C. Dental professionals' perception of their role in the practice of oral health promotion: a qualitative interview study. BMC Oral Health. 2023;23(1):43.

21.Yusuf H, Tsakos G, Ntouva A, Murphy M, Porter J, Newton T, et al. Differences by age and sex in general dental practitioners' knowledge, attitudes and behaviours in delivering prevention. British Dental Journal. 2015;219(6):E7-E.

22.Nagarajappa R, Sanadhya S, Batra M, Daryani H, Ramesh G, Aapaliya P. Perceived barriers to the provision of preventive care among dentists of Udaipur, India. Journal of Clinical and Experimental Dentistry. 2015;7(1):e74.

23.Agrawal N, Mariam S, Gupta ND, Tewari RK, Gupta J, Garg AK. Identifying the Potential Determinants of Tobacco Counseling Implementation among Oral Health Professionals of India: A Cross-Sectional Survey. Pesquisa Brasileira em Odontopediatria e Clínica Integrada. 2023;23:e210171.

24.Alblowi JA, Mohamed H. Perception of tobacco counseling and cessation among dental practitioners. Journal of Smoking Cessation. 2021;2021:e15.

25.Chan H, Chan AK, Chu C, Tsang Y. Smoking cessation in dental setting: a narrative review on dental professionals' attitude, preparedness, practices and barriers. Frontiers in Oral Health. 2023;4:1266467.

26.Aloshaiby A, Gaber A, Arheiam A. The oral health care system in Libya: a case study. BMC Oral Health. 2024;24(1):888.

27.Arheiam A, Masoud I, Bernabé E. Perceived barriers to preventive dental care among Libyan dentists. Libyan Journal of Medicine. 2014;9(1).

Scientific Journal of University of Benghazi

SJUOB (2025) 38 (1) Medical Sciences: Elsherif, et al, 245 – 268
www.sjuob.uob.edu.ly

Effect of socio-demographic Factors and Dietary Behavior on psychological well-being, and mental distress among Adolescents in Benghazi

Sara Ahmed Elsherif[1]*, Salima Saad[1], Mouda Abdulrazak Abdulrahim Alsbehi[1], Hanaa Dou Salah[1], Ameera Salem Atiya[1], Fatima Salem Alnajjar[1]

1 Department of Nutrition , Faculty of Public Health, University of Benghazi, Benghazi, Libya.

Received: 27 / 02 / 2025 | Accepted: 05 / 09 / 2025 | Publishing: 29/06/2025

ABSTRACT

Despite the growing awareness of the importance of nutrition for overall health, the relationship between dietary habits and mental well-being in adolescents remains understudied. This gap in knowledge poses a significant concern, as adolescence is a critical period for developing healthy eating patterns and reducing the risk of mental health issues. This study is aimed to investigate the associations between adolescents' dietary behaviors, psychological well-being, and levels of mental distress in Benghazi, Libya. A cross-sectional descriptive design was employed, involving 391 students (189 (48.6%) boys, 202 (51.4%) girls) from 7 randomly selected secondary schools. Data collection utilized structured questionnaires assessing dietary patterns, psychological well-being, and mental distress indicators. The study revealed a significant association between dietary habits and adolescent mental health outcomes. Regular breakfast consumption, correlated positively with perceived health and sleep satisfaction (P-value 0.000). However, no significant associations were found between happiness and fruit, soft drinks, or fast-food consumption. Higher physical activity levels were consistently linked with better mental well-being (P-value 0.000), while gender differences were evident in stress and depression prevalence. Balanced eating—especially frequent breakfast—and regular physical activity are strongly linked to better psychological well-being and lower mental distress in Libyan adolescents. Nutrition interventions promoting these behaviors may help mitigate the risk of stress and depression during this critical developmental stage.

Keywords: Dietary behavior, psychological well-being, mental distress, Adolescent nutrition, Libya.

Corresponding Author: Sara Ahmed Elsherif, sara.elsherif@uob.edu.ly

 ISSN: Online 2790-1637, Print 2790-1629
National Library of Libya, Legal number: 154/2018

1.INTRODUCTION

Dietary behaviors and food choices play a crucial role in individual health, well-being, and socio-cultural identity, extending beyond mere nutrition to impact long-term health outcomes and disease prevention [1][2]. Adolescence is a critical developmental stage marked by increased autonomy in food choices, making it an opportune time to establish lifelong healthy eating habits. However, various challenges, including peer pressure, busy schedules, and the marketing of unhealthy foods, hinder adolescents from making nutritious choices [3][4][5].

Research consistently links dietary behaviors to both physical and psychological health outcomes. Unhealthy eating patterns, such as excessive consumption of processed foods and sugary drinks, contribute to obesity, chronic diseases, and mental health issues like depression and anxiety, whereas a well-balanced diet supports overall well-being [1][6][7][2]. In recent years, the focus has shifted towards the psychological effects of diet, recognizing that mental health is fundamental to overall health, particularly during adolescence [8][9].

Despite the global burden of adolescent mental health disorders [10,11], many remain undiagnosed. This study explores the link between diet, well-being, and distress among adolescents in Benghazi, Libya, hypothesizing that healthier diets improve mental health [6]. Understanding these associations is vital for public health [11].

Existing studies demonstrate strong associations between poor dietary behaviors and mental distress in adolescents. Research from multiple countries, including Korea, New Zealand, and Southeast Asia, indicates that healthier dietary habits are linked to lower levels of mental distress and improved well-being [1][7][2]. Studies in the UK and Norway have shown that higher fruit and vegetable intake correlates with better mental health, while research in China highlights links between specific dietary patterns and symptoms of anxiety and depression [12][13][14].

Multiple cross-sectional studies across different regions have demonstrated significant associations between unhealthy dietary patterns and mental health issues in adolescents. In Iran (CASPIAN-IV, 2011–2012), a study of 13,486 children and adolescents linked junk food consumption to

increased risks of psychiatric distress and violent behaviors, while a 2013.

Malaysian study of 1,565 adolescents found that skipping meals and frequent eating out were associated with higher stress and depression symptoms. Similarly, a 2010 Chinese study in Bengbu (5,003 adolescents, aged 11–16) revealed that dietary patterns—particularly traditional, snack, and animal food diets—were robustly associated with depression and anxiety symptoms in urban adolescents. Collectively, these findings underscore those poor dietary habits, including high junk food intake, irregular meals, and unbalanced diets, may significantly contribute to mental health disorders in youth across diverse populations. [15][16][17]

Another cross-sectional survey of 300 Saudi girls aged 15–19 in Taif City, 58.3% reported healthy lifestyles and 6.7% unhealthy ones. Despite this, over half (52.5%) showed depressive symptoms (14.8% moderate-severe; 6.9% severe), 42.1% had moderate to severe anxiety, and 18% experienced high stress. Poorer lifestyle scores correlated strongly with worse depression, anxiety, and stress ($p < 0.001$), highlighting that even modest declines in diet, exercise, sleep, or substance avoidance markedly increase psychological distress and underscoring the need for school-based wellness programs. [18]

This study explores the link between diet, well-being, and distress among adolescents in Benghazi, Libya, hypothesizing that healthier diets improve mental health [7]. Understanding these associations is vital for public health [11].

2.METHODOLOGY

2.1. Design:

A cross-sectional descriptive study was utilized to conduct this study.

2.2. Setting:

The study was carried out on Libyan Secondary school students in the city of Benghazi.

The information regarding government schools and student population was acquired from the Ministry of Education in Benghazi. The city accommodates 30 girls-only secondary schools, 21 boys-only secondary schools, and 8 mixed-gender secondary schools, collectively catering to 23,114 students, including 8,622 boys and 14,492 girls. According to Slovin's Formula Calculator a sample size of 391 (189 boys and 202 girls) Students was established for

the study.

A multistage stratified sampling procedure was employed for the selection of study participants. In the initial stage, 7 secondary schools were randomly sampled from the 59 secondary schools in Benghazi, representing a sample size of 12%. These schools were chosen from the 5 sectors (Benghazi square, Berka, El Selawi, Sidi Khalifa, West of Benghazi) within Benghazi and were segregated based on gender, comprising 3 secondary schools for boys, 3 for girls, and one mixed-gender secondary school. Subsequently, one class from each grade (first, second, and third year) of high school was randomly chosen, with students then selected randomly from these classes.

2.3. Study Period:

The data of the study was collected between January 2024 and February 2024.

2.4. Study Participants:

7 secondary school students in Benghazi were participating.

2.4.1. Inclusion Criteria:

The selection was made randomly from government schools for secondary students in the city of Benghazi.(government schools was more feasible since: first they are directly supervised by the Ministry of Education. Second - government school students generally have more homogeneous socio-economic backgrounds. Which helps reduce potential confounding factors related to socio-economic status. Furthermore, government schools accommodate the majority of adolescents in Benghazi, making the study sample more representative of the general adolescent's population).

2.4.2. Exclusion Criteria:

Private schools for secondary students were excluded.

2.5. Study Tools and Methods of Data Collection:

Data collection involved students completing a questionnaire that encompassed assessments of dietary behavior, psychological well-being, and mental distress. The questionnaire, derived from a study conducted in Korea [(1)] The Korean-based questionnaire was adapted for the Libyan cultural context through expert review by faculty members specializing in nutrition and Public .

Health at the University of Benghazi. Modifications were made to ensure the clarity and relevance of the questionnaire items. However, a formal pilot test was not

conducted before data collection. The questionnaire consisted of five parts.

_The first part, Demographic Information, this segment gathered various control variables such as gender, age, type of housing, parental educational attainment, perceived socioeconomic status, and school type (boys only, girls only, or mixed).

_The second part measured psychological well-being by employing three questions regarding self-rated health, happiness and sleep satisfaction.

_The third part measured perceived stress, and depression symptoms.

Self-rated health was measured using a query assessing regular health perception. The responses were categorized as above-average health or average/below-average health. Happiness levels were assessed by asking participants about their usual happiness level, which was then grouped into above-average happiness or average/below-average happiness. Sleep satisfaction was evaluated based on the adequacy of sleep to combat fatigue in the past week. Perceived stress levels were determined by inquiring about the typical stress degree experienced. Depression symptoms were examined by asking about the occurrence of significant sadness or despair affecting daily routines in the previous year.

_The fourth part was regarding dietary behaviors, breakfast regularity over the previous week was rated on an eight-day scale. Participants were also asked about the frequency of consuming various food groups, such as soft drinks, highly caffeinated drinks, sweetened drinks, fast foods, fruits, vegetable dishes, and milk, with response options ranging from none to multiple times per day.

_The fifth part regarding Anthropometric measurement.

The Body Mass Index (BMI) of students was calculated based on their self-reported weight and height to determine their weight status. Students were classified into different categories:[19]

1.Underweight: BMI less than 18.5

2.Normal Weight: BMI between 18.5 and 24.9

3.Overweight: BMI between 25 and 29.9

4.Obese: BMI ≥30

Participants' physical activity levels were categorized as low, medium, or high based on their weekly minutes of moderate or vigorous exercise according to World Health

Organization guidelines: [20]

_Low: less than 150 minutes of moderate OR 75 minutes of vigorous exercise per week. _Medium: 150-300 minutes of moderate OR 75-150 minutes of vigorous exercise per week. _High: More than 300 minutes of moderate OR 150 minutes of vigorous exercise per week.

2.6.Statistical analysis:

Statistical analysis of the data was fed to the computer and analyzed using SPSS software package version 18 (PASW Statistics18). Qualitative data were described using numbers, percent, and the statistically significant association between different variables by using chi-square test at significant level (P-value (probability value) <0.05).

2.7. Ethics:

Consent and approval were received from the Faculty of Public Health at the University of Benghazi, and the Libyan Ministry of Education approved the protocol. Subjects were provided with informed consent and reassured about the confidentiality of their information. The research also received approval from the administration of the schools involved. Before starting the project, written notification was given to the school administrations outlining the study's objectives to secure their maximum cooperation in conducting the study.

3.RESULT

A survey conducted in 2024 among 391 secondary school students provides valuable insights into their demographics, socioeconomic backgrounds, and health-related behaviors. The majority of students in the sample are 17 or 18 years old, and the genders are split almost evenly. Although they live in different types of residences, (93.6%) come from medium-income households and live in either traditional homes or apartments. The majority of parents are highly

educated; many have college or graduate degrees. 25.1% of teenagers are overweight or obese, 13.8% are underweight, and 61.1% maintain a normal weight in terms of health. The majority report low (44.8%) levels of physical activity, while just 12.5% engage in high-intensity exercise, which is concerning and may pose long-term health hazards. Table (1)

Table (1). Sample Characteristics of Secondary Students, 2024 (N = 391)

Variable name	Variable specification	No.	Percent (%)
Gender	Male	190	48.6
	Female	201	51.4
Age in year	15	36	9.2
	16	114	29.2
	17	159	40.7
	18	74	18.9
	19	8	2.0
Place of residence	Villa	75	19.2
	Classic newly built house	121	30.9
	Classic old house	57	14.6
	Flat	138	35.3
Economic status	Low	3	0.8
	Medium	366	93.6
	High	22	5.6
School address	The west of Benghazi	94	24.0
	Benghazi sequare	129	33.0
	Berka	60	15.3
	El_Selawi	54	13.8
	Sidi Khalifa	54	13.8
Mother's education level	Illiterate	6	1.5
	Basic education	30	7.7
	Secondary education	146	37.3
	University degree	169	43.2
	Postgraduate degree	40	10.2
Father's education level	Illiterate	4	1.0
	Basic education	31	7.9
	Secondary education	165	42.2
	University degree	156	39.9
	Postgraduate degree	35	9.0
BMI	<18.5	54	13.8
	18.5-24.99	239	61.1
	25-29.99	62	15.9
	30 and above	36	9.2
Physical activity	High	49	12.5
	Moderate	167	42.7
	Low	175	44.8

Even while the majority of adolescents have a favorable view of their health (62.4%) and are happy (48.5%), a significant part of them suffer from mental health and well-being, with 34.5% reporting symptoms of depression and 56% expressing dissatisfaction with their sleep. Overall, the data shows developments in the physical, mental, and nutritional health of adolescents that are both encouraging and alarming. Table (2).

Table (2). Prevalence of mental health among adolescents (Total= 391)

1. Well-being outcomes	No.	Percent (%)
Perceived health		
Very healthy Healthy Fair Poor Very poor	84 160 129 13 5	21.5 40.9 33.0 3.3 1.3
Perceived happiness		
Very happy Happy Fair Unhappy Very unhappy	60 130 160 29 12	15.3 33.2 40.9 7.4 3.1
Sleep satisfaction (Fatigue recovery from sleep)		
Quite sufficient Sufficient Neutral Not Sufficient	61 111 118 101	15.6 28.4 30.2 25.8
2. Mental distress outcomes		
Perceived stress		
Very much Somewhat Average Not so much	70 103 105 113	17.9 26.3 26.9 28.9
Signs and symptoms of depression during the last year		
Yes No	135 256	34.5 65.5
Total	391	100.0

Tables (3) demonstrate the association between patient characteristics and well-being outcome health. Physical activity and gender significantly impact perceived health, while happiness is influenced by paternal education, and sleep satisfaction is influenced by age and economic status. Teenagers who were male and engaged in physical activity reported higher health. while older, less well-off teenagers reported higher levels of sleep satisfaction; No significant correlations with other socio-demographic characteristics.

Significant correlations between gender, physical activity, and teenage mental health are seen in Tables 4 Perceived stress and depression were higher among females. Stress and depression were significantly correlated with low levels of physical activity. BMI did not correlate with depression (p=0.352), although it did correlate with stress (p=0.003). Other factors, including place of residence, parental education, and economic status, did not show any significant association. These findings demonstrate the impact of gender and physical activity on adolescents' mental health.

The association between dietary practices and teenagers' perceptions of their health, happiness, and sleep satisfaction are examined in Tables 5. Frequent breakfast eating was not substantially associated with happiness, but it was significantly associated with improved sleep satisfaction and felt health. Increased consumption of highly caffeinated beverages was linked to lower levels of sleep pleasure (p=0.021) and exhibited a marginally positive correlation with dissatisfaction

(p=0.058). There was a non-significant tendency toward decreased sleep satisfaction with fast food consumption (p=0.067). These results highlight the benefits of eating a balanced diet, especially one that includes breakfast, veggies, and milk, in promoting teenagers, while highlighting the potential negative effects of high caffeine intake on sleep and happiness. Note that: Good" = above-average health, "Bad" = average/below-average health)

Tables (6) examine the association between dietary behaviors and perceived stress and depression among adolescents. There is no obvious correlation between eating habits and perceived stress because all of the p-values are more than 0.05. However, Table demonstrates that eating breakfast

 ISSN: Online 2790-1637, Print 2790-1629
National Library of Libya, Legal number: 154/2018

(p=0.000) and drinking a lot of caffeinated beverages (p=0.007) are significantly linked to depression. Regular consumption of highly caffeinated beverages and adolescents who eat breakfast infrequently or never are also associated with higher probabilities of depression. Foods including milk, fruit, vegetables, soft drinks, sweetened beverages, and fast food are also not substantially associated with sadness.

Table (3): Association between socio-demographic factors and wellbeing outcomes

Factors		Wellbeing outcomes No (%)						*Significance=P-value < 0.05		
		1.Perceived health			2.Perceived happiness			3.sleep satisfaction		
		Good	Bad	P-value	Happy	Un Happy	P-value	Sufficient	In Sufficient	P-value
Gender:	Male	189(50.7)	1(5.6)	P=0.000	168(48.0)	22(53.7)	P=0.493	147(50.7)	43(42.6)	P=0.160
	Female	184(49.3)	17(94.4)		182(52.0)	19(46.3)		143(49.3)	58(57.4)	
Age	14-16	143(38.3)	7(38.9)	P=0.693	140(40)	10(8.9)	P=0.052	123(42.2)	27(26.7)	P=0.005
	17-19	230(61.7)	11(61.1)		210(60.0)	31(75.6)		167(57.6)	74(73.3)	
Place of residence:										
Villa		74(19.8)	1(5.6)	P=0.053	69(19.7)	1(5.6)	P=0.723	52(17.9)	23(22.8)	P=0.306
Classic newly build house		114(30.6)	7(38.9)		106(30.3)	7(38.9)		97(33.4)	24(23.8)	
Classic old house		51(13.7)	6(33.3)		50(14.3)	6(33.3)		42(5.14)	15(14.9)	
Flat		134(35.9)	4(22.2)		125(35.7)	4(22.2)		99(34.1)	39(38.6)	
Economic status:										
Low-medium		352(94.4)	17(94.4)	P=0.989	330(94.3)	39(95.1)	P=0.826	278(95.9)	91(90.1)	P=0.030
Haigh		21(5.6)	1(5.6)		20(5.7)	2(4.9)		12(4.1)	10(9.9)	
Mother educational level:										
Illiterate		6(1.6)	0(0.0)	P=0,582	4(1.1)	2(4.9)	P=0.205	5(1.7)	1(1.0)	P=0.826
Basic education		30(8.0)	0(0.0)		26(7.4)	4(9.8)		21(7.2)	9(8.9)	
Secondary		139(37.3)	7(38.9)		129(36.9)	17(41.5)		111(38.3)	35(43.7)	
University		198(53.1)	11(61.1)		191(54.6)	18(43.9)		153(52.8)	56(55.4)	
Father educational level:										
Illiterate		3(0.8)	1(5.6)	P=0.162	1(0.3)	3(7.3)	P=0.000	0(2.7)	2(2.0)	P=0.537
Basic education		29(7.8)	2(11.1)		27(7.7)	4(9.8)		25(8.6)	6(5.9)	
Secondary		160(42.9)	5(27.8)		148(42.3)	17(41.5)		124(42.8)	41(40.6)	
University		181(48.5)	10(55.6)		174(49.7)	17(41.5)		139(47.9)	52(51.5)	
BMI:										
Underweight		53(14.2)	1(5.6)	P=0.236	50(14.3)	4(9.8)	P=0.735	39(13.4)	15(14.9)	P=0.702
Normal weight		224(60,1)	15(83.3)		213(60.9)	26(63.4)		180(62.1)	59(58.4)	
Overweight		61(16.4)	1(5.6)		54(15.4)	8(19.5)		47(16.2)	15(14.9)	
Obese		35(9.4)	1(5.6)		33(9.4)	3(7.3)		24(8.3)	12(11.9)	
Physical activity: High		49(13.1)	0(0.00)	P=0.012	47(13.4)	2(4.9)	P=0.165	39(13.4)	10(9.9)	P=0.454
Moderate		163(43.7)	4(22.2)		151(43.1)	16(39.0)		126(43.4)	41(40.6)	
Low		163(43.2)	14(77.8)		152(43.4)	23(56.1)		125(43.1)	50(49.5)	

 ISSN: Online 2790-1637, Print 2790-1629
National Library of Libya, Legal number: 154/2018

Table (4): Association between socio-demographic factors and Mental distress

Factors		Wellbeing outcomes No (%)			*Significance=P-value < 0.05		
		1.Perceived health			2.Depression		
		Much	Less	P-value	Yes	No	P-value
Gender:	Male	113(40.6)	77(68.1)	P=0.000	37(50.0)	140(54.7)	P=0.001
	Female	165(59.4)	36(31.9)		85(63.0)	116(45.3)	
Age	14-16	106(38.1)	44(38.9)	P=0.882	42(31.1)	108(42.2)	P=0,032
	17-19	172(61.9)	69(61.1)		93(68.9)	148(57.8)	
Place of residence:							
Villa		61(21.9)	14(12.4)	P=0.062	27(20.0)	48(18.8)	P=0.853
Classic newly build		85(30.6)	36(31.9)		39(28.9)	82(32.0)	
house		43(15.5)	14(12.4)		22(16.3)	35(13.7)	
Classic old house		89(32.0)	49(43.4)		47(34.8)	91(35.5)	
Flat		264(95.0)	105(92.9)		128(94.8)	241(94.1)	
Economic status:							
Low-medium		14(5.0)	8(7.1)	P=0.427	7(5.2)	15(5.9)	P=0.783
Haigh		6(2.2)	0(0.0)		2(1.5)	4(1.2)	
Mother educational level:							
Illiterate		24(8.6)	6(5.3)	P=0.152	10(7.4)	20(7.8)	P=0.675
Basic education		107(38.5)	39(34.5)		56(41.5)	90(35.2)	
Secondary		141(50.7)	68(60.2)		67(49.6)	142(55.5)	
University		3(1.1)	1(0.9)		2(1.5)	2(0.8)	
Father educational level:							
Illiterate		24(8.6)	7(6.2)	P=0.596	13(9.6)	18(7.0)	P=0.5603
Basic education		121(43.5)	44(38.9)		59(43.7)	106(41.4)	
Secondary		130(46.8)	61(54.0)		61(45.2)	130(50.8)	
University		28(10.1)	26(23.0)		16(11.9)	30(14.8)	
BMI:							
Underweight		173(62.1)	66(58.4)	P=0.003	78(57.8)	161(62.9)	P=0.352
Normal weight		51(18.3)	11(9.7)		26(19.3)	36(14.1)	
Overweight		26(9.4)	10(8.8)		15(11.1)	21(8.2)	
Obese		25(9.0)	24(21.2)		11(8.1)	38(14.8)	
Physical activity:							
High Moderate		110(39.6)	57(50.4)	P=0.000	42(31.1)	125(48.8)	P=0.000
Low		143(51.4)	32(28.3)		82(60.7)	93(36.3)	

Table (5): Association between dietary behavior and wellbeing outcomes of adolescents

Food groups consumed over the past 7 days	Wellbeing outcomes No (%)						*Significance=P-value < 0.05		
	1.Perceived health			2.Perceived happiness			3.sleep satisfaction		
	Good	Bad	P-value	Happy	Un Happy	P-value	Sufficient	In Sufficient	P-value
Breakfast									
Almost every day	212(56.8)	2(11.1)	P=0.00	197(56.3)108	17(41.5)	P=0.174	167(60.7)	38 (37.6)	P=0.000
Sometimes	115(30.8)	11(61.1)		(30.9)45	18(43.9)		87(30.0)	39(38.6)	
Rarely or never	46(12.3)	5(27.8)		(12.9)208	6(14.6)		27(9.3)	24(23.8)	
Soft Drink									
Never or 1-2 time per week	217(58.2)	13(72.2)	P=0.479	(59.4)	22(53.7)	P=0.479	171(59.0)	59(58.4)	P=0.801
6-3 times per day	74(19.8)	2(11.1)		65(18.6)77	11(26.8)		58(20)	18(17.8)	
At least once per week	82(22.0)	3(16.7)		(22.0)	8(19.5)		61(21.0)	24(23.8)	
Highly caffeinated Drink									
Never or 1-2 times per week	208(55.8)	12(66.7)	P=0.627	204(58.3)	16(39.0)	P=0.058	175(60.3)	45(44.6)	P=0.021
6-3 times per week	38(10.2)	1(5.6)		34(9.7)	5(12.2)		27(9.3)	12(11.9)	
At least once per day	127(34)	5(27.8)		112(32)	20(48.8)		188(30.3)	44(43.6)	
Sweetened Drink									
Never or 1-2 times per week	134(35.9)	7(38.9)	P=0.697	124(35.9)	17(41.5)	P=0.737	108(37.2.6)	33(32.7)	P=0.102
6-3 times per week	95(25.5)	3(16.7)		89(25.4)	9(22.0)		78(26.9)	20(19.8)	
At least once per day	144(38.6)	8(44.4)		137(39.1)	15(36.6)		104(35.9)	48(47.5)	
Fast Food:									
Never or 1-2 times per week	237(63.5)	13(72.2)	P=0.496	232(63.7)	27(65.9)	P=0.533	191(65.9)	59(58.4)	P=0.067
6-3 times per week	59(15.8)	1(5.6)		59(16)	4(9.8)		47(16.2)	13(12.9)	
At least once per day	77(20.6)	4(22.2)		71(20.3)	10(24.4)		52(17.9)	29(28.7)	
Fruit									
Never or 1-2 times per week	115(30.8)	9(50)	P=0.233	106(30.3)	18(43.90)	P=0.533	91(31.4)	33(32.7)	P=0.710
6-3 times per week	117(31.4)	4(22.2)		101(31.4)	11(26.8)		93(32.1)	28(27.7)	
At least once per day	141(37.8)	5(27.8)		134(38.3)	12(29.3)		106(36.6)	40(39.6)	
Vegetables									
Never or 1-2 times per week	141(37.8)	14(77.8)	P=0.003	133(38)	22(53.7)	P=0.150	111(38.3)	44(43.6)	P=0.642
6-3 times per week	78(20.9)	2(11.1)		74(21.1)	6(14.6)		61(21.0)	19(18.8)	
At least once per day	154(41.3)	2(11.1)		143(40.9)	13(31.7)		118(40.7)	38(37.6)	
Milk consumption									
Never or 1-2 times per week	128(34.3)	12(66.7)	P=0.001	119(34.0)	21(51.2)	P=0.079	97(33.4)	43(42.6)	P=0.257
6-3 times per week	55(14.7)	5(27.8)		54(15.4)	6(14.6)		46(15.9)	14(13.9)	
At least once per day	190(50.9)	1(5.6)		177(50.6)	14(34.1)		147(50.7)	44(34.6)	

Table (6): Association between dietary behavior and Mental distress of adolescents

Food groups consumed over the past 7 days	Mental Distress No (%)					
	1.Perceived stress			2.Depression		
	Much	Less	P-value	Much	Less	P-value
Breakfast						
Almost every day	145(52.2)	69(61.1)		56(41.1)	158(61.7)	
Sometimes	95(34.2)	31(27.4)	P=0.257	54(40)	72(28.1)	P=0.000
Rarely or never	38(13.7)	13(11.5)		25(18.5)	26(10.2)	
Soft Drink						
Never or 1-2 time per week	164(59.0)	66(58.4)		77(57.0)	153(59.8)	
6-3 times per day	51(18.3)	25(22.1)	P=0.615	24(17.8)	52(20.3)	P=0.465
At least once per week	63(22.7)	22(19.5)		34(25.2)	51(19.9)	
Highly caffeinated Drink						
Never or 1-2 times per week	161(57.9)	95(52.2)		62(45.9)	158(61.7)	
6-3 times per week	27(9.7)	12(10.6)	P=0.548	14(10.4)	25(9.8)	P=0.007
At least once per day	90(32.4)	42(37.2)		59(43.7)	73(28.5)	
Sweetened Drink						
Never or 1-2 times per week	98(35.3)	43(38.00)		51(37.8)	90(35.2)	
6-3 times per week	76(27.3)	22(19.5)	P=0.260	30(22.2)	68(26.6)	P=0.638
At least once per day	104(37.4)	48(42.5)		54(40.0)	98(38.3)	
Fast Food:						
Never or 1-2 times per week	173(36.3)	77(33.5)		50(37.0)	168(56.6)	
6-3 times per week	48(16.2)	12(31.3)	P=0.250	37(27.4)	39(15.2)	P=0.542
At least once per day	57(47.5)	24(35.3)		48(35.6)	49(19.1)	
Fruit						
Never or 1-2 times per week	93(33.5)	31(27.4)		93(33.5)	74(28.9)	
6-3 times per week	87(31.3)	34(30.1)	P=0.354	87(31.3)	84(32.8)	P=0.240
At least once per day	98(35.3)	48(42.5)		98(35.3)	98(38.3)	
Vegetables						
Never or 1-2 times per week	117(42.1)	38(33.6)		59(43.7)	96(37.5)	
6-3 times per week	57(20.5)	23(20.4)	P=0.230	27(20.0)	53(20.7)	P=0.461
At least once per day	104(37.4)	52(46.0)		49(36.3)	107(41.8)	
Milk consumption						
Never or 1-2 times per week	101(36.3)	34(42.6)		57(42.2)	83(32.4)	
6-3 times per week	45(16.2)	13.3(13.9)	P=0.642	19(14.1)	41(16.0)	P=0.157
At least once per day	132(47.5)	52.2(34.6)		95(43.7)	132(51.6)	

4.DISCUSSION

This Benghazi study examined the intricate association between eating habits and psychological health. The findings show a strong correlation between eating patterns and mental health outcomes, highlighting the significance of nutrition for teenagers' general well-being.

The study found that age had little impact on self-reported health, consistent with Currie et al. (2012) (21). Men reported better health than women, in line with Wade & Pevalin (2005) (22) and Hong & Peltzer (2017) (1), but differing from Sweeting & West (2003) (23). No significant association was found between health and economic status, supporting Chen et al. (2002) (24). Parents' education showed no correlation with perceived health, agreeing with Basu & Stephenson (2005) (25), but conflicting with Schwimmer (2003) (26). There was no link between BMI and perceived health, but a strong correlation between physical activity and perceived health, supporting the Korean study (1). These emphasize physical activity as important to perceived health.

The findings of this study suggest that gender and age were not significantly associated with perceived happiness, aligning with Weech-Maldonado et al. (2017) (27), but in contrast to a Korean study (1) that found a significant correlation. Furthermore, this study revealed no correlation between residential settings and well-being, despite Cicognani et al. (2008) (28) confirming this effect. In contrast to a Malaysian study that found a positive correlation between happiness and both parents' educational attainment, this study found a favorable correlation between teenage happiness and the father's education while the mother's education had no discernible impact (29). There was no correlation between happiness and BMI, which runs counter to research from Italy that shows happiness decreases as BMI rises (30). In a similar vein, no link between happiness and physical activity was found, although Zhang et al. (2019) (31), van Woudenberg et al. (2020) (32), and An et al. (2020) (33) found a positive correlation.

In contrast to studies from India, which showed that higher economic status was related to worse sleep, people of low to medium economic status reported better sleep (34). Economic status was also linked to sleep satisfaction. There was no correlation

between gender and sleep satisfaction, which is consistent with Nepalese studies (35). Furthermore, contrary to a Korean study that found a positive association, our study found no significant association between physical activity and sleep satisfaction (36).

The study found significant association between gender and stress; women reported higher levels of stress, which differs from Karnataka (37).

In contrast to research from Bangladesh (38) and Karnataka (39), no correlation was detected between stress and parents' age or level of education (40) or both. In contrast to findings in Bangladesh, BMI was substantially correlated with stress, with adolescents of normal weight reporting higher levels of stress (38). There was a significant association between stress and physical activity, with lower levels of exercise leading to higher stress levels, consistent with studies from Bangladesh (39).

Depression was also significantly linked with age and gender, with older adolescents and females reporting higher levels, which is consistent with studies from Bangladesh (41, 42) and China (43). Depression did not significantly correlate with parental education (41, 43), economic position (44), or area of residence (41, 45). Furthermore, BMI did not substantially correlate with depression, which is in contrast to research from Bangladesh (42) and Australia (46). Low levels of physical exercise, however (47), and Korea (1). No direct link was found between soft drink consumption and perceived health, similar to Norwegian research (48), though Korean studies indicated indirect effects (1). The study also supported research from Korea (1) and Tuscan (49) on the positive impact of vegetable consumption and aligned with Korean findings on milk consumption (1).

In contrast to Korean studies that connected fast food intake to obesity and ill health, no meaningful correlation between the two variables was discovered (1). These variations demonstrate how dietary customs, health beliefs, and research methods can differ among groups and impact results.

Remarkably, there was no significant correlation between breakfast eating and happiness levels. This result is in contrast to research that found a similar association between regular breakfast consumption and happiness in other nations, including Korea (50), Japan (47), the United States, Japan, and

Switzerland [51, 52].

Furthermore, there was no clear correlation between the use of soft drinks and caffeine and happiness, which is consistent with Norwegian study (48) but contradicts U.S. research (53), which associated high consumption with negative emotional states. Similarly, contrary to the findings of Huth et al., there was no correlation between happiness and milk consumption (54). Although eating more vegetables was associated with better feelings of happiness, this correlation was not statistically significant, which contrasts with research from Switzerland (51) and New

Zealand (55). The study confirmed a positive association between breakfast consumption and sleep satisfaction, which is in line with research done in the United States (56,53). No significant correlations were found between the consumption of fruit, vegetables, and fast food and sleep satisfaction, which is in contrast to studies by St-Onge et al. (57), which found a link between healthy eating habits and better sleep.

The study found no significant correlation between breakfast eating and stress or unhappiness, consistent with Spanish research (50).

There was no discernible link between stress and caffeine-containing beverages, in contrast to a Korean study (58).

Similarly, contrary to Australian findings, fast food and sugary beverages were not linked to stress (54). In line with Dutch (49) and Canadian (51) studies, the study also showed no connection between stress and consuming fruits, vegetables, or milk.

These differences in conclusions between the current study and prior research may be due to several contextual and methodological factors. Differences in sample characteristics—such as age group, cultural background, or socioeconomic distribution—could influence how individuals perceive and report their health and happiness. and even self-reporting tendencies can greatly influence outcomes related to health and well-being.

importantly, it must be noted that the cross-sectional nature of the study limits the ability to infer causal relationships. For instance, it remains unclear whether unhealthy eating patterns contribute to psychological distress or if existing mental health issues lead to poor dietary choices.

5.CONCLUSION AND RECOMMENDATIONS

This study emphasizes the importance of socio-demographic characteristics, food habits, and physical exercise on adolescent mental health. Gender disparities were noticeable, with girls reporting higher levels of stress and despair. Regular breakfast eating, vegetable intake, and physical activity were connected to improved health and reduced stress, whereas fast food and soft drinks had no meaningful impact.

To increase adolescent well-being, interventions should focus on a balanced diet (e.g, promoting regular breakfast programs in schools and reducing access to highly caffeinated drinks for adolescents), physical activity, and mental health support through school programs. Longitudinal studies are required to evaluate intervention efficacy and inform future health measures. Implementing these practices can lead to a healthier and more resilient adolescent population.

While this study sheds light on the association between demographics, food habits, and mental well-being, it does have some drawbacks. The cross-sectional study doesn't determine cause-and-effect linkages. In addition, self-reported data (e.g., self-report bias for dietary habits and BMI) may be impacted by memory biases or the proclivity to provide socially desired results. And the lack of diversity in the sample (only government schools). Lastly, differences in gender comparisons may be affected by an imbalance in sample size.

6. ACKNOWLEDGMENT

We sincerely thank the secondary school administrations and staff for their assistance in conducting this research. thanks also to the Ministry of Education for providing vital information. Most importantly, we thank the students for their contributions, which were critical to the success of this project.

7.REFERENCES

1. Hong SA, Peltzer K. Dietary behaviour, psychological well-being and mental distress among adolescents in Korea. Child and adolescent psychiatry and mental health. 2017 Dec;11(1):1-2. DOI 10.1186/s13034-017-0194-z

2.Puloka I, Utter J, Denny S, Fleming T. Dietary behaviours and the mental well-being of New Zealand adolescents. Journal of paediatrics and child health. 2017 Jul;53(7):657-

62.DOI: https://doi.org/10.1111/jpc.13524

3.Lerner RM, Boyd MJ, Du D. Adolescent development. The corsini encyclopedia of psychology. 2010 Jan 30:1-2. DOI https://doi.org/10.1002/9780470479216.corpsy0019

4.Lassi Z, Moin A, Bhutta Z. Nutrition in middle childhood and adolescence. Disease Control Priorities, (Volume 8): Child and Adolescent Health and Development. 2017 Nov 20:1896. DOI: 10.1596/978-1-4648-0423-6_ch11.

5.Heslin AM, McNulty B. Adolescent nutrition and health: Characteristics, risk factors and opportunities of an overlooked life stage. Proceedings of the Nutrition Society. 2023 May;82(2):142-56. doi: 10.1017/S0029665123002689.

6.Granero R. Role of Nutrition and Diet on Healthy Mental State. Nutrients. 2022 Feb 10;14(4):750.DOI: https://doi.org/10.3390/nu14040750.

7.Peltzer K, Pengpid S. Dietary behaviors, psychological well-being, and mental distress among university students in ASEAN. Iranian Journal of Psychiatry and Behavioral Sciences. 2017 Jun 30;11(2).DOI: https://doi.org/10.5812/ijpbs.10118

8.Firth J, Gangwisch JE, Borsini A, Wootton RE, Mayer EA. Food and mood: how do diet and nutrition affect mental wellbeing?. Bmj. 2020 Jun 29;369. doi: https://doi.org/10.1136/bmj.m2382

9.Muscaritoli M. The impact of nutrients on mental health and well-being: insights from the literature. Frontiers in nutrition. 2021:97.DOI:https://doi.org/10.3389/fnut.2021.656290

10. World Health Organization. Mental health of adolescents. https://www.who.int/news-room/fact-sheets/detail/adolescent-mental-health (2023).

11. Shawon MS, Rouf RR, Jahan E, Hossain FB, Mahmood S, Gupta RD, Islam MI, Al Kibria GM, Islam S. The burden of psychological distress and unhealthy dietary behaviours among 222,401 school-going adolescents from 61 countries. Scientific Reports. 2023 Dec 11;13(1):21894. DOI: https://doi.org/10.1038/s41598-023-49500-8

12.Blanchflower DG, Oswald AJ, Stewart-Brown S. Is psychological well-being linked to the consumption of fruit and vegetables?. Social Indicators Research. 2013 Dec;114:785-801. doi:10.3386/w18469

13. Hayhoe R, Rechel B, Clark AB, Gummerson C, Smith SL, Welch AA. Cross-sec-

tional associations of schoolchildren's fruit and vegetable consumption, and meal choices, with their mental well-being: a cross-sectional study. BMJ Nutrition, Prevention & Health. 2021;4(2):447. doi: 10.1136/bmjnph-2020-000205

14. Weng TT, Hao JH, Qian QW, Cao H, Fu JL, Sun Y, Huang L, Tao FB. Is there any relationship between dietary patterns and depression and anxiety in Chinese adolescents?. Public health nutrition. 2012 Apr;15(4):673-82. DOI: https://doi.org/10.1017/S1368980011003077

15.Zahedi H, Kelishadi R, Heshmat R, Motlagh ME, Ranjbar SH, Ardalan G, Payab M, Chinian M, Asayesh H, Larijani B, Qorbani M. Association between junk food consumption and mental health in a national sample of Iranian children and adolescents: the CASPIAN-IV study. Nutrition. 2014 Nov 1;30(11-12):1391-7. DOI: 10.1016/j.nut.2014.04.014

16. Tajik E, Awang H, Nur'Asyura AS, Chin YS, Shah AB, Koh CH, Hariz CG. Unhealthy diet practice and symptoms of stress and depression among adolescents in Pasir Gudang, Malaysia. Obesity research & clinical practice. 2016 Mar 1;10(2):114-23. DOI: 10.1016/j.orcp.2015.06.001

17.Weng TT, Hao JH, Qian QW, Cao H, Fu JL, Sun Y, Huang L, Tao FB. Is there any relationship between dietary patterns and depression and anxiety in Chinese adolescents?. Public health nutrition. 2012 Apr;15(4):673-82. DOI: 10.1017/S1368980011003077

18.Baz SS, Malibarey WM, Alsalmi HA, Alzaydi MD, Alqahtani AM, Alghamdi RY, Baz Sr SS, Malibarey II WM, Alsalmi Sr H, Alghamdi R. The Impact of a Healthy Lifestyle on Psychological Well-Being Among Saudi Adolescent Girls Attending Secondary Schools in Taif City, Saudi Arabia. Cureus. 2023 Dec 8;15(12). DOI: 10.7759/cureus.50189

19.Zierle-Ghosh A, Jan A. Physiology, body mass index.2018

20.WHO O. WHO guidelines on physical activity and sedentary behaviour. Geneva: World Health Organization. 2020 Apr 21:1-582.

21.Currie C, Zanotti C, Morgan A, Currie D, De Looze M, Roberts C, Samdal O, Smith OR, Barnekow V. Social determinants of health and well-being among young people. Health Behaviour in School-aged Children (HBSC) study: international report from the. 2009;2010:271.

22.Wade T, Pevalin D. Adolescent delinquency and health. Canadian Journal of Criminology and Criminal Justice. 2005 Oct 1;47(4):619-54. DOI: https://doi.org/10.3138/cjccj.47.4.61

23.Sweeting H, West P. Sex differences in health at ages 11, 13 and 15. Social science & medicine. 2003 Jan 1;56(1):31-9. DOI: https://doi.org/10.1016/S0277-9536(02)00010-2

24.Chen E, Matthews KA, Boyce WT. Socioeconomic differences in children's health: how and why do these relationships change with age?. Psychological bulletin. 2002 Mar;128(2):295. DOI: https://doi.org/10.1037/0033-2909.128.2.295

25.Basu AM, Stephenson R. Low levels of maternal education and the proximate determinants of childhood mortality: a little learning is not a dangerous thing. Social science & medicine. 2005 May 1;60(9):2011-23.DOI:https://doi.org/10.1016/j.socscimed.2004.08.057

26.Schwimmer JB, Burwinkle TM, Varni JW. Health-related quality of life of severely obese children and adolescents. Jama. 2003 Apr 9;289(14):1813-9. doi:10.1001/jama.289.14.1813

27.Weech-Maldonado R, Miller MJ, Lord JC. The relationships among socio-demographics, perceived health, and happiness. Applied research in quality of life. 2017 Jun;12:289-302. DOI: https://doi.org/10.1007/s11482-017-9517-8

28.Cicognani E, Albanesi C, Zani B. The impact of residential context on adolescents' subjective well being. Journal of Community & Applied Social Psychology. 2008 Nov;18(6):558-75. DOI: https://doi.org/10.1002/casp.972

29.Mohd Hashim IH, Mohd Zaharim N. Happiness among Malaysian adolescents: The role of sociodemographic factors and everyday events. Sage Open. 2020 Jul;10(3): DOI: https://doi.org/10.1177/2158244020940695

30.Di Giacomo D, Ranieri J, Fiasca F, Mattei A. Lifestyle, body mass index and wellness in youth: Strengthens and weakness in Italian youth. Health psychology research. 2019 Mar 3;7(1).DOI: 10.4081/hpr.2019.8035

31.Zhang Z, Chen W. A systematic review of the relationship between physical activity and happiness. Journal of happiness studies. 2019 Apr;20(4):1305-22. DOI: https://doi.org/10.1007/s10902-018-9976-0

32.van Woudenberg TJ, Bevelander KE, Burk WJ, Buijzen M. The reciprocal effects

of physical activity and happiness in adolescents. International Journal of Behavioral nutrition and physical activity. 2020 Dec;17:1-0. DOI: https://doi.org/10.1186/s12966-020-01058-8

33.An HY, Chen W, Wang CW, Yang HF, Huang WT, Fan SY. The relationships between physical activity, life satisfaction, and happiness among young, middle-aged, and older adults. International journal of environmental research and public health. 2020 Jul;17(13):4817. DOI: https://doi.org/10.3390/ijerph19148629

34.Sarveswaran G, Arikrishnan K, Krishnamoorthy Y, Sakthivel M, Majella MG, Lakshminarayanan S. Prevalence and determinants of poor quality of sleep among adolescents in rural Puducherry, South India. International journal of adolescent medicine and health. 2021 Apr 28;33(2):20180101. DOI: https://doi.org/10.1515/ijamh-2018-0101

35.Gautam P, Dahal M, Baral K, Acharya R, Khanal S, Kasaju A, Sangroula RK, Gautam KR, Pathak K, Neupane A. Sleep Quality and Its Correlates among Adolescents of Western Nepal: A Population-Based Study. Sleep disorders. 2021;2021(1):5590715.DOI: https://doi.org/10.1155/2021/5590715

36.Park S. Associations of physical activity with sleep satisfaction, perceived stress, and problematic Internet use in Korean adolescents. BMC public health. 2014 Dec;14:1-6. DOI: https://doi.org/10.1186/1471-2458-14-1143

37.Gajula M, Bant D, Bathija GV. Perceived stress among adolescent school students in Hubli: A cross-sectional study. National Journal of Community Medicine. 2021 Jul 31;12(07):169-74. DOI: https://doi.org/10.5455/njcm.20210625054326

38.Anjum A, Hossain S, Hasan MT, Christopher E, Uddin ME, Sikder MT. Stress symptoms and associated factors among adolescents in Dhaka, Bangladesh: findings from a crosssectional study. BMC psychiatry. 2022 Dec 19;22(1):807. DOI: https://doi.org/10.1186/s12888-022-04340-0

39.Verma A, Rao AP, Andrews T, Binu VS. Assessment of level of stress and depression among adolescents in Udupi taluk, Karnataka. Indian Journal of Community Health. 2019 Apr 20;31(1):132-6. DOI: https://doi.org/10.47203/IJCH.2019.v31i01.022

40.Watode BK, Kishore J, Kohli C. Prevalence of stress among school adolescents in Delhi. Indian J Youth Adolesc Health.

2015;2(4):5-9.

41.Mridha MK, Hossain MM, Khan MS, Hanif AA, Hasan M, Mitra D, Hossaine M, Ullah MA, Sarker SK, Rahman SM, Bulbul MM. Prevalence and associated factors of depression among adolescent boys and girls in Bangladesh: findings from a nationwide survey. BMJ open. 2021 Jan 1;11(1):e038954. doi: 10.1136/bmjopen-2020-038954

42.Khan A, Ahmed R, Burton NW. Prevalence and correlates of depressive symptoms in secondary school children in Dhaka city, Bangladesh. Ethnicity & health. 2020 Jan 2;25(1):34-46.DOI: https://doi.org/10.1080/13557858.2017.1398313

43.Fang YN, Cao Q. Effect of Mother's Educational Level on Depression in Children and Adolescents. In2022 5th International Conference on Humanities Education and Social Sciences (ICHESS 2022) 2022 Dec 30 (pp. 709-717). Atlantis Press. DOI: 10.2991/978-2-494069-89-3_84

44.Niu Y, Guo X, Cai H, Luo L. The relation between family socioeconomic status and depressive symptoms among children and adolescents in mainland China: a meta-analysis. Frontiers in Public Health. 2024 Jan 9;11: 1292411.DOI: https://doi.org/10.3389/fpubh.2023.1292411

45.Anjum A, Hossain S, Sikder T, Uddin ME, Rahim DA. Investigating the prevalence of and factors associated with depressive symptoms among urban and semi-urban school adolescents in Bangladesh: a pilot study. International health. 2022 Jul;14(4):354-62. DOI: https://doi.org/10.1093/inthealth/ihz092

46.Al Mamun A, Cramb S, McDermott BM, O'callaghan M, Najman JM, Williams GM. Adolescents' perceived weight associated with depression in young adulthood: a longitudinal study. Obesity. 2007 Dec;15(12):3097-105. DOI: https://doi.org/10.1038/oby.2007.369

47. Rampersaud GC, Pereira MA, Girard BL, Adams J, Metzl JD. Breakfast habits, nutritional status, body weight, and academic performance in children and adolescents. Journal of the american dietetic association. 2005 May 1;105(5):743-60. DOI: https://doi.org/10.1016/j.jada.2005.02.007

48.Bere E, Veierød MB, Bjelland M, Klepp KI. Outcome and process evaluation of a Norwegian school-randomized fruit and vegetable intervention: Fruits and Vegetables Make the Marks (FVMM). Health Educ Res. 2008;23(6):997-1007.DOI: https://doi.

org/10.1093/her/cyh062

49.Lazzeri G, Pammolli A, Azzolini E, Simi R, Meoni V, de Wet DR, Giacchi MV. Association between fruits and vegetables intake and frequency of breakfast and snacks consumption: a cross-sectional study. Nutrition journal. 2013 Dec;12:1-0.DOI: https://doi.org/10.1186/1475-2891-12-123

50. Kang M, Choi SY, Jung M. Dietary intake and nutritional status of Korean children and adolescents: a review of national survey data. Clinical and Experimental Pediatrics. 2020 Dec 28;64(9):443.DOI: : 10.3345/cep.2020.01655

51.Lesani A, Mohammadpoorasl A, Javadi M, Esfeh JM, Fakhari A. Eating breakfast, fruit and vegetable intake and their relation with happiness in college students. Eating and weight disorders-studies on anorexia, bulimia and obesity. 2016 Dec;21:645-51.DOI: https://doi.org/10.1007/s40519-016-0261-0

52.Tani Y, Isumi A, Doi S, Fujiwara T. Food categories for breakfast and mental health among children in Japan: Results from the A-CHILD Study. Nutrients. 2023 Feb 22;15(5):1091. https://doi.org/10.3390/nu15051091

53.Park S, Sherry B, Foti K, Blanck HM. Self-reported academic grades and other correlates of sugar-sweetened soda intake among US adolescents. J Acad Nutr Diet. 2012;112(1):125131. DOI: https://doi.org/10.1016/j.jada.2011.08.045

54.Quann EE, Fulgoni VL, Auestad N. Consuming the daily recommended amounts of dairy products would reduce the prevalence of inadequate micronutrient intakes in the United States: diet modeling study based on NHANES 2007–2010. Nutrition journal. 2015 Dec;14:1-1.DOI: https://doi.org/10.1186/s12937-015-0057-5

55.White BA, Horwath CC, Conner TS. Many apples a day keep the blues away–Daily experiences of negative and positive affect and food consumption in young adults. British journal of health psychology. 2013 Nov;18(4):782-98.DOI: https://doi.org/10.1111/bjhp.12021

56.Leidy HJ, Ortinau LC, Douglas SM, Hoertel HA. Beneficial effects of a higher-protein breakfast on the reduction of body fat and cardiovascular disease risk in overweight and obese late-adolescent girls. Am J Clin Nutr. 2009;87(1):149-157. DOI: https://doi.org/10.3945/ajcn.112.053116

57.St-Onge MP, Mikic A, Pietrolungo CE.

Effects of diet on sleep quality. *Advances in Nutrition*. 2016;7(5):938-949.DOI: https://doi.org/10.3945/an.116.012336

58.Jin MJ, Yoon CH, Ko HJ, Kim HM, Kim AS, Moon HN, Jung SP. The relationship of caffeine intake with depression, anxiety, stress, and sleep in Korean adolescents. Korean journal of family medicine. 2016 Mar;37(2):111. DOI: 10.4082/kjfm.2016.37.2.111.